

UNIVERSITAT JAUME I
ESCUELA SUPERIOR DE TECNOLOGIA Y CIENCIAS EXPERIMENTALES
DEPARTAMENTO DE SISTEMAS INDUSTRIALES Y DISEÑO
DOCTORADO EN TECNOLOGIAS INDUSTRIALES, MATERIALES Y EDIFICACIÓN



TESIS DOCTORAL

**Desarrollo y caracterización de formulaciones poliméricas
biodegradables y termoconformables para envasado**

Autora:

Jennifer González Ausejo

Dirigida por:

Luis Cabedo Mas

José Gámez Pérez

Castellón, febrero 2017

Agradecimientos

En primer lugar, me gustaría agradecer la labor de mis directores de tesis, José Gámez Pérez y Luís Cabedo Mas. Os agradezco enormemente la confianza depositada, el apoyo mostrado, el tiempo invertido y todo lo que me habéis enseñado en estos cuatro años.

Agradecer a los coautores de las publicaciones que forman parte de esta tesis, por permitirme realizar esta tesis por compendio de publicaciones y por el esfuerzo en el desarrollo de las mismas.

Agradecer a las distintas instituciones que han financiado las investigaciones desarrolladas en este trabajo:

- A la Universitat Jaume I por la ayuda predoctoral para la formación de personal investigador (PREDOC/2012/32), las dos becas para realizar estancias temporales en otros centros de investigación, para el personal docente e investigador de la Universidad (E-2015-22 y E-2016-32) y el proyecto de investigación financiado (UJI-B2016-35).
- Al Ministerio de Economía y Competitividad por el soporte financiero de este trabajo (AGL2015-63855-C2-2-R).
- A la Generalitat Valenciana por el soporte financiero de este trabajo (GV/2014/123).
- Al grupo de Novel Materials and Nanotechnology del Instituto de Agrotecnología y Tecnología de alimentos (IATA) del Consejo Superior de Investigaciones Científicas (CSIC) donde se han desarrollado parte del experimental de este trabajo.
- Al Instituto de Tecnología de Materiales de la Universitat Politècnica de València-Campus de Alcoy donde se llevó a cabo una estancia de investigación.
- Al Centre of Polymer and Carbon Materials, Polish Academy of Sciences (Zabrze, Polonia), donde se llevó a cabo una estancia de investigación.
- Al School of Biology, Chemistry and Forensic Science, Faculty of Science and Engineering, University of Wolverhampton (Wolverhampton, Reino Unido), donde se llevó a cabo una breve estancia de investigación.

Quisiera dar las gracias a cada una de las personas que han formado parte del grupo PIMA durante estos años. Todos y cada uno habéis sido unos maravillosos compañeros de trabajo. Unos me habéis ayudado con trámites burocráticos, otros en docencia, y la mayoría en el día a día en los laboratorios y delante del ordenador para culminar este trabajo. Gracias de todo corazón por vuestra voluntad de ayudarme, apoyarme, escucharme, darme fuerzas y enseñarme no sólo en aspectos del ámbito académico-profesional sino en el ámbito personal. Gracias a todos por los almuerzos, las comida y las cenas, cada "mone a fumar", cada congreso y tiempo compartido conmigo estos años.

Me siento muy afortunada de haber podido compartir despacho y laboratorio con todos y cada uno de vosotros: Ane, Montse, Sara, Javi, Fran, Estefanía, Adrià... y especialmente mi gran agradecimiento a Raquel y Pepe. Gracias a todos por vuestro tiempo, consejos, enseñanzas, ... habéis dejado una gran marca en mi durante este tiempo. Espero que nuestros caminos se vuelvan a cruzar en el futuro.

Águeda, gràcies pel teu suport durant l'estada a Polònia i aconsellar-me durant aquests 4 anys, gràcies per deixar-me conèixer-te i compartir amb mi tants congressos.

Así mismo, me gustaría agradecer a todos aquellos que habéis pasado por los laboratorios o acabáis de llegar a estos, por las ilusiones, experiencia, apoyo y ayuda que me habéis aportado. Gracias María José, Nuno, Braulio, Jorge, Lourdes, Ileana, Jaume, Balma, Patricia, Andrea, Alejandra, Alejandro, Vesa, Erik, Mika, Mafer, Florian, Julien, Omar, Andrea, Natalia, Atenas, ...

Quiero también agradecer a los miembros del GROC por sus enseñanzas en mis primeros meses de incursión en la investigación, especialmente a Gladys, Salva, Jorge y Rocío. Fue para mí una maravillosa y grata experiencia trabajar junto a vosotros en un campo tan desconocido para mí como es la física del láser de femtosegundo.

Agradecer la disposición mostrada por los técnicos del SCIC para ayudarme en la preparación y análisis de las muestras.

En cuanto a las colaboraciones científicas realizadas con otros centros de investigación, me gustaría agradecer a todos los miembros del Novel Materials and Nanotechnology group del IATA, por las

colaboraciones realizadas y la amabilidad y disponibilidad para utilizar sus equipos. Especialmente agradecer a Chema, María José, Amparo, Toni, Jesús y Lorena.

Con respecto a mi estancia en Alcoy, sólo tengo palabras de agradecimiento para cada uno de los miembros del Instituto de Tecnología de Materiales de la Escuela Politécnica Superior de Alcoy, por abrirme de par en par las puertas de sus laboratorios y sus despachos. Trabajar conjuntamente con vosotros me permitió aprender mucho, utilizar equipos nuevos, conocer distintas maneras de trabajar, pero sobretodo conocer lo maravillosas personas que sois. Me hicisteis sentir desde el primer día una más de vuestro grupo. Muchas gracias: Rafa, Lourdes, Teo, Juan, Tayo, Vicent, David, Néstor, Mado, Alfredo, Dani, Pelayo, Marina, ...

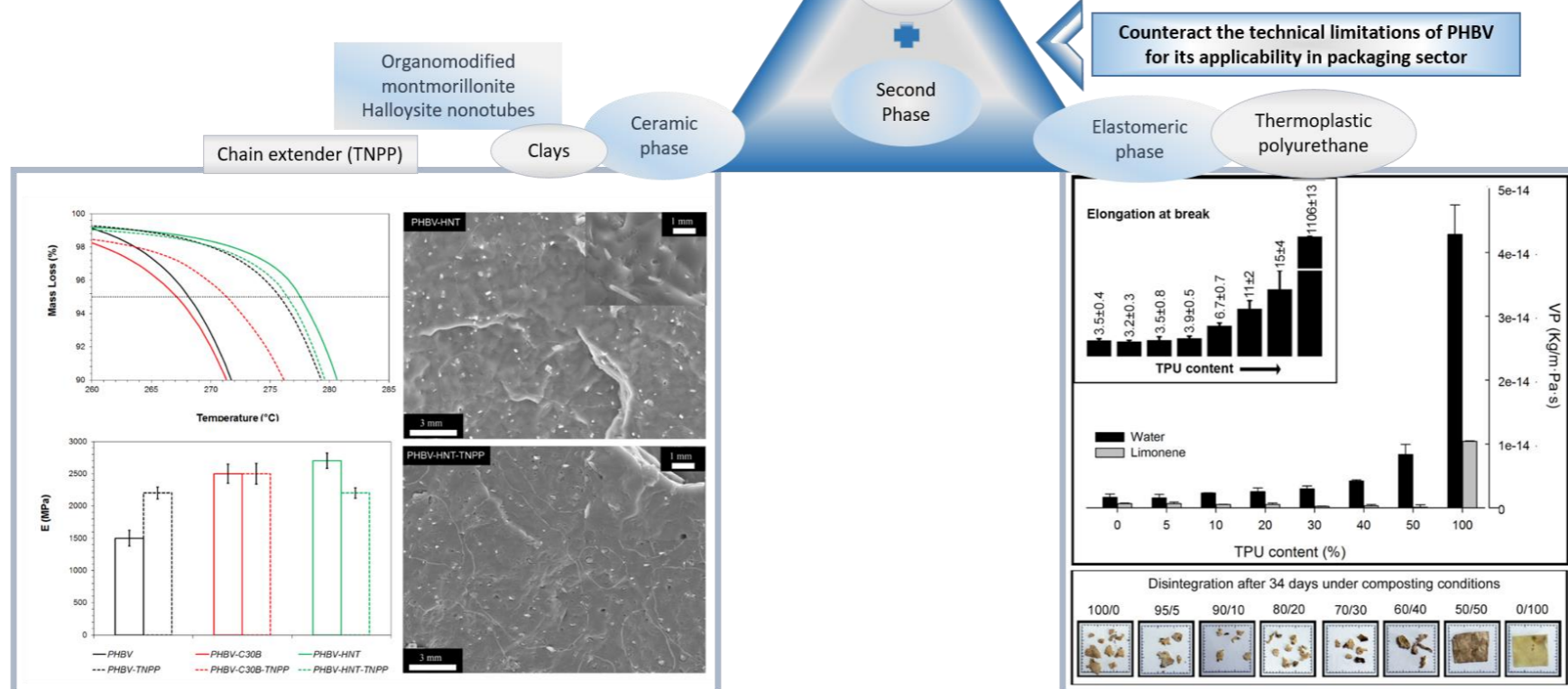
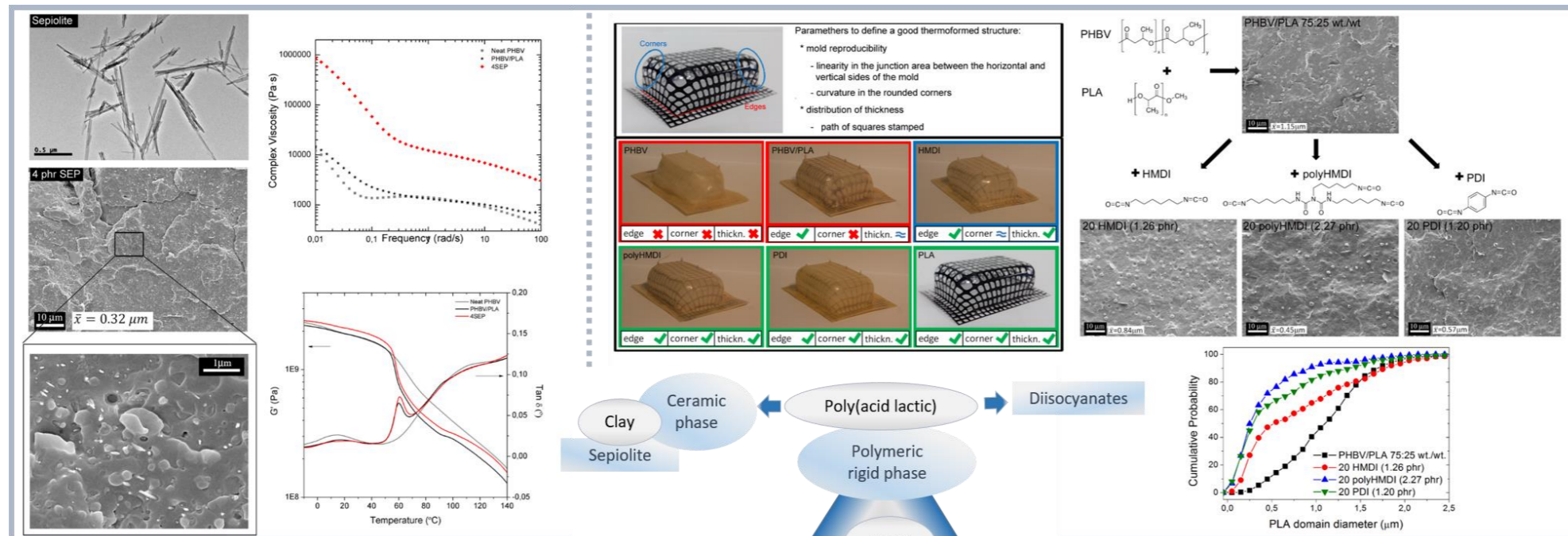
I would like to thank Marek Kowalczyk and Grażyna Adamus for giving me the opportunity to work at Centre of Polymer and Carbon Materials, Polish Academy of Sciences in Zabrze. Thanks to all the members of your group who made me feel like at home and thanks for your hospitality, thanks Marek, Grażyna, Joanna, Marta, Wanda, Paweł, Iwona, Kuba and all the Michał in the group. My stay in Poland was a wonderful experience, I learnt a lot on the laboratory, but also about the polish traditions and habits, it has only been possible because of your help and friendship: Joanna, Marta and Wanda. Dziękuję bardzo.

I would like to thank Marek Kowalczyk and Iza Radecka for giving me the opportunity to visit the University of Wolverhampton. Thanks Brian for your hospitality and your patience teaching me the biotechnological aspects of the PHAs synthesis.

En el terreno más personal, quisiera agradecer a toda mi familia por el apoyo recibido. Aunque no tenéis muy claro que he estado haciendo estos años y el porqué de tanto esfuerzo y horas de dedicación, siempre me habéis escuchado y me habéis animado a seguir adelante y conseguir aquello que me he propuesto.

Finalment, gràcies a Raúl per ser tan comprensiu, per suportar-me, animar-me en tot moment, donar-me ànims, per aguantar-me aquests últims mesos de redacció i les estades fora de casa i lluny de tu i per evolucionar amb mi tot aquest temps.

Resumen gráfico



Resumen

El deterioro ambiental causado por la contaminación de los vertidos de polímeros procedentes de combustibles fósiles y los problemas de la gestión de estos residuos ha generado gran interés por los polímeros biodegradables. El poli (3-hidroxibutirato-co-3-hidroxivalerato) (PHBV) se postula como un candidato para sustituir materiales no biodegradables derivados del petróleo, contribuyendo a la reducción de los desechos sólidos poliméricos destinados a vertederos. Concretamente, este interés se ha manifestado en el sector industrial del envasado ya que consume la mayor parte de la producción mundial de plásticos, lo que implica la más alta generación de residuos.

El PHBV posee unas excelentes propiedades mecánicas y barrera que lo hacen útil para su uso en envasado. Sin embargo, su aplicación práctica en este extensivo campo se ha visto limitada por presentar algunas desventajas frente a los plásticos de uso común, tales como mayor fragilidad, menor resistencia térmica, estrecha ventana de procesado y un mayor coste.

Con el fin de contrarrestar estas limitaciones técnicas, en este trabajo de tesis, se han desarrollado nuevas formulaciones biodegradables por adición al PHBV de una segunda fase para modular su comportamiento. Las estrategias de mejora se han abordado desde una perspectiva de viabilidad técnica y de aplicabilidad sencilla en un entorno industrial.

Así pues, se ha estudiado la adición de una segunda fase cerámica (nanoarcillas), elastomérica (poliuretano termoplástico) o polimérica rígida (poli (ácido láctico)-PLA), así como la mezcla ternaria de PHBV con PLA y una nanoarcilla. Todas las composiciones se han obtenido mediante mezclado en fundido en equipos convencionales de procesado de polímeros termoplásticos haciendo uso, en ocasiones, de agentes reactivos compatibilizantes.

Los resultados obtenidos presentan sistemas en los que se palió, al menos parcialmente, las limitaciones técnicas de este copolímero para su aplicación en el sector del envasado, sin que sus ventajas principales, biodegradabilidad y buen comportamiento barrera, se vean muy afectadas.

Abstract

The environmental deterioration caused by the contamination of the waste residues produced by plastics derived from fossil fuels and the management problems of such residues have generated great interest in biodegradable polymers. Poly (3-hydroxybutyrate-co-3-hydroxyvalerate) (PHBV) is postulated as a candidate to replace commodity plastics, which are non-biodegradable and petroleum-derived materials, contributing to the reduction of solid wastes destined for landfills. Specifically, this interest has arisen in the packaging industry as it consumes most of the world's plastics production, implying the highest generation of waste.

The PHBV has excellent mechanical and barrier properties that would make it useful for its use in food packaging. However, its applicability in this field has been so far limited, due to some severe disadvantages, when compared to commonly used plastics, like greater brittleness, lower thermal resistance, narrow processing window and higher cost.

In order to counteract these technical limitations, in this thesis work, new biodegradable formulations have been developed by addition to PHBV of a second phase to modulate their behavior. The improvement strategies have been approached from a perspective of technical feasibility and simple applicability in an industrial environment.

Thus, the addition of a second ceramic phase (nanoclay), elastomeric (thermoplastic polyurethane) or rigid polymer (Polylactic acid – PLA), as well as the ternary PHBV blends with PLA and a nanoclay has been studied. All compositions have been obtained by melt blending in conventional thermoplastic polymer processing equipment using sometimes reactive compatibilizing agents.

The results obtained present systems that at least partially overcome the technical limitations of this copolymer for its application in the packaging sector, keeping its main advantages, i.e. barrier properties, mechanical behavior and biodegradability.

La deterioració ambiental causada per la contaminació produïda pels abocaments dels residus de polímers procedents de combustibles fòssils i els problemes de gestió dels residus ha generat gran interès pels polímers biodegradables. El poli (3-hidroxibutirat-co-3-hidroxivalerat) (PHBV) es postula com un candidat per a substituir materials no biodegradables derivats del petroli, contribuint a la reducció de les deixalles sòlides polimèriques destinades a abocadors. Concretament, aquest interès s'ha manifestat en el sector industrial de l'envasament ja que consumeix la major part de la producció mundial de plàstics, la qual cosa implica la més alta generació de residus.

El PHBV posseeix unes excel·lents propietats mecàniques i barrera que el fan útil per al seu ús en envasament. No obstant això, la seua aplicació pràctica en aquest extensiu camp s'ha vist limitada per presentar alguns desavantatges enfront dels plàstics d'ús comú, tals com major fragilitat, menor resistència tèrmica, estreta finestra de processament i un major cost.

Amb la finalitat de contrarestar aquestes limitacions tècniques, en aquest treball de tesi, s'han desenvolupat noves formulacions biodegradables per addició al PHBV d'una segona fase per a modular el seu comportament. Les estratègies de millora s'han abordat des d'una perspectiva de viabilitat tècnica i d'aplicabilitat senzilla en un entorn industrial.

Així doncs, s'ha estudiat l'addició d'una segona fase ceràmica (nanoargila), elastomèrica (poliuretà termoplàstic) o polimèrica rígida (poliàcid làctic-PLA), així com la mescla ternària de PHBV amb PLA i una nanoargila. Totes les composicions s'han obtingut mitjançant mesclat en fos en equips convencionals de processament de polímers termoplàstics fent ús, en ocasions, d'agents reactius compatibilitzants.

Els resultats obtinguts presenten sistemes en els quals es pal·lia, almenys parcialment, les limitacions tècniques d'aquest copolímer per a la seua aplicació en el sector de l'envasament, sense que els seus avantatges principals, biodegradabilitat i bon comportament barrera, es vegien molt afectats.

Índice

Agradecimientos	3
Resumen gráfico	7
Resumen	9
Abstract.....	11
Resum	13
Índice	15
1. Introducción.....	21
1.1. Antecedentes	23
1.2. Planteamiento del problema.....	27
1.3. Objetivos de la investigación.....	29
1.4. Planificación de la investigación.....	31
1.5. Justificación de la investigación	34
Referencias	36
2. Marco teórico	39
2.1. Polímeros biodegradables	41
2.2. Poli(hidroxialcanoatos) (PHAs): Poli(3-hidroxi- butirato) (PHB) y Poli(3-hidroxi- butirato-co-3-hidroxi- valerato) (PHBV)	45
2.3. Limitaciones del PHBV asociadas al uso para envasado.....	48
2.3.1. Estabilidad térmica durante el procesado	48
2.3.2. Propiedades mecánicas	49
2.3.3. Ventana de procesado por termoconformado	51
2.4. Metodologías de actuación para la mejora de las propiedades del PHBV para envasado	53
2.4.1. Extensores de cadena	53
2.4.2. Nanocompuestos poliméricos	55
2.4.3. Mezclas de polímeros	56
2.4.4. Compatibilización de mezclas poliméricas.....	57
2.5. Degradabilidad en compostaje.....	58
2.6. Métodos de procesado y conformado	61
2.6.1. Termoconformado	61
Referencias	64

3. Capítulo 1.....	79
On the use of TNPP as a chain extender in melt blended PHBV/clay nanocomposites: morphology, thermal stability, and mechanical properties	79
ABSTRACT	83
GRAFICAL ABSTRACT.....	85
3.1. INTRODUCTION	87
3.2. EXPERIMENTAL.....	89
3.2.1. Materials	89
3.2.2. Nanocomposite preparation	89
3.2.3. Characterization	90
3.3. RESULTS AND DISCUSSION	92
3.3.1. Morphology.....	92
3.3.2. Thermal characterization	95
3.3.3. Mechanical properties	98
3.4. CONCLUSIONS	100
ACKNOWLEDGEMENTS	101
REFERENCES.....	101
4. Capítulo 2.....	107
Biodegradable poly(3-hydroxybutyrate-co-3-hydroxyvalerate) / thermoplastic polyurethane blends with improved mechanical and barrier performance	107
ABSTRACT	111
GRAFICAL ABSTRACT.....	113
4.1. INTRODUCTION	115
4.2. EXPERIMENTAL.....	117
4.2.1. Materials	117
4.2.2. Blend processing	117
4.2.3. Morphology.....	117
4.2.4. Thermal properties	118
4.2.5. Mechanical properties	119
4.2.6. Permeability measurements	119
4.2.7. Biodisintegration in composting conditions	120
4.3. RESULTS AND DISCUSSION	120
4.3.1. Morphological characterisation	120

4.3.2.	Thermal characterisation	124
4.3.3.	Mechanical properties	127
4.3.4.	Barrier performance	130
4.3.5.	Biodisintegration	131
4.4.	CONCLUSIONS	134
	ACKNOWLEDGEMENTS	134
	REFERENCES	134
5.	Capítulo 3	139
	Compatibilization of PHBV/PLA blends with diisocyanates	139
	ABSTRACT	143
	GRAFICAL ABSTRACT	145
5.1.	INTRODUCTION	147
5.2.	EXPERIMENTAL	150
5.2.1.	Materials	150
5.2.2.	Blend preparation	150
5.2.3.	Characterization	152
5.3.	RESULTS AND DISCUSSION	153
5.3.1.	Morphology	153
5.3.2.	Thermal characterization	156
5.3.3.	Mechanical properties	160
5.3.4.	Rheological behavior	163
5.4.	CONCLUSIONS	166
	ACKNOWLEDGEMENTS	167
	REFERENCES	167
6.	Capítulo 4	171
	Assessing the thermoformability of poly(3-hydroxybutyrate-co-3-hydroxyvalerate) / poly(acid lactic) blends compatibilized with Diisocyanates	171
	ABSTRACT	175
	GRAFICAL ABSTRACT	177
6.1.	INTRODUCTION	179
6.2.	EXPERIMENTAL	180
6.2.1.	Materials	180
6.2.2.	Blend preparation	181

6.2.3.	Characterization	181
6.2.4.	Thermoforming setup	183
6.3.	RESULTS AND DISCUSSION	185
6.3.1.	Morphology.....	185
6.3.2.	Barrier performance	187
6.3.3.	Thermoforming study	188
6.3.4.	Degradation in composting conditions.....	194
6.4.	CONCLUSIONS	197
	ACKNOWLEDGEMENTS.....	197
	REFERENCES.....	198
7.	Capítulo 5.....	201
	Effect of the addition of sepiolite on the morphology and properties of melt compounded PHBV/PLA blends	201
	ABSTRACT	205
	GRAFICAL ABSTRACT.....	207
7.1.	INTRODUCTION	209
7.2.	EXPERIMENTAL.....	211
7.2.1.	Materials	211
7.2.2.	Sample preparation	212
7.2.3.	Characterization	213
7.3.	RESULTS AND DISCUSSION	216
7.3.1.	Melt compounding and rheology of the blends	216
7.3.2.	Morphology.....	220
7.3.3.	Thermal characterization	223
7.3.4.	Mechanical properties	225
7.3.5.	Mechanical properties at high temperatures	228
7.3.6.	Barrier properties.....	231
7.4.	CONCLUSIONS	232
	ACKNOWLEDGEMENTS.....	233
	REFERENCES.....	233
8.	Discusión general.....	239
9.	Conclusiones	247
10.	Conclusions	251

11. Trabajos en curso y futuros	255
12. Anexos	261
12.1. Lista de publicaciones.....	263
12.2. Imagen de la primera página de los artículos publicados expuestos en la sección de resultados y discusión.....	265
12.3. Presentaciones en congresos nacionales e internacionales	268
12.4. Lista de abreviaturas y siglas	271
12.5. Lista de figuras.....	274
12.6. Lista de tablas.....	279
12.7. Lista de ecuaciones.....	280

1. Introducción

1. Introducción

1.1. Antecedentes

Los materiales que tradicionalmente se han utilizado en el envasado incluyen vidrio, metales (aluminio, hojalata y acero libre de estaño), papel y cartón y plásticos. Hoy en día los envases a menudo combinan varios materiales para explotar las propiedades funcionales o estéticas de cada material.

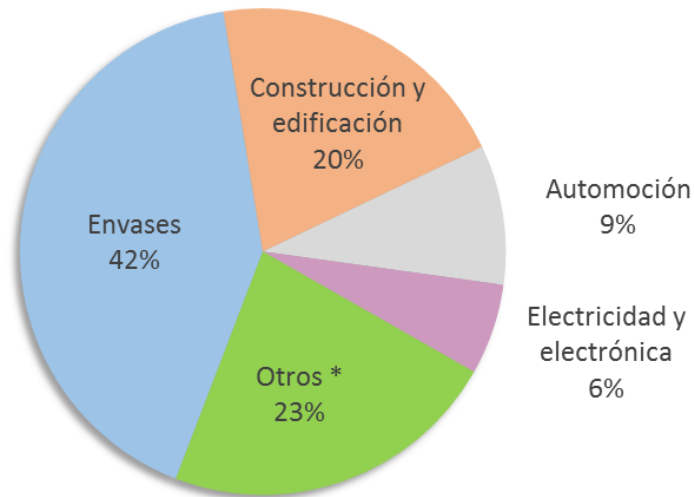
El uso de los plásticos en el envasado ha ido en aumento debido al bajo coste de los materiales y las ventajas funcionales (tales como termosellabilidad, capacidad de calentar en microondas, propiedades ópticas y tamaños y formas ilimitados) [1].

Los materiales plásticos más ampliamente utilizados en el mercado del envasado son polietileno (PE) (bolsas de plástico para comestibles, envases opacos para leche, agua y zumos, lejía, botellas de detergente y champú, bolsas de basura); polietilentereftalato (PET) (botellas, bandejas listas para el horno y comidas para microondas, envases de detergente); policloruro de vinilo (PVC) (recipientes para comida para llevar, botellas de champú, botellas de enjuague bucal, botellas de detergente, blísteres); polipropileno (PP) (recipientes de alimentos como salsa de tomate, yogur, requesón, margarina, jarabe, envases para llevar, tapas de botellas); poliestireno (PS) (espuma de poliestireno para envases de alimentos en general, cartones de huevos, productos de un solo uso, como cubiertos, vasos y platos desechables, envases de comida para llevar) y poliamida (PA) (envases flexibles de alimentos perecederos, como la carne y el queso), entre otros.

Anualmente alrededor de 300 millones de toneladas de materiales plásticos se consumen en todo el mundo [2]. En las últimas décadas ha habido una progresión en el consumo de plástico que se espera que continúe hasta el año 2020. Los envases plásticos representan al menos el 40 % del mercado de plástico en Europa [2] (Fig. 1.1). Las consecuencias de estas grandes demandas de plásticos derivados del petróleo han generado graves problemas de contaminación ambiental. En Europa, el 29,7 por ciento, o 7,7 millones de toneladas, de los plásticos post-consumo producido en el año 2014 se reciclaron, mientras que el 39,5 por ciento fue incinerado para la generación de

1.Introducción

energía. El 30,8 por ciento restante de plásticos post-consumo en Europa fue a vertederos [2] (Fig. 1.2).



*Otros *: Hace referencia a sectores de aplicación tales como electrodomésticos, hogar y productos de consumo, muebles, productos médicos y agricultura.*

Fig.1.1: Demanda de plásticos en Europa por segmentos, datos de 2016. Fuente: Plastics Europe, Association of Plastics Manufacturers [2].

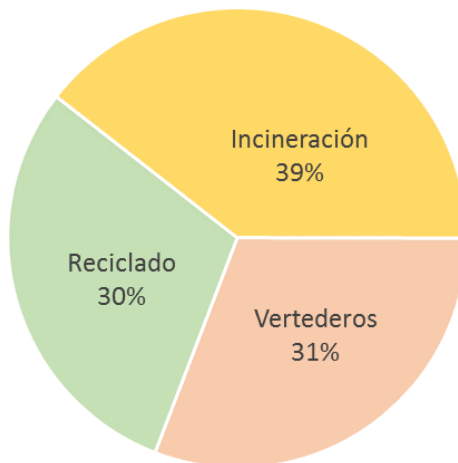


Fig.1.2: El tratamiento para los residuos plásticos post-consumo, datos de 2016. Fuente: Plastics Europe, Association of Plastics Manufacturers [2].

En los vertederos, las velocidades de degradación son tremendamente lentas. Las poliolefinas son resistentes a la degradación microbiana debido a la falta de un grupo funcional activo, su naturaleza hidrófoba, su alto peso molecular, su estructura ramificada y la presencia de aditivos [3].

La incineración permite recuperar la energía química contenida en los residuos plásticos. Si este proceso es realizado de manera controlada en reactores de incineración, el hidrocarburo del plástico es convertido en dióxido de carbono y agua. El residuo de fusión del incinerador está libre de peligros de toxicidad y puede ser eliminado en vertederos [4]. Sin embargo, la incineración incontrolada de los materiales plásticos tiene graves riesgos para la salud. Los gases de efecto invernadero y otros compuestos tóxicos, tales como partículas, gases ácidos (especialmente dióxido de azufre y óxidos de nitrógeno), metales pesados, halógenos, dioxinas y productos de combustión incompleta, se liberan en el medio ambiente durante la incineración de plásticos [4,5].

En cuanto al reciclado, es difícil llevar a cabo una adecuada clasificación y separación de los plásticos, debido a la amplia variedad de plásticos existentes. Hay que tener en cuenta que el reciclado cambia las propiedades de los materiales, lo que limita sus aplicaciones [4,6]. Además, la presencia de aditivos como los recubrimientos, las cargas y los pigmentos limitan el uso del material reciclado. Adicionalmente, el uso de materiales reciclados en el envasado alimentario entraña problemas de seguridad alimentaria, por lo que su uso está muy limitado legalmente.

La problemática asociada a la gestión de los residuos plásticos a nivel global y la contaminación producida por los vertidos incontrolados de los mismos, ha derivado en un aumento de la investigación en el desarrollo de materiales de envase y embalaje sostenibles ambiental y económicamente. Las principales estrategias actuales que se emplean para resolver estos problemas incluyen la revalorización de los mismos después de su ciclo de vida útil para que no terminen en vertederos, mediante el reciclaje y el aprovechamiento energético. Sin embargo, el desarrollo de los polímeros obtenidos a partir de fuentes renovables, considerados como biopolímeros, y su potencial biodegradabilidad ha sido objeto de estudio y análisis como una posible alternativa a esta problemática. Así pues, desde hace algún tiempo, debido a la política medioambiental que se está imponiendo a nivel mundial, se ha empezado a observar un considerable interés en desarrollar materiales para envases basados en polímeros obtenidos a

1.Introducción

partir de fuentes no fósiles, como alternativa a los plásticos convencionales, y que además sean biodegradables [7]. Su empleo permitiría contribuir a una mejor gestión de los desechos sólidos orgánicos junto a los poliméricos, destinados a su biodegradación en plantas de compostaje y con un menor impacto ambiental en caso de vertido descontrolado [9,9].

La base renovable y la biodegradabilidad de estos nuevos polímeros suponen un valor añadido adicional muy demandado en la actualidad por la industria del envasado, y es consecuencia lógica de la vasta cantidad de materiales de envase que se producen, así como del gran impacto medioambiental asociado a sus residuos [10].

1.2. Planteamiento del problema

Tal como se ha citado, los polímeros biodegradables se postulan como una alternativa viable a la sustitución de los plásticos convencionales no biodegradables para aplicaciones de envasado.

Los polihidroxicanoatos (PHAs) son poliésteres producidos naturalmente por algunas bacterias cultivadas en las materias primas agrícolas. Estos polímeros son termoplásticos biodegradables cuyas propiedades dependen de su composición química (homo- o copoliésteres, contenido en ácidos grasos hidroxilados, etc.) [11].

Entre los PHAs el polihidroxitirato-co-hidroxiclerato (PHBV) está siendo postulado como un sustituto sostenible de los plásticos convencionales derivados del petróleo en el sector del envasado dadas las excelentes propiedades barrera que presenta, equiparables a las del PET [12], y un comportamiento mecánico equilibrado en términos de rigidez y resistencia similares a la del PP [11,13], así como su origen renovable y su rápida biodegradabilidad [14]. No obstante, su aplicabilidad en la actualidad se ve dificultada por cuatro principales motivos [15,16]:

- i. Baja estabilidad térmica en fundido: el PHBV, como el resto de biopoliésteres, presentan una baja estabilidad térmica a sus temperaturas de procesado en fundido, lo que compromete su transformación en condiciones industriales.
- ii. Baja ductilidad: El PHBV presenta una deformación a rotura inferior al 5% que limita su aplicación en el sector del envasado.
- iii. Dificultad para ser termoconformado: la elevada cristalinidad del PHBV, que le dota de las excelentes propiedades barrera, hace que su termoconformado sea inviable en la práctica.
- iv. Elevado coste: el PHBV es aún un material poco competitivo desde el punto de vista de los costes. No obstante, se trata de un aspecto económico que se prevé se resuelva en el futuro con el aumento de la demanda y la mejora de los procesos productivos.

Por otro lado, el mercado de PHBV se encuentra en un estado incipiente, es decir, existe una baja disponibilidad industrial de PHBV en el mercado en comparación con las demandas actuales de

1.Introducción

polímero para envasado. Ello, sumado a las limitaciones que presenta, compromete sustancialmente su implantación en el sector del envasado.

El presente trabajo de tesis busca desarrollar nuevas formulaciones dirigidas a contrarrestar las tres principales limitaciones técnicas que presenta el PHBV para su aplicación inmediata en el campo del envasado. Las distintas estrategias que se proponen para abordar estos inconvenientes son las siguientes:

- i. Baja estabilidad térmica en fundido. La propuesta para abordar esta limitación es la introducción de un agente extensor de cadena. Se analizará el efecto de este agente tanto en el polímero puro como en presencia de nanoarcillas.
- ii. Baja ductilidad. Con el fin de incrementar la ductilidad del PHBV, se van a desarrollar mezclas con un elastómero termoplástico biodegradable, concretamente un poliuretano termoplástico (TPU) comercial en base éster y no estabilizado contra hidrólisis.
- iii. Dificultad para ser termoconformado. Para ampliar la ventana de termoconformado, así como la estabilidad de la lámina, principales motivos de la baja termoconformabilidad del PHBV, se plantean mezclas con poliláctico (PLA). Con estas mezclas, se busca aumentar la viscosidad en fundido del material y la elasticidad de la lámina durante el procesado. Dada la naturaleza inmiscible de ambos biopoliésteres, se va a recurrir a diferentes aditivos (reactivos químicos compatibilizantes y nanoarcillas) para mejorar el comportamiento de las mezclas.

Para garantizar que el resultado de esta investigación sea susceptible de ser trasladado a aplicaciones industriales se emplean técnicas de mezclado en fundido convencionales y todos los materiales (resinas y aditivos) están disponibles a nivel comercial.

1.3. Objetivos de la investigación

El objetivo principal del presente trabajo es contrarrestar las limitaciones técnicas que plantea el copolímero PHBV mediante el desarrollo de nuevas formulaciones biodegradables a partir de mezclas y compuestos de PHBV con otros polímeros y aditivos con el fin de aumentar la aplicabilidad del PHBV en el sector del envasado.

Los objetivos específicos planteados para la consecución de este fin se describen a continuación:

- Desarrollo y caracterización de materiales nanocompuestos PHBV/arcilla con propiedades mecánicas y estabilidad térmica mejoradas. Se pretende evaluar la incorporación de un extensor de cadena, tris(nonilfenil)fosfito (TNPP) y dos tipos de arcillas, una arcilla montmorillonita comercial (de tipo laminar) modificada con sales de amonio cuaternarias (Cloysite® 30B) (C30B) y nanotubos de halloysita (HNT) no modificada al PHBV. Se comparará la influencia del extensor de cadena, así como de las diferentes arcillas sobre la estabilidad térmica, la morfología y las propiedades mecánicas del PHBV. (Capítulo 1)
- Estudio de la influencia de la adición al PHBV de un elastómero (poliuretano termoplástico (TPU)) por mezclado en fundido. Caracterización del comportamiento de las mezclas sobre la morfología, la ductilidad, las propiedades térmicas y barrera y desintegrabilidad en condiciones de compostaje. (Capítulo 2)
- Desarrollo y caracterización de mezclas compatibilizadas mediante diisocianatos de PHBV/ poli (ácido láctico) (PLA). Estudio del efecto del tipo y contenido de diisocianato sobre la compatibilidad de las fases poliméricas, la morfología, las propiedades térmicas, mecánicas, reológicas, barrera y desintegrabilidad en condiciones de compostaje. (Capítulos 3 y 4)
- Estudio de la procesabilidad por termoconformado del PHBV y sus mezclas. Desarrollo de una metodología sencilla de evaluación de la termoconformabilidad y determinación del rango de temperaturas en una ventana de procesado para termoconformado de polímeros. (Capítulo 4)
- Obtención de nanocompuestos de PHBV para la mejora de las propiedades barrera y el moldeo del PHBV por termoconformado. Evaluación del efecto de la adición de distintos

1.Introducción

contenidos de sepiolita sobre la morfología, las propiedades térmicas, mecánicas, reológicas, barrera y temperatura de servicio de nanocompuestos sepiolita/PHBV/PLA.
(Capítulo 5)

1.4. Planificación de la investigación

De acuerdo con los objetivos planteados, en el presente trabajo se planifican las siguientes investigaciones, distribuidas en tres líneas generales de actuación, correspondientes con los tres problemas técnicos que comprometen la aplicabilidad del PHBV al sector del envasado. Se pretende la mejora de las propiedades del PHBV introduciendo una segunda fase de naturaleza cerámica, polimérica elastomérica o polimérica rígida. Además, para el último tipo de aditivo, se estudia la mejora de la interacción entre la fase principal y la fase polimérica rígida con el uso de agentes reactivos compatibilizantes, así como la mezcla de fase polimérica rígida y cerámica.

Con el fin de mejorar la estabilidad térmica durante el procesado del PHBV, en el presente trabajo, se estudia el efecto de la adición de un extensor de cadena y nanomateriales de origen mineral (Capítulo 1). La hipótesis planteada es contrarrestar la caída de peso molecular durante el procesado mediante la reacción entre los grupos carboxilos terminales del poliéster y los grupos funcionales del extensor de cadena, dando lugar a la mejora de la estabilidad térmica del PHBV durante el procesado. Estas composiciones fueron estudiadas en términos morfológicos, térmicos y mecánicos mediante SEM, TEM, WAXS, DSC, TGA y ensayos de tracción a temperatura ambiente. Los resultados se muestran en el punto 3 de este trabajo (Capítulo 1).

En el capítulo 2 se pretende la mejora de la ductilidad del PHBV mediante la adición de un modificador de impacto durante el mezclado en fundido en un mezclado interno, un poliuretano termoplástico comercial en base éster no estabilizado contra hidrólisis. La hipótesis planteada es la mejora de la elongación a rotura sin repercutir en exceso sobre las excelentes propiedades barrera del PHBV, ni sobre su capacidad de biodegradarse en condiciones de compostaje. Concretamente, se estudia la morfología, propiedades térmicas, mecánicas, barrera y desintegración en compostaje de las mezclas obtenidas en función del contenido en TPU.

Con la intención de mejorar la procesabilidad para el moldeo por termoconformado del PHBV, en el presente trabajo, se estudia el efecto de la adición de una segunda fase polimérica, el PLA, que presenta una buena termoconformabilidad a unas temperaturas de procesado similares a las del PHBV (Capítulos 3, 4 y 5). Se espera que la adición del PLA incremente la viscosidad en fundido del material, aumentando la estabilidad mecánica de la lámina a las temperaturas de procesado tras

1.Introducción

el proceso de calentamiento previo al estirado por termoconformado, así como la elasticidad de la lámina durante el conformado. Debido a la inmiscibilidad entre ambos poliésteres, se estudia la adición de reactivos químicos compatibilizantes y nanoarcillas para mejorar el comportamiento de las mezclas.

Concretamente, en los capítulos 3 y 4 se estudia el efecto de la adición de tres diisocianatos distintos sobre la compatibilización de las fases poliméricas. Las propiedades térmicas y mecánicas, dinamo-mecánicas y comportamiento reológico se estudian en el Capítulo 3. Posteriormente, en el Capítulo 4 se estudia la capacidad de termoconformado del PHBV, su comportamiento a barrera y desintegración en compostaje de las composiciones más prometedoras del Capítulo 3.

Por último, en el Capítulo 5, se evalúa el efecto de la adición de la fase cerámica, sepiolita, sobre la morfología, propiedades térmicas, mecánicas a temperatura ambiente y a altas temperaturas, dinamo-mecánicas, barrera, temperatura de reblandecimiento Vicat y comportamiento reológico del PHBV.

Estas líneas de investigación han sido desarrolladas siguiendo los siguientes esquemas (Figura 1.3):

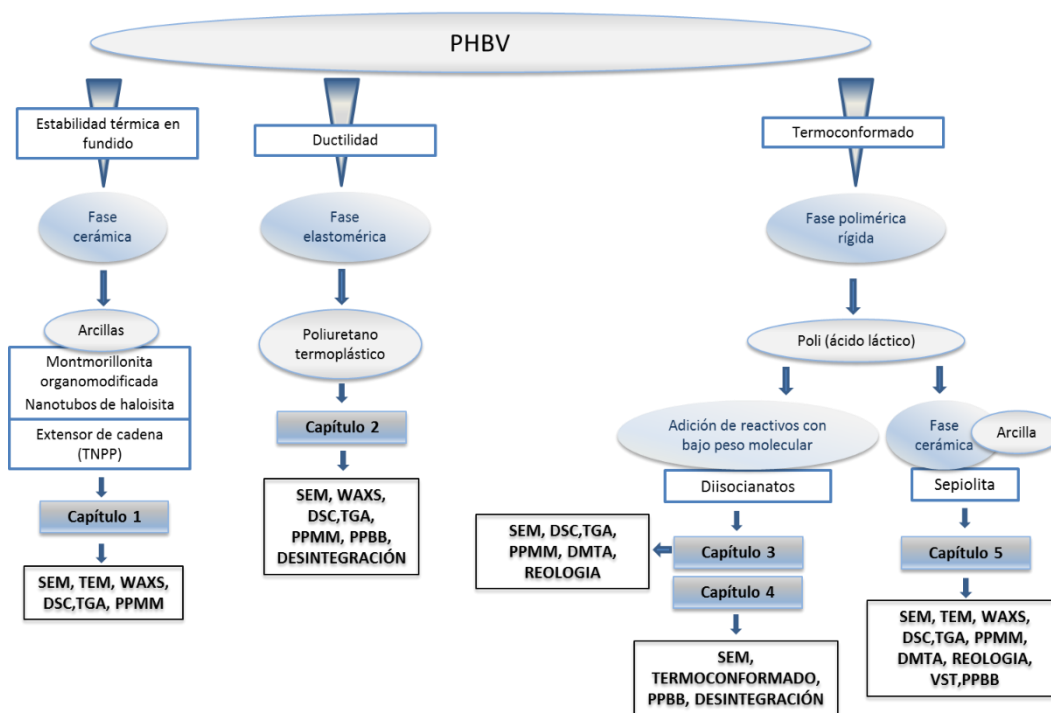


Fig. 1.3: Esquema de las líneas de investigación desarrolladas en el presente trabajo

La nomenclatura abreviada utilizada en la Fig. 1.3 para definir las técnicas utilizadas en las distintas investigaciones desarrolladas se define en el apartado 12.4 de los anexos.

1.Introducción

1.5. Justificación de la investigación

La industria del envasado consume la mayor parte de la producción mundial de plásticos, lo que implica la generación de una gran cantidad de residuos, como consecuencia de la corta vida útil de estos productos y la vasta cantidad de envases que se fabrican. Ello ha generado una gran preocupación por la gestión de estos residuos, así como por el deterioro ambiental causado por la contaminación derivada de los mismos. Esta situación ha convertido el reemplazamiento de los plásticos convencionales por bioplásticos que se degradan en un corto período de tiempo en una necesidad industrial, social y medioambiental.

Tal y como se ha comentado previamente, el PHBV es uno de los biopolíesteres que mayor interés está despertando en la actualidad dada la buena combinación de sus propiedades con su origen renovable y no procedente de fuentes alimenticias [17]. Además, su síntesis biológica a partir de la fermentación por microorganismos, hace que sea intrínsecamente biodegradable [14]. Este hecho hace que se trate de un material que está llamado a ser un potencial sustituto renovable de algunos plásticos procedentes del petróleo.

Cabe destacar que existe una expectativa de futuro a que los polímeros obtenidos por síntesis biológica a partir de microorganismos sean competitivos económicamente. Hoy por hoy, los polímeros procedentes del petróleo son baratos debido al reducido coste del petróleo. Sin embargo, las fuentes de carbono para la síntesis de estos biopolímeros pueden provenir de la valorización de residuos que no necesiten de procesos caros de extracción, purificación y síntesis, etc., como es el caso de los derivados del petróleo. Esto hace que el potencial de precio que presentan los procesos biológicos sean atractivos frente a la síntesis de plásticos a partir de derivados del petróleo. A estas ventajas futuras, se debe añadir que la huella de carbono de los polímeros obtenidos por síntesis biológica a partir de microorganismos es menor a la de los polímeros derivados del petróleo [18].

Por consiguiente, teniendo en cuenta estas consideraciones y la biodegradabilidad intrínseca del PHBV, el impacto económico y medioambiental potencial que presenta el PHBV es muy relevante.

Sin embargo, el PHBV posee una serie de limitaciones técnicas que no han sido suficientemente estudiadas en la actualidad. Es decir, a día de hoy, se tiene muy poco conocimiento sobre su

comportamiento en servicio y procesado industrial. Esto se debe, en parte, a su novedad, y a que no se ha conseguido aún desarrollar formulaciones que permitan contrarrestar las limitaciones para su aplicación masiva en el sector del envasado.

La mayoría de las publicaciones que existen en la literatura científica sobre el PHBV se limitan a un estudio morfológico y de sus propiedades físico-químicas, como propiedades barrera y mecánicas, cinéticas de degradación, etc. [19-23]. No obstante, no existen trabajos en los que se profundice en el comportamiento en servicio, la procesabilidad o la biodegradabilidad de los materiales resultantes de realizar modificaciones químicas y físicas sobre el PHBV. Además, en muchos de los estudios realizados hasta el momento, el procesado del PHBV se ha llevado a cabo mediante técnicas no convencionales industrialmente, como es la técnica de *solvent casting* [23-30], con grados poliméricos y aditivos o modificadores no comerciales ni disponibles comercialmente a gran escala [31–35]. Por todo ello, aun obteniendo unos buenos resultados a escala de laboratorio son difícilmente extrapolables a la industria.

Por ello, en el presente trabajo se busca aumentar el conocimiento que se tiene del procesado del PHBV mediante el desarrollo de nuevas formulaciones para modular el comportamiento del PHBV desde una perspectiva de viabilidad técnica y de aplicabilidad sencilla en un entorno industrial como es el sector del envase.

Además, cabe remarcar que entre los retos sociales que propone Europa en Horizonte 2020 se encuentra: “Seguridad alimentaria, agricultura y silvicultura sostenibles, investigación marina, marítima y de aguas interiores y bioeconomía” y más concretamente en la línea de actividad: 2.4. “Bioindustria: Bioindustrias sostenibles y competitivas que favorecen el desarrollo de una bioeconomía europea” [36]. Por consiguiente, el uso de materiales poliméricos biodegradables y provenientes de fuentes renovables para su aplicación en el sector del envasado se trata pues sin duda de un tema de gran importancia e impacto en la sociedad actual, no únicamente una demanda de la industria.

1.Introducción

Referencias

- [1] A. López-Rubio, E. Almenar, P. Hernandez-Muñoz, J.M. Lagarón, R. Català, R. Gavara, Overview of Active Polymer-Based Packaging Technologies for Food Applications, *Food Rev. Int.* 20 (2004) 357–387. doi:10.1081/LFRI-200033462.
- [2] Association of Plastics Manufacturers in Europe, *Plastics -The Facts 2016*. An analysis of European plastics production, demand and waste data.<http://www.plasticseurope.org/Document/plastics---the-facts-2016-15787.aspx?Page=DOCUMENT&FolID=2>, (2016) accessed 23/10/16.
- [3] P.V. a. Arutchelvi, J., Sudhakar, M., Arkatkar, A., Doble, M. , Bhaduri, S., Uppara, Biodegradation of polyethylene and polypropylene, *Indian J. Biotechnol.* 7 (2008) 9–22.
- [4] V. Sinha, M.R. Patel, J. V. Patel, Pet waste management by chemical recycling: A review, *J. Polym. Environ.* 18 (2010) 8–25. doi:10.1007/s10924-008-0106-7.
- [5] K. Marsh, B. Bugusu, Food packaging - Roles, materials, and environmental issues: Scientific status summary, *J. Food Sci.* 72 (2007). doi:10.1111/j.1750-3841.2007.00301.x.
- [6] K. Hamad, M. Kaseem, F. Deri, Recycling of waste from polymer materials: An overview of the recent works, *Polym. Degrad. Stab.* 98 (2013) 2801–2812. doi:10.1016/j.polymdegradstab.2013.09.025.
- [7] M. Vert, Y. Doi, K.-H. Hellwich, M. Hess, P. Hodge, P. Kubisa, M. Rinaudo, F. Schué, Terminology for biorelated polymers and applications (IUPAC recommendations 2012), *Pure Appl. Chem.* 84 (2012).
- [8] G. Kale, T. Kijchavengkul, R. Auras, M. Rubino, S.E. Selke, S.P. Singh, Compostability of bioplastic packaging materials: An overview, *Macromol. Biosci.* 7 (2007). doi:10.1002/mabi.200600168.
- [9] S. Philip, T. Keshavarz, I. Roy, Polyhydroxyalkanoates: Biodegradable polymers with a range of applications, *J. Chem. Technol. Biotechnol.* 82 (2007) 233–247. doi:10.1002/jctb.1667.
- [10] F. Haugaard, V. K., Udsen, A. M., Mortensen, G., Hoegh, L., Petersen, K., & Monahan, Biobased packaging materials for the food industry. Status and perspectives, in: . C. J. Weber (Ed.), *A Eur. Concert. Action*, 2001.
- [11] E. Bugnicourt, Polyhydroxyalkanoate (PHA): Review of synthesis, characteristics, processing and potential applications in packaging, *Express Polym. Lett.* 8 (2014) 791–808. doi:10.3144/expresspolymlett.2014.82.
- [12] D. Cava, E. Gimenez, R. Gavara, J.M. Lagaron, Comparative Performance and Barrier Properties of Biodegradable Thermoplastics and Nanobiocomposites versus PET for Food Packaging Applications, *J. Plast. Film Sheeting.* 22 (2006) 265–274. <http://www.scopus.com/inward/record.url?eid=2-s2.0-33845203640&partnerID=tZotx3y1> (accessed January 14, 2015).
- [13] D.Z. Bucci, L.B.B. Tavares, I. Sell, PHB packaging for the storage of food products, *Polym. Test.* 24 (2005) 564–571. doi:10.1016/j.polymertesting.2005.02.008.
- [14] Y.-X. Weng, Y. Wang, X.-L. Wang, Y.-Z. Wang, Biodegradation behavior of PHBV films in a pilot-scale composting condition, *Polym. Test.* 29 (2010) 579–587. doi:10.1016/j.polymertesting.2010.04.002.
- [15] K.K. Yang, X.L. Wang, Y.Z. Wang, Progress in nanocomposite of biodegradable polymer, *J. Ind. Eng. Chem.* 13 (2007) 485–500. <http://www.scopus.com/inward/record.url?eid=2-s2.0-34547635623&partnerID=tZotx3y1>.

- [16] J.W. Rhim, H.M. Park, C.S. Ha, Bio-nanocomposites for food packaging applications, *Prog. Polym. Sci.* 38 (2013) 1629–1652. doi:10.1016/j.progpolymsci.2013.05.008.
- [17] G. Jiang, D.J. Hill, M. Kowalczyk, B. Johnston, G. Adamus, V. Irorere, I. Radecka, Carbon sources for polyhydroxyalkanoates and an integrated biorefinery, *Int. J. Mol. Sci.* (2016). doi:10.3390/ijms17071157.
- [18] A. Javadi, S. Pilla, S. Gong, L.S. Turng, Biobased and Biodegradable PHBV-Based Polymer Blends and Biocomposites: Properties and Applications, *Handb. Bioplastics Biocomposites Eng. Appl.* (2011) 372–396. doi:10.1002/9781118203699.ch14.
- [19] E. Hablot, P. Bordes, E. Pollet, L. Avérous, Thermal and thermo-mechanical degradation of poly(3-hydroxybutyrate)-based multiphase systems, *Polym. Degrad. Stab.* 93 (2008) 413–421. doi:10.1016/j.polymdegradstab.2007.11.018.
- [20] P. Bordes, E. Hablot, E. Pollet, L. Avérous, Effect of clay organomodifiers on degradation of polyhydroxyalkanoates, *Polym. Degrad. Stab.* 94 (2009) 789–796. doi:10.1016/j.polymdegradstab.2009.01.027.
- [21] J.P. Mofokeng, A.S. Luyt, Morphology and thermal degradation studies of melt-mixed PLA/PHBV biodegradable polymer blend nanocomposites with TiO₂ as filler, *J. Appl. Polym. Sci.* 132 (2015) n/a-n/a. doi:10.1002/app.42138.
- [22] Q. Liu, C. Wu, H. Zhang, B. Deng, Blends of polylactide and poly(3-hydroxybutyrate-co-3-hydroxyvalerate) with low content of hydroxyvalerate unit: Morphology, structure, and property, *J. Appl. Polym. Sci.* 132 (2015) n/a-n/a. doi:10.1002/app.42689.
- [23] B.M.P. Ferreira, C.A.C. Zavaglia, E.A.R. Duek, Films of PLLA/PHBV: Thermal, morphological, and mechanical characterization, *J. Appl. Polym. Sci.* 86 (2002) 2898–2906. doi:10.1002/app.11334.
- [24] E. Fortunati, M. Peltzer, I. Armentano, L. Torre, A. Jiménez, J.M. Kenny, Effects of modified cellulose nanocrystals on the barrier and migration properties of PLA nano-biocomposites, *Carbohydr. Polym.* 90 (2012) 948–956. doi:10.1016/j.carbpol.2012.06.025.
- [25] H.-Y. Yu, Z.-Y. Qin, B. Sun, X.-G. Yang, J.-M. Yao, Reinforcement of transparent poly(3-hydroxybutyrate-co-3-hydroxyvalerate) by incorporation of functionalized carbon nanotubes as a novel bionanocomposite for food packaging, *Compos. Sci. Technol.* 94 (2014) 96–104. doi:10.1016/j.compscitech.2014.01.018.
- [26] K. Wang, Y. Wang, R. Zhang, Q. Li, C. Shen, Preparation and characterization of microbial biodegradable poly(3-hydroxybutyrate-co-4-hydroxybutyrate)/organoclay nanocomposites, *Polym. Compos.* 33 (2012) 838–842. doi:10.1002/pc.22220.
- [27] C. Xu, Z. Qiu, Crystallization behavior and thermal property of biodegradable poly(3-hydroxybutyrate)/multi-walled carbon nanotubes nanocomposite, *Polym. Adv. Technol.* 22 (2011) 538–544. doi:10.1002/pat.1540.
- [28] E. Ten, J. Turtle, D. Bahr, L. Jiang, M. Wolcott, Thermal and mechanical properties of poly(3-hydroxybutyrate-co-3-hydroxyvalerate)/cellulose nanowhiskers composites, *Polymer (Guildf)*. 51 (2010). doi:10.1016/j.polymer.2010.04.007.
- [29] H.-Y. Yu, Z.-Y. Qin, B. Sun, X.-G. Yang, J.-M. Yao, Reinforcement of transparent poly(3-hydroxybutyrate-co-3-hydroxyvalerate) by incorporation of functionalized carbon nanotubes as a novel bionanocomposite for food packaging, *Compos. Sci. Technol.* 94 (2014). doi:10.1016/j.compscitech.2014.01.018.
- [30] E. Ten, L. Jiang, M.P. Wolcott, Preparation and properties of aligned poly(3-hydroxybutyrate-co-3-hydroxyvalerate)/cellulose nanowhiskers composites, *Carbohydr. Polym.* 92 (2013). doi:10.1016/j.carbpol.2012.09.033.

1.Introducción

- [31] A. Martínez-Abad, L. Cabedo, C.S.S. Oliveira, L. Hilliou, M. Reis, J.M. Lagarón, Characterization of polyhydroxyalkanoate blends incorporating unpurified biosustainably produced poly(3-hydroxybutyrate-co-3-hydroxyvalerate), *J. Appl. Polym. Sci.* 133 (2016). doi:10.1002/app.42633.
- [32] M. Martínez-Sanz, M. Villano, C. Oliveira, M.G.E. Albuquerque, M. Majone, M. Reis, A. Lopez-Rubio, J.M. Lagaron, Characterization of polyhydroxyalkanoates synthesized from microbial mixed cultures and of their nanobiocomposites with bacterial cellulose nanowhiskers, *N. Biotechnol.* 31 (2014). doi:10.1016/j.nbt.2013.06.003.
- [33] L.N. Carli, T.S. Daitx, G.V. Soares, J.S. Crespo, R.S. Mauler, The effects of silane coupling agents on the properties of PHBV/halloysite nanocomposites, *Appl. Clay Sci.* 87 (2014). doi:10.1016/j.clay.2013.11.032.
- [34] M. Martínez-Sanz, M. Villano, C. Oliveira, M.G.E. Albuquerque, M. Majone, M. Reis, A. Lopez-Rubio, J.M. Lagaron, Characterization of polyhydroxyalkanoates synthesized from microbial mixed cultures and of their nanobiocomposites with bacterial cellulose nanowhiskers, *N. Biotechnol.* 31 (2014) 364–376. doi:10.1016/j.nbt.2013.06.003.
- [35] S. Zainuddin, A. Fahim, S. Shoieb, F. Syed, M. V. Hosur, D. Li, C. Hicks, S. Jeelani, Morphological and mechanical behavior of chemically treated jute-PHBV bio-nanocomposites reinforced with silane grafted halloysite nanotubes, *J. Appl. Polym. Sci.* (2016). doi:10.1002/app.43994.
- [36] Ministerio de Economía y Competitividad. Gobierno de España, ES HORIZONTE 2020 <http://eshorizonte2020.cdti.es/index.asp?MP=87&MS=716&MN=2&TR=C&IDR=2002>, (n.d.).

2. Marco teórico

2. Marco teórico

2.1. Polímeros biodegradables

En los últimos años los biopolímeros han atraído más y más interés ya que las políticas de desarrollo sostenible tienden a expandirse debido a la creciente preocupación por el medio ambiente. En consecuencia, los biopolímeros han sido objeto de investigación académica e industrial con el fin de desarrollar nuevos materiales producidos a partir de fuentes alternativas y renovables, con menor consumo de energía, biodegradables y sin generar residuos perjudiciales para el medio ambiente.

El término polímero biodegradable hace referencia a materiales poliméricos en los que al menos una etapa en el proceso de degradación tiene lugar por medio de la acción metabólica de organismos de origen natural [1]. Para que la biodegradación de los materiales plásticos se produzca se requiere de condiciones idóneas de humedad, temperatura y oxígeno. Este proceso se da a través de la fragmentación o la desintegración de los materiales plásticos sin generar residuos tóxicos o perjudiciales para el medio ambiente [2].

En diversos *reviews* de la literatura [1,3,4] se clasifican los biopolímeros en función del origen de las materias primas y sus procesos de fabricación en:

- (i) biopolímeros naturales, es decir, extraídos directamente de la biomasa, tales como el almidón, la celulosa, el quitosano, el alginato, el agar, el carragenato, etc., y las proteínas de origen vegetal como la proteína de soja, la zeína de maíz, el gluten de trigo; o animal como la gelatina, el colágeno, la proteína de suero de leche animal, la seda de araña, etc.;
- (ii) polímeros sintéticos biodegradables obtenidos a través de las rutas clásicas de síntesis química a partir de monómeros derivados del petróleo o de la biomasa, tales como el poli (ácido láctico) (PLA), el poli (ácido glicólico) (PGA), la poli (ϵ -caprolactona) (PCL), el poli (sucinato de butileno) (PBS), el poli (alcohol vinílico) (PVA), etc.;
- (iii) biopolímeros producidos por fermentación microbiana como los poliésteres microbianos, tales como los poli (hidroxialcanoatos) (PHA), incluyendo el poli (β -hidroxibutirato) (PHB),

2. Marco teórico

el poli(3-hidroxibutirato-co-3-hidroxivalerato) (PHBV), etc., y los polisacáridos microbianos, tales como el pululano y el curdlano.

En estos trabajos se destaca que la mayoría de los biopolímeros son costosos en comparación con los termoplásticos convencionales y presentan relativamente pobres propiedades mecánicas y barrera, lo que limitan actualmente su uso industrial. Por lo general, los problemas asociados con los biopolímeros son tres aspectos: el rendimiento, el procesado y el coste [3,5]. Por lo tanto, parece necesario mejorar estos biopolímeros para que sean plenamente competitivos con los termoplásticos comunes.

De entre los biopolímeros, los más investigados y que están atrayendo más interés comercial son algunos poliésteres biodegradables, que pueden ser procesados empleando equipos convencionales de procesado y que ya están siendo utilizados comercialmente en aplicaciones de envases monocapa y multicapa, sobre todo en el envasado de alimentos, así como en el campo biomédico. Estos son el PLA y los PHAs, más concretamente el PHB y su copolímero PHBV [6–8]. La Fig. 2.1 muestra la evolución de trabajos publicados en referencia a estos polímeros, lo que da una idea del creciente interés que la comunidad científica está mostrando por aumentar el conocimiento que se tiene de estos materiales.

Como se muestra en la Fig.2.1.a el PLA ha sido ampliamente estudiado y sigue siendo en la actualidad un biopoliéster de gran interés científico e industrial debido a sus potenciales propiedades y a que se produce comercialmente a unos precios que son competitivos dentro del rango de los plásticos técnicos. El PLA es un poliéster alifático que puede presentar una resistencia y un módulo relativamente alto, similares a los del PET y que muestra una excelente termoconformabilidad en comparación con otros biopolímeros [9], debido a su amplia ventana de procesado, derivada de su estado amorfo en las condiciones de procesado normales. Estas propiedades han resultado en la producción industrial de artículos desechables de PLA, ya que es biodegradable.

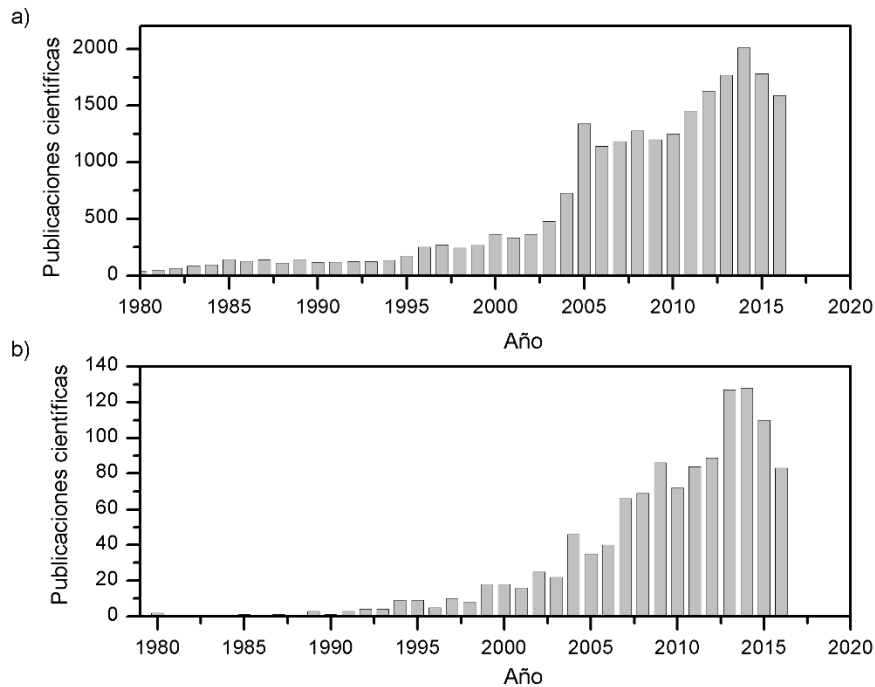


Fig. 2.1: Investigaciones científicas publicadas cada año desde 1980 hasta 2016 acerca de a) PLA y b) PHBV. Fuente de datos Scopus.

Sin embargo, diferentes estudios muestran que el PLA presenta una elevada permeabilidad a los gases [10,11] y una reducida tenacidad [12–14], lo cual limitan su aplicabilidad en el sector del envasado e impiden la sustitución de polímeros no biodegradables tales como el PET. Debido a estas limitaciones técnicas, se encuentran en la bibliografía numerosos intentos de mejora de las propiedades del PLA mediante mezclado con otros polímeros, como PHB [15,16], PHBV [17–20], PCL [21,22], PBAT [23,24], entre otros; e incorporación de materiales orgánicos y/o inorgánicos, tales como sepiolita [25], montmorillonita [26–28], nanotubos de carbono [29], etc.

En cuanto a los PHAs, éstos están siendo también ampliamente investigados en la actualidad para aplicaciones comerciales debido al excelente comportamiento a barrera que poseen en comparación con otros biopolíesteres, tal como el PLA. En concreto, el PHBV posee unas propiedades barrera similares a las del PET [30]. Sin embargo, tal y como ha sido mencionado previamente en el apartado (1.2), su aplicabilidad en la actualidad se ve dificultada por tres

2. Marco teórico

limitaciones técnicas y una limitación económica [31–34]: la baja estabilidad térmica en fundido la baja ductilidad, la dificultad para ser termoconformado y el elevado coste.

Diferentes métodos han sido estudiados con el fin de resolver estas limitaciones técnicas y disminuir su coste total. Se han propuesto varios enfoques tales como la formación de mezclas con polímeros biodegradables, o compuestos con cargas naturales o cargas inorgánicas [35].

A fin de conocer en mayor profundidad el origen, las propiedades y las características de los PHAs, especialmente el PHBV, así como los avances científicos para la adaptación de sus propiedades a su aplicación industrial, a continuación se analiza el estado del arte de estos biopolímeros tan prometedores.

2.2. Poli(hidroxicanoatos) (PHAs): Poli(3-hidroxiбутирато) (PHB) y Poli(3-hidroxiбутирато-co-3-hidroxiуалерато) (PHBV)

Los PHAs son biopolímeros producidos naturalmente por bacterias. Dentro de esta familia, el PHB, homopolímero del 3-hidroxiбутирато, es el miembro más extendido y mejor caracterizado de la familia de los polihidroxicanoatos [34,36–38].

El PHB es producido por microorganismos (tales como *Ralstonia eutrophus* o *Bacillus megaterium*) en respuesta a condiciones de estrés fisiológico y se puede producir ya sea por cultivo puro [39–41] o mediante cultivo mixto de bacterias [42,43].

Este polímero es principalmente un producto de la asimilación de carbono y se emplea por los microorganismos como una forma de almacenamiento de energía de la molécula para ser metabolizados cuando otras fuentes de energía común no están disponibles.

Las fuentes de carbono pueden ser muy diversas, tradicionalmente se usa glucosa y almidón, pero estas fuentes de carbono compiten con la producción de suministro de alimentos. Sin embargo, se están utilizando otras fuentes de carbono no procedentes de recursos alimentarios para una producción sostenible, como son el suero de lácteo [44], la melaza [45], el efluente de moler el aceite de palma [46], las aguas residuales de conservas de tomate [47], los efluentes de moler aceite de oliva [48], entre otros [49]. Recientemente se ha publicado el uso de hidrocarburos derivados de residuos plásticos como la cera de polietileno oxidado para la producción de PHB [50].

El PHB se acumula como inclusiones granulares en el citoplasma de la célula (gránulos intracelulares) de una amplia variedad de organismos Gram-positivos y Gram-negativos bajo condiciones de limitación de nutrientes que no son la fuente de carbono, por ejemplo nitrógeno [34,51]. Típicamente estos gránulos poseen un diámetro de entre 0,2 a 0,5 μm y se pueden visualizar con un microscopio óptico de contraste de fase debido a su alta refractividad [52] (Fig.2.2). El peso molecular del PHB difiere dependiendo del organismo, la fuente de carbono, las condiciones de crecimiento y el método de extracción, y puede variar de 10.000 a 3.000.000 Da [53].

Este polímero es termoplástico y biodegradable en condiciones de compostaje, así como en otros ambientes diversos [54]. En consecuencia, ha generado un gran interés medioambiental y

2. Marco teórico

comercial. El PHB es altamente cristalino, insoluble en agua y relativamente resistente a la degradación hidrolítica. Tiene baja permeabilidad a oxígeno con propiedades mecánicas, limitadas en cuanto que es muy frágil. Sin embargo, presenta un módulo de Young y una resistencia a la tracción comparables o superiores a otros termoplásticos de gran uso, como el PP [55].

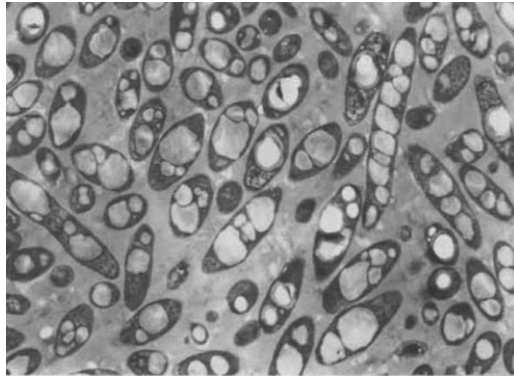


Fig. 2.2: PHB acumulado en el interior de las células como gránulos intracelulares. Imagen reportada por Lee en la revista *Biotechnology and bioengineering* en 1996 [56].

Una estrategia muy utilizada para mejorar las propiedades del PHB es la incorporación de diferentes monómeros secundarios en la cadena del polímero para formar copolímeros, tales como el 3-hidroxivalerato (HV), el 3-hidroxihexanoato (HH), el 3-hidroxipropionato (HP) y el 4-hidroxibutirato (4HV). La formación de estos copolímeros afecta a propiedades tales como la cristalinidad, el punto de fusión, la rigidez y la tenacidad. Entre los copolímeros, el más conocido es el PHBV. Al incorporar el monómero de HV se genera un copolímero al azar cuya estructura química se muestra en la Fig.2.3.

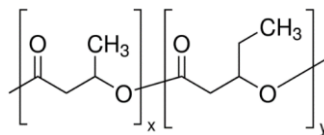


Fig. 2.3: Estructura química del PHBV

El PHBV es un poliéster alifático lineal, que posee propiedades termoplásticas con la ventaja de ser 100% biodegradable, compostable, biocompatible y producido por fuentes renovables no procedentes de recursos alimentarios [57–61]. Otra de las ventajas del PHBV son sus excelentes

propiedades barrera a oxígeno, cercanas a las del PET [30], siendo mucho mejores que las de otros biopolíester tales como el PLA [62]. Además el PHBV presenta un comportamiento mecánico equilibrado en términos de rigidez y resistencia y una elevada temperatura de servicio, semejantes a la del PP [34,63].

Sin embargo, las propiedades del PHBV dependen del contenido en valerato. La incorporación del monómero HV en el copolímero reduce el nivel de cristalinidad y el punto de fusión, resultando en una disminución de la rigidez pero el incremento de la tenacidad, el aumento de la elongación a rotura y la resistencia al impacto [64,65]. El PHBV con contenido inferior al 40% molar en HV cristaliza en la misma forma cristalina del PHB, sin embargo, para contenidos superiores lo hace en la estructura cristalina del PHV [66]. Aunque la disminución del nivel de cristalinidad del PHBV mejora su comportamiento mecánico por incremento de la flexibilidad, altos contenidos en HV conducen a la disminución de las propiedades barrera [67]. Por lo tanto, los grados de PHBV con bajo contenido en HV son todavía los más adecuados para aplicaciones de envasado con efecto barrera.

Concretamente en el campo del envasado, el PHBV presenta gran interés debido a que es inerte y estable químicamente, lo que lo hace adecuado para aplicaciones como películas de materiales en contacto con cualquier tipo de alimento [68].

Sin embargo, el PHBV aún presenta una serie de propiedades e inconvenientes de procesado que limitan su uso. Cuando se compara con otros polímeros lineales, el PHBV posee un rango de temperaturas en su ventana de procesado muy estrecha; es excesivamente frágil, tiene una baja resistencia térmica durante el procesado y en la actualidad sigue siendo una alternativa más cara que otros materiales utilizados comúnmente en el sector del envasado [1,30].

El estrecho rango de temperaturas durante el procesado del PHBV es debido a la elevada cristalinidad, que en algunos casos es del 60% [69] y que es la responsable de las excelentes propiedades barrera. Esta elevada cristalinidad resulta en un inconveniente en el termoconformado de bandejas o blísteres, ya que la viscosidad de fundido cae muy rápidamente al aumentar la temperatura pocos grados por encima de la fusión de la fase cristalina.

2. Marco teórico

2.3. Limitaciones del PHBV asociadas al uso para envasado

Como ha sido expuesto anteriormente, el PHBV presenta unas excelentes propiedades barrera, un comportamiento mecánico equilibrado en términos de rigidez y resistencia y una elevada temperatura de servicio. Sin embargo, muestra algunos inconvenientes en comparación con los polímeros convencionales, tales como alta fragilidad, pobre estabilidad térmica a temperaturas próximas al punto de fusión y un rango de temperaturas en su ventana de procesado muy estrecha, lo que limita su aplicabilidad.

A continuación, se exponen con detalle las principales limitaciones del PHBV; en el siguiente apartado (2.4), se tratarán las posibles formas de actuación y modificación del PHBV, para mejorar su aplicabilidad en el sector del envasado.

2.3.1. Estabilidad térmica durante el procesado

Una de las principales limitaciones del PHBV es la inestabilidad térmica durante el procesado. El principal mecanismo de degradación térmica del PHB y el PHBV es una reacción de escisión aleatoria de cadenas no radicalaria por el mecanismo de *cis*-eliminación. El esquema de este mecanismo se muestra en la Fig. 2.4 [34,70–73]. Como consecuencia de este proceso de degradación por escisión de cadenas se produce una drástica reducción del peso molecular del polímero durante el procesado [74]. Así mismo, mediante este mecanismo de degradación se genera ácido *trans*-crotónico y oligómeros del PHB [75].

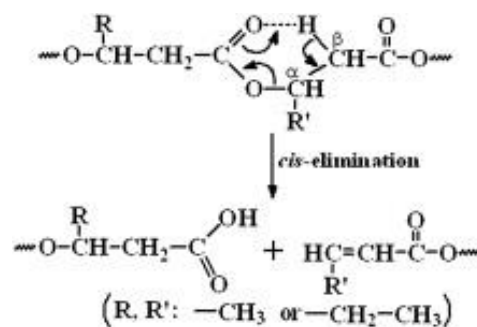


Fig. 2.4: El mecanismo general de degradación del PHBV [31].

El mecanismo de degradación del PHB y PHBV por cis-eliminación es debido a la presencia de ésteres con un enlace C-H activado. De acuerdo con el estudio reportado por Abe [76] para que tenga lugar el mecanismo de cis-eliminación en el enlace éster se requiere de la presencia de un enlace β -C-H con el oxígeno del éster para formar un estado de transición con un éster de anillo de seis miembros (tal y como se muestra en la Fig. 2.4). La molécula de PHB (y la de PHBV) contiene un grupo carbonilo en un átomo de carbono vecino al grupo β -metileno, de modo que el enlace β -C-H del grupo metileno puede ser activado por el grupo carbonilo vecino. Esta disposición resulta en la degradación térmica del PHB y PHBV a temperaturas reducidas a través de la reacción de cis-eliminación, en comparación con otros poliésteres, como el PLA o el poli(ácido 4-hidroxi-butírico) [76].

Por consiguiente, durante el procesado del PHBV los enlaces éster de la cadena del polímero se degradan de manera aleatoria dando lugar a la disminución de la masa molecular de las cadenas resultantes afectando a las propiedades finales del material.

2.3.2. Propiedades mecánicas

La aplicabilidad del PHBV se ha visto comprometida por las inferiores propiedades mecánicas, tales como fragilidad, baja resistencia al impacto y reducida elongación a la rotura, en comparación con los polímeros convencionales. Existen distintos estudios que atribuyen la fragilidad del PHBV a varios factores relacionados con la cristalinidad del PHBV.

Por un lado, la baja densidad de nucleación, conjuntamente con el alto grado de cristalinidad y la lenta velocidad de cristalización conducen a la formación de grandes esferulitas [77,78]. En el interior de estas grandes esferulitas se pueden formar fisuras circulares y radiales debido a la diferencia entre el coeficiente de expansión térmica radial y circunferencial [79]. Estas fisuras pueden actuar como puntos de concentración de tensiones y promover la fragilidad del PHBV [80–82].

El segundo factor es el proceso de envejecimiento del PHBV durante el almacenamiento a temperatura ambiente. Este fenómeno no está claramente elucidado, pero se supone que las cadenas amorfas interlamelares son progresivamente restringidas de movimiento, lo que resulta en un aumento de la fracción amorfa rígida [83,84]. Se proponen dos explicaciones para esclarecer

2. Marco teórico

este fenómeno: la cristalización secundaria de la fase amorfa [77,78] y el envejecimiento físico de la fase amorfa [85–87].

Por último, se debe tener en cuenta que la temperatura de transición vítrea (T_g) del PHBV es cercana a la temperatura ambiente.

Por estas razones, para mejorar la tenacidad del PHBV las modificaciones en la composición del PHBV reportadas se centran principalmente en la reducción y el control del proceso de cristalización y no en aumentar la movilidad de la fracción amorfa. En la bibliografía existente estos objetivos se han abarcado mediante cuatro métodos.

Uno de los métodos es la incorporación de agentes de nucleación, mediante los cuales se incrementa la densidad de nucleación, el tamaño de las esferulitas se reduce y se aumenta la velocidad de cristalización [93–98]. Este método ya está siendo implementado en los grados comerciales de los PHAs. Por ejemplo, el PHBV de grado comercial utilizado en este trabajo de investigación (ENMAT Y1000P de Tianan Biologic Material Co.) posee alrededor de un 1% en peso de nitruro de boro como agente nucleante.

El segundo de los métodos reportados hace referencia a la realización de un enfriamiento rápido durante el procesado del material, reduciendo de este modo el grado de cristalinidad y el tamaño de las esferulitas [99]. Sin embargo, este método no es deseable, ya que la cristalización secundaria y el envejecimiento físico de la fase amorfa tiene lugar durante el almacenamiento a la temperatura ambiente.

El tercer de los métodos es la realización de un tratamiento de recocido tras el envejecimiento de los materiales basados en PHBV [88,90,100,101]. Con este método se pretende rejuvenecer el material, sin embargo, se produce un efecto temporal [88]. Recientemente, Crétois et al. [90] han demostrado la reversibilidad del envejecimiento físico y la irreversibilidad de la segunda cristalización tras el recocido. Aunque la realización del tratamiento de recocido reduce la fragilización del PHBV, no previene el posterior envejecimiento físico. Por lo que no permite mantener la ductilidad del PHBV rejuvenecido con el tiempo.

El cuarto método reportado para la mejora de la tenacidad del PHBV es el mezclado con otros polímeros. La plastificación es una de las estrategias más ampliamente utilizada para la mejora de

la tenacidad en polímeros. Recientemente Jost et al. [102] ha estudiado la idoneidad del uso de plastificantes en matrices de PHBV procesadas mediante técnicas de procesamiento industriales. Se demuestra que las propiedades mecánicas de las películas fabricadas por mezclado en fundido y posterior extrusión conducen a películas relativamente inelásticas con una baja elongación a la rotura, limitando la aplicación de estos materiales para el procesamiento industrial. Dado este contexto, se han reportado un amplio número de investigaciones centradas en el mezclado del PHBV con otros polímeros [17,20,23,24,103–110]. Desafortunadamente, la mayoría de las mezclas de PHBV no son exitosas como consecuencia de la inmiscibilidad del PHBV con la mayoría de los polímeros. Por lo que para lograr mezclas exitosas es necesario recurrir al uso de agentes compatibilizantes. No obstante, como se tratará más adelante en el presente trabajo, esta estrategia se plantea como la más viable a corto plazo y algunos de los resultados obtenidos en esta tesis indican que es adecuada.

Por otro lado, se debe tener en cuenta que las excelentes propiedades barrera del PHBV son debidas al elevado grado de cristalinidad del PHBV. Por consiguiente, aquellas modificaciones que se realicen sobre la composición del PHBV que resulten en la reducción de la cristalinidad conllevan la caída de las propiedades barrera del PHBV.

2.3.3. Ventana de procesamiento por termoconformado

La procesabilidad por termoconformado de los materiales poliméricos está fuertemente influenciada por el grado de cristalinidad de los mismos. El elevado grado de cristalinidad que posee el PHBV resulta en una ventana de procesamiento estrecha cuando se compara con otros biopolímeros [64,109,111–114].

La elevada cristalinidad del PHBV, su baja temperatura de transición vítrea, así como la inestabilidad térmica del PHBV a temperaturas próximas a su temperatura de fusión, (c.f. punto 2.2.1.), condicionan la reología del PHBV y, por consiguiente, su procesabilidad.

Para temperaturas inferiores a la temperatura de fusión del PHBV la movilidad de las cadenas en las regiones amorfas es muy limitada como consecuencia de que las regiones cristalinas (alrededor de un 60% de cristalinidad) siguen en estado sólido, lo que se traduce en una elevada viscosidad y rigidez del material hasta temperaturas próximas a la fusión (ver Fig. 2.5.b). Por consiguiente, el

2. Marco teórico

procesado del PHBV, como material altamente cristalino, debe realizarse a temperaturas próximas a su punto de fusión.

Por otro lado, cuando se alcanza el punto de fusión de los cristales la estructura colapsa y todas las cadenas adquieren movilidad, disminuyendo drásticamente la viscosidad del material. Esto hace que el material pierda completamente la consistencia y la estabilidad de la lámina no sea la suficiente como para poderse conducir a un conformado adecuado.

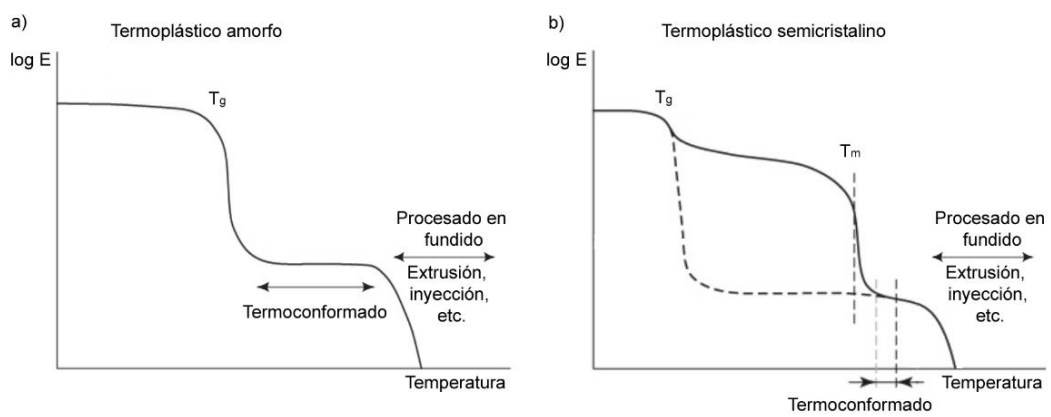


Fig. 2.5: Rango de temperaturas en el que diferentes técnicas de procesamiento pueden ser aplicadas en función de la cristalinidad del polímero. Adaptación de [115]

Por otro lado, para procesos en los cuales el polímero se encuentre en estado completamente fundido, se debe tener en cuenta que el rango de temperaturas de procesamiento efectivo del PHBV se encuentra restringido por el proceso de degradación térmica, lo que también limita su procesamiento en estas condiciones.

2.4. Metodologías de actuación para la mejora de las propiedades del PHBV para envasado

Con el fin de mejorar la aplicabilidad del PHBV en el sector del envasado, en el presente trabajo se han abordado una serie de metodologías de actuación para la modificación de las propiedades del PHBV.

Las metodologías de actuación aplicadas han sido el uso de extensores de cadena, la adición de nanoarcillas y el mezclado con otros polímeros. A continuación, se exponen con detalle cada una de éstas.

2.4.1. Extensores de cadena

La tecnología de mezclado y extrusión reactiva puede ser utilizada para la mejora de la resistencia térmica de los biopoliésteres durante el procesado. Ha sido reportado el uso de extensores de cadena en biopoliésteres para evitar la caída de peso molecular debido a la degradación térmica producida durante el procesado en fundido [116–125]. Este efecto está sustentado en la reacción entre los grupos carboxílicos e hidroxilos finales de los poliésteres y los grupos funcionales del extensor de cadena. Los grupos carboxílicos e hidroxilos de los poliésteres son reactivos con muchos grupos funcionales, tales como los grupos hidroxilo, amino, anhídrido, epoxi, ácido carboxílico o isocianato [126].

Este enfoque ha sido aplicado con éxito sobre el PHBV utilizando peróxido de dicumilo (DCP) [127,128] y Joncryl® ADR-4368 [32].

En el presente trabajo se ha planteado el uso del tris(nonilfenil)fosfito (TNPP) y el estudio de su influencia sobre la morfología y las propiedades mecánicas y térmicas del PHBV. Este extensor de cadena ha sido utilizado con éxito en otras matrices, tales como el PLA, resultando en la estabilización térmica de los polímeros con bajos contenidos de extensor [122–124], pero nunca se ha estudiado su efecto en el PHBV. (Capítulo 1).

Najafi et al. [117] reporta el mecanismo de acción del TNPP en la estabilización térmica del PLA a partir de los mecanismos de reacción propuestos por Cicero et al. [123]. Este mecanismo se muestra en la Figura 2.6. De acuerdo con el mecanismo mostrado, los grupos fosfato de TNPP

2. Marco teórico

reaccionan con los grupos terminales hidroxilo de las cadenas PLA para producir una cadena con un grupo terminal fosfito (Reacción I en la Figura 2.6). La cadena fosfatada de PLA se somete a continuación a transesterificación con una cadena de PLA con un grupo terminal carboxilo (Reacción II), dando como resultado la producción de una cadena de PLA más larga y fosfito de bis (nonilfenilo). Los dos grupos activos restantes del fosfito pueden entonces proceder a reaccionar con otro grupo hidroxilo terminal. Si todos los grupos activos en TNPP reaccionan de esta manera, se espera que el producto final esté libre de grupos aromáticos y fosfato.

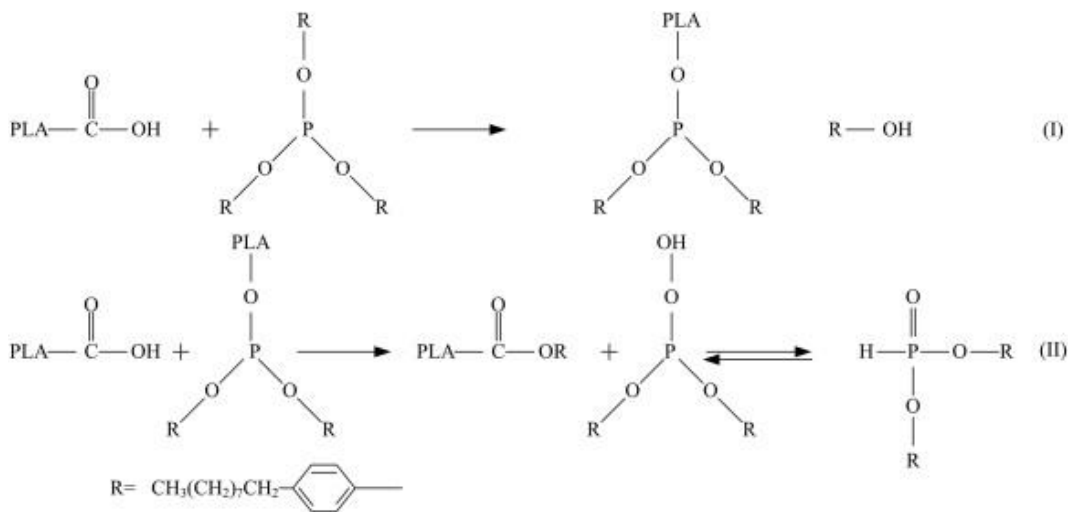


Fig. 2.6: Reacciones potenciales en el sistema PLA-TNPP. (I) Reacción entre grupos hidroxilo terminales del PLA con el TNPP y (II) transesterificación entre un grupo terminal PLA fosfatado y un grupo terminal ácido carboxílico del PLA. [117]

Este mismo mecanismo se cree que puede tener lugar en el caso del PHBV, reaccionando los grupos fosfato de TNPP con los grupos terminales hidroxilo de las cadenas del PHBV generados tras la escisión aleatoria de cadenas no radicalaria por el mecanismo de cis-eliminación del PHBV. Se produciría la formación de cadenas de PHBV más largas evitando la caída de peso molecular durante el procesado en fundido.

2.4.2. Nanocompuestos poliméricos

En los últimos años, los nanocompuestos poliméricos han generado gran interés a nivel científico e industrial debido a las interesantes propiedades resultantes de los mismos. En el caso de los polímeros biodegradables, los nanocompuestos pueden mejorar el comportamiento en los aspectos donde los polímeros derivados del petróleo aún son superiores [129–131]. Ha sido ampliamente reportada la mejora de las propiedades mecánicas, la estabilidad térmica y las propiedades barrera a gases, aromas y vapor de agua de matrices de biopolímeros por la adición de pequeñas fracciones volumétricas de nanopartículas, tales como, nanotubos de carbono [132–134], bentonitas [20,135], nanotubos de haloisita [136–139], montmorillonitas [136,139–143], agujas de sepiolita [144–148], vermiculita [149] y nanocelulosa [150–153], entre otros.

Algunas de estas nanopartículas requieren de la modificación de los grupos funcionales superficiales para lograr un adecuado grado de dispersión en la matriz polimérica. Las arcillas montmorillonitas, las más comúnmente utilizadas en los nanocompuestos poliméricos, requieren de modificación superficial, organomodificación, para alcanzar un buen grado de exfoliación durante el mezclado con el polímero, resultando en la mejora de la afinidad con el polímero y dispersión homogénea en la matriz [139,154,155]. Sin embargo, la estabilidad térmica de los nanocompuestos con arcillas organomodificadas puede verse perjudicada debido a la degradación del organomodificador de las arcillas durante el mezclado en fundido [139,154,155].

El efecto de refuerzo mecánico constatado en biopolímeros por la adición de reducidas cantidades de nanomateriales es debido a la buena dispersión de los nanomateriales en la matriz polimérica y su elevada área superficial, condicionada por la relación de aspecto [139,156–158]. Por ello, la eficiencia del refuerzo mecánico es generalmente mayor en nanocompuestos que la obtenida con los compuestos convencional micro y macro para la misma cantidad de materiales de carga [159].

En cuanto a la reducción de la permeabilidad a gases, vapores y aromas de los nanocompuestos con respecto a las matrices poliméricas es debido al aumento en la longitud de las trayectorias de difusión, mediante el incremento de la tortuosidad inducida por la presencia de los nanomateriales impermeables [1,3,10,143,160]. Por consiguiente, el efecto resultante de la adición de

2. Marco teórico

nanorellenos depende de la relación de aspecto de estos materiales, el contenido, su morfología, la orientación en la matriz polimérica, el grado de dispersión, etc. [143,161,162].

Los estudios realizados sobre nanocompuestos PHBV/arcilla atribuyen el efecto de estabilización térmica al hecho de que las arcillas, junto con los productos de degradación sólido del PHBV, generan un recubrimiento denso que impide el desarrollo de una degradación adicional al oponer una fuerte resistencia al transporte másico de los agentes volátiles implicados en la reacción, dando como resultado una disminución de la cinética de degradación [112,163].

Por otro lado, la introducción de partículas nanométricas con una elevada relación de aspecto a materiales poliméricos conduce generalmente a un incremento de la viscosidad en fundido [164]. Este hecho puede ser deseable para el sistema objeto de este trabajo, como se verá más adelante; de manera que las nanoarcillas pueden emplearse como agentes de procesado.

2.4.3. Mezclas de polímeros

La mezcla física de polímeros en fundido es una estrategia conveniente de modificación de las propiedades de los biopolímeros para obtener propiedades similares a las de los termoplásticos tradicionales haciendo uso de los equipamientos de procesado de polímeros convencionalmente utilizados en la industria del envasado. Las propiedades de la mezcla resultante pueden ser ajustadas a través de la correcta elección de las fases poliméricas, así como de la composición de la mezcla.

Como ha sido expuesto anteriormente al abordar las limitaciones mecánicas del PHBV, una de las opciones reportadas para mejorar la flexibilidad y aumentar el alargamiento a rotura del PHBV es el mezclado con otros polímeros. Tradicionalmente para mejorar la tenacidad de los polímeros se han utilizado plastificantes. Sin embargo, un reciente estudio reportado por Jost et al. acerca de la idoneidad del uso de plastificantes en matrices de PHBV muestra la falta de eficacia de los plastificantes para aumentar el alargamiento a rotura del PHBV [102]. Incluso, en este estudio, se cuestiona la utilización de plastificantes en PHBV en aplicaciones de envasado a gran escala en un futuro próximo dados los resultados del estudio. En este contexto, la adición de una segunda fase elastomérica o un polímero amorfo se plantea como alternativa para mejorar la elasticidad del

PHBV [165]. Sin embargo, en muchos casos la adición de una segunda fase resulta en la caída de las propiedades barrera del PHBV y la pérdida de la deseada biodegradabilidad [166–168].

En cuanto a la procesabilidad del PHBV por termoconformado, ha sido reportado que la mezcla de polímeros altamente cristalino con polímeros amorfos puede conducir al aumento de la ventana de procesado y la estabilidad de la lámina para aplicaciones de termoconformado [169,170].

Desafortunadamente es difícil obtener mezclas de PHBV de alto rendimiento por simple mezclado, en la mayoría de los casos no se obtienen mezclas exitosas como consecuencia de la inmiscibilidad del PHBV con la mayoría de los polímeros. Este es el caso concreto de las mezclas PHBV/PLA.

El rendimiento de las mezclas PHBV/PLA puede verse comprometido por la baja adhesión interfacial entre los componentes debido a la naturaleza inmiscible del PHBV y el PLA [19,171,172], lo que resulta en la formación de una morfología de fase dispersa. Debido a la baja viscosidad en fundido de las mezclas PHBV/PLA, el mezclado en fundido a alta cizalla de estas mezclas no logra una buena dispersión de la fase dispersa, dada la competencia entre las fuerzas de cizallamiento (mecanismo de ruptura) y las fuerzas de tensión interfacial (mecanismo de coalescencia) [173,174]. Por lo que para lograr mezclas con propiedades excelentes es necesario recurrir al uso de aditivos (bien sean agentes compatibilizantes que mejoren la interacción entre ambos biopolíesteres o aditivos destinados a aumentar la eficiencia del mezclado mediante el aumento de la viscosidad en fundido).

2.4.4. Compatibilización de mezclas poliméricas

El uso de agentes compatibilizantes es una técnica para mejorar la interacción y las propiedades de las mezclas de polímeros inmiscibles. Las funciones más importantes de la compatibilización son la reducción del tamaño de la fase dispersa a través de la reducción de la tensión interfacial y la prevención de la coalescencia de la fase dispersa, para estabilizar la morfología de fase fina formada [159,165].

Existen varias estrategias de compatibilización, como son la adición de copolímeros, la adición de polímeros reactivos, la adición de productos químicos de bajo peso molecular o la adición de nanopartículas [159].

2. Marco teórico

La adición de copolímeros es la manera convencional y más eficiente de compatibilizar las mezclas de polímeros. Sin embargo, existe limitación en la disponibilidad comercial de los copolímeros específicos, que deben ser sintetizados antes del mezclado, lo que supone un coste adicional elevado para la aplicación industrial de esta estrategia.

La compatibilización por adición de sustancias reactivas implica reacción química entre el PHBV y los compatibilizantes de la mezcla. Las sustancias reactivas de bajo peso molecular pueden contener más de un grupo funcional, lo que resulta en una alta y rápida reactividad durante el mezclado en fundido. Estos aditivos son, por ejemplo, diisocianatos, oxazolinas y anhídridos, los cuales poseen una alta reactividad con los grupos hidroxilos y carboxilos terminales del PHBV. Esta estrategia es mucho más favorable para su aplicación industrial debido a la disponibilidad de diversas sustancias reactivas y la alta eficiencia de compatibilización de esta técnica.

En cuanto a la introducción de nanopartículas para modificar las propiedades interfaciales y la morfología de las fases no sólo permite la mejora de la compatibilidad entre los componentes de la mezcla, sino que puede incluso aportar nuevas funcionalidades a los nanocompuestos resultantes, como son la mejora de las propiedades mecánicas, el incremento del comportamiento a barrera, etc., es decir, las ventajas adicionales de los nanocompuestos poliméricos.

Por lo tanto, de entre las estrategias de compatibilización expuestas, las más convenientes para su aplicación sobre las mezclas de PHBV/PLA en la industria del envasado son el uso de reactivos químicos de bajo peso molecular y la adición de nanopartículas.

2.5. Degradabilidad en compostaje

Es de gran importancia social y medioambiental el estudio de la degradación de los materiales utilizados en envases al finalizar la vida útil de estos. Como ha sido comentado en la introducción, los polímeros de mayor uso en el sector del envase, los plásticos convencionales, presentan grandes tiempos de degradación (entre 100 y 300 años), produciéndose grandes problemas ambientales por acumulación de deshechos en las aguas marinas y en los vertederos [175]. Las alternativas a la acumulación de los deshechos plásticos derivados de polímeros no biodegradables son la incineración o el reciclaje. Sin embargo, debido a las consecuencias medioambientales derivadas de la mala gestión de los residuos plásticos a nivel global y la contaminación producida

por los vertidos o incineración incontrolada de los mismos, el reciclaje y la valorización energética están perdiendo interés últimamente en favor de los polímeros biodegradables y su comportamiento en condiciones de compostaje.

Es importante remarcar que todos los plásticos compostables son biodegradables, pero no todos los plásticos biodegradables son compostables. De acuerdo con la IUPAC, un polímero biodegradable es aquél susceptible de sufrir degradación por la acción enzimática resultado de la acción de células [176]. Por otro lado, de acuerdo con la ISO 17088 [177], un plástico compostable es aquel que sufre degradación por procesos biológicos durante el compostaje para producir dióxido de carbono, agua, compuestos inorgánicos y biomasa a una velocidad consistente con otros materiales compostables conocidos y no deja residuos visibles o tóxicos. Por lo tanto, la evaluación de la compostabilidad incluye tres fases: desintegración, biodegradación y ecotoxicidad.

La desintegración es el proceso de fragmentación física en fragmentos de reducido tamaño. Se considera que un producto plástico es desintegrable cuando después de un periodo de tiempo, que es función de la norma, bajo el ensayo controlado de compostaje no queda más del 10% de su masa seca original después de tamizar a través de un tamiz de 2,0 mm. El ensayo se puede llevar a cabo de acuerdo a las normas ISO 16929, ISO 20200, ISO 14855-1 o ASTM D 5338 en condiciones de compostaje térmico, sin el equipo de captura de CO₂.

El ensayo de biodegradación puede realizarse de acuerdo a las normas ISO 14855-1, ISO 14855-2 o ASTM D 5338. Se considera que un producto plástico es biodegradable cuando alcanza la relación de conversión a dióxido de carbono del 90% del carbono orgánico, con respecto a un material de referencia de control positivo en un periodo máximo de 180 días.

En cuanto a la toxicidad del compost se evalúa mediante el contenido en metales y otras sustancias tóxicas, el contenido en sólidos volátiles y la capacidad de germinación de semillas en el compost resultante de acuerdo con la norma EN 13432.

En la bibliografía existente la desintegración en condiciones de compostaje del PLA y los PHAs es la metodología de ensayo más ampliamente utilizada para estudiar el comportamiento de estos materiales en condiciones de compostaje, siendo la norma ISO 20200 la más utilizada en la bibliografía para el estudio del PLA y los PHAs a escala de laboratorio [15,16,178–188]. Sin embargo,

2. Marco teórico

en los últimos años Sikorska, Rydz y Musiol están llevando a cabo una intensa investigación del comportamiento en compostaje de PLA y PHAs en condiciones industriales de compostaje en Zabrze, Polonia [6,189–191]. En estas investigaciones se constata que el proceso de biodegradación en condiciones industriales de compostaje del PLA y los PHAs se produce por los mismos mecanismos que en las condiciones de laboratorio.

La degradación en compostaje se produce inicialmente en la región amorfa y, por lo tanto, la velocidad de degradación se encuentra marcadamente influenciada por el grado de cristalinidad del polímero [189,192,193]. Por consiguiente, debido a las diferencias de cristalinidad de los polímeros el proceso de degradación en compostaje es distinto.

El proceso de degradación del PLA en condiciones de compostaje se produce en dos etapas secuenciales. La primera etapa implica una hidrólisis química simple (que ocurre a través de la escisión de cadena aleatoria) conduciendo a la reducción del peso molecular y la formación de ácido láctico y/o oligómeros de ácido láctico. La hidrólisis abiótica parece ser un paso crucial durante un proceso de compostaje convencional. En la segunda etapa se produce la asimilación microbiana de los oligómeros de ácido láctico de bajo peso molecular convirtiéndose en biomasa, agua y dióxido de carbono, que se emite a la atmósfera [189,191,193,194].

Sin embargo, los PHAs son directamente biodegradados por muchos microorganismos presentes en el medio ambiente [195,196]. En condiciones de compostaje controlado los PHAs pueden ser consumidos por los microorganismos como fuente de energía. Las enzimas secretadas por los microorganismos descomponen los polímeros en monómeros. Los monómeros son entonces utilizados por la célula como fuente de carbono para el crecimiento de la biomasa. Los productos finales de la degradación en ambientes anaeróbicos son dióxido de carbono y agua [197]. Los microorganismos producen, en primer lugar, la degradación de las cadenas de PHA en estado amorfo sobre la superficie del material y erosionan, a continuación, las cadenas de PHA en estado cristalino [192].

El compost resultante de la degradación de los envases biodegradables puede usarse para diferentes propósitos, como por ejemplo, como fertilizante en la agricultura y la horticultura, como sustrato de crecimiento vegetal y para el re-cultivo de la tierra [198].

2.6. Métodos de procesado y conformado

Los métodos más ampliamente utilizados para el procesado y conformado de materiales poliméricos son: el soplado, la inyección, la extrusión, el mezclado en fundido, el moldeo rotacional, el termoconformado, la espumación, la compresión, el *casting* y el moldeo por transferencia de resina. Sin embargo, en los últimos años se han desarrollado nuevas metodologías de procesado de polímeros, como son el *electrospinning* o la impresión 3D.

Para el desarrollo de las composiciones de estudio de este trabajo y la obtención de las láminas o probetas para caracterizar estas composiciones se han empleado varias técnicas de procesado. Éstas son: mezclado en fundido y compresión, extrusión e inyección. El PHBV ha mostrado ser un biopolíéster capaz de ser transformado en equipos convencionales y en condiciones habituales a los polímeros de amplio uso en el sector del envasado. No obstante, el PHBV presenta una gran limitación en su procesado por termoconformado, que es uno de los procesos más comunes en la industria del envasado. Por ello, con el fin de mejorar la aplicabilidad de los biopolímeros en el sector del envasado, se ha llevado a cabo el desarrollo de varias composiciones buscando mejorar la termoconformabilidad del PHBV. En la siguiente sección se explica brevemente esta técnica de conformado muy ampliamente empleada para la obtención de envases.

2.6.1. Termoconformado

El moldeo por termoconformado, es un proceso muy ampliamente extendido para el conformado de formas muy diversas, como por ejemplo carcasas de equipos, bandejas para el transporte y almacenamiento de objetos o alimentos, paneles de vehículos, como por ejemplo salpicaderos de coches, contenedores para diversos fines, etc. Se trata de una de las tecnologías de conformado de láminas más utilizada en envasado debido al coste relativamente bajo de las máquinas de termoconformado, el reducido coste de los moldes, la sencillez y la alta velocidad de producción de grandes superficies, de amplia variedad de formas y de partes con secciones delgadas. Además, una de las grandes ventajas del proceso de moldeo por termoconformado es que puede ser utilizado cuando se desea modelar una lámina compuesta por múltiples capas. Los competidores directos de esta técnica son el moldeo por soplado y el moldeo por inyección [199].

2. Marco teórico

El proceso de termoconformado consiste en aplicar temperatura y presión o vacío sobre una preforma, normalmente una lámina, para que ésta tome la forma de un molde. La lámina es sujeta por un bastidor y se calienta hasta que reblandece, normalmente mediante radiación infrarroja. Posteriormente, la lámina caliente y tensa es sometida a condiciones de vacío o presión con el fin de que alcance la forma de un molde frío (Fig. 2.7) [200]. La aplicación de vacío genera unas condiciones más severas de termoconformado. En contacto con el molde, el calor se pierde y el material recupera la rigidez a medida que se enfría. Existen dos tipos de molde: molde macho o positivo y molde hembra o negativo, como el esquematizado en la Fig. 2.7.

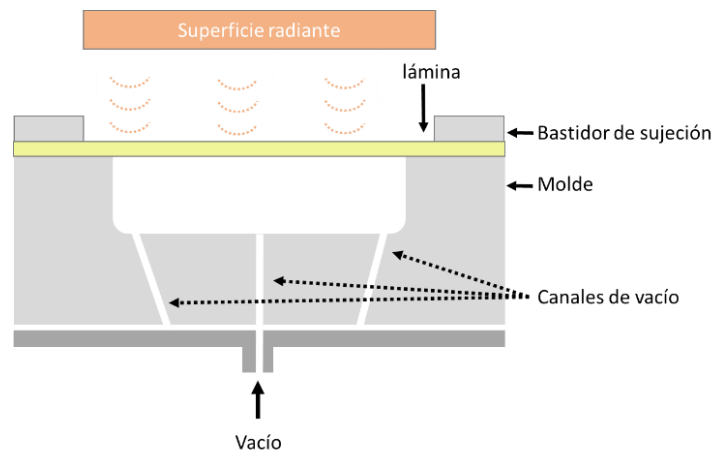


Fig. 2.7: Esquema de un sistema de termoconformado asistido a vacío. Reproducción del sistema de termoconformado utilizado en esta investigación.

De acuerdo con el procedimiento expuesto, para llevar a cabo el proceso de termoconformado los polímeros deben poseer un rango de temperaturas en el que el polímero sea lo suficientemente deformable y resistente para obtener la forma deseada (ventana de termoconformado). Por ello, los materiales comúnmente utilizados en termoconformado son materiales termoplásticos, especialmente amorfos, como PS, ABS, PVC, PLA, etc. En los polímeros amorfos la ventana de termoconformado se extiende desde unos grados por encima de la temperatura de transición vítrea hasta aproximadamente donde estaría su temperatura de fusión en caso de presentar cristalinidad. Sin embargo, en los polímeros altamente cristalinos, por lo general, la ventana de termoconformado es muy estrecha, localizándose unos grados por debajo de la temperatura de fusión (ver Fig. 2.5). La amplitud del rango de temperaturas de la región plástica determina la facilidad del conformado por termoconformado [115].

Además, se debe tener en cuenta que uno de los inconvenientes que presenta esta técnica es la baja uniformidad de espesor de pared. Durante el proceso de termoconformado la lámina es tensionada de manera no uniforme, es decir, sólo la parte de la lámina que no se encuentra en contacto con el molde es estirada. Por consiguiente, para obtener un espesor mínimo de pared en las zonas más tensionadas, en otras el espesor es mucho mayor del requerido. Si el material en las condiciones de termoconformado tiene una buena respuesta elástica, se deformará rápidamente cuando se aplica el vacío, alcanzando una mayor uniformidad de espesores en la pieza final [200]. Este inconveniente de procesado se ve incrementado en el caso del PHBV, debido al reducido comportamiento elástico de este material en el rango de temperaturas de moldeo por termoconformado.

Como ha sido expuesto anteriormente en el punto 2.3.3, la estrecha ventana de procesado del PHBV, debido a su alta cristalinidad, restringe el rango de temperaturas de moldeo por termoconformado de este biopolímero a temperaturas cercanas a su punto de fusión. El PHBV es muy rígido hasta su punto de fusión y muy fluido después. Esto conduce a un fenómeno de flacidez derivada de la pérdida de la estabilidad mecánica de la lámina antes del proceso de estirado, lo que resulta en una pobre termoconformabilidad en comparación con los polímeros convencionales u otros biopoliésteres como el PLA.

Adicionalmente a toda la problemática asociada al termoconformado del PHBV, existe muy poca literatura científica donde se trate de manera específica este proceso, y no hay, hasta donde sabemos, ninguna metodología para evaluar de manera rigurosa los resultados obtenidos de un proceso de termoconformado. Por este motivo, en el presente trabajo de tesis se va a definir una metodología para evaluar de manera muy sencilla (mediante inspección visual) la termoconformabilidad de un material y analizar su ventana de termoconformado.

Referencias

- [1] J.W. Rhim, H.M. Park, C.S. Ha, Bio-nanocomposites for food packaging applications, *Prog. Polym. Sci.* 38 (2013) 1629–1652. doi:10.1016/j.progpolymsci.2013.05.008.
- [2] R. Chandra, R. Rustgi, Biodegradable polymers, *Prog. Polym. Sci.* 23 (1998) 1273–1335. doi:10.1016/S0079-6700(97)00039-7.
- [3] P. Bordes, E. Pollet, L. Averous, Nano-biocomposites: Biodegradable polyester/nanoclay systems, *Prog. Polym. Sci.* 34 (2009) 125–155. doi:10.1016/j.progpolymsci.2008.10.002.
- [4] A. Sorrentino, G. Gorrasi, V. Vittoria, Potential perspectives of bio-nanocomposites for food packaging applications, *Trends Food Sci. Technol.* 18 (2007) 84–95. doi:10.1016/j.tifs.2006.09.004.
- [5] S. Pilla, *Handbook of Bioplastics and Biocomposites Engineering Applications*, Firts, Jonh Wiley & Sons, INC, Salem, Massachusetts, 2011. doi:10.1002/9781118203699.
- [6] M. Musioł, W. Sikorska, G. Adamus, H. Janeczek, M. Kowalczyk, J. Rydz, (Bio)degradable polymers as a potential material for food packaging: studies on the (bio)degradation process of PLA/(R,S)-PHB rigid foils under industrial composting conditions, *Eur. Food Res. Technol.* (2015) 1–9. doi:10.1007/s00217-015-2611-y.
- [7] T. Keshavarz, I. Roy, Polyhydroxyalkanoates: bioplastics with a green agenda., *Curr. Opin. Microbiol.* 13 (2010) 321–6. doi:10.1016/j.mib.2010.02.006.
- [8] M. Jamshidian, E.A. Tehrani, M. Imran, M. Jacquot, S. Desobry, Poly-Lactic Acid: Production, applications, nanocomposites, and release studies, *Compr. Rev. Food Sci. Food Saf.* 9 (2010) 552–571. doi:10.1111/j.1541-4337.2010.00126.x.
- [9] R.M. Rasal, A. V. Janorkar, D.E. Hirt, Poly(lactic acid) modifications, *Prog. Polym. Sci.* 35 (2010) 338–356. doi:10.1016/j.progpolymsci.2009.12.003.
- [10] M.D. Sanchez-García, J.M. Lagaron, Novel clay-based nanobiocomposites of biopolyesters with synergistic barrier to UV light, gas, and vapour, *J. Appl. Polym. Sci.* 118 (2010) 188–199. doi:10.1002/app.31986.
- [11] M. Martínez-Sanz, A. Lopez-Rubio, J.M. Lagaron, Optimization of the dispersion of unmodified bacterial cellulose nanowhiskers into polylactide via melt compounding to significantly enhance barrier and mechanical properties, *Biomacromolecules.* 13 (2012). doi:10.1021/bm301430j.
- [12] J. Gámez-Pérez, J.C. Velazquez-Infante, E. Franco-Urquiza, P. Pages, F. Carrasco, O.O. Santana, M.L. MasPOCH, Fracture behavior of quenched poly(lactic acid), *Express Polym. Lett.* 5 (2011) 82–91. doi:10.3144/expresspolymlett.2011.9.
- [13] Y. Li, H. Shimizu, Toughening of polylactide by melt blending with a biodegradable poly(ether)urethane elastomer., *Macromol. Biosci.* 7 (2007) 921–8. doi:10.1002/mabi.200700027.
- [14] H. Balakrishnan, A. Hassan, M. Imran, M.U. Wahit, Toughening of Polylactic Acid Nanocomposites: A Short Review, *Polym. Plast. Technol. Eng.* (2012). doi:10.1080/03602559.2011.618329.
- [15] M.P. Arrieta, J. López, D. López, J.M. Kenny, L. Peponi, Development of flexible materials based on plasticized electrospun PLA–PHB blends: Structural, thermal, mechanical and disintegration properties, *Eur. Polym. J.* 73 (2015) 433–446. doi:10.1016/j.eurpolymj.2015.10.036.
- [16] M.P. Arrieta, J. López, A. Hernández, E. Rayón, Ternary PLA – PHB – Limonene blends

- intended for biodegradable food packaging applications, *Eur. Polym. J.* 50 (2014) 255–270. doi:10.1016/j.eurpolymj.2013.11.009.
- [17] J.P. Mofokeng, A.S. Luyt, Morphology and thermal degradation studies of melt-mixed PLA/PHBV biodegradable polymer blend nanocomposites with TiO₂ as filler, *J. Appl. Polym. Sci.* 132 (2015) n/a-n/a. doi:10.1002/app.42138.
- [18] V. Jost, Blending of Polyhydroxybutyrate-co-valerate with Polylactic Acid for Packaging Applications – Reflections on Miscibility and Effects on the Mechanical and Barrier Properties, *Chem. Biochem. Eng. Q.* 29 (2015) 221–246. doi:10.15255/CABEQ.2014.2257.
- [19] S. Modi, K. Koelling, Y. Vodovotz, Miscibility of poly(3-hydroxybutyrate-co-3-hydroxyvalerate) with high molecular weight poly(lactic acid) blends determined by thermal analysis, *J. Appl. Polym. Sci.* 124 (2012) 3074–3081. doi:10.1002/app.35343.
- [20] M.J. John, Biopolymer blends based on polylactic acid and polyhydroxy butyrate-co-valerate: Effect of clay on mechanical and thermal properties, *Polym. Compos.* (2014). doi:10.1002/pc.23114.
- [21] J.M. Ferri, O. Fenollar, A. Jorda-Vilaplana, D. García-Sanoguera, R. Balart, Effect of miscibility on mechanical and thermal properties of poly(lactic acid)/ polycaprolactone blends, *Polym. Int.* 65 (2016) 453–463. doi:10.1002/pi.5079.
- [22] J.P. Mofokeng, a. S. Luyt, Dynamic mechanical properties of PLA/PHBV, PLA/PCL, PHBV/PCL blends and their nanocomposites with TiO₂ as nanofiller, *Thermochim. Acta.* 613 (2015) 41–53. doi:10.1016/j.tca.2015.05.019.
- [23] J. Yu, J. Han, F. Zhu, J. Su, L. Ou, Structures and properties of fully biodegradable PLA/PBAT/PHBV blends, *Fuhe Cailiao Xuebao/Acta Mater. Compos. Sin.* (2016). doi:10.13801/j.cnki.fhclxb.20151014.004.
- [24] W. Pivsa-Art, A. Chaiyasat, S. Pivsa-Art, H. Yamane, H. Ohara, Preparation of polymer blends between poly(lactic acid) and poly(butylene adipate-co-terephthalate) and biodegradable polymers as compatibilizers, *Energy Procedia.* (2013). doi:10.1016/j.egypro.2013.06.784.
- [25] M. Liu, M. Pu, H. Ma, Preparation, structure and thermal properties of polylactide/sepiolite nanocomposites with and without organic modifiers, *Compos. Sci. Technol.* 72 (2012) 1508–1514. doi:10.1016/j.compscitech.2012.05.017.
- [26] K. Fukushima, Properties of poly(lactic acid) nanocomposites based on montmorillonite, sepiolite and zirconium phosphonate, *Express Polym. Lett.* 6 (2012) 914–926. doi:10.3144/expresspolymlett.2012.97.
- [27] J.-W. Rhim, H.-M. Park, C.-S. Ha, Bio-nanocomposites for food packaging applications, *Prog. Polym. Sci.* 38 (2013). doi:10.1016/j.progpolymsci.2013.05.008.
- [28] M.-A. Paul, M. Alexandre, P. Degée, C. Henrist, A. Rulmont, P. Dubois, New nanocomposite materials based on plasticized poly(L-lactide) and organo-modified montmorillonites: Thermal and morphological study, *Polymer (Guildf)*. 44 (2002). doi:10.1016/S0032-3861(02)00778-4.
- [29] G.Z. Papageorgiou, D.S. Achilias, S. Nanaki, T. Beslikas, D. Bikiaris, PLA nanocomposites: Effect of filler type on non-isothermal crystallization, *Thermochim. Acta.* 511 (2010). doi:10.1016/j.tca.2010.08.004.
- [30] D. Cava, E. Gimenez, R. Gavara, J.M. Lagaron, Comparative Performance and Barrier Properties of Biodegradable Thermoplastics and Nanobiocomposites versus PET for Food Packaging Applications, *J. Plast. Film Sheeting.* 22 (2006) 265–274. <http://www.scopus.com/inward/record.url?eid=2-s2.0->

2. Marco teórico

- 33845203640&partnerID=tZOtx3y1 (accessed January 14, 2015).
- [31] Q.-S. Liu, M.-F. Zhu, W.-H. Wu, Z.-Y. Qin, Reducing the formation of six-membered ring ester during thermal degradation of biodegradable PHBV to enhance its thermal stability, *Polym. Degrad. Stab.* 94 (2009) 18–24. doi:10.1016/j.polymdegradstab.2008.10.016.
- [32] S. Duangphet, D. Szegda, J. Song, K. Tarverdi, The Effect of Chain Extender on Poly(3-hydroxybutyrate-co-3-hydroxyvalerate): Thermal Degradation, Crystallization, and Rheological Behaviours, *J. Polym. Environ.* 22 (2013) 1–8. doi:10.1007/s10924-012-0568-5.
- [33] W. V. Srubar, Z.C. Wright, A. Tsui, A.T. Michel, S.L. Billington, C.W. Frank, Characterizing the effects of ambient aging on the mechanical and physical properties of two commercially available bacterial thermoplastics, *Polym. Degrad. Stab.* 97 (2012) 1922–1929. doi:10.1016/j.polymdegradstab.2012.04.011.
- [34] E. Bugnicourt, Polyhydroxyalkanoate (PHA): Review of synthesis, characteristics, processing and potential applications in packaging, *Express Polym. Lett.* 8 (2014) 791–808. doi:10.3144/expresspolymlett.2014.82.
- [35] A. Javadi, S. Pilla, S. Gong, L.S. Turng, Biobased and Biodegradable PHBV-Based Polymer Blends and Biocomposites: Properties and Applications, *Handb. Bioplastics Biocomposites Eng. Appl.* (2011) 372–396. doi:10.1002/9781118203699.ch14.
- [36] B.S. Kushwah, A.V.S. Kushwah, V. Singh, Towards understanding polyhydroxyalkanoates and their use, *J. Polym. Res.* 23 (2016). doi:10.1007/s10965-016-0988-3.
- [37] A. Anjum, M. Zuber, K.M. Zia, A. Noreen, M.N. Anjum, S. Tabasum, Microbial production of polyhydroxyalkanoates (PHAs) and its copolymers: A review of recent advancements, *Int. J. Biol. Macromol.* 89 (2016) 161–174. doi:10.1016/j.ijbiomac.2016.04.069.
- [38] J. Możejko-Ciesielska, R. Kiewisz, Bacterial polyhydroxyalkanoates: Still fabulous?, *Microbiol. Res.* 192 (2016) 271–282. doi:10.1016/j.micres.2016.07.010.
- [39] B. Laycock, P. Halley, S. Pratt, A. Werker, P. Lant, The chemomechanical properties of microbial polyhydroxyalkanoates, *Prog. Polym. Sci.* 38 (2013) 536–583. doi:10.1016/j.progpolymsci.2012.06.003.
- [40] G. Kedia, P. Passanha, R.M. Dinsdale, A.J. Guwy, S.R. Esteves, Evaluation of feeding regimes to enhance PHA production using acetic and butyric acids by a pure culture of *Cupriavidus necator*, *Biotechnol. Bioprocess Eng.* 19 (2014). doi:10.1007/s12257-014-0144-z.
- [41] C. Kourmentza, I. Ntaikou, M. Kornaros, G. Lyberatos, Production of PHAs from mixed and pure cultures of *Pseudomonas* sp. using short-chain fatty acids as carbon source under nitrogen limitation, *Desalination.* 248 (2009) 723–732. doi:10.1016/j.desal.2009.01.010.
- [42] M.A.M. Reis, L.S. Serafim, P.C. Lemos, A.M. Ramos, F.R. Aguiar, M.C.M. Van Loosdrecht, Production of polyhydroxyalkanoates by mixed microbial cultures., *Bioprocess Biosyst. Eng.* 25 (2003) 377–85. doi:10.1007/s00449-003-0322-4.
- [43] L.S. Serafim, P.C. Lemos, R. Oliveira, M.A.M. Reis, Optimization of polyhydroxybutyrate production by mixed cultures submitted to aerobic dynamic feeding conditions, *Biotechnol. Bioeng.* (2004). doi:10.1002/bit.20085.
- [44] C. Bianca, P.S. Tommy, R. Maria, S. Barbara, A. Fabrizio, Polyhydroxyalkanoates (PHAs) production from fermented cheese whey by using a mixed microbial culture, *Bioresour. Technol.* (2016). doi:10.1016/j.biortech.2016.07.024.
- [45] G. Carvalho, A. Oehmen, M.G.E. Albuquerque, M.A.M. Reis, The relationship between mixed microbial culture composition and PHA production performance from fermented molasses, *N. Biotechnol.* 31 (2014). doi:10.1016/j.nbt.2013.08.010.
- [46] M.F. Md. Din, P. Mohanadoss, Z. Ujang, M. van Loosdrecht, S.M. Yunus, S. Chelliapan, V.

- Zambare, G. Olsson, Development of Bio-PORec® system for polyhydroxyalkanoates (PHA) production and its storage in mixed cultures of palm oil mill effluent (POME), *Bioresour. Technol.* 124 (2012). doi:10.1016/j.biortech.2012.08.036.
- [47] H.-Y. Liu, P.V. Hall, J.L. Darby, E.R. Coats, P.G. Green, D.E. Thompson, F.J. Loge, Production of polyhydroxyalkanoate during treatment of tomato cannery wastewater, *Water Environ. Res.* 80 (2008). doi:10.2175/106143007X221535.
- [48] D. Dionisi, G. Carucci, M. Petrangeli Papini, C. Riccardi, M. Majone, F. Carrasco, Olive oil mill effluents as a feedstock for production of biodegradable polymers, *Water Res.* 39 (2005). doi:10.1016/j.watres.2005.03.011.
- [49] G. Jiang, D.J. Hill, M. Kowalczuk, B. Johnston, G. Adamus, V. Irorere, I. Radecka, Carbon sources for polyhydroxyalkanoates and an integrated biorefinery, *Int. J. Mol. Sci.* (2016). doi:10.3390/ijms17071157.
- [50] I. Radecka, V. Irorere, G. Jiang, D. Hill, C. Williams, G. Adamus, M. Kwiecień, A.A. Marek, J. Zawadiak, B. Johnston, M. Kowalczuk, Oxidized polyethylene wax as a potential carbon source for PHA production, *Materials (Basel)*. 9 (2016). doi:10.3390/ma9050367.
- [51] R.A.J. Verlinden, D.J. Hill, M.A. Kenward, C.D. Williams, I. Radecka, Bacterial synthesis of biodegradable polyhydroxyalkanoates, *J. Appl. Microbiol.* (2007). doi:10.1111/j.1365-2672.2007.03335.x.
- [52] E.A. Dawes, P.J. Senior, The Role and Regulation of Energy Reserve Polymers in Microorganisms, *Adv. Microb. Physiol.* (1973). doi:10.1016/S0065-2911(08)60088-0.
- [53] A. Anjum, M. Zuber, K.M. Zia, A. Noreen, M.N. Anjum, S. Tabasum, Microbial production of polyhydroxyalkanoates (PHAs) and its copolymers: A review of recent advancements, *Int. J. Biol. Macromol.* (2016). doi:10.1016/j.ijbiomac.2016.04.069.
- [54] J.M. Puglia, D. Fortunati, E. D'Amico, D.A. Manfredi, L.B. Cyras, V.P. Kenny, Influence of organically modified clays on the properties and disintegrability in compost of solution cast poly(3-hydroxybutyrate) films, *Polym. Degrad. Stab.* 99 (2014) 127–135. <http://www.scopus.com/inward/record.url?eid=2-s2.0-84892372731&partnerID=tZOtx3y1> (accessed January 29, 2014).
- [55] K. Sudesh, H. Abe, Y. Doi, Synthesis, structure and properties of polyhydroxyalkanoates: Biological polyesters, *Prog. Polym. Sci.* (2000). doi:10.1016/S0079-6700(00)00035-6.
- [56] S.Y. Lee, Bacterial Polyhydroxyalkanoates, *Biotechnol. Bioeng.* 49 (1996) 1–14. doi:10.1002/(SICI)1097-0290(19960105)49:1<1::AID-BIT1>3.0.CO;2-P.
- [57] M.A.M. Reis, L.S. Serafim, P.C. Lemos, A.M. Ramos, F.R. Aguiar, M.C.M. Van Loosdrecht, Production of polyhydroxyalkanoates by mixed microbial cultures, *Bioprocess Biosyst. Eng.* (2003). doi:10.1007/s00449-003-0322-4.
- [58] L.S. Serafim, P.C. Lemos, R. Oliveira, M.A.M. Reis, Optimization of polyhydroxybutyrate production by mixed cultures submitted to aerobic dynamic feeding conditions., *Biotechnol. Bioeng.* 87 (2004) 145–60. doi:10.1002/bit.20085.
- [59] B. Laycock, P. Halley, S. Pratt, A. Werker, P. Lant, The chemomechanical properties of microbial polyhydroxyalkanoates, *Prog. Polym. Sci.* 38 (2013) 536–583. doi:10.1016/j.progpolymsci.2012.06.003.
- [60] S. Khanna, A.K. Srivastava, Recent advances in microbial polyhydroxyalkanoates, *Process Biochem.* (2005). doi:10.1016/j.procbio.2004.01.053.
- [61] R.W. Lenz, R.H. Marchessault, Bacterial polyesters: biosynthesis, biodegradable plastics and biotechnology., *Biomacromolecules*. 6 (2005) 1–8. <http://www.scopus.com/inward/record.url?eid=2-s2.0->

2. Marco teórico

- 14044254667&partnerID=tZOtx3y1 (accessed January 14, 2015).
- [62] Y.M. Corre, S. Bruzaud, J.L. Audic, Y. Grohens, Morphology and functional properties of commercial polyhydroxyalkanoates: A comprehensive and comparative study, *Polym. Test.* (2012). doi:10.1016/j.polymertesting.2011.11.002.
- [63] D.Z. Bucci, L.B.B. Tavares, I. Sell, PHB packaging for the storage of food products, *Polym. Test.* 24 (2005) 564–571. doi:10.1016/j.polymertesting.2005.02.008.
- [64] S. Modi, K. Koelling, Y. Vodovotz, Assessment of PHB with varying hydroxyvalerate content for potential packaging applications, *Eur. Polym. J.* 47 (2011) 179–186. doi:10.1016/j.eurpolymj.2010.11.010.
- [65] J.M. Nduko, K. Matsumoto, S. Taguchi, Biological lactate-polymers synthesized by one-pot microbial factory: Enzyme and metabolic engineering, in: *ACS Symp. Ser.*, 2012. doi:10.1021/bk-2012-1105.ch014.
- [66] T.L. Bluhm, G.K. Hamer, R.H. Marchessault, C.A. Fyfe, R.P. Veregin, Isodimorphism in bacterial poly(β -hydroxybutyrate-co- β -hydroxyvalerate), *Macromolecules.* 19 (1986).
- [67] R. Shogren, Water vapor permeability of biodegradable polymers, *J. Environ. Polym. Degrad.* 5 (1997).
- [68] V. Chea, H. Angellier-Coussy, S. Peyron, D. Kemmer, N. Gontard, Poly(3-hydroxybutyrate-co-3-hydroxyvalerate) films for food packaging: Physical-chemical and structural stability under food contact conditions, *J. Appl. Polym. Sci.* (2015) Article in press. doi:10.1002/app.41850.
- [69] M. Kunioka, A. Tamaki, Y. Doi, Crystalline and thermal properties of bacterial copolyesters: poly(3-hydroxybutyrate-co-3-hydroxyvalerate) and poly(3-hydroxybutyrate-co-4-hydroxybutyrate), *Macromolecules.* 22 (1989) 694–697. doi:10.1021/ma00192a031.
- [70] N. Grassie, E.J. Murray, P.A. Holmes, The thermal degradation of poly(-(d)-??-hydroxybutyric acid): Part 2-Changes in molecular weight, *Polym. Degrad. Stab.* (1984). doi:10.1016/0141-3910(84)90075-2.
- [71] N. Grassie, E.J. Murray, P.A. Holmes, The thermal degradation of poly(-(d)-??-hydroxybutyric acid): Part 3-The reaction mechanism, *Polym. Degrad. Stab.* (1984). doi:10.1016/0141-3910(84)90032-6.
- [72] M. Kunioka, Y. Doi, Thermal degradation of microbial copolyesters. Poly(3-hydroxybutyrate-co-3-hydroxyvalerate) and poly(3-hydroxybutyrate-co-4-hydroxybutyrate), *Macromolecules.* 23 (1990).
- [73] E. Hablot, P. Bordes, E. Pollet, L. Avérous, Thermal and thermo-mechanical degradation of poly(3-hydroxybutyrate)-based multiphase systems, *Polym. Degrad. Stab.* 93 (2008) 413–421. doi:10.1016/j.polymdegradstab.2007.11.018.
- [74] S. Nguyen, G.E. Yu, R.H. Marchessault, Thermal degradation of poly(3-hydroxyalkanoates): Preparation of well-defined oligomers, *Biomacromolecules.* (2002). doi:10.1021/bm0156274.
- [75] F.D. Kopinke, M. Remmler, K. Mackenzie, Thermal decomposition of biodegradable polyesters - I: Poly(??-hydroxybutyric acid), *Polym. Degrad. Stab.* (1996). doi:10.1016/0141-3910(95)00221-9.
- [76] H. Abe, Thermal degradation of environmentally degradable poly(hydroxyalkanoic acid)s, *Macromol. Biosci.* (2006). doi:10.1002/mabi.200600070.
- [77] G.J.M. de Koning, P.J. Lemstra, Crystallization phenomena in bacterial poly[(R)-3-hydroxybutyrate]: 2. Embrittlement and rejuvenation, *Polymer (Guildf).* 34 (1993) 4089–4094. doi:10.1016/0032-3861(93)90671-V.

- [78] F. Biddlestone, a Harris, J.N. Hay, T. Hammond, The physical ageing of amorphous poly(hydroxybutyrate), *Polym. Int.* 39 (1996) 221–229. doi:10.1002/(SICI)1097-0126(199603)39:3<221::AID-PI511>3.0.CO;2-O.
- [79] J. Martinez-Salazar, M. Sanchez-Cuesta, P.J. Barham, A. Keller, Thermal expansion and spherulite cracking in 3-hydroxybutyrate/3-hydroxyvalerate copolymers, *J. Mater. Sci. Lett.* 8 (1989). doi:10.1007/BF00720717.
- [80] P.J. Barham, A. Keller, The relationship between microstructure and mode of fracture in polyhydroxybutyrate, *J. Polym. Sci. Part B Polym. Phys.* 24 (1986). doi:10.1002/polb.1986.180240108.
- [81] A. El-Hadi, R. Schnabel, E. Straube, G. Müller, S. Henning, Correlation between degree of crystallinity, morphology, glass temperature, mechanical properties and biodegradation of poly (3-hydroxyalkanoate) PHAs and their blends, *Polym. Test.* 21 (2002) 665–674. doi:10.1016/S0142-9418(01)00142-8.
- [82] J.K. Hobbs, T.J. McMaster, M.J. Miles, P.J. Barham, Cracking in spherulites of poly(hydroxybutyrate), *Polymer (Guildf)*. 37 (1996). doi:10.1016/0032-3861(96)88468-0.
- [83] M.L. Di Lorenzo, M.C. Righetti, Effect of thermal history on the evolution of crystal and amorphous fractions of poly[(R)-3-hydroxybutyrate] upon storage at ambient temperature, *Eur. Polym. J.* 112 (2013) 1439-1446-. doi:10.1007/s10973-012-2734-3.
- [84] C. Schick, A. Wurm, A. Mohamed, Vittrification and devitrification of the rigid amorphous fraction of semicrystalline polymers revealed from frequency-dependent heat capacity, *Colloid Polym. Sci.* 279 (2001) 800–806. doi:10.1007/s003960100507.
- [85] M. Scandola, G. Ceccorulli, M. Pizzoli, The physical aging of bacterial poly(D-B-hydroxybutyrate), *Makromol Chem, Rapid Commun.* 50 (1989) 47–50.
- [86] B.L. Hurrell, R.E. Cameron, Physical ageing and the embrittlement of poly(hydroxybutyrate) on storage: a time resolved small angle X-ray scattering study, *Polym. Int.* 45 (1998) 308–312. doi:10.1002/(SICI)1097-0126(199803)45:3<308::AID-PI934>3.0.CO;2-V.
- [87] B.L. Hurrell, R.E. Cameron, A wide-angle X-ray scattering study of the ageing of poly (hydroxybutyrate), *J. Mater. Sci.* 33 (1998) 1709–1713.
- [88] G.J.M. de Koning, A.H.C. Scheeren, P.J. Lemstra, M. Peeters, H. Reynaers, Crystallization phenomena in bacterial poly[(R)-3-hydroxybutyrate]: 3. Toughening via texture changes, *Polymer (Guildf)*. 35 (1994) 4598–4605. doi:10.1016/0032-3861(94)90809-5.
- [89] G.J.. de Koning, P.. Lemstra, D.J.. Hill, T.. Carswell, J.. O'Donnell, Ageing phenomena in bacterial poly[(R)-3-hydroxybutyrate], *Polymer (Guildf)*. 33 (1992) 3295–3297. doi:10.1016/0032-3861(92)90250-Z.
- [90] R. Crétois, J.-M. Chenal, N. Sheibat-Othman, A. Monnier, C. Martin, O. Astruz, R. Kurusu, N.R. Demarquette, Physical explanations about the improvement of PolyHydroxyButyrate ductility: Hidden effect of plasticizer on physical ageing, *Polym. (United Kingdom)*. 102 (2016) 176–182. doi:10.1016/j.polymer.2016.09.017.
- [91] L.C.E. Struik, The mechanical behaviour and physical ageing of semicrystalline polymers: 2., *Polymer (Guildf)*. 28 (1987) 1534–1542.
- [92] L.C.E. Struik, The mechanical and physical ageing of semicrystalline polymers: 1, *Polymer (Guildf)*. 28 (1987) 1521–1533. doi:10.1016/0032-3861(87)90353-3.
- [93] J. Qian, L. Zhu, J. Zhang, R.S. Whitehouse, Comparison of different nucleating agents on crystallization of poly(3-hydroxybutyrate-co-3-hydroxyvalerates), *J. Polym. Sci. Part B Polym. Phys.* (2007). doi:10.1002/polb.21157.
- [94] W. Kai, Y. He, Y. Inoue, Fast crystallization of poly(3-hydroxybutyrate) and poly(3-

2. Marco teórico

- hydroxybutyrate-co-3-hydroxyvalerate) with talc and boron nitride as nucleating agents, *Polym. Int.* (2005). doi:10.1002/pi.1758.
- [95] J.A.S. Puente, A. Esposito, F. Chivrac, E. Dargent, Effects of size and specific surface area of boron nitride particles on the crystallization of bacterial poly(3-hydroxybutyrate-co-3-hydroxyvalerate), *Macromol. Symp.* (2013). doi:10.1002/masy.201350601.
- [96] L. Jiang, J. Huang, J. Qian, F. Chen, J. Zhang, M.P. Wolcott, Y. Zhu, Study of poly(3-hydroxybutyrate-co-3-hydroxyvalerate) (PHBV)/bamboo pulp fiber composites: Effects of nucleation agent and compatibilizer, *J. Polym. Environ.* (2008). doi:10.1007/s10924-008-0086-7.
- [97] M. Öner, A.A. Çöl, celine Pochat-Bohatier, M. Bechelany, Effect of Incorporation of Boron Nitride Nanoparticles on Oxygen Barrier and Thermal Properties of Poly(3-hydroxybutyrate-co-3-hydroxyvalerate), *RSC Adv.* (n.d.). doi:10.1039/C6RA19198C.
- [98] P. Pan, G. Shan, Y. Bao, Z. Weng, Crystallization kinetics of bacterial poly(3-hydroxybutyrate) copolyesters with cyanuric acid as a nucleating agent, *J. Appl. Polym. Sci.* (2013). doi:10.1002/app.38825.
- [99] W.J. Liu, H.L. Yang, Z. Wang, L.S. Dong, J.J. Liu, Effect of nucleating agents on the crystallization of poly(3-hydroxybutyrate-co-3-hydroxyvalerate), *J. Appl. Polym. Sci.* 86 (2002). doi:10.1002/app.11023.
- [100] R.S. Kurusu, C.A. Siliki, É. David, N.R. Demarquette, C. Gauthier, J.M. Chenal, Incorporation of plasticizers in sugarcane-based poly(3-hydroxybutyrate)(PHB): Changes in microstructure and properties through ageing and annealing, *Ind. Crops Prod.* 72 (2015) 166–174. doi:10.1016/j.indcrop.2014.12.040.
- [101] R.S. Kurusu, N.R. Demarquette, C. Gauthier, J.M. Chenal, Effect of ageing and annealing on the mechanical behaviour and biodegradability of a poly(3-hydroxybutyrate) and poly(ethylene-co-methyl-acrylate-co-glycidyl-methacrylate)blend, *Polym. Int.* (2014). doi:10.1002/pi.4616.
- [102] V. Jost, H.-C. Langowski, Effect of different plasticisers on the mechanical and barrier properties of extruded cast PHBV films, *Eur. Polym. J.* 68 (2015) 302–312. doi:10.1016/j.eurpolymj.2015.04.012.
- [103] S.P.C. Gonçalves, S.M. Franchetti, Biodegradability of PP/PHBV (70/30) blend films, *Adv. Polym. Technol.* (2013). doi:10.1002/adv.21377.
- [104] P. Ma, X. Cai, W. Wang, F. Duan, D. Shi, P.J. Lemstra, Crystallization behavior of partially crosslinked poly(3-hydroxyalkonates)/poly(butylene succinate) blends, *J. Appl. Polym. Sci.* (2014). doi:10.1002/app.41020.
- [105] Q. Liu, C. Wu, H. Zhang, B. Deng, Blends of polylactide and poly(3-hydroxybutyrate-co-3-hydroxyvalerate) with low content of hydroxyvalerate unit: Morphology, structure, and property, *J. Appl. Polym. Sci.* (2015). doi:10.1002/app.42689.
- [106] V. Jost, Blending of Polyhydroxybutyrate-co-valerate with Polylactic Acid for Packaging Applications – Reflections on Miscibility and Effects on the Mechanical and Barrier Properties, *Chem. Biochem. Eng. Q.* (2015). doi:10.15255/CABEQ.2014.2257.
- [107] J.P. Mofokeng, A.S. Luyt, Morphology and thermal degradation studies of melt-mixed poly(hydroxybutyrate-co-valerate) (PHBV)/poly(ε-caprolactone) (PCL) biodegradable polymer blend nanocomposites with TiO₂ as filler, *J. Mater. Sci.* (2015). doi:10.1007/s10853-015-8950-z.
- [108] Y.J. Phua, A. Pegoretti, T.M. Araujo, Z.A.M. Ishak, Mechanical and thermal properties of poly(butylene succinate)/poly(3-hydroxybutyrate-co-3-hydroxyvalerate) biodegradable

- blends, *J. Appl. Polym. Sci.* (2015). doi:10.1002/app.42815.
- [109] L.H. Mara Cunha, Bruno Fernandes, Jose A. Covas, Antonio A. Vicente, Film blowing of PHBV blends and PHBV-based multilayers for the production of biodegradable packages, *J. Appl. Polym. Sci.* 133 (2016). doi:10.1002/app.42971.
- [110] S.P. Pawar, A. Misra, S. Bose, K. Chatterjee, V. Mittal, Enzymatically degradable and flexible bio-nanocomposites derived from PHBV and PBAT blend: assessing thermal, morphological, mechanical, and biodegradation properties, *Colloid Polym. Sci.* (2015). doi:10.1007/s00396-015-3700-y.
- [111] Y. Zhou, N. Yang, X. Wang, Y. Weng, X. Diao, M. Zhang, Y. Jin, Biomanufactured polyhydroxyalkanoates (PHA) modification: A review, *Shengwu Gongcheng Xuebao/Chinese J. Biotechnol.* 32 (2016). doi:10.13345/j.cjb.160027.
- [112] K. Wang, Y. Wang, R. Zhang, Q. Li, C. Shen, Preparation and characterization of microbial biodegradable poly(3-hydroxybutyrate-co-4-hydroxybutyrate)/organoclay nanocomposites, *Polym. Compos.* 33 (2012) 838–842. doi:10.1002/pc.22220.
- [113] P. Ma, X. Cai, W. Wang, F. Duan, D. Shi, P.J. Lemstra, Crystallization behavior of partially crosslinked poly(β -hydroxyalkanoates)/poly(butylene succinate) blends, *J. Appl. Polym. Sci.* 41020 (2014) n/a-n/a. doi:10.1002/app.41020.
- [114] T. Gerard, T. Budtova, Morphology and molten-state rheology of polylactide and polyhydroxyalkanoate blends, *Eur. Polym. J.* 48 (2012) 1110–1117. doi:10.1016/j.eurpolymj.2012.03.015.
- [115] E. Saldívar-Guerra, E. Vivaldo-Lima, *Handbook of Polymer Synthesis, Characterization, and Processing*, 2013. doi:10.1002/9781118480793.
- [116] N. Najafi, M.C. Heuzey, P.J. Carreau, Crystallization behavior and morphology of polylactide and PLA/clay nanocomposites in the presence of chain extenders, *Polym. Eng. Sci.* 53 (2013) 1053–1064. doi:10.1002/pen.23355.
- [117] N. Najafi, M.C. Heuzey, P.J. Carreau, P.M. Wood-Adams, Control of thermal degradation of polylactide (PLA)-clay nanocomposites using chain extenders, *Polym. Degrad. Stab.* 97 (2012) 554–565. doi:10.1016/j.polymdegradstab.2012.01.016.
- [118] N. Najafi, M.C. Heuzey, P.J. Carreau, Polylactide (PLA)-clay nanocomposites prepared by melt compounding in the presence of a chain extender, *Compos. Sci. Technol.* 72 (2012) 608–615. doi:10.1016/j.compscitech.2012.01.005.
- [119] R. Al-Itry, K. Lamnawar, A. Maazouz, Improvement of thermal stability, rheological and mechanical properties of PLA, PBAT and their blends by reactive extrusion with functionalized epoxy, *Polym. Degrad. Stab.* 97 (2012) 1898–1914. doi:10.1016/j.polymdegradstab.2012.06.028.
- [120] Q. Meng, M.-C. Heuzey, P.J. Carreau, Control of thermal degradation of polylactide/clay nanocomposites during melt processing by chain extension reaction, *Polym. Degrad. Stab.* 97 (2012) 2010–2020. doi:10.1016/j.polymdegradstab.2012.01.030.
- [121] P. Rytlewski, M. Żenkiewicz, R. Malinowski, Influence of Dicumyl Peroxide Content on Thermal and Mechanical Properties of Polylactide, *Int. Polym. Process.* 26 (2011) 580–586. doi:10.3139/217.2521.
- [122] J. Burlet, M.C. Heuzey, C. Dubois, P. Wood-Adams, J. Brisson, Thermal stabilization of high molecular weight L-polylactide, *Annu. Tech. Conf. - ANTEC, Conf. Proc.* 3 (2005) 281–285. <http://www.scopus.com/inward/record.url?eid=2-s2.0-33644949024&partnerID=tZ0tx3y1>.
- [123] J.A. Cicero, J.R. Dorgan, S.F. Dec, D.M. Knauss, Phosphite stabilization effects on two-step

2. Marco teórico

- melt-spun fibers of polylactide, *Polym. Degrad. Stab.* 78 (2002) 95–105. doi:10.1016/S0141-3910(02)00123-4.
- [124] H.J. Lehermeier, J.R. Dorgan, Melt rheology of poly(lactic acid): Consequences of blending chain architectures, *Polym. Eng. Sci.* 41 (2001) 2172–2184. doi:10.1002/pen.10912.
- [125] P. D'Haene, E.E. Remsen, J. Asrar, Preparation and Characterization of a Branched Bacterial Polyester, *Macromolecules.* 32 (1999) 5229–5235. doi:10.1021/ma981911k.
- [126] D. Bikiaris, G. Karayannidis, Chain extension of polyesters PET and PBT with two new diimidodiepoxides. II, *J. Polym. Sci. Part A Polym. Chem.* 34 (1996) 1337–1342. [http://onlinelibrary.wiley.com/doi/10.1002/\(SICI\)1099-0518\(199605\)34:7%3C1337::AID-POLA22%3E3.0.CO;2-9/abstract](http://onlinelibrary.wiley.com/doi/10.1002/(SICI)1099-0518(199605)34:7%3C1337::AID-POLA22%3E3.0.CO;2-9/abstract) (accessed December 23, 2014).
- [127] P. D'Haene, E.E. Remsen, J. Asrar, Preparation and Characterization of a Branched Bacterial Polyester, *Macromolecules.* 32 (1999) 5229–5235. doi:10.1021/ma981911k.
- [128] B. Fei, C. Chen, S. Chen, S. Peng, Y. Zhuang, Y. An, L. Dong, Crosslinking of poly[(3-hydroxybutyrate)-co-(3-hydroxyvalerate)] using dicumyl peroxide as initiator, *Polym. Int.* 53 (2004) 937–943. doi:10.1002/pi.1477.
- [129] J. Matusik, E. Stodolak, K. Bahranowski, Synthesis of polylactide/clay composites using structurally different kaolinites and kaolinite nanotubes, 51 (2011) 102–109. doi:10.1016/j.clay.2010.11.010.
- [130] N.F. Magalhães, K. Dahmouche, G.K. Lopes, C.T. Andrade, Using an organically-modified montmorillonite to compatibilize a biodegradable blend, *Appl. Clay Sci.* 72 (2013) 1–8. doi:10.1016/j.clay.2012.12.008.
- [131] A. Botana, M. Mollo, P. Eisenberg, R.M. Torres Sanchez, Effect of modified montmorillonite on biodegradable PHB nanocomposites, 47 (2010) 263–270. doi:10.1016/j.clay.2009.11.001.
- [132] Y. Ma, Y. Zheng, G. Wei, W. Song, T. Hu, H. Yang, R. Xue, Processing, structure, and properties of multiwalled carbon nanotube/poly(hydroxybutyrate-co-valerate) biopolymer nanocomposites, *J. Appl. Polym. Sci.* 125 (2012) E620–E629. doi:10.1002/app.35650.
- [133] G.-F. Shan, X. Gong, W.-P. Chen, L. Chen, M.-F. Zhu, Effect of multi-walled carbon nanotubes on crystallization behavior of poly(3-hydroxybutyrate-co-3-hydroxyvalerate), *Colloid Polym. Sci.* 289 (2011) 1005–1014. doi:10.1007/s00396-011-2412-1.
- [134] H.-Y. Yu, Z.-Y. Qin, B. Sun, X.-G. Yang, J.-M. Yao, Reinforcement of transparent poly(3-hydroxybutyrate-co-3-hydroxyvalerate) by incorporation of functionalized carbon nanotubes as a novel bionanocomposite for food packaging, *Compos. Sci. Technol.* 94 (2014) 96–104. doi:10.1016/j.compscitech.2014.01.018.
- [135] B. Bittmann, R. Bouza, L. Barral, J. Diez, C. Ramirez, Poly(3-hydroxybutyrate-co-3-hydroxyvalerate)/clay nanocomposites for replacement of mineral oil based materials, *Polym. Compos.* 34 (2013) 1033–1040. <http://www.scopus.com/inward/record.url?eid=2-s2.0-84879208437&partnerID=tZOtx3y1> (accessed February 15, 2014).
- [136] T.S. Daitx, L.N. Carli, J.S. Crespo, R.S. Mauler, Effects of the organic modification of different clay minerals and their application in biodegradable polymer nanocomposites of PHBV, *Appl. Clay Sci.* 115 (2015) 157–164. doi:10.1016/j.clay.2015.07.038.
- [137] S. Zainuddin, A. Fahim, S. Shoieb, F. Syed, M. V. Hosur, D. Li, C. Hicks, S. Jeelani, Morphological and mechanical behavior of chemically treated jute-PHBV bio-nanocomposites reinforced with silane grafted halloysite nanotubes, *J. Appl. Polym. Sci.* (2016). doi:10.1002/app.43994.

- [138] T.S. Daitx, L.N. Carli, J.S. Crespo, R.S. Mauler, Effects of the organic modification of different clay minerals and their application in biodegradable polymer nanocomposites of PHBV, *Appl. Clay Sci.* 115 (2015) 157–164. doi:10.1016/j.clay.2015.07.038.
- [139] L.N. Carli, J.S. Crespo, R.S. Mauler, PHBV nanocomposites based on organomodified montmorillonite and halloysite: The effect of clay type on the morphology and thermal and mechanical properties, *Compos. Part A Appl. Sci. Manuf.* 42 (2011) 1601–1608. doi:10.1016/j.compositesa.2011.07.007.
- [140] N.F. Magalhães, K. Dahmouche, G.K. Lopes, C.T. Andrade, Using an organically-modified montmorillonite to compatibilize a biodegradable blend, *Appl. Clay Sci.* 72 (2013) 1–8. doi:10.1016/j.clay.2012.12.008.
- [141] S. Wang, C. Song, G. Chen, T. Guo, C. Yang, J. Liu, X. Zhang, B. Zhang, Thermal characteristics, crystallization behavior and biodegradability of poly (β -hydroxybutyrate-co- β -hydroxyvalerate)/organophilic montmorillonite (PHBV/OMMT) nanocomposites, *Lizi Jiaohuan Yu Xifu/Ion Exch. Adsorpt.* 20 (2004) 299. <http://www.scopus.com/inward/record.url?eid=2-s2.0-5744247878&partnerID=tZOtx3y1>.
- [142] L.N. Carli, O. Bianchi, G. Machado, J.S. Crespo, R.S. Mauler, Morphological and structural characterization of PHBV/organoclay nanocomposites by small angle X-ray scattering, *Mater. Sci. Eng. C* 33 (2013) 932–937. doi:10.1016/j.msec.2012.11.023.
- [143] R. Crétois, N. Follain, E. Dargent, J. Soulestin, S. Bourbigot, S. Marais, L. Lebrun, Microstructure and barrier properties of PHBV/organoclays bionanocomposites, *J. Memb. Sci.* 467 (2014) 56–66. doi:10.1016/j.memsci.2014.05.015.
- [144] J. Wu, X. Zou, B. Jing, W. Dai, Effect of sepiolite on the crystallization behavior of biodegradable poly(lactic acid) as an efficient nucleating agent, *Polym. Eng. Sci.* 55 (2015) 1104–1112. doi:10.1002/pen.23981.
- [145] A. Nuzzo, E. Bilotti, T. Peijs, D. Acierno, G. Filippone, Nanoparticle-induced co-continuity in immiscible polymer blends – A comparative study on bio-based PLA-PA11 blends filled with organoclay, sepiolite, and carbon nanotubes, *Polymer (Guildf)*. 55 (2014) 4908–4919. doi:10.1016/j.polymer.2014.07.036.
- [146] M.D. Samper-Madrigal, O. Fenollar, F. Dominici, R. Balart, J.M. Kenny, The effect of sepiolite on the compatibilization of polyethylene–thermoplastic starch blends for environmentally friendly films, 50 (2014) 863–872. doi:10.1007/s10853-014-8647-8.
- [147] J.B. Olivato, J. Marini, E. Pollet, F. Yamashita, M.V.E. Grossmann, L. Avérous, Elaboration, morphology and properties of starch/polyester nano-biocomposites based on sepiolite clay, 118 (2015) 250–256. doi:10.1016/j.carbpol.2014.11.014.
- [148] H.E. Miltner, N. Watzeels, N.A. Gotzen, A.L. Goffin, E. Duquesne, S. Benali, B. Ruelle, S. Peeterbroeck, P. Dubois, B. Goderis, G. Van Assche, H. Rahier, B. Van Mele, The effect of nano-sized filler particles on the crystalline-amorphous interphase and thermal properties in polyester nanocomposites, 53 (2012) 1494–1506. doi:10.1016/j.polymer.2012.01.047.
- [149] D.C. da Costa Reis, A.C. Lemos Morais, L.H. de Carvalho, T.S. Alves, R. Barbosa, Assessment of the Morphology and Interaction of PHBV/Clay Bionanocomposites: Uses as Food Packaging, *Macromol. Symp.* 367 (2016). doi:10.1002/masy.201500143.
- [150] K.Y. Kim, S.Y. Yoon, M.J. Yoon, D.Y. Lim, The study on nanocellulose and their biocomposites, in: *Tech. Proc. 2012 NSTI Nanotechnol. Conf. Expo, NSTI-Nanotech 2012, 2012*.
- [151] J. Trifol, D. Plackett, C. Sillard, J. Bras, O. Hassager, A.E. Daugaard, P. Szabo, Reinforcement of PLA nanocomposite with nanoclay and nanocellulose extracted from sisal, in: *TAPPI Int.*

2. Marco teórico

- Conf. Nanotechnol. Renew. Mater. 2014, 2014.
- [152] Q. Zhou, L.A. Berglund, PLA-nanocellulose biocomposites, 2015.
- [153] J. Trifol, D. Plackett, C. Sillard, O. Hassager, A.E. Daugaard, J. Bras, P. Szabo, A comparison of partially acetylated nanocellulose, nanocrystalline cellulose, and nanoclay as fillers for high-performance polylactide nanocomposites, *J. Appl. Polym. Sci.* 133 (2016). doi:10.1002/app.43257.
- [154] L. Cabedo, D. Plackett, E. Giménez, J.M. Lagarón, Studying the degradation of polyhydroxybutyrate-co-valerate during processing with clay-based nanofillers, *J. Appl. Polym. Sci.* 112 (2009) 3669–3676. doi:10.1002/app.29945.
- [155] P. Bordes, E. Hablot, E. Pollet, L. Avérous, Effect of clay organomodifiers on degradation of polyhydroxyalkanoates, *Polym. Degrad. Stab.* 94 (2009) 789–796. doi:10.1016/j.polymdegradstab.2009.01.027.
- [156] P. Russo, B. Vetrano, D. Acierno, M. Mauro, Thermal and structural characterization of biodegradable blends filled with halloysite nanotubes, *Polym. Compos.* 34 (2013) 1460–1470. <http://www.scopus.com/inward/record.url?eid=2-s2.0-84882252115&partnerID=tZ0tx3y1> (accessed February 18, 2014).
- [157] A. Javadi, Y. Srithep, S. Pilla, Microcellular poly (hydroxybutyrate-co-hydroxyvalerate) hyperbranched polymer–nanoclay nanocomposites, *Polym. Eng. Sci.* 51 (2011) 1815–1826. doi:10.1002/pen.
- [158] D. Rawtani, Y. Agrawal, Multifarious applications of halloysite nanotubes: a review, *Rev. Adv. Mater. Sci.* 30 (2012) 282–295. http://mp.ipme.ru/e-journals/RAMS/no_33012/08_rawtani.pdf (accessed December 2, 2014).
- [159] J.-B. Zeng, K.-A. Li, A.-K. Du, Compatibilization strategies in poly(lactic acid)-based blends, *RSC Adv.* (2015). doi:10.1039/C5RA01655J.
- [160] M.M. Reddy, S. Vivekanandhan, M. Misra, S.K. Bhatia, A.K. Mohanty, Biobased plastics and bionanocomposites: Current status and future opportunities, *Prog. Polym. Sci.* 38 (2013) 1653–1689. doi:10.1016/j.progpolymsci.2013.05.006.
- [161] B. Tan, N.L. Thomas, A review of the water barrier properties of polymer/clay and polymer/graphene nanocomposites, *J. Memb. Sci.* 514 (2016). doi:10.1016/j.memsci.2016.05.026.
- [162] G. Choudalakis, A.D. Gotsis, Permeability of polymer/clay nanocomposites: A review, *Eur. Polym. J.* 45 (2009). doi:10.1016/j.eurpolymj.2009.01.027.
- [163] A. Javadi, Y. Srithep, C.C. Clemons, L.-S. Turng, S. Gong, Processing of poly(hydroxybutyrate-co-hydroxyvalerate)-based bionanocomposite foams using supercritical fluids, *J. Mater. Res.* 27 (2012) 1506–1517. doi:10.1557/jmr.2012.74.
- [164] L. Elias, F. Fenouillot, J.C. Majeste, P. Cassagnau, Morphology and rheology of immiscible polymer blends filled with silica nanoparticles, *Polymer (Guildf)*. 48 (2007) 6029–6040. doi:10.1016/j.polymer.2007.07.061.
- [165] B. Imre, B. Puk??nszky, Compatibilization in bio-based and biodegradable polymer blends, *Eur. Polym. J.* 49 (2013) 1215–1233. doi:10.1016/j.eurpolymj.2013.01.019.
- [166] F. Gassner, A.J. Owen, On the physical properties of BIOPOL/ethylene-vinyl acetate blends, *Polymer (Guildf)*. (1992). doi:10.1016/0032-3861(92)91131-K.
- [167] C.C. Han, J. Ismail, H.-W. Kammer, Melt reaction in blends of poly(3-hydroxybutyrate-co-3-hydroxyvalerate) and epoxidized natural rubber, *Polym. Degrad. Stab.* 85 (2004) 947–955. doi:10.1016/j.polymdegradstab.2003.11.020.
- [168] E.-S. Park, H.K. Kim, J.H. Shim, H.S. Kim, L.W. Jang, J.-S. Yoon, Compatibility of

- poly(butadiene-co-acrylonitrile) with poly(L-lactide) and poly(3-hydroxybutyrate-co-3-hydroxyvalerate), *J. Appl. Polym. Sci.* 92 (2004) 3508–3513. doi:10.1002/app.20356.
- [169] E. Giménez, J.M. Lagarón, M.L. MasPOCH, L. Cabedo, J.J. Saura, Uniaxial tensile behavior and thermoforming characteristics of high barrier EVOH-based blends of interest in food packaging, *Polym. Eng. Sci.* 44 (2004) 598–608. doi:10.1002/pen.20054.
- [170] E. Giménez, J. Lagaron, R. Gavara, L. Cabedo, J.J. Saura, Study of the thermoformability of ethylene-vinyl alcohol copolymer based barrier blends of interest in food packaging applications, *J. Appl. Polym. Sci.* 96 (2004) 3851–3855. <http://onlinelibrary.wiley.com/doi/10.1002/app.13584/full> (accessed December 9, 2014).
- [171] I. Zembouai, S. Bruzaud, M. Kaci, A. Benhamida, Y. Corre, Y. Grohens, J.-M. Lopez-Cuesta, Synergistic Effect of Compatibilizer and Cloisite 30B on the Functional Properties of Poly (3-hydroxybutyrate- co -3-hydroxyvalerate)/ Polylactide Blends, *Polym. Eng. Sci.* 54 (2014) 2239–2251. doi:10.1002/pen.
- [172] I. Zembouai, M. Kaci, S. Bruzaud, A. Benhamida, Y.-M. Corre, Y. Grohens, A study of morphological, thermal, rheological and barrier properties of Poly(3-hydroxybutyrate-Co-3-Hydroxyvalerate)/polylactide blends prepared by melt mixing, *Polym. Test.* 32 (2013) 842–851. doi:10.1016/j.polymertesting.2013.04.004.
- [173] A. Monfared, A. Jalali-Arani, Morphology and rheology of (styrene-butadiene rubber/acrylonitrile-butadiene rubber) blends filled with organoclay: The effect of nanoparticle localization, *Appl. Clay Sci.* 108 (2015) 1–11. doi:10.1016/j.clay.2015.02.012.
- [174] J. Huitric, J. Ville, P. Médéric, M. Moan, T. Aubry, Rheological, morphological and structural properties of PE/PA/nanoclay ternary blends: Effect of clay weight fraction, *J. Rheol. (N. Y. N. Y.)* 53 (2009) 1101. doi:10.1122/1.3153551.
- [175] P.V. a. Arutchelvi, J., Sudhakar, M., Arkatkar, A., Doble, M. , Bhaduri, S., Uppara, Biodegradation of polyethylene and polypropylene, *Indian J. Biotechnol.* 7 (2008) 9–22.
- [176] M. Vert, Y. Doi, K.-H. Hellwich, M. Hess, P. Hodge, P. Kubisa, M. Rinaudo, F. Schué, Terminology for biorelated polymers and applications (IUPAC recommendations 2012), *Pure Appl. Chem.* 84 (2012).
- [177] ISO 17088:2012 Specifications for compostable plastics, (2012).
- [178] M.P. Arrieta, E. Fortunati, F. Dominici, E. Rayón, J. López, J.M. Kenny, PLA-PHB/cellulose based films: Mechanical, barrier and disintegration properties, *Polym. Degrad. Stab.* 107 (2014) 139–149. doi:10.1016/j.polymdegradstab.2014.05.010.
- [179] M.P. Arrieta, J. López, E. Rayón, a. Jiménez, Disintegrability under composting conditions of plasticized PLA-PHB blends, *Polym. Degrad. Stab.* (2014) 1–12. doi:10.1016/j.polymdegradstab.2014.01.034.
- [180] M.P. Arrieta, J. López, D. López, J.M. Kenny, L. Peponi, Development of flexible materials based on plasticized electrospun PLA-PHB blends: Structural, thermal, mechanical and disintegration properties, *Eur. Polym. J.* 73 (2015) 433–446. doi:10.1016/j.eurpolymj.2015.10.036.
- [181] M.P. Arrieta, E. Fortunati, F. Dominici, J. L??pez, J.M. Kenny, Bionanocomposite films based on plasticized PLA-PHB/cellulose nanocrystal blends, *Carbohydr. Polym.* 121 (2015) 265–275. doi:10.1016/j.carbpol.2014.12.056.
- [182] M.P. Arrieta, J. López, A. Hernández, E. Rayón, Ternary PLA-PHB-Limonene blends intended for biodegradable food packaging applications, *Eur. Polym. J.* 50 (2014) 255–270. doi:10.1016/j.eurpolymj.2013.11.009.
- [183] M.P. Arrieta, M.D. Samper, J. López, A. Jiménez, Combined Effect of Poly(hydroxybutyrate)

2. Marco teórico

- and Plasticizers on Polylactic acid Properties for Film Intended for Food Packaging, *J. Polym. Environ.* (2014) 460–470. doi:10.1007/s10924-014-0654-y.
- [184] M. Ramos, E. Fortunati, M. Peltzer, A. Jimenez, J.M. Kenny, M.C. Garrigós, Characterization and disintegrability under composting conditions of PLA-based nanocomposite films with thymol and silver nanoparticles, *Polym. Degrad. Stab.* (2016) 1–9. doi:10.1016/j.polymdegradstab.2016.05.015.
- [185] D. Puglia, E. Fortunati, D.A. D'Amico, L.B. Manfredi, V.P. Cyras, J.M. Kenny, Influence of organically modified clays on the properties and disintegrability in compost of solution cast poly(3-hydroxybutyrate) films, *Polym. Degrad. Stab.* (2014). doi:10.1016/j.polymdegradstab.2013.11.013.
- [186] F. Luzi, E. Fortunati, D. Puglia, R. Petrucci, J.M. Kenny, L. Torre, Study of disintegrability in compost and enzymatic degradation of PLA and PLA nanocomposites reinforced with cellulose nanocrystals extracted from *Posidonia Oceanica*, *Polym. Degrad. Stab.* 121 (2015) 105–115. doi:10.1016/j.polymdegradstab.2015.08.016.
- [187] N. Bitinis, E. Fortunati, R. Verdejo, I. Armentano, L. Torre, J.M. Kenny, M.Á. López-Manchado, Thermal and bio-disintegration properties of poly(lactic acid)/natural rubber/organoclay nanocomposites, *Appl. Clay Sci.* 93–94 (2014) 78–84. doi:10.1016/j.clay.2014.02.024.
- [188] D. Puglia, E. Fortunati, D. a. D'Amico, L.B. Manfredi, V.P. Cyras, J.M. Kenny, Influence of organically modified clays on the properties and disintegrability in compost of solution cast poly(3-hydroxybutyrate) films, *Polym. Degrad. Stab.* 99 (2014) 127–135. doi:10.1016/j.polymdegradstab.2013.11.013.
- [189] W. Sikorska, P. Dacko, M. Sobota, J. Rydz, M. Musioł, M. Kowalczyk, Degradation Study of Polymers from Renewable Resources and their Compositions in Industrial Composting Pile, *Macromol. Symp.* 272 (2008) 132–135. doi:10.1002/masy.200851219.
- [190] W. Sikorska, J. Richert, J. Rydz, M. Musioł, G. Adamus, H. Janeczek, M. Kowalczyk, Degradability studies of poly(l-lactide) after multi-reprocessing experiments in extruder, *Polym. Degrad. Stab.* 97 (2012) 1891–1897. doi:10.1016/j.polymdegradstab.2012.03.049.
- [191] W. Sikorska, M. Musiol, B. Nowak, J. Pajak, S. Labuzek, M. Kowalczyk, G. Adamus, Degradability of polylactide and its blend with poly[(R,S)-3-hydroxybutyrate] in industrial composting and compost extract, *Int. Biodeterior. Biodegrad.* 101 (2015) 32–41. doi:10.1016/j.ibiod.2015.03.021.
- [192] Y. Kumagai, Y. Kanesawa, Enzymatic degradation of microbial poly (3-hydroxybutyrate) films., *Die Makromol. Chemie.* 193 (1992) 53–57.
- [193] M. Scandola, M.L. Focarete, G. Adamus, W. Sikorska, I. Baranowska, S. Świerczek, M. Gnatowski, M. Kowalczyk, Z. Jedliński, Polymer Blends of Natural Poly(3-hydroxybutyrate-co-3-hydroxyvalerate) and a Synthetic Atactic Poly(3-hydroxybutyrate). Characterization and Biodegradation Studies, *Macromolecules.* 30 (1997) 2568–2574. doi:10.1021/ma961431y.
- [194] M. Musioł, H. Janeczek, S. Jurczyk, I. Kwiecień, M. Sobota, A. Marcinkowski, J. Rydz, (Bio)degradation studies of degradable polymer composites with jute in different environments, *Fibers Polym.* 16 (2015) 1362–1369. doi:10.1007/s12221-015-1362-5.
- [195] M. Rutkowska, K. Krasowska, A. Heimowska, G. Adamus, M. Sobota, M. Musioł, H. Janeczek, W. Sikorska, A. Krzan, E. Żagar, M. Kowalczyk, Environmental degradation of blends of atactic poly[(R,S)-3-hydroxybutyrate] with natural PHBV in baltic sea water and compost with activated sludge, *J. Polym. Environ.* 16 (2008). doi:10.1007/s10924-008-0100-0.

- [196] C. Kunze, H.E. Bernd, R. Androsch, C. Nischan, T. Freier, S. Kramer, B. Kramp, K.-P. Schmitz, In vitro and in vivo studies on blends of isotactic and atactic poly (3-hydroxybutyrate) for development of a dura substitute material, *Biomaterials*. 27 (2006). doi:10.1016/j.biomaterials.2005.05.095.
- [197] L. Jiang, J. Zhang, *Biodegradable Polymers and Polymer Blends*, 2012. doi:10.1016/B978-1-4557-2834-3.00006-9.
- [198] H. Abe, Y. Doi, H. Aoki, T. Akehata, Y. Hori, A. Yamaguchi, Physical properties and enzymatic degradability of copolymers of (R)-3-hydroxybutyric and 6-hydroxyhexanoic acids, *Macromolecules*. 28 (1995).
- [199] P. Klein, *Fundamentals of plastics thermoforming*., *Synthesis Lectures on Materials Engineering*, 2009.
- [200] M. Beltrán, A. Marcilla, *Tecnología de Polímeros, Procesado y Propiedades*., 2012.

3. Capítulo 1

On the use of TNPP as a chain extender in melt blended PHBV/clay nanocomposites: morphology, thermal stability, and mechanical properties

3. Capítulo 1

**On the use of TNPP as a chain extender in melt blended PHBV/clay nanocomposites:
morphology, thermal stability, and mechanical properties.**

Jennifer Gonzalez-Ausejo,¹ Estefania Sanchez-Safont,¹ Jose Gamez-Perez,¹ Luis Cabedo¹

¹ Polymer and Advanced Materials Group (PIMA), Universidad Jaume I, 12071, Castellon, Spain.

Journal of Applied Polymer Science (2015)

ABSTRACT

The influence of the incorporation of tris(nonylphenyl) phosphite (TNPP) as a chain extender on the morphology and thermal stability of poly(hydroxybutyrate-co-hydroxyvalerate) (PHBV)/clay nanocomposites obtained by melt mixing has been studied. Two different clays have been used: a laminar organomodified montmorillonite (Cloisite® 30B) and a tubular unmodified halloysite (HNT). The morphology of the so-obtained nanocomposites has been assessed by TEM, SEM, and WAXS, showing a partially exfoliated structure for PHBV/Cloisite® 30B nanocomposites, as well as a good dispersion of the HNT in the PHBV matrix. The crystallinity of the resulting nanocomposites, determined by DSC, does not change when clays or TNPP are added. An increase in the onset temperature of thermal degradation of PHBV has been obtained with the addition of TNPP, as determined by TGA. With regard to the effect of the nanoclays on the thermal stability of PHBV, the onset temperature of the PHBV/HNT nanocomposites is higher than that of the pure PHBV, while this trend is not observed for the nanocomposites containing Cloisite® 30B. The addition of TNPP to the PHBV/Cloisite® 30B nanocomposites resulted in an improved thermal stability; however, for the HNT nanocomposites, the TNPP does not seem to have a significant effect. For all studied systems, it was shown that the variation of mechanical properties of the nanocomposites is due to the reinforcing effect of the nanoclays on the PHBV matrix. In the case of TNPP it is due to the increased molecular weight and formation of a long chain branching structure.

GRAFICAL ABSTRACT

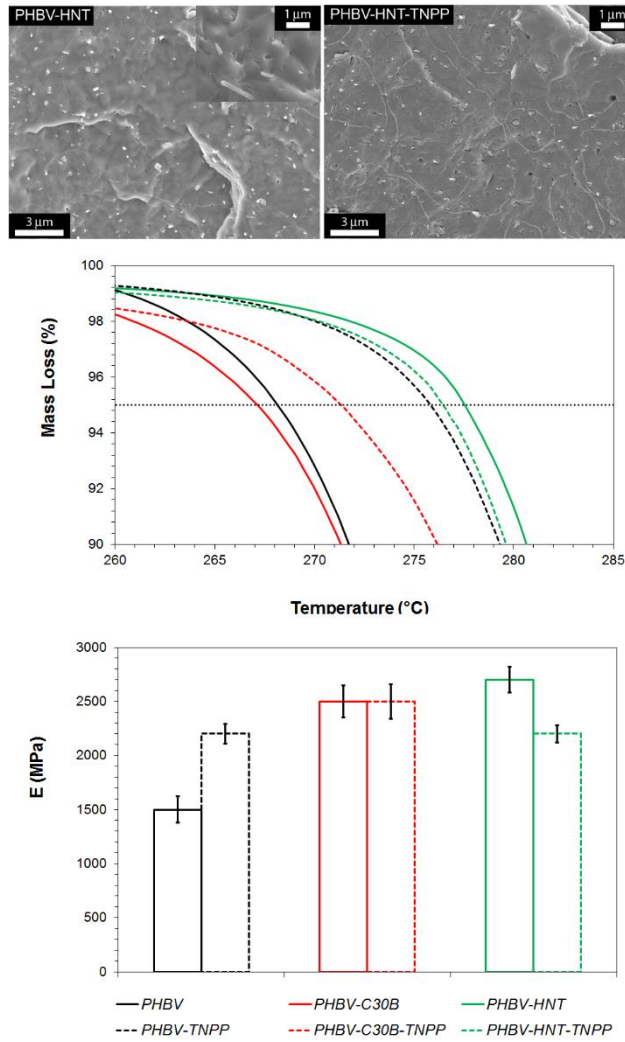


Fig 3.1: Graphical abstract of the work named On the use of TNPP as a chain extender in melt blended PHBV/clay nanocomposites: morphology, thermal stability, and mechanical properties.

3.1. INTRODUCTION

Poly(hydroxybutyrate-co-hydroxyvalerate) (PHBV), a biodegradable copolyester from the polyhydroxyalkanoate family (PHA), has gained a lot of attention because of its fast biodegradability and biocompatibility as well as a non-food-competitive origin [1]. Particularly in the packaging field, PHBV has shown a great interest because its inertness and chemical stability that makes it suitable for applications as films for food contact material with any type of food [2]. It has been suggested that PHBV could replace polypropylene [3] or poly(ethylene terephthalate) [4] in many applications where it would not be necessary to modify their processing. In spite of the significant potential of PHBV to substitute commodity polymers, it still presents a number of property and processing shortcomings that hinder its use in many applications. [5] When compared to other linear polymers, PHBV has shown lower mechanical and gas barrier properties, as well as lower thermal resistance during processing [4,6].

Nanotechnology brings significant opportunities to improve the applicability of PHBV to the food packaging field. [5,7] The increase in mechanical properties of biopolymers by incorporating low amounts of nanoparticles has been widely reported [6,8,9]. Indeed, some works have shown that the use of nanocomposites in food packaging applications, when properly prepared, is harmless and free potential migration issues. [7] The obtaining of polymer nanocomposites has been reported to be a promising way to improve the barrier properties against gases, aromas, and water vapor. Some reported nanofillers are carbon nanotubes, nanoclays and halloysite nanotubes, among others [10,11].

The montmorillonite is the most commonly used nanoclay in the field of polymer nanocomposites [8]. It is a natural clay belonging to the family of 2:1 layered silicates, also called 2:1 phyllosilicates. Its structure consists of layers made up of two tetrahedrally coordinated silicon atoms bonded to an edge-shared octahedral sheet of either aluminum or magnesium hydroxide. This nanoclay requires surface modification (organomodification) to achieve a good degree of delamination when mixed with polymers. The chemicals more widely used for organomodification of montmorillonites are alkylammonium cations. In the case of PHBV nanocomposites, the use of organomodified clays containing surfactants appears to be a suitable way to improve their affinity to the polymer and dispersion within the matrix [12–14]. However, the addition of organomodified

3. Capítulo 1

clays can lead to higher polymer degradation during melt processing [12–14], due to a catalytic effect of their decomposition products [14–16].

Recently, halloysite nanotubes (HNTs) have attracted interest as nanoparticles for biopolymers because they are economical and abundantly available and have rich functionality, good biocompatibility, and high mechanical strength [17]. Halloysite belongs to the kaolin group of clay minerals. It exhibits a predominantly hollow tubular structure in the nanoscale range and a large aspect ratio [18].

As mentioned before, the degradation of biopolyesters, more specifically PHBV, during processing in molten conditions is a factor that inevitably limits the range of applications [19]. The use of chain extenders is a convenient approach for improving the thermal stability of biopolyesters during processing [20–29]. The chain extension is a reaction that avoids a drop in molecular weight. The reaction between carboxylic end groups on polyesters and the functional groups of chain extenders, such as hydroxyl, amine, anhydride, epoxy, or carboxylic acid, are the key reactions for improving thermal resistance [30]. This approach has been successfully applied to blends from several matrices [20,21,26–28].

Some studies have developed the use of DCP [31,32] or Joncryl® ADR-4368 [33] in PHBV. Haene et al. [31] studied the branching behavior of PHBV using low levels of DCP, reporting a branching process of PHBV observed from the increase in strain hardening with the addition of higher concentrations of DCP. Fei et al. [32] studied the cross-linking of PHBV using a high level of DCP and observed enhanced melt viscosity and mechanical properties without compromising the biodegradability. Duangphet et al. [33] studied the effect of an epoxy-functionalized chain extender (Joncryl® ADR-4368 S) on degradation during melt blending of PHBV conducted in a twin screw extruder, showing an improvement in the resistance to thermal decomposition of PHBV, an enhancement of PHBV melt viscosity, and also a reduction of the crystallization rate by introducing the chain extender due to the increase in molecular weight and chain rigidity.

The use of chain extenders in the production of polymer-based nanocomposites has been studied [20–22,24]. According to Najafi et al. [20–22], the incorporation of a chain extender into the nanocomposites had a profound effect on controlling the degradation and also increasing the molecular weight, resulting in an increase of the polymer viscosity [20–22]. Also, Meng et al. [24]

found that the chain extenders have a remarkable stabilization effect on PLA/clay nanocomposites without negatively affecting the clay dispersion [24].

Tris(nonylphenyl) phosphite (TNPP) has been successfully used as chain extender in other matrices [26–28] leading to thermal stabilization with low contents. Indeed, TNPP is characterized by being suitable for food contact [34], thus being suitable for food packaging applications. However, to the best of our knowledge, its effect in PHBV has never been studied.

Within this context, the aim of this study was to evaluate the effect of the addition of TNPP as a chain extender with two types of clays (Cloisite®30B and halloysite nanotubes) on the morphology, thermal and mechanical properties of PHBV nanocomposites for food packaging applications.

3.2. EXPERIMENTAL

3.2.1. Materials

Poly(hydroxybutyrate-co-hydroxyvalerate) (PHBV) with 3 mol% hydroxyvalerate content was purchased from Tianan Biologic Material Co. (Ningbo, P.R. China) in pellet form (ENMAT Y1000P). Two different commercial nanoclays were used in this study: organomodified montmorillonite Cloisite® 30B (hereafter referred to as C30B) containing a methyl bis-2- hydroxyethyl ammonium quaternary salt, supplied by Southern Clay Products; and halloysite (HNT), an unmodified tubular clay from NaturalNano Inc. The chain extender used was tris(nonylphenyl) phosphite (TNPP) supplied by Sigma Aldrich.

3.2.2. Nanocomposite preparation

PHBV and the clays used in this study were dried under vacuum at 80 °C for 2 h before use, while the chain extender was used as received. The PHBV blends and nanocomposites were obtained by melt blending using an internal mixer (Rheomix 3000P ThermoHaake, Karlsruhe, Germany) during a mixing time of less than 6 minutes at a temperature of 180 °C and rotor speed of 100 rpm. The mixer is provided with a software for displaying the variation of temperature (chamber and melt) and the torque during mixing. According to the record of the sensor of melt temperature during mixing, the melt temperature never reached 195°C, which guaranteed that there was no severe

3. Capítulo 1

thermal degradation during blending. Plates (0.8 mm thick) and films (0.1 mm thick) were obtained from the blends by melting in a hot-plate press at 185 °C and applying during 2 min for premelting followed by 3 bar for 3. Plates were used for morphological and thermal characterization, while films were used for the mechanical characterization. All the samples were stored in a vacuum desiccator at ambient temperature during two weeks to allow full crystallization to take place [35–37].

Samples of both PHBV (referred to as neat PHBV) and PHBV with 1 wt. % TNPP (PHBV-TNPP) were processed. The nomenclature used for the nanocomposites is as follows: PHBV-C30B and PHBV-HNT for the systems containing 5 wt. % of Cloisite 30B and halloysite nanotubes, respectively, and PHBV-C30B-TNPP and PHBV-HNT-TNPP for the systems containing 5 wt. % of Cloisite 30B and halloysite nanotubes together with 1 wt. % TNPP as a chain extender.

3.2.3. Characterization

Transmission electron microscopy (TEM) of the nanocomposites was performed using a Jeol 2100 operated at 200 kV. The ultrathin sections with a thickness of 80 nm were prepared at room temperature using an RMC ultramicrotome (Model Powertome XL). The so-obtained films were placed on a carbon-coated copper grid for observation.

The morphology of the cryofractured surface of PHBV nanocomposites was evaluated by Scanning Electron Microscopy (SEM) using a JEOL 7001F. The samples were fractured in liquid nitrogen and subsequently coated by sputtering with a thin layer of Pt.

Wide angle X-ray diffraction (WAXS) measurements were performed using a Bruker AXS D4 Endeavour diffractometer. The samples were scanned at room temperature in reflection mode using incident Cu K α radiation ($k = 1.54 \text{ \AA}$), while the generator was set up at 40 kV and 40 mA. The data were collected over a range of scattering angles (2θ) of 2–30°. The basal spacing (d-spacing) of the clays was estimated from the (001) diffraction peak using Bragg's law, where λ is the wavelength of incident wave:

$$\lambda = 2 \cdot d \cdot \sin\theta \quad (3.1)$$

The thermal stability of the nanocomposites was investigated by means of thermogravimetric analysis (TGA) using a TG-SDTA Mettler Toledo model TGA/SDTA851e/LF/1600. The samples were heated from 50 to 900 °C at a heating rate of 10 °C/min under nitrogen flow. The characteristic temperatures $T_{5\%}$ and T_d corresponded, respectively, to the initial decomposition temperature (5% of degradation) and to the maximum degradation rate temperature measured at the DTG peak maximum.

Differential scanning calorimeter (DSC) experiments were conducted using a PerkinElmer DSC-7. The weight of the DSC samples was typically 6 mg. Samples were first heated from 45 to 200 °C at 40 °C/min, kept for 1 min at 200 °C, cooled down to 45 °C at 10 °C/min, and then finally heated to 200 °C at 10 °C/min. The crystallization temperature (T_c), melt temperature (T_m), and melting enthalpy (ΔH_m) were determined from the cooling and second heating curve. T_m and ΔH_m were taken as the peak temperature and the area of the melting endotherm, respectively. The crystallinity (X_c) of the PHBV phase was calculated by the following expression:

$$X_c (\%) = \frac{\Delta H_m}{w \cdot \Delta H_m^0} \cdot 100 \quad (3.2)$$

where ΔH_m (J/g) is the melting enthalpy of the polymer matrix, ΔH_m^0 is the melting enthalpy of 100% crystalline PHBV (perfect crystal) (146 J/g), and w is the polymer weight fraction of PHBV in the blend [9]. The DSC instrument was calibrated with an indium standard before use.

Tensile properties were measured in a universal testing machine (Instron 4469) at a crosshead speed of 10 mm/min and room temperature. All samples were conditioned under ambient conditions (25 °C and 50% R.H. for 24 hours). Tests were carried out according to ASTM D638 using films of approximately 100- μ m thickness prepared by hot press. Five specimens of each sample were tested and the average results with standard deviation were reported.

3.3. RESULTS AND DISCUSSION

3.3.1. Morphology

The morphology of the PHBV nanocomposites was evaluated by means of SEM, TEM, and WAXS. Figures 3.2.a and 3.2.b present the TEM micrographs of the PHBV nanocomposites with 5 wt. % of C30B and HNT, respectively.

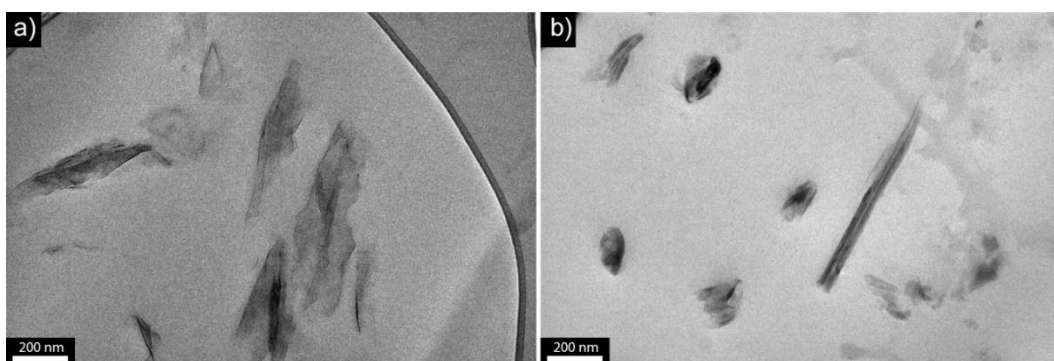


Fig. 3.2: TEM micrograph of (a) PHBV-C30B and (b) PHBV-HNT

The effect of nanoclays on the properties of the polymer matrix is highly dependent on the degree of dispersion achieved during mixing [9]; hence sometimes surface modification of the nanoclays is required in order to increase their compatibility.

As seen in Fig. 3.2.a, the presence of small intercalated structures with a large aspect ratio (tactoids) in the PHBV-C30B is observed. Nevertheless, the nanocomposite shows a good dispersion of the montmorillonite platelets, also indicating that a high degree of delamination of the clay during melt processing was achieved.

The TEM micrograph of the PHBV-HNT sample (Fig. 3.2.b) shows the presence of isolated nanotubes. In this figure, it is possible to identify a parallel-oriented nanotube showing the internal structure of the halloysite, which can be described as a hollow tubular morphology produced by the stacking of the clay mineral layers. From the TEM pictures, the dimensions of the halloysite tubes could be estimated: a length below 1 μm and external and internal nanotube diameters of 70 and 25 nm, respectively. The good dispersion of the unmodified halloysite can be ascribed to its structure; i.e. the surface of HNTs is comprised of siloxane and hydroxyl groups, which gives

halloysites potential for the formation of hydrogen bonds and hence improves the dispersion in some polymer matrixes without any chemical modification, especially when compared to other two-dimensional nanoclay fillers such as montmorillonites [38,39].

SEM micrographs of PHBV nanocomposites with and without TNPP are presented in Fig. 3.3. In the case of montmorillonite nanocomposites (Figs. 3.3.a and 3.3.b), a strong adhesion between the clay and the polymer matrix can be deduced from the look of the platelets, covered with the polymer matrix. In these figures it is possible to observe the presence of individual platelets (indicated with an arrow), as well as a good dispersion, in agreement with the TEM micrographs. Hence, it can be inferred that an effective mixing has been achieved.

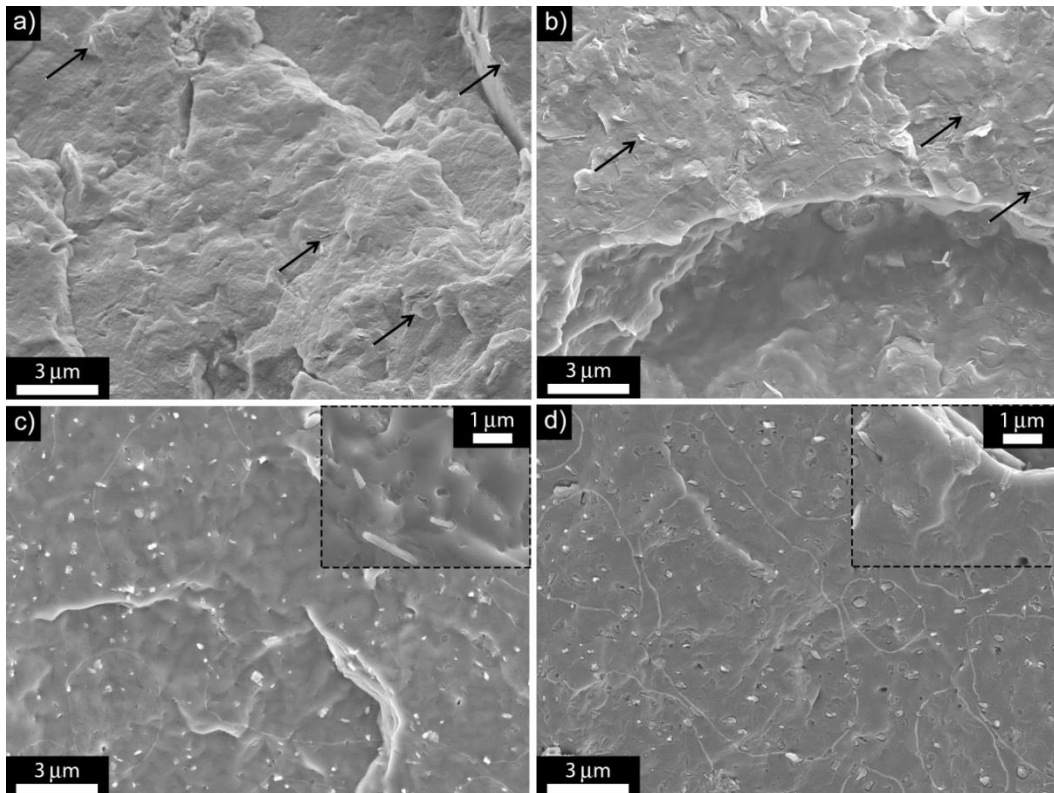


Fig. 3.3: SEM images of the fracture surface of a) PHBV-C30B, b) PHBV-C30B-TNPP, c) PHBV-HNT, and d) PHBV-HNT-TNPP

The SEM micrographs of PHBV-HNT nanocomposites present a uniform dispersion of the halloysite nanotubes in both cases (with and without TNPP), shown as white dots in Fig. 3.3.c and 3.3.d. These

3. Capítulo 1

micrographs are in agreement with TEM observations. However, different surface interaction between the halloysite and the PHBV can be observed depending on the presence of the chain extender. The sample without TNPP exhibits a good degree of adhesion of the polymer matrix on the nanoclay surface. The sample containing TNPP shows a slight detachment of the nanotubes from the polymer matrix. A possible explanation for this behavior is that the TNPP is partially absorbed on the surface of the nanotubes, thus leading to a decrease in the interaction between the nanoclay surface and the polymer matrix.

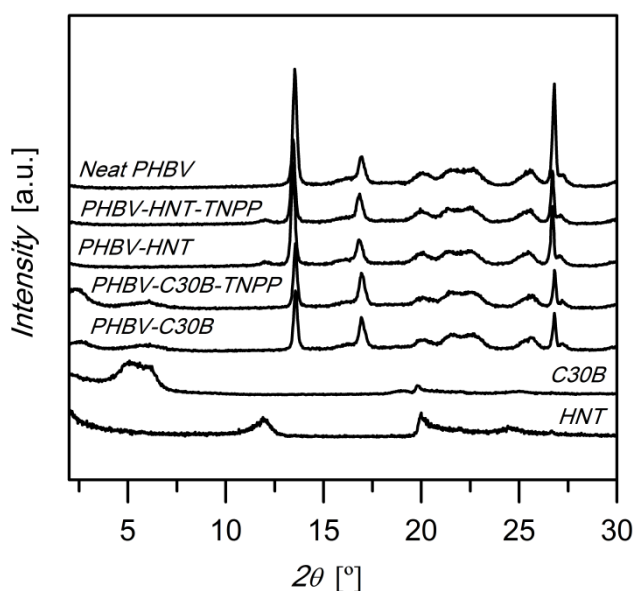


Fig 3.4: WAXS pattern of neat PHBV, PHBV-C30B, and PHBV-HNT nanocomposites

The WAXS diffractograms of the clays and PHBV nanocomposites are shown in Fig. 3.4. The PHBV diffractogram presents three main peaks at 2θ values of 13° , 17° , and 26° . The first two peaks can be associated with the (020) and (110) reflections of the orthorhombic lattice of the PHBV respectively. The most intense peak at $2\theta = 26^\circ$ corresponds to the (002) reflexion of the boron nitride, which is present as a nucleating agent in the commercial grade used in this work. No noticeable difference in the peak positions and relative intensities can be observed when the clays or the TNPP are introduced; therefore, it can be concluded that the crystalline form of the PHBV is not affected by the addition of these nanoclays or the chain extender.

The diffraction pattern of C30B exhibits a peak at $2\theta = 5^\circ$, corresponding to a basal spacing (001) of 1.76 nm according to the Bragg equation. The PHBV-C30B diffractogram shows the peak associated with the basal reflection of the C30B, which suggests that fully exfoliated morphology has not been achieved. However, a shift towards lower angles is observed, indicating an increase in the interlayer gallery, associated with a predominantly intercalated morphology.

Regarding the samples containing HNTs, it is possible to observe the most intense diffraction peak of HNT (001) at $2\theta = 11.95^\circ$ (corresponding to a basal spacing of 0.74 nm). No changes were observed in the shape or position of this peak in the PHBV-HNT nanocomposites. This result indicates that after blending no changes occur in the tubular structure of the primary particles of halloysite. The addition of chain extender does not affect either the crystalline structure of PHBV or the interlayer distance of the clay.

3.3.2. Thermal characterization

TGA experiments were carried out to investigate the effect of the addition of clay and chain extenders on the thermal stability of PHBV. Figure 3.5 plots the mass loss and the DTG versus temperature for the neat PHBV and PHBV nanocomposites, while Table 3.I summarizes the values of $T_{5\%}$ and T_d for all the samples studied.

The thermal degradation of neat PHBV consists of a single weight loss step between 240 and 320 °C (Figure 3.5), according to the random chain scission reaction [40]. The maximum rate of mass loss takes place at 285 °C and $T_{5\%}$ (the temperature at which the mass loss is 5%) is of 268 °C. Some differences in the thermal degradation of PHBV are observed with the incorporation of the clays.

Once the degradation has begun, the reaction rate clearly decreases with respect to the pure polymer, showing a higher T_d with respect PHBV, from 285 to 288 and 294 °C for C30B and HNT, respectively. This behavior can be explained by the fact that the clays, together with the solid degradation products, generate a dense coating that hinders the development of further degradation by opposing a strong mass transport resistance to the volatile agents involved in the reaction, resulting in a decrease of the degradation kinetics [41]. These results are in agreement with the work reported by Bittmann et al. and Bruzaud et al. in which different nanoclays (non-

3. Capítulo 1

modified montmorillonite, bentonite and Cloisite®15A) showed similar trends in thermogravimetric analysis.

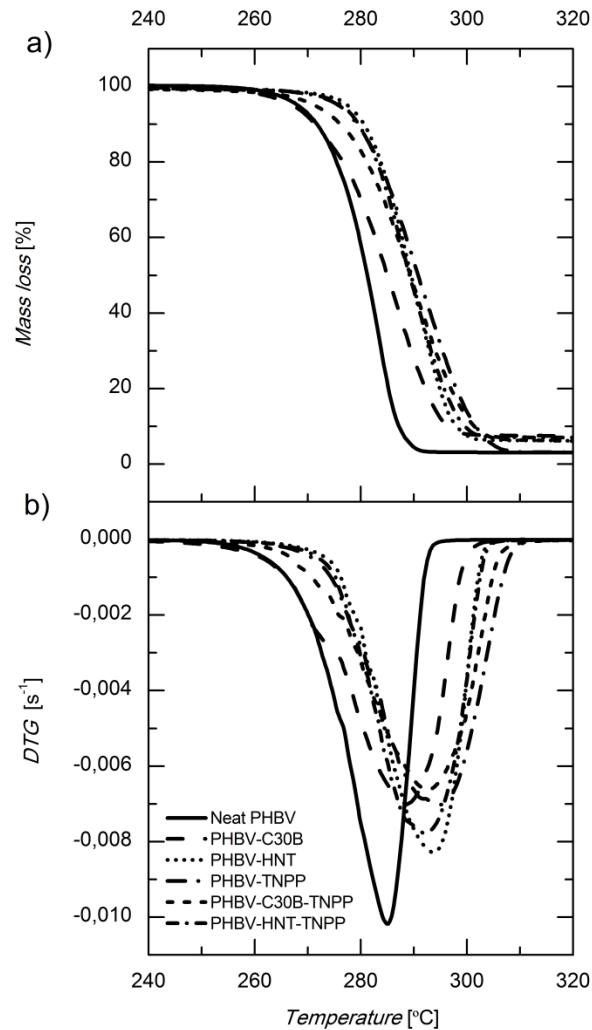


Fig. 3.5: TGA and DTG curves of PHBV and PHBV/clay nanocomposites with and without chain extender

With respect to the presence of HNT in the PHBV matrix, it also increases the thermal stability of PHBV, with a rise in $T_{5\%}$ from 268 to 277 °C. The sample containing C30B exhibits a degradation onset similar to that of the neat PHBV, as derived from the $T_{5\%}$. In other works, it has been reported a decrease on the $T_{5\%}$ for PHBV/C30B composites [42–45]. This behaviour is generally attributed to the clay modifiers that may have a catalytic action in the degradation of PHBV [15]. In our case,

the opposed phenomena of stabilizing by the clays [46,47] compensates the catalytic degradation generated by the organomodifier [12–14], resulting in no significant variation on the $T_{5\%}$. Additionally, it has been suggested that the water adsorbed to the clays may contribute to accelerate the degradation rate in clay/PHBV composites, hindering the thermal stabilizing effect of the clays [42]. The thermal history and severity of processing conditions, especially with clays, may have also an influence in the degradation kinetics of the samples [48].

The effect of the addition of TNPP to both neat PHBV and the nanocomposites on the thermal degradation behavior can be seen in Fig. 3.5. As expected, the presence of the chain extender improves the thermal stability of PHBV, as derived from the increases of $T_{5\%}$ and T_d by 8 and 10 °C, respectively. This issue is of special relevance since during food packaging operations there are many thermic cycles (film processing, stretching, thermoforming, hot sealing, etc.) where some local thermal degradation can occur, being the products of such degradation susceptible to migrate towards the content of the package [49]. This trend is in concordance with the literature where the TNPP has been used as chain extender in other matrices [26–28].

The addition of TNPP to the sample containing the C30B clay revealed a shift of the curve towards higher temperatures, thus showing an increase of ca. 5 °C in both $T_{5\%}$ and T_d with respect to that without the chain extender. These results would indicate that the addition of TNPP to PHBV/clay nanocomposites may improve their thermal resistance. The PHBV-HNT-TNPP sample does not show relevant changes in thermal degradation when compared with that without the chain extender. This lack of a synergetic effect between the TNPP and the halloysite could be explained by the fact that, as inferred from the SEM analysis, the TNPP is partially adsorbed over the surface of the clay, thus decreasing the chain extender activity.

DSC experiments were conducted in order to evaluate the influence of the addition of the nanoclays and chain extender on the crystallization characteristics of PHBV. Table 3.1 summarizes the crystallization and melting temperatures, crystallization enthalpy, and degree of crystallinity of all the samples studied in this work.

After analyzing the resulting DSC parameters, it can be appreciated that the crystallization temperature (T_c) of PHBV was not significantly modified when the nanoclays were incorporated. The degree of crystallinity (X_c) also remained similar, at around 66%, in agreement with other works

3. Capítulo 1

and a similar processing history [33,50]. During the second heating scan it could be observed that the peak melting temperature (T_m) decreased by about 5 °C with C30B and 3°C with HNT. These results suggest that nanoclays make the formation of thick lamella more difficult than neat PHBV, being more pronounced in the case of C30B.

Table 3.1: DSC and TGA data of the samples studied.

	TGA parameters		DSC parameters			
	T_c (°C)	T_m (°C)	ΔH_c (J/g)	X_c (%)	$T_{5\%}$ (°C)	T_d (°C)
Neat PHBV	115	169	96	66	268	285
PHBV-C30B	115	164	96	66	267	288
PHBV-HNT	115	166	98	67	277	294
PHBV-TNPP	113	166	97	66	276	295
PHBV-C30B-TNPP	114	165	100	68	272	293
PHBV-HNT-TNPP	115	169	97	66	277	292

When TNPP was added to PHBV, a small decrease on T_m is detected, pointing to some reduction in lamellar thickness; but when it is combined with C30B or HNT, the T_m increases slightly with respect to the composites without TNPP. In any case, it is considered that the variations in T_c , X_c and T_m shown are not of great significance, indicating that 1%wt of TNPP has little interference with the crystallization processes of PHBV.

3.3.3. Mechanical properties

Tensile tests to rupture were conducted on hot-pressed films for all the samples studied. Figure 3.6 shows the strain-stress representative curves for the neat PHBV and PHBV nanocomposites. From the stress-strain curves were obtained the average values of Young's modulus, tensile strength and elongation at break of PHBV with the addition of clays and TNPP, these values are shown in Figure 3.7. The Young's modulus of PHBV showed significant increases of 69 and 80% with the addition of 5 wt.% C30B and HNT, respectively. Regarding the tensile strength, increases of 12 and 34% were detected with the addition of both C30B and HNT. This enhancement in stiffness and tensile strength of PHBV/clay nanocomposites was at the expense of a significant reduction in the elongation at break (see Fig. 3.7.c). In this sense, drops of 63 and 50% in the elongation at break can be observed with the addition of 5 wt.% C30B and HNTs, respectively. Altogether these results show a clear reinforcing effect of the nanoclays on the PHBV matrix. The

higher reinforcement observed for the samples containing HNTs as compared to the ones with montmorillonite platelets can be explained by the higher stiffness and length-to-diameter aspect ratio of the nanotubes. This behavior has been also reported in other works [12,39,46,51].

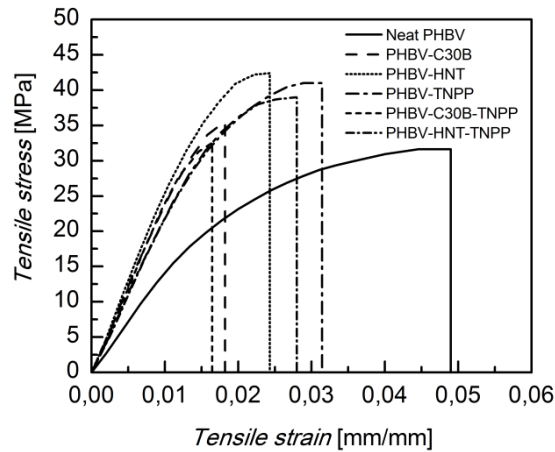


Fig. 3.6: Stress-strain curves of PHBV and PHBV/clay nanocomposites with and without chain extender

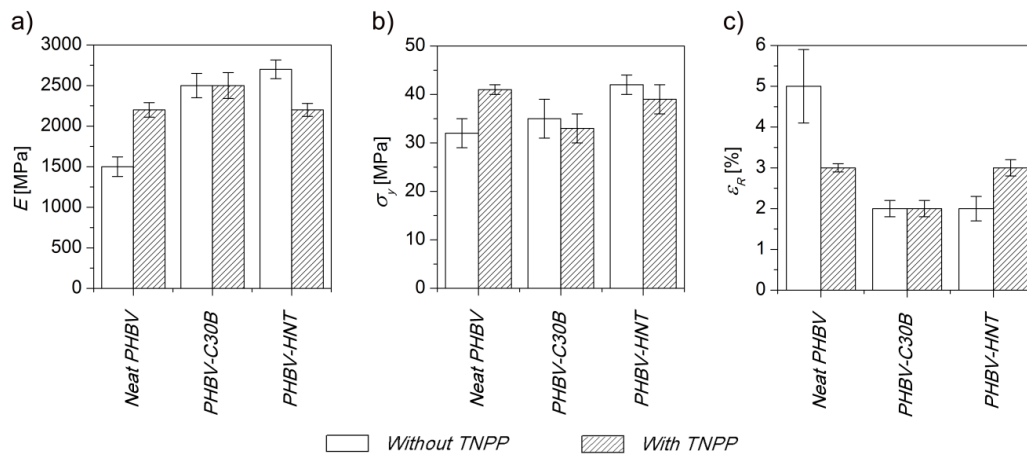


Fig. 3.7: Young's modulus (E), tensile strength (σ_y), and elongation at break (ϵ_R) of PHBV/clay nanocomposites with and without chain extender

The addition of TNPP to the neat PHBV resulted in increases in the Young's modulus (44%) and the tensile strength (30%), similar to those obtained by the addition of nanoclays. Some studies with PCL and PLA showed that the increase in the Young's modulus and tensile strength with the

3. Capítulo 1

addition of chain extenders could be ascribed to the increased molecular weight, together with the formation of a long chain branching structure [21,52,53]. The strain at break of PHBV containing the chain extender decreases compared to that of the original polymer. This can be explained by the fact that the increased density of entanglements of the polymer structure with the long chain branching hinders the slipping of the polymer chains [21,54,55].

Regarding the combined effect of the nanoclays with the TNPP on the mechanical properties of PHBV, surprisingly, no relevant changes were observed when TNPP was added to PHBV-C30B nanocomposites. However, an increase in elongation at break and a decreased Young's modulus and tensile strength with respect to the PHBV-HNT nanocomposite were observed. Such different behavior could be attributed to the effect of partial absorption of TNPP on the clay surface discussed previously on the morphological and thermal stability analysis. This can also explained why mechanical properties of the PHBV/HNT/TNPP nanocomposites are similar to those of PHBV/TNPP, since the reinforcement of the HNT is limited by the partial absorption of the TNPP on its surface. These results suggest that the properties of PHBV/HNT nanocomposites could be improved by modifying the mixing procedures, in order to minimize the absorption of TNPP on the active surface of HNT.

The improvement on mechanical properties opens up the possibility to reduce thickness in food packaging products, thus decreasing the overall costs while preserving the other characteristics of the package. It is worthwhile to recall that this type of industry uses large amounts of raw material and a reduction of 5-10% in volume may have a huge impact of the final economic and environmental balance of the package.

3.4. CONCLUSIONS

PHBV nanocomposites with two different clays (Cloisite®30B and halloysite nanotubes) and a chain extender (TNPP) were successfully obtained by melt blending. Favorable morphologies were achieved during processing for both nanoadditives (i.e. predominantly intercalated morphology in the PHBV-C30B and good distribution of halloysite nanotubes within the polymer matrix) as derived from TEM, SEM, and WAXS experiments.

The properties of such compounds are characterized by an increase in the thermal stability of PHBV through incorporation of TNPP as a chain extender or HNT. The addition of C30B only improves the thermal stability by decreasing the degradation rate. The crystallization temperature and overall crystallinity of the compounds was not altered by the addition of clays or TNPP.

Regarding the mechanical properties, the nanocomposites prepared with C30B and HNT revealed a reinforced behavior when compared to the neat PHBV, with higher stiffness and tensile strength and a decreased elongation at break. However, no relevant changes were observed when TNPP was added to PHBV nanocomposites.

ACKNOWLEDGEMENTS

Financial support for this research from Ministerio de Economía y Competitividad (project MAT2012-38947-C02-01), Generalitat Valenciana (GV/2014/123), and Pla de Promoció de la Investigació de la Universitat Jaume I (PREDOC/2012/32) is gratefully acknowledged. The authors are also grateful to Raquel Oliver and José Ortega for experimental support.

REFERENCES

- [1] R.W. Lenz, R.H. Marchessault, Bacterial polyesters: biosynthesis, biodegradable plastics and biotechnology., *Biomacromolecules*. 6 (2005) 1–8. <http://www.scopus.com/inward/record.url?eid=2-s2.0-14044254667&partnerID=tZOtx3y1> (accessed January 14, 2015).
- [2] V. Chea, H. Angellier-Coussy, S. Peyron, D. Kemmer, N. Gontard, Poly(3-hydroxybutyrate-co-3-hydroxyvalerate) films for food packaging: Physical-chemical and structural stability under food contact conditions, *J. Appl. Polym. Sci.* (2015) Article in press. doi:10.1002/app.41850.
- [3] D.Z. Bucci, L.B.B. Tavares, I. Sell, PHB packaging for the storage of food products, *Polym. Test.* 24 (2005) 564–571. doi:10.1016/j.polymertesting.2005.02.008.
- [4] D. Cava, E. Gimenez, R. Gavara, J.M. Lagaron, Comparative Performance and Barrier Properties of Biodegradable Thermoplastics and Nanobiocomposites versus PET for Food Packaging Applications, *J. Plast. Film Sheeting*. 22 (2006) 265–274. <http://www.scopus.com/inward/record.url?eid=2-s2.0-33845203640&partnerID=tZOtx3y1> (accessed January 14, 2015).
- [5] J.M. Lagaron, A. Lopez-Rubio, Nanotechnology for bioplastics: opportunities, challenges and strategies, *Trends Food Sci. Technol.* 22 (2011) 611–617. doi:10.1016/j.tifs.2011.01.007.
- [6] J.W. Rhim, H.M. Park, C.S. Ha, Bio-nanocomposites for food packaging applications, *Prog. Polym. Sci.* 38 (2013) 1629–1652. doi:10.1016/j.progpolymsci.2013.05.008.

3. Capítulo 1

- [7] J.M. Lagarón, L. Cabedo, D. Cava, J.L. Feijoo, R. Gavara, E. Gimenez, Improving packaged food quality and safety. Part 2: nanocomposites., *Food Addit. Contam.* 22 (2005) 994–998. doi:10.1080/02652030500239656.
- [8] P. Bordes, E. Pollet, L. Averous, Nano-biocomposites: Biodegradable polyester/nanoclay systems, *Prog. Polym. Sci.* 34 (2009) 125–155. doi:10.1016/j.progpolymsci.2008.10.002.
- [9] M.D. Sanchez-Garcia, J.M. Lagaron, Novel clay-based nanobiocomposites of biopolyesters with synergistic barrier to UV light, gas, and vapour, *J. Appl. Polym. Sci.* 118 (2010) 188–199. doi:10.1002/app.31986.
- [10] J.-W. Rhim, H.-M. Park, C.-S. Ha, Bio-nanocomposites for food packaging applications, *Prog. Polym. Sci.* 38 (2013) 1629–1652. doi:10.1016/j.progpolymsci.2013.05.008.
- [11] M.M. Reddy, S. Vivekanandhan, M. Misra, S.K. Bhatia, A.K. Mohanty, Biobased plastics and bionanocomposites: Current status and future opportunities, *Prog. Polym. Sci.* 38 (2013) 1653–1689. doi:10.1016/j.progpolymsci.2013.05.006.
- [12] L.N. Carli, J.S. Crespo, R.S. Mauler, PHBV nanocomposites based on organomodified montmorillonite and halloysite: The effect of clay type on the morphology and thermal and mechanical properties, *Compos. Part A Appl. Sci. Manuf.* 42 (2011) 1601–1608. doi:10.1016/j.compositesa.2011.07.007.
- [13] L. Cabedo, D. Plackett, E. Giménez, J.M. Lagarón, Studying the degradation of polyhydroxybutyrate-co-valerate during processing with clay-based nanofillers, *J. Appl. Polym. Sci.* 112 (2009) 3669–3676. doi:10.1002/app.29945.
- [14] P. Bordes, E. Hablot, E. Pollet, L. Avérous, Effect of clay organomodifiers on degradation of polyhydroxyalkanoates, *Polym. Degrad. Stab.* 94 (2009) 789–796. doi:10.1016/j.polymdegradstab.2009.01.027.
- [15] F. Bellucci, G. Camino, A. Frache, A. Sarra, Catalytic charring–volatilization competition in organoclay nanocomposites, *Polym. Degrad. Stab.* 92 (2007) 425–436. doi:10.1016/j.polymdegradstab.2006.11.006.
- [16] E. Hablot, P. Bordes, E. Pollet, L. Avérous, Thermal and thermo-mechanical degradation of poly(3-hydroxybutyrate)-based multiphase systems, *Polym. Degrad. Stab.* 93 (2008) 413–421. doi:10.1016/j.polymdegradstab.2007.11.018.
- [17] Y.-F. Shi, Z. Tian, Y. Zhang, H.-B. Shen, N.-Q. Jia, Functionalized halloysite nanotube-based carrier for intracellular delivery of antisense oligonucleotides., *Nanoscale Res. Lett.* 6 (2011) 608–614. doi:10.1186/1556-276X-6-608.
- [18] L. Guimarães, A.N. Enyashin, G. Seifert, H.A. Duarte, Structural, Electronic, and Mechanical Properties of Single-Walled Halloysite Nanotube Models, *J. Phys. Chem. C.* 114 (2010) 11358–11363. doi:10.1021/jp100902e.
- [19] Q.-S. Liu, M.-F. Zhu, W.-H. Wu, Z.-Y. Qin, Reducing the formation of six-membered ring ester during thermal degradation of biodegradable PHBV to enhance its thermal stability, *Polym. Degrad. Stab.* 94 (2009) 18–24. doi:10.1016/j.polymdegradstab.2008.10.016.
- [20] N. Najafi, M.C. Heuzey, P.J. Carreau, Crystallization behavior and morphology of polylactide and PLA/clay nanocomposites in the presence of chain extenders, *Polym. Eng. Sci.* 53 (2013) 1053–1064. doi:10.1002/pen.23355.
- [21] N. Najafi, M.C. Heuzey, P.J. Carreau, P.M. Wood-Adams, Control of thermal degradation of polylactide (PLA)-clay nanocomposites using chain extenders, *Polym. Degrad. Stab.* 97 (2012) 554–565. doi:10.1016/j.polymdegradstab.2012.01.016.

- [22] N. Najafi, M.C. Heuzey, P.J. Carreau, Polylactide (PLA)-clay nanocomposites prepared by melt compounding in the presence of a chain extender, *Compos. Sci. Technol.* 72 (2012) 608–615. doi:10.1016/j.compscitech.2012.01.005.
- [23] R. Al-Itry, K. Lamnawar, A. Maazouz, Improvement of thermal stability, rheological and mechanical properties of PLA, PBAT and their blends by reactive extrusion with functionalized epoxy, *Polym. Degrad. Stab.* 97 (2012) 1898–1914. doi:10.1016/j.polymdegradstab.2012.06.028.
- [24] Q. Meng, M.-C. Heuzey, P.J. Carreau, Control of thermal degradation of polylactide/clay nanocomposites during melt processing by chain extension reaction, *Polym. Degrad. Stab.* 97 (2012) 2010–2020. doi:10.1016/j.polymdegradstab.2012.01.030.
- [25] P. Rytlewski, M. Żenkiewicz, R. Malinowski, Influence of Dicumyl Peroxide Content on Thermal and Mechanical Properties of Polylactide, *Int. Polym. Process.* 26 (2011) 580–586. doi:10.3139/217.2521.
- [26] J. Bulet, M.C. Heuzey, C. Dubois, P. Wood-Adams, J. Brisson, Thermal stabilization of high molecular weight L-polylactide, *Annu. Tech. Conf. - ANTEC, Conf. Proc.* 3 (2005) 281–285. <http://www.scopus.com/inward/record.url?eid=2-s2.0-33644949024&partnerID=tZOtx3y1>.
- [27] J.A. Cicero, J.R. Dorgan, S.F. Dec, D.M. Knauss, Phosphite stabilization effects on two-step melt-spun fibers of polylactide, *Polym. Degrad. Stab.* 78 (2002) 95–105. doi:10.1016/S0141-3910(02)00123-4.
- [28] H.J. Lehermeier, J.R. Dorgan, Melt rheology of poly(lactic acid): Consequences of blending chain architectures, *Polym. Eng. Sci.* 41 (2001) 2172–2184. doi:10.1002/pen.10912.
- [29] P. D’Haene, E.E. Remsen, J. Asrar, Preparation and Characterization of a Branched Bacterial Polyester, *Macromolecules.* 32 (1999) 5229–5235. doi:10.1021/ma981911k.
- [30] D. Bikiaris, G. Karayannidis, Chain extension of polyesters PET and PBT with two new diimidodiepoxides. II, *J. Polym. Sci. Part A Polym. Chem.* 34 (1996) 1337–1342. [http://onlinelibrary.wiley.com/doi/10.1002/\(SICI\)1099-0518\(199605\)34:7%3C1337::AID-POLA22%3E3.0.CO;2-9/abstract](http://onlinelibrary.wiley.com/doi/10.1002/(SICI)1099-0518(199605)34:7%3C1337::AID-POLA22%3E3.0.CO;2-9/abstract) (accessed December 23, 2014).
- [31] P. D’Haene, E.E. Remsen, J. Asrar, Preparation and Characterization of a Branched Bacterial Polyester, *Macromolecules.* 32 (1999) 5229–5235. doi:10.1021/ma981911k.
- [32] B. Fei, C. Chen, S. Chen, S. Peng, Y. Zhuang, Y. An, L. Dong, Crosslinking of poly[(3-hydroxybutyrate)-co-(3-hydroxyvalerate)] using dicumyl peroxide as initiator, *Polym. Int.* 53 (2004) 937–943. doi:10.1002/pi.1477.
- [33] S. Duangphet, D. Szegda, J. Song, K. Tarverdi, The Effect of Chain Extender on Poly(3-hydroxybutyrate-co-3-hydroxyvalerate): Thermal Degradation, Crystallization, and Rheological Behaviours, *J. Polym. Environ.* 22 (2013) 1–8. doi:10.1007/s10924-012-0568-5.
- [34] R.J. Fensterheim, TNPP - Update on global risk assessments, in: *Soc. Plast. Eng. - Int. Polyolefins Conf. - FLEXPACON 2008, 2008: pp. 643–650.* <http://www.scopus.com/inward/record.url?eid=2-s2.0-52649151771&partnerID=tZOtx3y1>.
- [35] L. Savenkova, Z. Gercberga, I. Bibers, M. Kalnin, Effect of 3-hydroxy valerate content on some physical and mechanical properties of polyhydroxyalkanoates produced by *Azotobacter chroococcum*, *Process Biochem.* 36 (2000) 445–450. doi:10.1016/S0032-9592(00)00235-1.
- [36] K. Heo, J. Yoon, K. Jin, S. Jin, Structural evolution in microbial polyesters, *J. Phys. Chem.* 112 (2008) 4571–4582. <http://pubs.acs.org/doi/abs/10.1021/jp711136x> (accessed December 9, 2014).
- [37] H. Alata, T. Aoyama, Y. Inoue, Effect of Aging on the Mechanical Properties of Poly(3-hydroxybutyrate-co-3-hydroxyhexanoate), *Macromolecules.* 40 (2007) 4546–4551. doi:10.1021/ma070418i.

3. Capítulo 1

- [38] E. Joussein, S. Petit, J. Churchman, B. Theng, D. Righi, B. Delvaux, Halloysite clay minerals – a review, *Clay Miner.* 40 (2005) 383–426. doi:10.1180/0009855054040180.
- [39] D. Rawtani, Y. Agrawal, Multifarious applications of halloysite nanotubes: a review, *Rev. Adv. Mater. Sci.* 30 (2012) 282–295. http://mp.ipme.ru/e-journals/RAMS/no_33012/08_rawtani.pdf (accessed December 2, 2014).
- [40] N. Grassie, E.J. Murray, P.A. Holmes, The thermal degradation of poly(-d)- β -hydroxybutyric acid): Part 3-The reaction mechanism, *Polym. Degrad. Stab.* 6 (1984) 127–134. <http://www.scopus.com/inward/record.url?eid=2-s2.0-0021208453&partnerID=tZOtx3y1>.
- [41] M. Du, B. Guo, D. Jia, Thermal stability and flame retardant effects of halloysite nanotubes on poly(propylene), *Eur. Polym. J.* 42 (2006) 1362–1369. <http://www.scopus.com/inward/record.url?eid=2-s2.0-33646175070&partnerID=tZOtx3y1> (accessed February 3, 2015).
- [42] L.N. Carli, J.S. Crespo, R.S. Mauler, PHBV nanocomposites based on organomodified montmorillonite and halloysite: The effect of clay type on the morphology and thermal and mechanical properties, *Compos. Part A Appl. Sci. Manuf.* 42 (2011) 1601–1608. doi:10.1016/j.compositesa.2011.07.007.
- [43] L.N. Carli, T.S. Daitx, G. V. Soares, J.S. Crespo, R.S. Mauler, The effects of silane coupling agents on the properties of PHBV/halloysite nanocomposites, *Appl. Clay Sci.* 87 (2014) 311–319. doi:10.1016/j.clay.2013.11.032.
- [44] S. Wang, C. Song, G. Chen, T. Guo, J. Liu, B. Zhang, S. Takeuchi, Characteristics and biodegradation properties of poly(3-hydroxybutyrate-co-3-hydroxyvalerate)/organophilic montmorillonite (PHBV/OMMT) nanocomposite, *Polym. Degrad. Stab.* 87 (2005) 69–76. doi:10.1016/j.polymdegradstab.2004.07.008.
- [45] P. Bordes, E. Pollet, S. Bourbigot, L. Avérous, Structure and Properties of PHA/Clay Nano - Biocomposites Prepared by Melt Intercalation, *Macromol. Chem. Phys.* 209 (2008) 1473 – 1484. doi:10.1002/macp.200800022.
- [46] A. Javadi, Y. Srithep, S. Pilla, Microcellular poly (hydroxybutyrate-co-hydroxyvalerate) hyperbranched polymer–nanoclay nanocomposites, *Polym. Eng. Sci.* 51 (2011) 1815–1826. doi:10.1002/pen.
- [47] S. Bruzaud, A. Bourmaud, Thermal degradation and (nano)mechanical behavior of layered silicate reinforced poly(3-hydroxybutyrate-co-3-hydroxyvalerate) nanocomposites, *Polym. Test.* 26 (2007) 652–659. doi:10.1016/j.polymertesting.2007.04.001.
- [48] M. Zaverl, M.Ö. Seydibeyoğlu, M. Misra, A. Mohanty, Studies on recyclability of polyhydroxybutyrate-co-valerate bioplastic: Multiple melt processing and performance evaluations, *J. Appl. Polym. Sci.* 125 (2012) E324–E331. doi:10.1002/app.36840.
- [49] L. Incarnato, L. Di Maio, D. Acierno, M. Denaro, L. Arrivabene, Relationships between processing-structure-migration properties for recycled polypropylene in food packaging, *Food Addit. Contam.* 15 (1998) 195–202. <http://www.scopus.com/inward/record.url?eid=2-s2.0-0031919783&partnerID=tZOtx3y1>.
- [50] R. Crétois, N. Follain, E. Dargent, J. Soulestin, S. Bourbigot, S. Marais, L. Lebrun, Microstructure and barrier properties of PHBV/organoclays bionanocomposites, *J. Memb. Sci.* 467 (2014) 56–66. doi:10.1016/j.memsci.2014.05.015.
- [51] P. Russo, B. Vetrano, D. Acierno, M. Mauro, Thermal and structural characterization of biodegradable blends filled with halloysite nanotubes, *Polym. Compos.* 34 (2013) 1460–1470. <http://www.scopus.com/inward/record.url?eid=2-s2.0-84882252115&partnerID=tZOtx3y1> (accessed February 18, 2014).

- [52] J. Liu, L. Lou, W. Yu, R. Liao, R. Li, C. Zhou, Long chain branching polylactide: Structures and properties, *Polymer (Guildf)*. 51 (2010) 5186–5197. doi:10.1016/j.polymer.2010.09.002.
- [53] M. Grosvenor, The effect of molecular weight on the rheological and tensile properties of poly(ϵ -caprolactone), *Int. J. Pharm.* 135 (1996) 103–109. doi:10.1016/0378-5173(95)04404-3.
- [54] M.A. Kennedy, A.J. Peacock, L. Mandelkern, Tensile properties of crystalline polymers: Linear polyethylene, *Macromolecules*. 27 (1994) 5297–5310. <http://www.scopus.com/inward/record.url?eid=2-s2.0-0028497889&partnerID=tZOtx3y1>.
- [55] G. Lin, H. Shih, Influence of side - chain structures on the viscoelasticity and elongation viscosity of polyethylene melts, *Polym. Eng. Sci.* 42 (2002) 2213 – 2221. <http://onlinelibrary.wiley.com/doi/10.1002/pen.11111/abstract> (accessed September 5, 2014).

4. Capítulo 2

Biodegradable poly(3-hydroxybutyrate-co-3-hydroxyvalerate) / thermoplastic polyurethane blends with improved mechanical and barrier performance

4. Capítulo 2

Biodegradable poly(3-hydroxybutyrate-co-3-hydroxyvalerate)/ thermoplastic polyurethane blends with improved mechanical and barrier performance

Antonio Martinez-Abad ¹, Jennifer Gonzalez-Ausejo ², Jose Maria Lagaron ¹, Luis Cabedo ²

¹ Novel Materials and Nanotechnology Group, IATA, CSIC, Avda. Agustín Escardino 7, 46980, Burjassot, Spain

² Polymers and Advanced Materials Group (PIMA), Universitat Jaume I, 12071, Castellon, Spain

Polymer Degradation and Stability (2015)

ABSTRACT

Poly(3-hydroxybutyrate-co-3-hydroxyvalerate) (PHBV) polymers pose a green alternative to fossil-fuel derived polymers, as they exhibit good biocompatibility, biodegradability and outstanding barrier performance compared to other biopolyesters. However, their excessive brittleness has not yet been overcome without compromising barrier performance. In this work, a native ester-based thermoplastic polyurethane (TPU) not stabilised against hydrolysis, has been thoroughly assessed for the first time as an additive in melt blends with PHBV. Phase segregation in scanning electron microscopy (SEM) confirmed the immiscibility of the two polymers, however a degree of interaction has been found. Wide-angle X-ray scattering and differential scanning calorimetry revealed no major effect of the TPU on the crystallinity of the PHBV phase. The onset and kinetics of thermal degradation was not altered by the presence of the TPU up to 50 wt.% content. Blends with increasing TPU contents showed a gradual decrease in the modulus of elasticity and tensile strength, while a substantial increase in elongation at break has been found for contents of TPU above 20 wt.%, which resulted an improvement in the overall toughness of the blends. The excellent barrier performance of the PHBV against water vapour and aroma compounds was shown to be unaffected by TPU loads of ≤ 30 wt.%. Full decomposition of neat PHBV and PHBV/TPU blends below 50 wt.% TPU content was achieved after 40 days according to biodegradation standards (ISO 20200). The study puts forward the potential use of TPU to improve the mechanical performance of these natural biopolyesters without compromising the barrier properties or the biodegradability of the melt blends.

GRAFICAL ABSTRACT

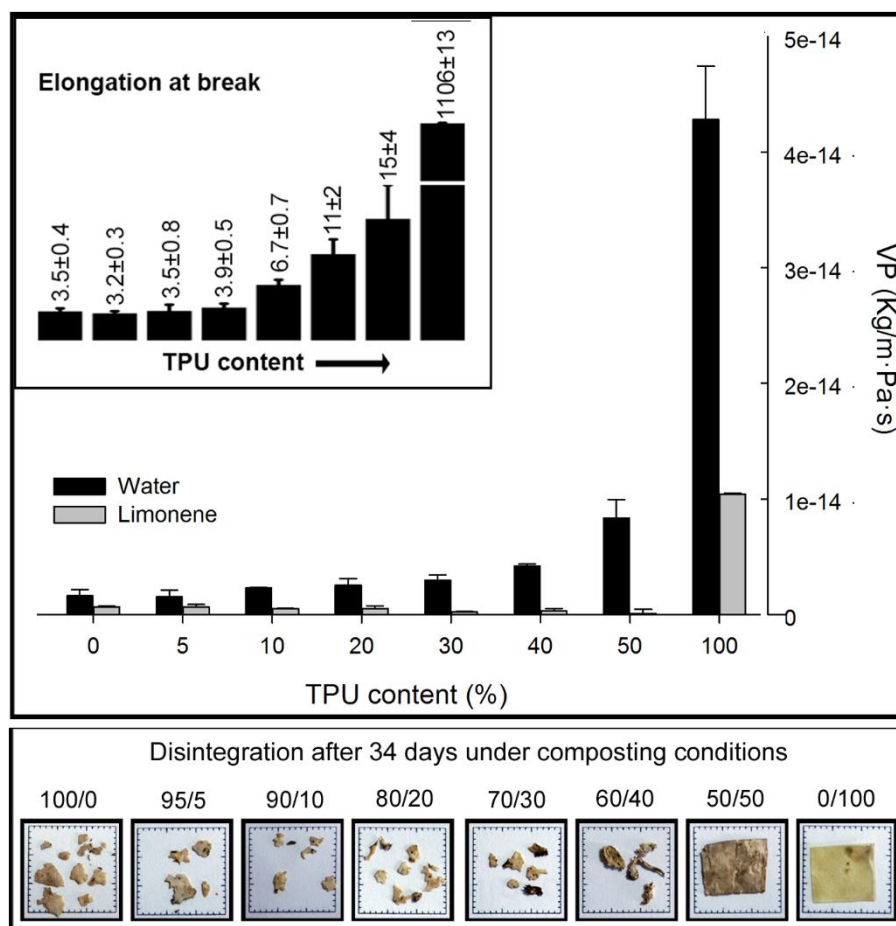


Fig. 4.1: Graphical abstract of the work named Biodegradable poly(3-hydroxybutyrate-co-3-hydroxyvalerate)/ thermoplastic polyurethane blends with improved mechanical and barrier performance.

4.1. INTRODUCTION

Polyhydroxyalkanoates (PHAs) are a family of naturally occurring storage biopolyesters synthesised by more than 300 species of Gram-positive and Gram-negative bacteria [1]. Among the various biodegradable polymers, PHAs provide a good alternative to fossil-fuel based plastics as they possess thermoplastic properties similar to conventional polyolefins, with the advantage of being 100% biodegradable, compostable and produced from renewable resources [2–5]. Another key advantage of PHAs is their excellent barrier properties, which are similar to those of polyethylene terephthalate (PET) [6], and are much better than other biopolyesters such as poly(lactic acid) [7]. In the areas of food and cosmetic packaging, PHAs are already commercialised as cosmetic containers, shampoo bottles, covers, milk cartons, films, moisture barriers in nappies and sanitary towels, pens and combs, among others (reviewed by [8]).

Nevertheless, PHAs have a very narrow processing window, are excessively brittle, and currently constitute a more expensive alternative to other commonly used materials in the packaging sector. These application limitations have been confronted by using different approaches, including the addition of plasticisers, enhancing the synthesis of poly(3-hydroxybutyrate-co-3-hydroxyvalerate; PHBV) heteropolymers, or blending with other polymers. Although increasing valerate contents in PHBV results in higher flexibility, higher strength and a lower melting temperature [9], high contents of hydroxyvalerate (HV) lead to a decrease in the barrier properties [10]. Moreover, the improvement in elongation at break with HV wanes with storage time [11]. Therefore, low HV-content grades might still be more suitable for packaging applications. A recent work reported the effect of different plasticisers on the mechanical and barrier properties of PHBV [12]. Researchers found that, although the barrier properties could be maintained with the addition of some plasticisers, the elongation at break of PHBV could not be substantially modified. The authors thus concluded that it is questionable whether plasticised PHBV may be used in larger scale packaging applications in the near future [12]. The approach of blending it with other polymers by melt compounding is a very convenient method since it uses conventional polymer processing equipment widely used in the packaging industry. This strategy has also been assessed for the PHBV copolymers [13–15]. Biodegradable polyesters [13] such as polylactides, polycaprolactone, polybutylene succinate (PBS) [16] and butylene (adipate-co-terephthalate) (PBAT) [17] have been

4. Capítulo 2

studied in this sense. However, the barrier properties of the blends were found to be considerably lower than that of the pure PHBV [18].

A conventional approach for increasing elongation at break in brittle polymers is the addition of an elastomeric second phase. This is commonly known as rubber toughening of polymers and has been successfully carried out for many years, leading to many engineering materials such as high impact polystyrene (HIPS), acrylonitrile-butadiene-styrene (ABS) or styrene-butadiene-styrene copolymers (SBS). Recently, interest in this approach to increase the toughness of biopolyesters has grown, as brittleness is one of the main drawbacks in their application in the packaging field. In this regard, intense work in toughening polylactic acid (PLA) has been conducted in recent years [19–23]. Toughening PHBV with elastomers such as ethylene vinyl acetate [24], epoxidized natural rubber [25] and poly(butadiene-co-acrylonitrile) [26] has also been investigated. In most cases, the addition of the elastomeric phase showed either no great improvement [26] or loss of the desired biodegradability [24–26]. In line with blending with an elastomeric material, the use of a biodegradable thermoplastic polyurethane is proposed in the present work. Thermoplastic polyurethanes (TPUs) are a widely used class of polymers with excellent mechanical properties and good biocompatibility, which have already been successfully evaluated in a number of biomedical applications [27]. Although conventional TPUs are typically not intended to degrade quickly, they are susceptible to hydrolytic, oxidative and enzymatic degradation, which could be deliberately exploited to design biodegradable systems [28]. In fact, good biodegradability of TPUs has been reported under composting conditions [29], especially when the TPU comes from an ester diol [30]. In this sense, the use of TPU for the development of biodegradable blends has been already explored with other biopolyesters such as PLA [31–33]. Moreover, the use of TPU to increase the elongation at break of PHBV has already been explored by solvent casting [34]. In this work, Wang et al. obtained blends of PHBV/TPU with an increased elongation at break of up to 6% for TPU contents of 40%. The addition of the TPU by solvent cast resulted in a decrease in the crystallinity of PHBV by close to 20%, which may lead to a drop in the gas barrier performance.

In the present work, the use of a native ester-based TPU (not stabilised against hydrolysis) has been assessed for the first time in melt blends with PHBV as an additive for decreasing the brittleness of these natural biopolyesters without compromising the barrier properties or the biodegradability of the PHBV. A thorough study on the effect of the interaction of the two

polymers in the blends behaviour has been carried out, as well as an assessment of the final biodegradability of the system by measuring the biodegradation of the blends under standard conditions.

4.2. EXPERIMENTAL

4.2.1. Materials

Commercial grade PHBV with 3 mol% valerate content was purchased from Tianan Biopolymer (Ningbo, China) in pellet form (ENMAT Y1000P). The native thermoplastic polyurethane Elastollan® 880AN was kindly supplied by BASF (Germany).

4.2.2. Blend processing

Prior to the blending step, both the PHBV and TPU pellets were vacuum dried at 80°C for 3 hours. The PHBV blends were obtained by mixing different amounts of pellets of both polymers in a Brabender Plastograph mixer (Brabender, Germany) for 8 min at 100 rpm and at 175°C. To avoid severe thermal degradation during blending, the melt temperature was not allowed to reach 185°C. The batches were subsequently compression moulded into films using a hot-plate hydraulic press (Carver 4122, USA) at 177°C, 2 MPa and 4 min to produce films with a thickness of 200 µm. All the samples were stored in a vacuum desiccator at ambient temperature for 2 weeks to allow full crystallisation to take place [35]. Blends containing 5 wt% (95/5), 10 wt% (90/10), 20 wt% (80/20), 30 wt% (70/30), 40 wt% (60/40) and 50 wt% (50/50) of TPU were obtained. For the sake of comparison, the pure PHBV (100/0) and TPU (0/100) were also processed under identical conditions and used as reference materials.

4.2.3. Morphology

Scanning Electron Microscopy (SEM) of all the samples was conducted using a high-resolution field-emission JEOL 7001F microscope. The samples were fractured in liquid nitrogen and then were coated by sputtering with a thin layer of Pt prior to SEM observation. The size of the dispersed phase (i.e. diameter of the spheres) was measured in the SEM microphotographs by using ImageJ software (the number of spheres measured for each sample was never below 200).

4. Capítulo 2

Wide-angle X-ray diffraction (WAXS) measurements were performed using a Bruker AXS D4 ENDEAVOR diffractometer. The samples were scanned at room temperature in reflection mode using incident Cu K-alpha radiation ($k = 1.54 \text{ \AA}$), while the generator was set at 40 kV and 40 mA.

4.2.4. Thermal properties

The thermal stability of the blends was investigated by means of thermogravimetric analysis (TGA) using a TG-STDA Mettler Toledo model TGA/SDTA851e/LF/1600. The samples were heated from 50°C to 900°C at a heating rate of 10°C/min under nitrogen flow. The characteristic temperatures $T_{5\%}$ and T_{\max} corresponded, respectively, to the initial decomposition temperature (5% of weight loss) and to the maximum degradation rate temperature measured at the derivative thermogravimetric (DTG) peak maximum.

Differential scanning calorimeter (DSC) experiments were conducted using a DSC2 (Mettler Toledo) with an intracooler (Julabo model FT900). The weight of the DSC samples was typically 6 mg. Samples were first heated from -20°C to 200°C at 10°C/min, kept for 1 min at 200°C, cooled down to -20°C at 10°C/min, and then finally reheated to 200°C at 10°C/min. The crystallisation temperature (T_c), melt temperature (T_m), melting enthalpy (ΔH_m) and crystallisation enthalpy (ΔH_c) were determined from the cooling and second heating curve. The crystallinity (X_c) of the PHBV phase was calculated by the following Equation (4.1), where (ΔH_m) (J/g) is the melting enthalpy of the polymer matrix, (ΔH_m^0) is the melting enthalpy of 100% crystalline PHBV (perfect crystal) (146 J/g), and w is the weight fraction of PHBV in the blend [36].

$$X_c (\%) = \frac{\Delta H_m}{w \cdot \Delta H_m^0} \cdot 100 \quad (4.1)$$

The DSC instrument was calibrated with an indium standard before use.

4.2.5. Mechanical properties

Tensile tests were conducted in a universal testing machine (Instron 4469) at a crosshead speed of 10 mm/min and at room temperature. Tests were conducted according to ISO 527:2012 using films prepared by hot press moulding and subsequently conditioned as previously detailed. A minimum of five specimens of each sample were tested and the average results with standard deviation were reported.

4.2.6. Permeability measurements

The water vapour permeability (WVP) of the PHBV/TPU blends was measured according to the ASTM E96 (2011) gravimetric method, using Payne permeability cups (Elcometer, Hermelle Argenteau, Belgium). Distilled water was placed inside the cup to expose the film (the exposed area was $9.6 \times 10^{-4} \text{ m}^2$) to 100% relative humidity on one side. Once the films were secured, each cup was placed in an equilibrated relative humidity desiccator at 24°C. Relative humidity at 0% was held constant using silica gel. The cups were weighed periodically ($\pm 0.0001 \text{ g}$), at least twice a day for 7 days. Aluminium foil was used as a control to rule out vapour loss through the seal. WVP was calculated from the steady-state permeation slopes obtained from the regression analysis of weight loss data over time. The permeability to D-limonene (Panreac, Barcelona, Spain) was measured analogously, filling the cups with the volatile compound instead of distilled water. The lower limit of vapour permeability detection of the permeation cells was $\sim 1.10^{-17}$ and $5.10^{-17} \text{ kg}\cdot\text{m}\cdot\text{s}^{-1}\cdot\text{m}^{-2}\cdot\text{Pa}^{-1}$ for water vapour and D-limonene, respectively, based on the weight loss through the seal in the aluminium samples. All measurements were performed in triplicate. The diffusivity coefficients of both permeants in the studied blends was calculated according to Equation (4.2), where P is the permeability, D the diffusivity and S, the solubility of the permeants as evaluated from the steady-state vapour sorption mass increase in the studied conditions.

$$P = DS \quad (4.2)$$

4. Capítulo 2

4.2.7. Biodisintegration in composting conditions

Disintegrability of neat PHBV and PHBV/TPU films, as well as neat TPU, was assessed by means of a disintegration test under lab-scale composting conditions according to the ISO 20200 standard, “Determination of the degree of disintegration of plastic materials under simulated composting conditions in a laboratory-scale test” [37]. For the preparation of solid synthetic waste, 10% of activated mature compost (VIGORHUMUS H-00, purchased from Burás Profesional, S.A., Girona, Spain) was mixed with 30% rabbit food, 10% starch, 5% sugar, 1% urea, 4% corn oil and 40% sawdust. The water content of the substrate was around 55 wt% and the aerobic conditions were guaranteed by gently mixing the compost and periodically adding water according to the standard requirements. The samples were cut from hot pressed plates (10 x 10 x 0.2 mm³) and buried inside iron mesh bags to simplify their extraction and allow the contact of the compost with the specimens, and were incubated at 58°C for 41 days. At different composting times samples were recovered for analysis, washed with distilled water, dried at 40°C under vacuum for 24 h, and weighed. The degree of disintegration was calculated by normalising the sample weight, at different days of incubation, to the initial weight with Equation (4.3), where m_i is the initial dry mass of the test material and m_f is the dry mass of the test material recovered at different incubation stages.

$$D = \frac{m_i - m_f}{m_i} \times 100 \quad (4.3)$$

Photographs of samples were taken for visual evaluation.

4.3. RESULTS AND DISCUSSION

4.3.1. Morphological characterisation

Figure 4.2.a-f presents the cryofractured surfaces of the PHBV/TPU blends with different TPU contents. A first observation shows that, in all cases, the morphology of the blends revealed the presence of a two-phase morphology, thus revealing an immiscible polymeric system. Hence, the TPU microstructure shows the TPU dispersed within a PHBV continuous matrix, thus revealing a characteristic discrete-phase structure (DPS, or drop-in matrix) [38]. For all the studied

compositions, the TPU is found to be homogeneously dispersed throughout the PHBV matrix, forming spheres which increase in size with a greater TPU content.

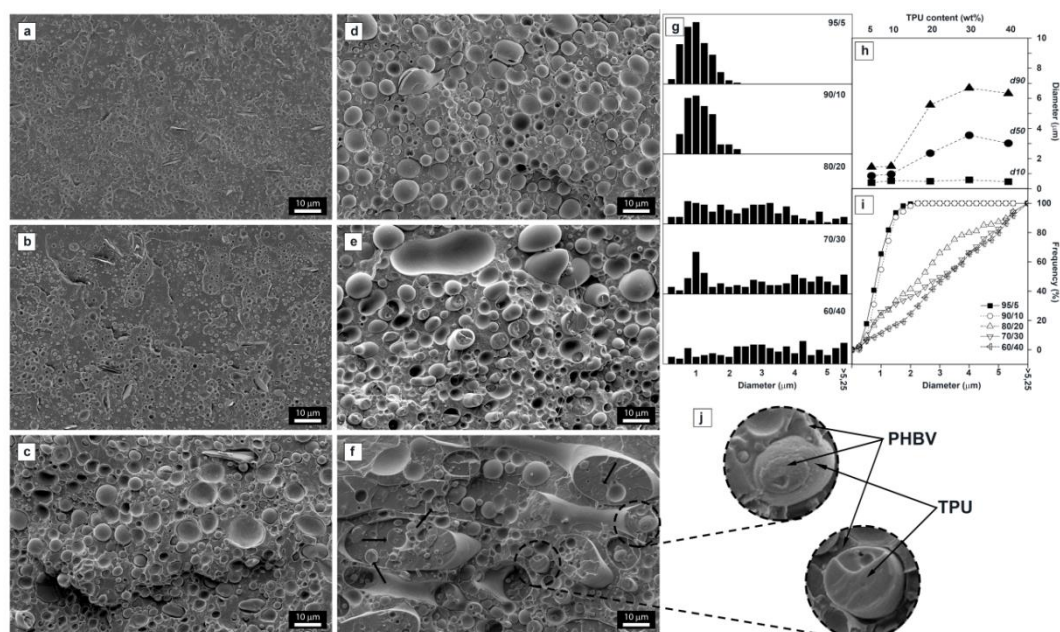


Fig. 4.2. Morphology of PHBV/TPU blends. Figure 1a-1f: Scanning electron images of 95/5 (a), 90/10 (b), 80/20 (c), 70/30 (d), 60/40 (e) and 50/50 (f). Particle size distribution for the PHBV/TPU blends (g). D10, D50 and D90 values of the PHBV/TPU blends (h). Accumulated frequency of particle sizes in the ester-blends (i). Detail of PHBV/TPU blend interfaces (j).

Figure 4.2.g shows the size distribution of the dispersed phase as a function of the TPU content, while Figure 4.2.h plots the D10, D50 and D90 values determined as the size below which 10%, 50% and 90% of the spheres respectively are comprised, respectively. In samples with TPU contents ≤ 10 wt%, the segregated TPU phase is observed to be confined in spheres of close to $1 \mu\text{m}$ on average ($0.9 \mu\text{m}$ and $1 \mu\text{m}$ for 5 wt% and 10 wt% respectively). When the amount of TPU is increased, the size of the dispersed phase is also gradually increased. Mean values of droplet size for 80/20, 70/30, 60/40 samples are $2.4 \mu\text{m}$, $3.6 \mu\text{m}$ and $3 \mu\text{m}$ in diameter, respectively. However, the d10 value seems unaffected, indicating the abundance of small particles is not altered. On the other hand, the number of spheres with a size $\geq 2 \mu\text{m}$ increases with TPU content. This behaviour could be explained by a droplet-droplet coalescence mechanism. Finally, for 50/50 samples, larger domains of both PHBV and TPU can be observed. These domains reveal a co-continuous

4. Capítulo 2

morphology, i.e. the TPU content is above the percolation threshold. Moreover, a phase reversion effect can be seen in Figure 4.2.f, as TPU and PHBV spheres are forming part of the dispersed phase.

As far as phase interaction is concerned, from a theoretical point of view and according to the literature [31,32,34], some degree of interaction should be expected between the PHBV and the TPU since both are polyesters. Moreover, as discussed in the following sections, the mechanical behaviour of the blends implies that a certain degree of adherence should exist on the interface between the two polymers. Additionally, the gas barrier performance results (see section 3.4) clearly reveal a continuous interface. For all these reasons, an immiscible system with good interfacial interaction should be expected. However, direct observation of the morphology by SEM, does not seem to corroborate this, as clear detachment of the spheres from the continuous matrix can be detected throughout the whole range of studied materials. This debonding of the TPU particles could be explained by the SEM sample preparation procedure rather than by an actual lack of adhesion on the interface between the two polymers. Quenching in liquid nitrogen can provoke high thermal stresses in heterogeneous systems when there is a difference in the coefficient of linear thermal expansion (CLTE) of the involved materials. In this case, the PHBV is a highly crystalline polymer with a relatively low CLTE, while TPU is an elastomer with a high CLTE [39]. Hence, during fast cooling, the TPU spheres would shrink in such a way that the interface adhesion would be exceeded and consequently, a pull-out effect is observed throughout the fracture. On the other hand, in a phase reversion situation in which the TPU is surrounding the PHBV, the relative shrinkage of the TPU will lead to a compressive strength over the PHBV spheres therefore, the adhesion at the interface will not be significantly affected by the fracture. This is illustrated in Figure 4.2.j (upper image), where the detail of a PHBV sphere in a TPU region can be seen interacting at the interface and the debonding of a TPU particle surrounded by PHBV is observed in the lower image. The black arrows indicate PHBV spheres in TPU regions where the fracture has taken place in a cohesive mode, probably due to adhesion at the interface (Figure 4.2.f).

WAXS experiments were conducted on both the neat polymers as well as on all the studied PHBV/TPU blends. The diffractograms are shown in Figure 4.3. Three characteristic peaks of PHBV were detected in the pure PHBV diffractogram: $13.4^\circ 2\theta$, $16.9^\circ 2\theta$ and $21.5^\circ 2\theta$. According to the literature, these peaks correspond to the (0 2 0), (1 1 0) and (1 0 1) lattice planes of the

orthorhombic unit cell of PHB lattices [36,39]. The PHB crystal lattice is characteristic for the PHBV with HV contents below 37% [40]. The most intense peak at $2\theta = 26^\circ$ corresponds to the (0 0 2) reflection of boron nitride, which is present as a nucleating agent in the commercial grade PHBV used in this work. There were no changes in position or in relative intensities of the PHBV diffraction peaks throughout the whole range of PHBV/TPU blends. This suggests that the crystalline structure of PHBV does not change with the addition of the elastomer. The pure TPU pattern does not show any peaks, but a single amorphous hump. Therefore, the decrease in the absolute intensity of the peaks with increasing TPU content can mostly be explained by a dilution effect.

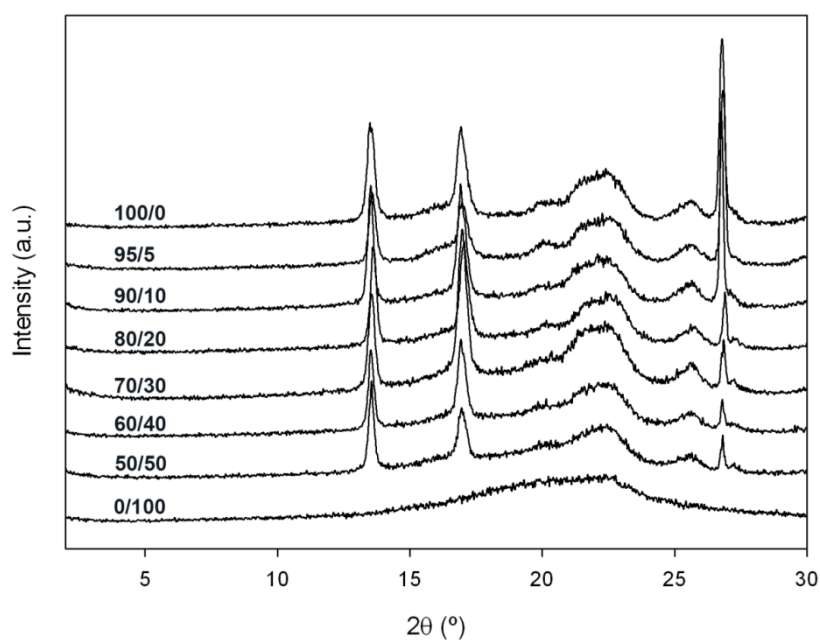


Fig. 4.3. WAXS patterns of neat PHBV, TPU and PHBV/TPU blends.

4. Capítulo 2

4.3.2. Thermal characterisation

4.3.2.1. Differential Scanning Calorimetry

Second phase additives can often affect the crystallinity of binary polymer blends with semicrystalline polymers such as PHBV. Table 4.1 gathers the crystallisation (ΔH_c) and melting enthalpies (ΔH_m) and crystallisation and (T_c) melting temperatures (T_m) of PHBV and PHBV/TPU blends as a function of the blend composition. The corresponding thermograms are presented in Figure 4.4. The appearance of two melting peaks in the thermograms is the result of melt-recrystallisation mechanisms that are typical for this type of biopolymer and has been reported in previous works dealing with PHBV blends [36,41]. A gradual decrease in both crystallisation and melting temperatures can be observed as the TPU concentration is increased (see Table 4.1). The slight decrease in the melting temperature accounts for $\leq 2^\circ\text{C}$ for TPU contents up to 30 wt%. This points towards a crystallite population of slightly decreasing size or decreased lamellar thickness. The crystalline fraction, as calculated from the melting enthalpies of the blends, is also shown to decrease with increasing TPU content, indicating that the presence of TPU might interfere with the crystallisation process to some extent.

Table 4.1. Thermal properties of the PHBV/TPU blends.

PHBV/TPU (%)	TGA			DSC				
	$T_{5\%}$ ($^\circ\text{C}$)	T_{max} ($^\circ\text{C}$)	Res (wt.%)	T_c ($^\circ\text{C}$)	ΔH_c (J/g)	T_c ($^\circ\text{C}$)	ΔH_m (J/g)	X_c (%)*
100	277 \pm 0	296 \pm 0	1.1 \pm 0.0	118 \pm 0	89.1 \pm 0.9	171 \pm 1	98.1 \pm 0.9	67.2 \pm 0.6
95/5	280 \pm 2	296 \pm 3	1.1 \pm 0.0	111 \pm 0	79.1 \pm 0.8	170 \pm 0	90.3 \pm 1.5	65.1 \pm 1.1
90/10	281 \pm 2	296 \pm 3	1.3 \pm 0.1	110 \pm 0	71.5 \pm 2.4	170 \pm 0	83.6 \pm 1.9	63.7 \pm 1.5
80/20	279 \pm 1	296 \pm 1	1.6 \pm 0.2	106 \pm 0	62.3 \pm 0.5	169 \pm 0	73.9 \pm 2.2	63.3 \pm 1.9
70/30	282 \pm 2	296 \pm 2	2.0 \pm 0.1	103 \pm 0	53.7 \pm 1.4	168 \pm 0	65.8 \pm 0.7	64.3 \pm 0.7
60/40	281 \pm 2	296 \pm 0	2.4 \pm 0.0	99 \pm 1	41.8 \pm 0.4	168 \pm 0	55.2 \pm 0.6	63.0 \pm 0.7
50/50	281 \pm 3	296 \pm 2	2.9 \pm 0.1	97 \pm 0	31.5 \pm 0.6	167 \pm 0	44.5 \pm 0.9	61.0 \pm 1.2
0/100	324 \pm 1	407 \pm 1	7.4 \pm 0.3	-	-	-	-	-

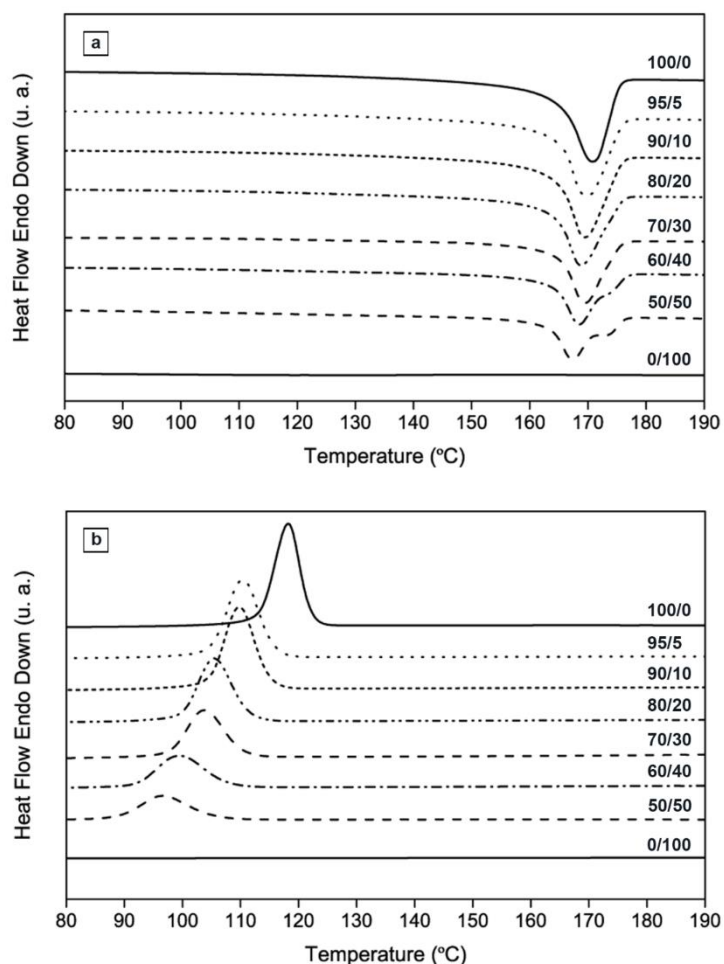


Fig. 4.4. DSC thermograms of neat PHBV, TPU and PHBV/TPU blends: a) Second heating run, b) Cooling run.

4.3.2.2. Thermogravimetric analysis

The thermal degradation behaviours of neat PHBV and TPU, as well their blends were examined using TGA under N_2 flow. The original thermogravimetric curves are shown in Figure 4.5, while their respective first derivative curves are presented in the inset. Experimental replicates are also shown on the graph to demonstrate the excellent reproducibility of the results. Data, including the onset of degradation ($T_{5\%}$), temperature for the maximum weight loss rate (T_{max}), and residual charge (Res), are shown in Table 4.1. It is well reported that PHB and its copolymers easily undergo thermal

4. Capítulo 2

degradation involving random chain scission in a one-step process with an onset between 270°C and 300°C [42,43].

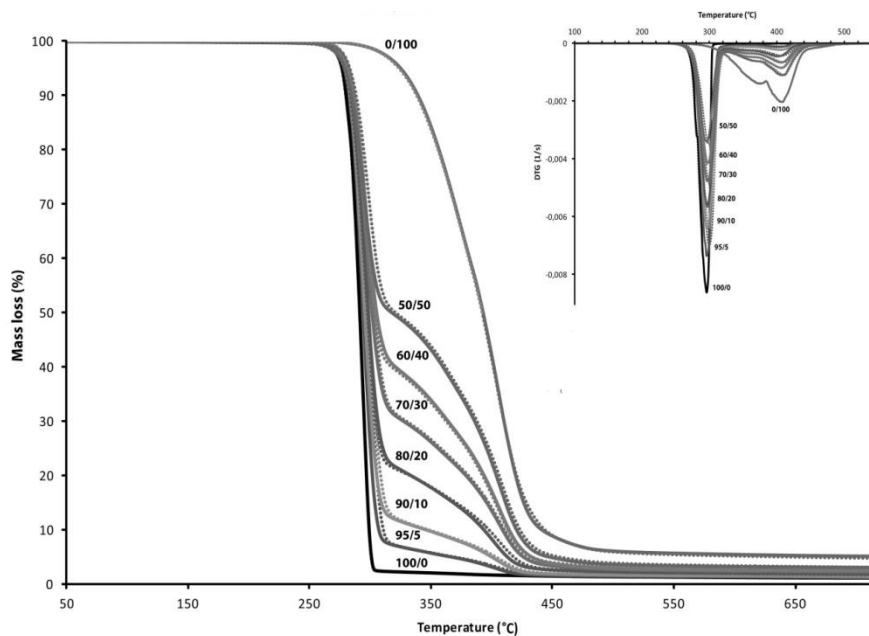


Fig. 4.5. Weight loss versus temperature of the tested materials as analysed by TGA. Inset displays the DTG curves for the same samples.

Degradation of the TPU proceeds at a later stage in a two-step process, in which it has been suggested that urethane linkages and unstable side chains degrade at temperatures of 300°C–400°C, followed by chain scission at the β -position to the carbon–carbon double bond occurring at around 450°C [44,45]. The residual charges in the tested specimens can be ascribed to the presence of boron nitride as a nucleating agent in the commercial grade PHBV and to the char formation of methylene diphenyl diisocyanate [46]. The onset of thermal degradation in all the PHBV/TPU blends was comparable to that of the neat PHBV (Table 4.1). Moreover, the temperature for the maximum rate of degradation in all the blends was the same as for neat PHBV. This indicates degradation in the blends is governed by the presence of the more labile PHBV and that TPU does not have an impact on this parameter. It is also remarkable that the degradation rate of the blends was reproducible and decreased linearly with an increasing TPU content, while the two-stage degradation of the TPU analogously increased together with the final residual charge. These results

suggest neither component has any impact on the other's degradation kinetics, so that thermal degradation of the blends might be predicted a result of their separate combination.

4.3.3. Mechanical properties

In order to evaluate the effect of the addition of the TPU to the mechanical performance of the PHBV, tensile tests up to failure were conducted on the pure PHBV and TPU, as well as all the blends. The interaction of the two polymers has been analysed by using different mechanical models, assuming different degrees of adhesion on the interface to study how the mechanical properties of the blends vary with the addition of the second elastomeric phase.

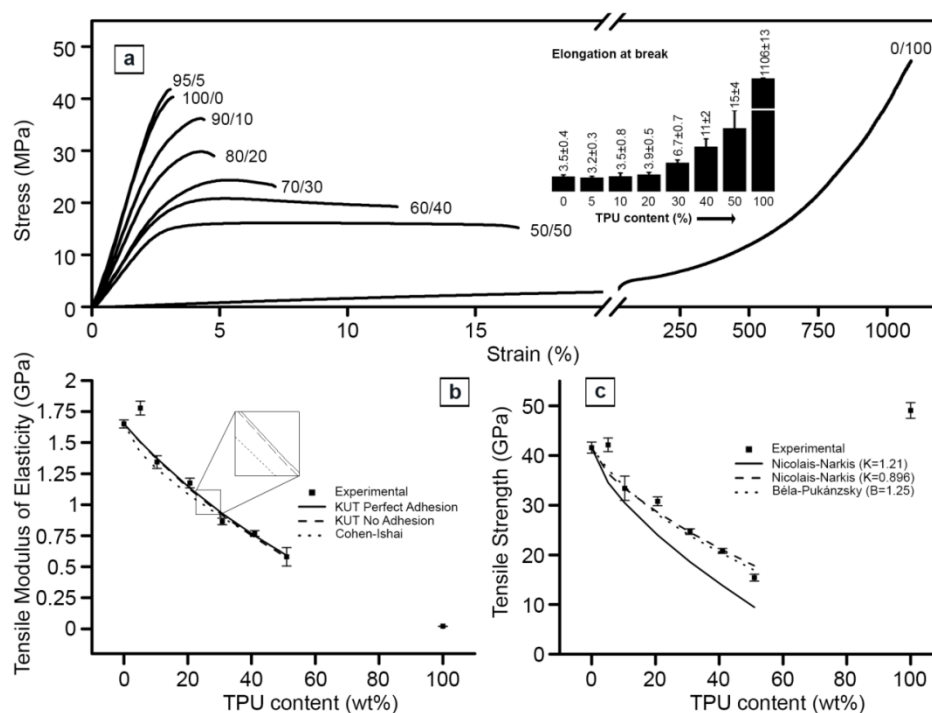


Fig. 4.6. Tensile stress curves of the PHBV/TPU blends. Inset displays the tendency in elongation at break of blends with increasing TPU content (a). Variation of the tensile modulus of elasticity (b) and tensile strength (c) with the incorporation of TPU and fitting to the respective predictive models.

Figure 4.6.a shows the strain-stress curves of the pure PHBV and TPU, as well as of all the studied blends. As expected, the addition of the TPU to the PHBV resulted in a decrease in the rigidity and resistance of the blend, but an increase in the elongation at break and tensile toughness. Thus, the

4. Capítulo 2

tensile modulus of elasticity decreased from ca.1.7GPa for the pristine PHBV to below 1GPa for the high TPU content blends, the decrease being dependent on the TPU content. The variation on the elastic modulus with the addition of the elastomer was compared with the theoretical values derived from two different models: Kerner–Uemura–Takayanagi (KUT) and Cohen–Ishai. Figure 4.6.b shows the experimental values of the modulus of elasticity of the PHBV/TPU blends as a function of the TPU content as well as the plots obtained from the predictive models. In both models, PHBV and TPU have been considered the continuous and dispersed phase respectively, and only the compositions in which the PHBV is the major phase have been represented.

The KUT model is commonly used to assess the interfacial adherence in immiscible polymer blends [47–50]. This model assumes the blend has spherical inclusions of a polymer (disperse, d), having an elastic modulus (E_d), in a continuous matrix of polymer (matrix, m), having an elastic modulus (E_m) and a Poisson's ratio (ν_m) taken to be 0.5. The KUT model has two equations: one for a perfect adhesion in the interface (Equation 4.4) and the other assumes no adhesion (Equation 4.5).

$$E_b = E_m \left(\frac{(7-5\nu_m)x E_m + (8-10\nu_m)x E_d - (7-5\nu_m)x (E_m - E_d)x \phi_d}{(7-5\nu_m)x E_m + (8-10\nu_m)x E_d + (8-10\nu_m)x (E_m - E_d)x \phi_d} \right) \quad (4.4)$$

$$E_b = E_m \left(\frac{(7-5\nu_m)x E_m - (7-5\nu_m)x E_m x \phi_d}{(7-5\nu_m)x E_m + (8-10\nu_m)x E_m x \phi_d} \right) \quad (4.5)$$

Where E_b is the elastic modulus of the blend and ϕ_d is the volume fraction of the dispersed phase.

As can be seen in Figure 4.6.b, the difference between the perfect adhesion and the no-adhesion curve is minimal for our system, as it is also from the experimental results for both of them (see Figure 4.6.b). This can be attributed to a very low elastic modulus of the dispersed phase when compared to that of the matrix. Hence, the contribution of the TPU to the elastic modulus of the blend is negligible. This can be confirmed when fitting the experimental results to the Cohen–Ishai model (Equation 4.6), in which no interaction between the phases is considered, with the dispersed phase considered as voids.

$$E_b = E_m (1 - \phi_d^{2/3}) \quad (4.6)$$

Figure 4.6.c shows the experimental values of the tensile strength as a function of the TPU content. The tensile strength of the blends also decreases gradually when the TPU is incorporated to the

PHBV. It can be pointed out that, although the pure TPU has a tensile strength close to that of the PHBV, the strength corresponding to the elongation at which rupture takes place is still very low. The interaction between the two polymers at the interface was assessed by fitting the experimental values to two different models: the Nicolais–Narkis model (NN) and the Béla Pukánszky model (BP). These two models allow for quantifying the adherence between two immiscible polymer blends [47,48,50,51]. The NN model (Equation 4.7) defines an interface interaction constant (K) which is a function of the blend structure. For spherical inclusions, $K = 1.21$ stands for the extreme case of poor adhesion, while a lower K value denotes better interfacial interaction. By fitting the experimental results to that model, a K value of 0.896 has been determined (see Figure 4.5.c), indicating a degree of interaction.

$$\sigma_b = \sigma_m (1 - K \phi_d^{2/3}) \quad (4.7)$$

On the other hand, the BP model (Equation 4.8) establishes parameter B that is related to the load-bearing capacity of the dispersed phase. This value depends on the size of the contact surface between the matrix and the dispersed phase and on the properties of the interface that is formed. For lower interactions of the interface, the B value decreases. A value of the B parameter of 1.25 is found when fitting the experimental data to the BP model. This also indicates some degree of interaction at the interface, thus in accordance with the NN value.

$$\sigma_b = \sigma_m \left(\frac{1 - \phi_d}{1 + 2.5 \phi_d} \right) e^{B \phi_d} \quad (4.8)$$

With respect to the elongation at break, the addition of small quantities of TPU to the PHBV does not seem to affect the yielding capacity of the PHBV (being below 4% for all the samples below 20 wt.% TPU). However, when the TPU content surpasses 20 wt.%, a clear increase in the elongation at break has been detected. Thus, the 70/30 samples exhibit a value for the elongation at break, double that of the pure PHBV and a clear yielding effect is detected. Therefore, the addition of a TPU above 20 wt.% would result in a change in the mechanical behaviour of the blend, thus decreasing the inherent fragility of the PHBV.

4. Capítulo 2

Overall, the mechanical results show that incorporating TPU promotes the potential applications of these materials, with higher ductility and similar tensile strength as polylactides, these being the natural competitors in the field of biodegradable polyesters.

4.3.4. Barrier performance

Water vapour permeability by weight loss or gain measurements (ASTM E96) are common methods to determine the water barrier properties of materials, while D-limonene is a commonly used standard compound to test mass transport of volatile compounds, such as aromas.

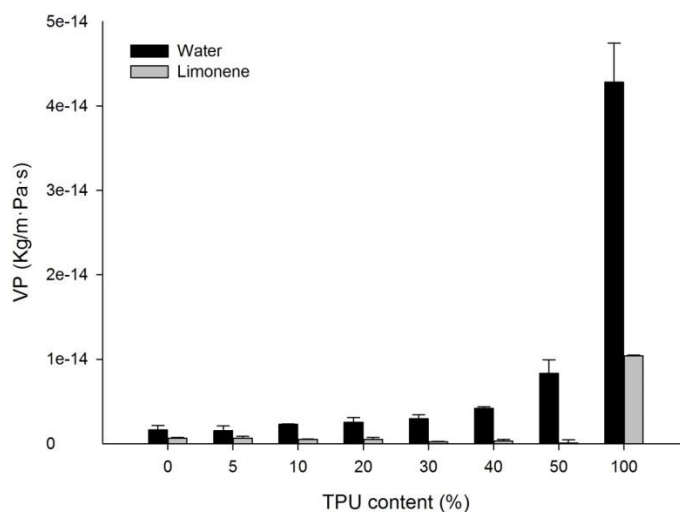


Fig. 4.7. Vapour permeability of the neat materials and their tested blends to water and limonene.

Figure 4.7 shows the vapour permeability (VP) values of both compounds and all PHBV-TPU blends with increasing TPU fraction. Values for both water and D-limonene vapour permeability of blends with up to 30 wt.% TPU are not significantly affected, as compared to neat PHBV. Indeed, permeability values are relatively low (close to the detection limit of the technique), especially for limonene permeability. The values are in agreement with previous studies on neat PHBV and reinforce the excellent water and aroma barrier properties of these bacterial polyesters [6,10,52,53]. A detrimental interaction between the PHBV and TPU phase would cause preferential diffusion pathways to drastically affect the permeability values even at low TPU load. However,

increased permeability only occurs at very high TPU contents. In fact, increased permeability is mostly a result of the increased sorption of the volatile compounds, while actual diffusion coefficients do not contribute as drastically to the decreasing barrier properties at very high TPU loads (Table 4.2). This suggests a degree of interaction between both phases, which supports the discussion elaborated in the morphology and mechanical properties section. This decrease may therefore be attributed to the considerable increase in free volume in the absence of PHBV from the combination. These results point out that the incorporation of high quantities of the TPU does not affect the excellent barrier properties of the materials against water or aroma compounds.

Table 4.2. Mass transfer parameters through PHBV/TPU blends.

PHBV/TPU (%)	Water			Limonene		
	Sorption (vol.%)	Diffusion coefficient (m^2/s) $\cdot 10^{-14}$	Permeability ($\text{kg}/\text{m}\cdot\text{Pa}\cdot\text{s}$) $\cdot 10^{-15}$	Sorption (vol.%)	Diffusion coefficient (m^2/s) $\cdot 10^{-14}$	Permeability ($\text{kg}/\text{m}\cdot\text{Pa}\cdot\text{s}$) $\cdot 10^{-15}$
100/0	2.5 \pm 0.2	6.6 \pm 0.2	1.6 \pm 0.5	0.4 \pm 0.1	17.5 \pm 0.5	0.7 \pm 0.1
95/5	2.1 \pm 0.1	7.2 \pm 0.1	1.5 \pm 0.6	0.4 \pm 0.1	15.3 \pm 1.2	0.6 \pm 0.2
90/10	2.6 \pm 0.4	8.8 \pm 0.4	2.3 \pm 0.1	0.4 \pm 0.0	12.4 \pm 0.1	0.5 \pm 0.1
80/20	3.2 \pm 0.8	7.8 \pm 0.3	2.5 \pm 0.6	0.3 \pm 0.0	16.0 \pm 0.2	0.5 \pm 0.3
70/30	3.7 \pm 0.0	7.9 \pm 0.0	2.9 \pm 0.5	0.3 \pm 0.0	7.3 \pm 0.1	0.2 \pm 0.6
60/40	4.2 \pm 0.6	9.8 \pm 0.1	4.2 \pm 0.2	0.5 \pm 0.0	6.3 \pm 0.3	0.3 \pm 0.3
50/50	5.6 \pm 1.0	14.9 \pm 0.5	8.3 \pm 1.6	1.2 \pm 0.1	1.7 \pm 0.2	0.1 \pm 0.1
0/100	7.6 \pm 0.9	56.5 \pm 0.7	42.8 \pm 4.6	3.2 \pm 0.1	32.3 \pm 0.1	10.4 \pm 0.1

4.3.5. Biodisintegration

Disintegration under composting conditions was evaluated by measuring the weight loss of PHBV and PHBV/TPU composite samples according to the ISO 20200 standard [37]. Figure 4.8 shows the evolution of the disintegration (%) over time for neat PHBV, neat TPU and PHBV/TPU blends in lab-scale composting conditions.

Weight loss remains practically unchanged until the 13th day of composting. After that, weight loss increases markedly for all the blends as well as for neat PHBV. In the case of 50/50 samples, up to about 65 wt.% had disintegrated at 41 days, and showed no tendency to plateau. It is estimated that the degree of disintegration would be higher if longer composting periods are considered. However, the blends with TPU content below 50 wt.% reached total disintegration after 36 days of

4. Capítulo 2

testing. No significant differences in weight loss rate were observed among samples with a content lower than 50 wt.%, demonstrating that this relatively high load of TPU does not affect the disintegration of the PHBV/TPU blends. As can be observed, thermoplastic polyurethane is only partially disintegrated after 41 days (8 wt.% disintegration). This rate of disintegration is in agreement with previous reports [29].

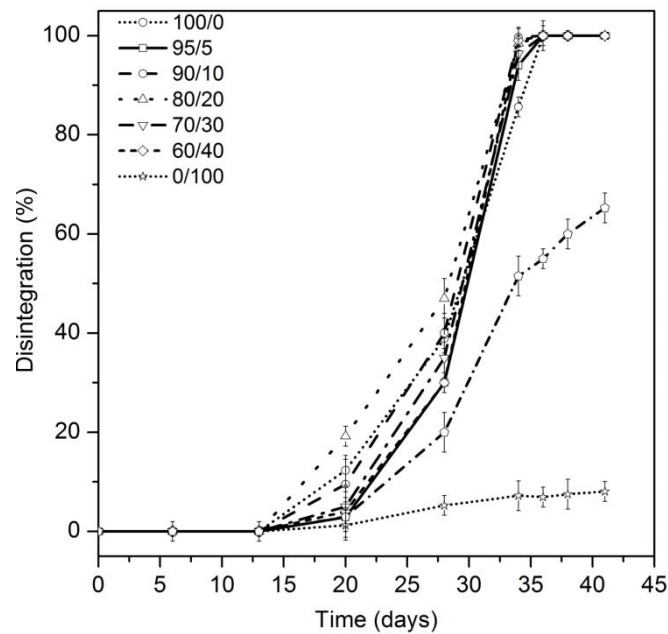


Fig. 4.8. Disintegration of the PHBV/TPU blends over time under composting conditions.

In order to visually assess the impact over time of the composting process on the tested samples, images of the studied blends were taken at different time points (Figure 4.9). All the samples with a TPU content below 50 wt.% exhibited considerable surface deformation and fractures started after 20 days under composting conditions. After 28 days, all these samples were broken into small pieces and showed similar roughening and physical alterations. At longer composting times, samples were found to be further disintegrated, leaving pieces smaller than 2 mm in size. Finally, after 36 days samples reached a level of disintegration where no visible fragments could be recovered.

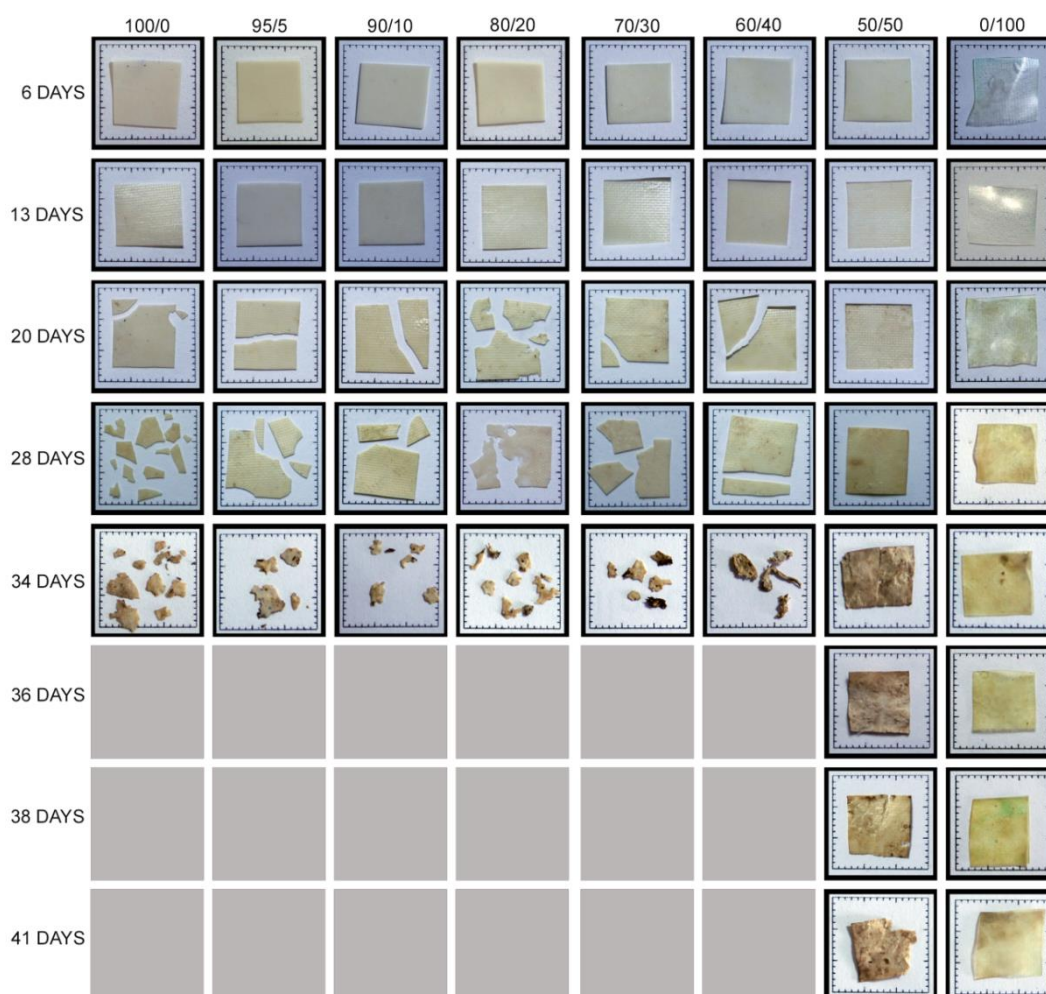


Fig. 4.9. Visual appearance of the tested blend films (PHBV/TPU) after selected time points during the composting process.

Nevertheless, 50/50 and 0/100 samples were still present after 41 days composting. The 50/50 samples showed slight surface roughening and were visibly affected after 34 days. This surface roughening indicates the beginning of the disintegration process. In fact, as reported in the literature, PHB and PHBV disintegration is primarily caused by microorganisms that erode the polymer surface and gradually spread into the bulk [54–56]

On the other hand, TPU does not show this surface alteration. However, a remarkable change in colour and loss of transparency is evident after 28 days. Similar behaviour has been reported for

4. Capítulo 2

PLA films [57,58]. This change in the appearance of the samples was attributed to changes in the refraction index of the materials, to water absorption and/or to the presence of products formed during bacterial hydrolytic processes.

4.4. CONCLUSIONS

Although PHBV polymers are a promising alternative to fossil fuel derived polymers, their excessive brittleness has yet to be overcome without compromising barrier performance. In this work, for the first time an ester-based TPU, which was not stabilised against hydrolysis, has been assessed as an additive in melt blends with PHBV. The incorporation of the TPU did not alter the overall crystallinity or the thermal degradation kinetics of the blends. Elongation at break was increased without drastically compromising the tensile performance. Barrier performance against water vapour and aroma compounds was shown to be comparable to benchmark barrier polyesters when the TPU content was ≤ 30 wt.% and the biodegradability was preserved for TPU loads of at least 40 wt.%. Overall, the blends show a combination of mechanical and barrier performance which exceeds that of commercial PLA, the closest competitor in biodegradable food packaging applications. The study indicates the suitability of these types of elastomers to create biodegradable materials based on PHBV with high barrier properties and better performance for potential food packaging applications.

ACKNOWLEDGEMENTS

The authors wish to thank the European project ECOBIOCAP and the Ministry of Economy and Competitiveness under project MAT2012-38947-C02 for financial support. Jennifer Gonzalez-Ausejo gratefully acknowledges financial support under grant "Pla de promocio de la investigació en la Universitat Jaume I" Predoc/2012/32.

REFERENCES

- [1] B.H. a Rehm, Polyester synthases: natural catalysts for plastics., *Biochem. J.* (2003). doi:10.1042/BJ20031254.
- [2] M.A.M. Reis, L.S. Serafim, P.C. Lemos, A.M. Ramos, F.R. Aguiar, M.C.M. Van Loosdrecht, Production of polyhydroxyalkanoates by mixed microbial cultures, *Bioprocess Biosyst. Eng.* (2003). doi:10.1007/s00449-003-0322-4.

- [3] L.S. Serafim, P.C. Lemos, R. Oliveira, M.A.M. Reis, Optimization of polyhydroxybutyrate production by mixed cultures submitted to aerobic dynamic feeding conditions., *Biotechnol. Bioeng.* 87 (2004) 145–60. doi:10.1002/bit.20085.
- [4] B. Laycock, P. Halley, S. Pratt, A. Werker, P. Lant, The chemomechanical properties of microbial polyhydroxyalkanoates, *Prog. Polym. Sci.* 38 (2013) 536–583. doi:10.1016/j.progpolymsci.2012.06.003.
- [5] S. Khanna, A.K. Srivastava, Recent advances in microbial polyhydroxyalkanoates, *Process Biochem.* (2005). doi:10.1016/j.procbio.2004.01.053.
- [6] D. Cava, E. Gimenez, R. Gavara, J.M. Lagaron, Comparative Performance and Barrier Properties of Biodegradable Thermoplastics and Nanobiocomposites versus PET for Food Packaging Applications, *J. Plast. Film Sheeting.* 22 (2006) 265–274. doi:10.1177/8756087906071354.
- [7] Y.M. Corre, S. Bruzaud, J.L. Audic, Y. Grohens, Morphology and functional properties of commercial polyhydroxyalkanoates: A comprehensive and comparative study, *Polym. Test.* (2012). doi:10.1016/j.polymertesting.2011.11.002.
- [8] T. Keshavarz, I. Roy, Polyhydroxyalkanoates: bioplastics with a green agenda., *Curr. Opin. Microbiol.* 13 (2010) 321–6. doi:10.1016/j.mib.2010.02.006.
- [9] J.M. Nduko, K. Matsumoto, S. Taguchi, Biological lactate-polymers synthesized by one-pot microbial factory: Enzyme and metabolic engineering, in: *ACS Symp. Ser.*, 2012. doi:10.1021/bk-2012-1105.ch014.
- [10] R. Shogren, Water vapor permeability of biodegradable polymers, *J. Environ. Polym. Degrad.* 5 (1997).
- [11] M.L. Di Lorenzo, M. Raimo, E. Cascone, E. Martuscelli, Poly(3-Hydroxybutyrate)-Based Copolymers and Blends: Influence of a Second Component on Crystallization and Thermal Behavior*, *J. Macromol. Sci. Part B.* 40 (2001) 639–667. doi:10.1081/MB-100107554.
- [12] V. Jost, H.-C. Langowski, Effect of different plasticisers on the mechanical and barrier properties of extruded cast PHBV films, *Eur. Polym. J.* 68 (2015) 302–312. doi:10.1016/j.eurpolymj.2015.04.012.
- [13] N. Peelman, P. Ragaert, B. De Meulenaer, D. Adons, R. Peeters, L. Cardon, F. Van Impe, F. Devlieghere, Application of bioplastics for food packaging, *Trends Food Sci. Technol.* (2013). doi:10.1016/j.tifs.2013.06.003.
- [14] L. Yu, K. Dean, L. Li, Polymer blends and composites from renewable resources, *Prog. Polym. Sci.* (2006). doi:10.1016/j.progpolymsci.2006.03.002.
- [15] C.S. Ha, W.J. Cho, Miscibility, properties, and biodegradability of microbial polyester containing blends, *Prog. Polym. Sci.* (2002). doi:10.1016/S0079-6700(01)00050-8.
- [16] P. Ma, D.G. Hristova-Bogaerds, P.J. Lemstra, Y. Zhang, S. Wang, Toughening of PHBV/PBS and PHB/PBS Blends via In situ Compatibilization Using Dicumyl Peroxide as a Free-Radical Grafting Initiator, *Macromol. Mater. Eng.* 297 (2012) 402–410. doi:10.1002/mame.201100224.
- [17] L.H. Mara Cunha, Bruno Fernandes, Jose A. Covas, Antonio A. Vicente, Film blowing of PHBV blends and PHBV-based multilayers for the production of biodegradable packages, *J. Appl. Polym. Sci.* 133 (2016). doi:10.1002/app.42971.
- [18] I. Zembouai, M. Kaci, S. Bruzaud, A. Benhamida, Y.-M. Corre, Y. Grohens, A study of morphological, thermal, rheological and barrier properties of Poly(3-hydroxybutyrate-Co-3-Hydroxyvalerate)/polylactide blends prepared by melt mixing, *Polym. Test.* 32 (2013) 842–851. doi:10.1016/j.polymertesting.2013.04.004.

4. Capítulo 2

- [19] S. Ishida, R. Nagasaki, K. Chino, T. Dong, Y. Inoue, Toughening of Poly(L-lactide) by melt blending with rubbers, *J. Appl. Polym. Sci.* (2009). doi:10.1002/app.30134.
- [20] H. Liu, J. Zhang, Toughening modification of poly(lactic acid) via melt blending, in: *ACS Symp. Ser.*, 2012. doi:10.1021/bk-2012-1105.ch003.
- [21] C. Zhang, C. Man, Y. Pan, W. Wang, L. Jiang, Y. Dan, Toughening of polylactide with natural rubber grafted with poly(butyl acrylate), *Polym. Int.* (2011). doi:10.1002/pi.3118.
- [22] C. Zhang, W. Wang, Y. Huang, Y. Pan, L. Jiang, Y. Dan, Y. Luo, Z. Peng, Thermal, mechanical and rheological properties of polylactide toughened by epoxidized natural rubber, *Mater. Des.* (2013). doi:10.1016/j.matdes.2012.09.024.
- [23] M. Kowalczyk, E. Piorkowska, Mechanisms of plastic deformation in biodegradable polylactide/poly(1,4-cis-isoprene) blends, *J. Appl. Polym. Sci.* (2012). doi:10.1002/app.35489.
- [24] F. Gassner, A.J. Owen, On the physical properties of BIOPOL/ethylene-vinyl acetate blends, *Polymer (Guildf)*. (1992). doi:10.1016/0032-3861(92)91131-K.
- [25] C.C. Han, J. Ismail, H.W. Kammer, Melt reaction in blends of poly(3-hydroxybutyrate-co-3-hydroxyvalerate) and epoxidized natural rubber, in: *Polym. Degrad. Stab.*, 2004. doi:10.1016/j.polymdegradstab.2003.11.020.
- [26] E.-S. Park, H.K. Kim, J.H. Shim, H.S. Kim, L.W. Jang, J.-S. Yoon, Compatibility of poly(butadiene-co-acrylonitrile) with poly(L-lactide) and poly(3-hydroxybutyrate-co-3-hydroxyvalerate), *J. Appl. Polym. Sci.* 92 (2004) 3508–3513. doi:10.1002/app.20356.
- [27] L. Tatai, T.G. Moore, R. Adhikari, F. Malherbe, R. Jayasekara, I. Griffiths, P.A. Gunatillake, Thermoplastic biodegradable polyurethanes: The effect of chain extender structure on properties and in-vitro degradation, *Biomaterials.* (2007). doi:10.1016/j.biomaterials.2007.08.035.
- [28] V. Jašo, G. Glenn, A. Klamczynski, Z.S. Petrović, Biodegradability study of polylactic acid/thermoplastic polyurethane blends, 2015. doi:10.1016/j.polymertesting.2015.07.011.
- [29] Y.D. Kim, S.C. Kim, Effect of chemical structure on the biodegradation of polyurethanes under composting conditions, *Polym. Degrad. Stab.* 62 (1998).
- [30] T. Seidenstücker, H.-G. Fritz, Innovative biodegradable materials based upon starch and thermoplastic poly(ester-urethane) (TPU), *Polym. Degrad. Stab.* 59 (1998).
- [31] Y. Li, H. Shimizu, Toughening of polylactide by melt blending with a biodegradable poly(ether)urethane elastomer, *Macromol. Biosci.* (2007). doi:10.1002/mabi.200700027.
- [32] R.L. Yu, L.S. Zhang, Y.H. Feng, R.Y. Zhang, J. Zhu, Improvement in toughness of polylactide by melt blending with bio-based poly(ester)urethane, *Chinese J. Polym. Sci. (English Ed.)* (2014). doi:10.1007/s10118-014-1487-9.
- [33] V. Jašo, M. Cvetinov, S. Rakić, Z.S. Petrović, Bio-plastics and elastomers from polylactic acid/thermoplastic polyurethane blends, *J. Appl. Polym. Sci.* 131 (2014) n/a-n/a. doi:10.1002/app.41104.
- [34] S. Wang, H. Xiang, R. Wang, C. Peng, Z. Zhou, M. Zhu, Morphology and properties of renewable poly(3-hydroxybutyrate-co-3-hydroxyvalerate) blends with thermoplastic polyurethane, *Polym. Eng. Sci.* (2014). doi:10.1002/pen.23655.
- [35] H. Alata, T. Aoyama, Y. Inoue, Effect of Aging on the Mechanical Properties of Poly(3-hydroxybutyrate-co-3-hydroxyhexanoate), *Macromolecules.* (2007). doi:10.1021/ma070418i.
- [36] Q.-S. Liu, M.-F. Zhu, W.-H. Wu, Z.-Y. Qin, Reducing the formation of six-membered ring ester during thermal degradation of biodegradable PHBV to enhance its thermal stability, *Polym. Degrad. Stab.* 94 (2009) 18–24. doi:10.1016/j.polymdegradstab.2008.10.016.
- [37] UNE-EN ISO 20200 Determinación del grado de desintegración de materiales plásticos bajo condiciones de compostaje simuladas en un laboratorio, (2006).

- [38] L.A. Utracki, Polymer alloys and blends. State of the art, *Polym. Networks & Blends*. 1 (1991).
- [39] R. Simha, R.F. Boyer, On a general relation involving the glass temperature and coefficients of expansion of polymers, *J. Chem. Phys.* 37 (1962).
- [40] M. Kunioka, A. Tamaki, Y. Doi, Crystalline and thermal properties of bacterial copolyesters: Poly(3-hydroxybutyrate-co-3-hydroxyvalerate) and poly(3-hydroxybutyrate-co-4-hydroxybutyrate), *Macromolecules*. 22 (1989).
- [41] L.M.W.K. Gunaratne, R.A. Shanks, Multiple melting behaviour of poly(3-hydroxybutyrate-co-hydroxyvalerate) using step-scan DSC, *Eur. Polym. J.* (2005). doi:10.1016/j.eurpolymj.2005.06.015.
- [42] N. Grassie, E.J. Murray, P.A. Holmes, The thermal degradation of poly(-D)-3-hydroxybutyric acid): Part 3-The reaction mechanism, *Polym. Degrad. Stab.* 6 (1984) 127–134. doi:10.1016/0141-3910(84)90032-6.
- [43] R. Abate, A. Ballistreri, G. Montaudo, G. Impallomeni, Thermal degradation of microbial poly(4-hydroxybutyrate), *Macromolecules*. 27 (1994).
- [44] M. Floros, L. Hojabri, E. Abraham, J. Jose, S. Thomas, L. Pothan, A.L. Leao, S. Narine, Enhancement of thermal stability, strength and extensibility of lipid-based polyurethanes with cellulose-based nanofibers, in: *Polym. Degrad. Stab.*, 2012. doi:10.1016/j.polymdegradstab.2012.02.016.
- [45] A.K. Barick, D.K. Tripathy, Thermal and dynamic mechanical characterization of thermoplastic polyurethane/organoclay nanocomposites prepared by melt compounding, *Mater. Sci. Eng. A.* (2010). doi:10.1016/j.msea.2009.10.063.
- [46] M. Herrera, G. Matuschek, A. Kettrup, Thermal degradation of thermoplastic polyurethane elastomers (TPU) based on MDI, *Polym. Degrad. Stab.* (2002). doi:10.1016/S0141-3910(02)00181-7.
- [47] C.L. Simões, J.C. Viana, A.M. Cunha, Mechanical properties of poly(ϵ -caprolactone) and poly(lactic acid) blends, *J. Appl. Polym. Sci.* (2009). doi:10.1002/app.29425.
- [48] N.C. Loureiro, J.L. Esteves, J.C. Viana, S. Ghosh, Mechanical characterization of polyhydroxyalkanoate and poly (lactic acid) blends, *J. Thermoplast. Compos. Mater.* (2013). doi:10.1177/0892705712475020.
- [49] M.E. Broz, D.L. VanderHart, N.R. Washburn, Structure and mechanical properties of poly(D,L-lactic acid)/poly(??-caprolactone) blends, *Biomaterials.* (2003). doi:10.1016/S0142-9612(03)00314-4.
- [50] E.D. Bliznakov, C.C. White, M.T. Shaw, Mechanical properties of blends of HDPE and recycled urea-formaldehyde resin, *J. Appl. Polym. Sci.* (2000). doi:10.1002/1097-4628(20000929)77:14<3220::AID-APP250>3.0.CO;2-4.
- [51] N. Tomar, S.N. Maiti, Mechanical properties of PBT/ABAS blends, *J. Appl. Polym. Sci.* 104 (2007). doi:10.1002/app.25831.
- [52] N. Follain, C. Chappey, E. Dargent, F. Chivrac, R. Crétois, S. Marais, Structure and barrier properties of biodegradable polyhydroxyalkanoate films, *J. Phys. Chem. C.* (2014). doi:10.1021/jp408150k.
- [53] A. Martínez-Abad, L. Cabedo, C.S.S. Oliveira, L. Hilliou, M. Reis, J.M. Lagarón, Characterization of polyhydroxyalkanoate blends incorporating unpurified biosustainably produced poly(3-hydroxybutyrate-co-3-hydroxyvalerate), *J. Appl. Polym. Sci.* (2016). doi:10.1002/app.42633.
- [54] D. Puglia, E. Fortunati, D.A. D'Amico, L.B. Manfredi, V.P. Cyras, J.M. Kenny, Influence of organically modified clays on the properties and disintegrability in compost of solution cast poly(3-hydroxybutyrate) films, *Polym. Degrad. Stab.* (2014). doi:10.1016/j.polymdegradstab.2013.11.013.

4. Capítulo 2

- [55] Y.-X. Weng, Y. Wang, X.-L. Wang, Y.-Z. Wang, Biodegradation behavior of PHBV films in a pilot-scale composting condition, *Polym. Test.* 29 (2010) 579–587. doi:10.1016/j.polymertesting.2010.04.002.
- [56] K. Iggui, N. Le Moigne, M. Kaci, S. Cambe, J.-R. Degorce-Dumas, A. Bergeret, A biodegradation study of poly(3-hydroxybutyrate-co-3-hydroxyvalerate)/organoclay nanocomposites in various environmental conditions, *Polym. Degrad. Stab.* 119 (2015) 77–86. doi:10.1016/j.polymdegradstab.2015.05.002.
- [57] M.P. Arrieta, J. López, E. Rayón, a. Jiménez, Disintegrability under composting conditions of plasticized PLA–PHB blends, *Polym. Degrad. Stab.* (2014) 1–12. doi:10.1016/j.polymdegradstab.2014.01.034.
- [58] E. Fortunati, I. Armentano, A. Iannoni, M. Barbale, S. Zaccheo, M. Scavone, L. Visai, J.M. Kenny, New multifunctional poly(lactide acid) composites: Mechanical, antibacterial, and degradation properties, *J. Appl. Polym. Sci.* (2012). doi:10.1002/app.35039.

5. Capítulo 3

Compatibilization of PHBV/PLA blends with diisocyanates

5. Capítulo 3

Compatibilization of PHBV/PLA blends with diisocyanates

Jennifer González-Ausejo¹, Estefania Sánchez-Safont¹, José Maria Lagarón², Rafael Balart³, Luis Cabedo¹ and José Gámez-Pérez¹

¹Polymer and Advanced Materials Group (PIMA), Universidad Jaume I, 12071 Castellon, Spain

²Novel Materials and Nanotechnology Group, IATA-CSIC, 46980 Paterna (Valencia), Spain

³Instituto de Tecnología de Materiales (ITM), Universidad Politécnica de Valencia, Campus de Alcoi, 03801 Alcoy (Alicante), Spain

Journal of Applied Polymer Science (2017)

ABSTRACT

Poly(3-hydroxybutyrate-co-3-hydroxyvalerate) (PHBV) was blended with poly(lactic acid) (PLA) using various reactive processing agents in order to decrease its brittleness and enhance its processability. Three diisocyanates, namely, hexamethylene diisocyanate (HMDI), poly(hexamethylene) diisocyanate (polyHMDI) and 1,4-phenylene diisocyanate (PDI), were used as compatibilizing agents. The morphology, thermomechanical properties and rheological behavior were investigated using scanning electron microscopy (SEM), thermogravimetric analysis (TGA), differential scanning calorimetry (DSC), tensile tests, dynamo-mechanical thermal analysis in torsion mode (DMTA) and oscillatory rheometry with a parallel plate setup. The presence of the diisocyanates resulted in an enhanced polymer blend compatibility, thus leading to an improvement in the overall mechanical performance without affecting the thermal stability of the system. A slight reduction in PHBV crystallinity was observed with the incorporation of the diisocyanates. The addition of diisocyanates to the PHBV/PLA blend resulted in a notable increase in the final complex viscosity at low frequencies when compared with the same system without compatibilizers.

GRAFICAL ABSTRACT

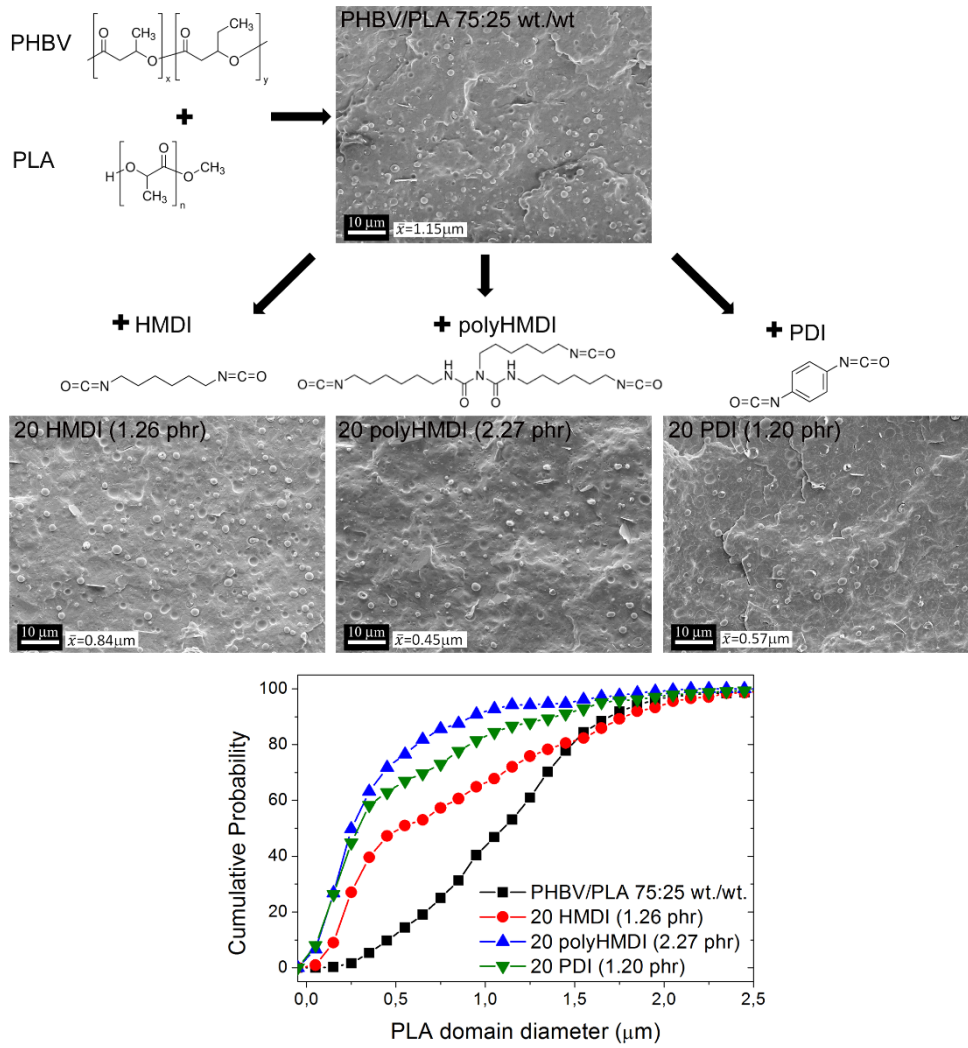


Fig 5.1: Graphical abstract of the work named Compatibilization of PHBV/PLA blends with diisocyanates.

5.1. INTRODUCTION

Biopolymers have generated significant interest in recent years due to increasing awareness of environmental problems involving large amounts of discarded plastic. Most plastic items are produced from fossil fuels and they show very high degradation times (about 100-300 years), meaning that in the worst case scenario, they are left in the sea or waste landfills. In some cases, they are burned to recover some of the embodied energy, but their incineration produces an increased concentration of carbon dioxide in the atmosphere, while toxic gases are also released to the environment during the combustion cycle. This has led to an increased interest in the study of polymers derived from renewable resources, such as aliphatic biopolyesters, with the ability to completely biodegrade in composting conditions due to their hydrolysable backbone, thus alleviating the problem of landfill saturation [1,2].

Among these biopolymers, there are two that are raising an increasing industrial interest, polylactic acid (PLA) and poly(3-hydroxybutyrate-co-3-hydroxyvalerate) (PHBV). PLA is a semicrystalline polymer which can present a relatively high strength and modulus, similar to that of PET and which shows an excellent thermoformability. However, its slow crystallization rate limits its potential applicability boundaries, such as permeability to gases and toughness, preventing its possible replacement of non-biodegradable polymers such as PET [3–5].

PHBV is a copolymer that presents similar crystallinity index that the homopolymer poly(hydroxybutyrate). The random valerate content in PHBV (below 25%) as a matter of fact, does not alter the usual PHB crystal structure and it shows similar properties as PHB, such as high tensile strength, high service temperature -similar to that of polypropylene (PP) [6] and barrier properties to oxygen close to that of the poly(ethylene terephthalate) (PET) [7]. However, PHB practical application has been restricted by some other disadvantages such as thermal degradation (close to melting temperature) during processing and consequently a narrow processing window. The addition of valerate in PHBV decreases partially the melting point of the homopolymer, allowing its processing at slightly lower temperatures, thus decreasing thermal degradation. Even though this improvement, PHBV as well as PHB shows brittleness and a much higher cost compared to the fossil equivalents [7–11].

5. Capítulo 3

Since polymer blending is a convenient approach to overcome the individual disadvantages of polymers and it allows for the production of new materials with improved properties [12–16], several researchers have reported the study of PHBV/PLA blends [17–24] as a way to overcome some limitations of PHBV. They claim that by decreasing the overall crystalline nature of the blend, brittleness, for instance, can be reduced. However, the resulting blends did not show the expected performance, being attributed to the lack of compatibility of these biopolyesters [18–20]. A possible solution to this problem can be reached by increasing the interfacial adhesion, using a compatibilizer capable of reacting with the terminal groups of both PHBV and PLA during melt processing. This method, known as reactive blending, is very convenient due to its easy implementation on an industrial scale, using conventional polymer processing facilities. By blending PHBV with PLA, one should expect to decrease the processing temperature of PHBV, enlarge the processing window of PHBV for thermoforming by increasing the melt strength and also reduce the brittleness of the PHBV associated to secondary crystallization [25,26]. Indeed, the use of such as compatibilizers may have another positive influence on the blends, acting as chain extender thermal stabilizers [27].

Recently, Zembouai et al. [19] prepared blends based on PLA and PHBV by grafting maleic anhydride onto PHBV as a compatibilizing agent in combination with the addition of Cloisite 30B. Their results revealed that the morphology of the blend changed from co-continuous to a dispersed-type. This was attributed to the reduction of interfacial tension (increased interaction) among the interface between the blend components and the location of the clay in the blend. The blends exhibited enhanced mechanical properties with respect to the uncompatibilized PHBV/PLA blend, especially when PHBV was previously compatibilized.

Pivsa-Art et al. [28] studied the mechanical properties and biodegradation effect of PLA and PHBV blends with polyethylene glycol (PEG) as the compatibilizer, with molecular weights of 4000 and 6000 for biodegradable textile applications. It was found that the addition of PEG improved the tensile strength and Young's Modulus.

One group of reagents that could be used as compatibilizers in PHBV/PLA blends and have not yet been explored are diisocyanates. Isocyanates can react with either hydroxyl or carboxyl groups to form urethane linkages, as described in the literature (see refs. [29–33] to mention a few). As Zeng

noted out in his excellent review about compatibilization of PLA blends [33], isocyanates containing more than one isocyanate group can be used to compatibilize PLA blends with other polymers that contain hydroxyl or amino groups, since the isocyanates can react with terminal groups randomly thus generating copolymers of both blend components that can compatibilize the blend. The systems studied by Zeng in that work included PLA with biodegradable polyesters, polyamides and natural polymers.

Therefore, diisocyanates are promising reactive compatibilizers for blending PHBV with PLA which. To the best of our knowledge, have not been reported. In order to investigate their potential to improve the properties of PHBV/PLA blends in terms of their rheological and mechanical properties, three different diisocyanates have been tested with a fixed PHBV/PLA ratio of 75/25 in weight.

The systems were chosen looking for its applicability in thermoformed packaging applications. So, one of the diisocyanates was chosen among those approved for food contact applications: hexamethylene diisocyanate (HMDI). Another diisocyanate worth to try was considered to be 1,4-phenylene diisocyanate (PDI), known to its high reactivity. Finally, to take advantage of the ability of the isocyanates to react with terminal groups of the polymer chains, a trifunctional isocyanate, poly(hexamethylene) diisocyanate (polyHMDI) was selected, with the aim of increasing the melt strength of the blend.

Even though isocyanates are known to be quite toxic, we are optimistic about their potential use as additives for compatibilizing blends, since they are used at very low contents ($\leq 1\%$) and they are submitted to an environment in which they are prompt to react to form polyurethanes (inside the extrusion barrel, with high temperature and high concentration of reactive species).

The ratio of PHBV/PLA 75/25 in wt. was selected since, according to literature, it presents the best compromise between barrier properties, maximum service temperature and deformation at rupture [20,34].

5.2. EXPERIMENTAL

5.2.1. Materials

PHBV with 3 mol.% hydroxyvalerate content was purchased from the Tianan Biologic Material Co. (Ningbo, P.R. China) in pellet form (ENMAT Y1000P). PLA Ingeo™ Biopolymer commercial grade 2003D was supplied by the NatureWorks® Co. LLC, USA. The three compatibilizers used (hexamethylene diisocyanate, poly(hexamethylene) diisocyanate and 1,4-phenylene diisocyanate) were supplied by Sigma Aldrich.

5.2.2. Blend preparation

The PHBV and PLA used in this study were dried under vacuum at 80 °C for 2 h before use by a Piovan DPA 10 (Santa Maria di Sala VE, Italy), while the compatibilizers were used as received. The PHBV/PLA blends with 75:25 wt./wt., respectively, and different contents of compatibilizers were obtained by melt blending using an internal mixer (Rheomix 3000P ThermoHaake, Karlsruhe, Germany). To avoid degradation, the mixing time was kept under 4 min at a temperature of 180 °C and a rotor speed of 100 rpm. The mixer is supplied with software for displaying the variation of temperature (chamber and melt) and the torque during mixing. According to the melt temperature sensor during mixing, the melt temperature never reached 195 °C, which guaranteed that there was no severe thermal degradation during blending.

Films (0.2 mm thick) for scanning electron microscopy (SEM), thermogravimetric analysis (TGA), differential scanning calorimetry (DSC) and mechanical property analysis were obtained from the blends by melting in a hot-plate press (180 °C, 2 min for pre-melting, followed by 2 min at 3 bar). DMTA specimens with a thickness of 4 mm were obtained from injected bars, in a Meteor 270/75 injection molding machine (Mateu & Sole, Barcelona, Spain) with an injection temperature of 180 °C at the nozzle. For rheological measurements, discs (25 mm diameter and 2 mm thick) were obtained from the blends by melting in a hot-plate press at 180 °C and applying 300 bar for 2.5 min. All the samples were stored in a vacuum desiccator at ambient temperature for two weeks to allow full crystallization to take place [35].

Samples of both PHBV and PLA (referred to as neat PHBV and neat PLA, respectively) were processed under the same conditions as the blends, for the sake of comparison. The nomenclature used for the blends is as follows: PHBV/PLA for the systems with 75:25 wt./wt. without compatibilizer, and XY for the compatibilized blends, where X is the compatibilizer content and Y is the compatibilizer type: hexamethylene diisocyanate (HMDI), poly(hexamethylene diisocyanate) (polyHMDI) and 1,4-phenylene diisocyanate (PDI).

The compatibilizer content X was indicated as the estimated molar ration between the functional polymer reactive sites (alcohol and carboxylic acid end groups) and the compatibilizer ones (isocyanates), according to the available Mn and molecular weight data of polymers and isocyanates. For comparison purposes, these ratios were set equally at 1:1, 1:10 and 1:20 for the three isocyanates studied. Table 5.1 summarizes the detailed compositions of all the blends studied.

Table 5.1: Nomenclature of studied PHBV, PLA and PHBV/PLA blends.

SAMPLE	Weigh percentage		Molar ratio			Compatibilizer phr
	PHBV	PLA	HMDI	polyHMDI	PDI	
Neat PHBV	100					
Neat PLA		100				
PHBV/PLA	75	25				
1HMDI	75	25	1:1			0.06
10HMDI	75	25	1:10			0.63
20HMDI	75	25	1:20			1.26
1polyHMDI	75	25		1:1		0.11
10polyHMDI	75	25		1:10		1.14
20polyHMDI	75	25		1:20		2.27
1PDI	75	25			1:1	0.06
10PDI	75	25			1:10	0.60
20PDI	75	25			1:20	1.20

5.2.3. Characterization

The morphology of the cryofractured surfaces of the PHBV/PLA blends was evaluated by SEM using a JEOL 7001F. The samples were fractured in liquid nitrogen and subsequently coated by sputtering with a thin layer of Pt. The size of the dispersed phase observed in the SEM micrograph was evaluated, measuring the length of the spheres in microphotographs with ImageJ software (the number of spheres analysed was over 400 in all cases).

The thermal stability of the blends was investigated by means of TGA using a TG-STDA Mettler Toledo model TGA/SDTA851e/LF/1600. The samples were heated from 50 to 900 °C at a heating rate of 10 °C/min under nitrogen flow. The characteristic temperatures, $T_{5\%}$ and T_d , corresponded, respectively, to the initial decomposition temperature (5% weight loss) and to the maximum degradation rate temperature measured at the derivative thermogravimetric analysis (DTG) peak maximum.

DSC experiments were conducted using a DSC2 (Mettler Toledo) with an intracooler (Julabo modelo FT900). The weight of the DSC samples was typically 6 mg. Samples were first heated from -20 to 200 °C at 10 °C/min, kept for 1 min at 200 °C, cooled down to -20 °C at 10 °C/min, and then finally heated to 200 °C at 10 °C/min. The crystallization temperature (T_c), melting temperature (T_m) and melting enthalpy (ΔH_m) were determined from the cooling and second heating curve. T_m and ΔH_m were taken as the peak temperature and the area of the melting endotherm, respectively. By overlapping DSC scans of PLA, PHBV and PLA/PHBV blends, it could be deduced that PLA remains amorphous in the blends. Therefore, the net crystallinity (X_c) of the blends (after removing cold crystallization of PLA) corresponds solely to the PHBV phase and was calculated by the following expression:

$$X_c (\%) = \frac{\Delta H_m}{w \cdot \Delta H_m^0} \cdot 100 \quad (5.1)$$

where ΔH_m (J/g) is the melting enthalpy of the polymer matrix, ΔH_m^0 is the melting enthalpy of 100% crystalline PHBV (perfect crystal) (146 J/g) and w is the polymer weight fraction of PHBV in the blend [36]. The DSC instrument was calibrated with an indium standard before use.

Tensile tests were carried out in a universal testing machine (Shimadzu AGS-X 500N) at a crosshead rate of 10 mm/min at room temperature. All samples were allowed to reach the equilibrium under ambient conditions (25 °C and 50% R.H. for 24 hours before the testing). Tests were performed according to ASTM D638 with dumb-bell samples die-cut from approximately 200 μm thick films prepared by hot press. Five specimens of each sample were tested and the average results with standard deviation were reported.

Dynamic mechanical analysis (DMTA) experiments were conducted in an oscillatory rheometer AR G2 (TA Instruments, New Castle, EEUU) equipped with a clamp system for solid samples (torsion mode). Samples sizing 40 x 10 x 4 mm^3 were subjected to a heating program from -20 to 130 °C with a heating rate of 2 °C/min at a constant frequency of 1 Hz. The maximum deformation (γ) was set to 0.1%.

Rheological Measurements. Oscillatory shear measurements were performed using an oscillatory rheometer AR G2 (TA Instruments, New Castle, EEUU) equipped with parallel plates of 25 mm diameter using a gap of 1.5 mm. Sample disks were vacuum dried at 60 °C for 24 h before testing. Strain sweep viscoelastic tests were first performed at a fixed angular frequency of 1 Hz in order to determine the extent of the linear regime, then, frequency sweep experiments were carried out at a fixed strain in the linear regime in order to determine the linear viscoelastic moduli, G' (storage modulus) and G'' (loss modulus), as well as the complex viscosity η^* . The angular frequencies were swept from 100 to 0.01 Hz with five points per decade at temperatures of 180 °C.

5.3. RESULTS AND DISCUSSION

5.3.1. Morphology

The morphology of the blends can be related with the degree of compatibility of their components. The morphology of the PHBV/PLA blends is clearly affected by the presence of the diisocyanates, as observed SEM.

Fig. 5.2 presents the SEM micrographs of all the PHBV/PLA blends studied as a function of diisocyanate type and content, as well as the histograms of the size for the dispersed phase. The SEM morphology observed for the PHBV/PLA blend without any compatibilizer (Fig. 5.2.a) shows

5. Capítulo 3

spheres of PLA (1.15 μm average diameter) evenly dispersed in the PHBV matrix. The neat separation between the phases and the presence of a detachment phenomenon is an evidence that indicates that the two phases are not compatible. Indeed, several authors have also reported the poor compatibility of PHBV/PLA blends with similar PHBV/PLA ratios blend [36].

The addition of diisocyanates produces a compatibilization effect that can be clearly observed with a reduction of the particle diameter of the dispersed PLA phase. Figs. 5.2.b, 5.2.e and 5.2.h show that the addition of HMDI reduces the PLA particle size to average diameter values ranging from 0.84 to 0.88 μm . However, even though the differences in particle size may not be very pronounced as the HMDI content increases, at a 1:10 molar ratio and above, two populations of sphere sizes can be identified, showing a significantly higher ratio of entities with less than 0.7 μm . Furthermore, an increase in the amount of particles that are not detached can be observed for a 1:20 HMDI molar ratio (Fig. 5.2.h), indicating better compatibility.

Regarding the effect of polyHMDI on the blends, there is a remarkable decrease in PLA domain size with increasing polyHMDI content, as seen in Figs. 5.2.c, 5.2.f and 5.2.i, with average particle diameters of 0.95, 0.66 and 0.45 μm , respectively. This reduction in domain size is clearly seen in the corresponding histogram (Fig. 5.2.l). Indeed, it can be observed that higher concentrations of polyHMDI seems to improve the adhesion between the phases decreasing the amount of detached particles, thus indicating higher compatibilization between both biopolymers [19].

As well as polyHMDI, the use of PDI leads to a noticeable reduction in the size of PLA domains for all the contents studied in this work (Figs. 5.2.d, 5.2.g and 5.2.j), with the average diameters being about 0.83, 0.58 and 0.57 μm for 1:1, 1:10 and 1:20 molar ratios, respectively. Although no differences in the morphology and domain size of PLA are observed at 1:20 with respect to a 1:10 molar ratios of PDI (Fig. 5.2.m), detached PLA particles in SEM micrographs are significantly reduced with the highest PDI content. This observation would be in agreement with an increase in the interfacial adhesion and compatibility between both phases, promoted by PDI.

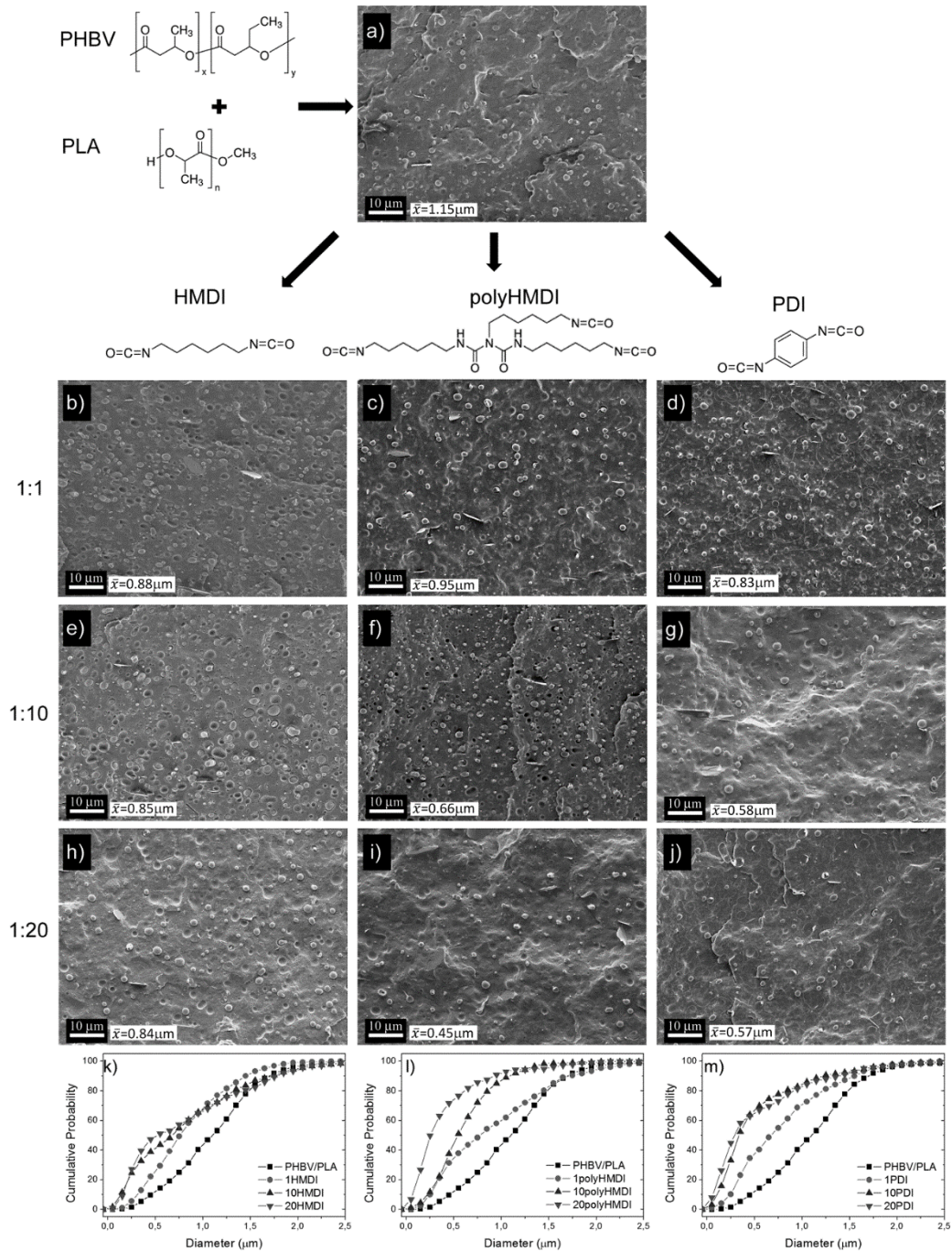


Fig. 5.2: SEM images of the fracture surfaces of PHBV/PLA blends with diisocyanates.

5.3.2. Thermal characterization

In order to study the effect of compatibilizer content and type on the thermal stability of PHBV/PLA blends, TGA experiments were carried out. The mass loss and the DTG versus temperature for the neat PHBV, neat PLA and PHBV/PLA blends (with and without compatibilizers) were recorded and the values of the onset degradation temperature ($T_{5\%}$) and maximum degradation rate temperature (T_d) were calculated for all samples studied. Table 5.2 summarises all the parameters obtained.

Table 5.2: DSC and TGA data of PHBV and PHBV/PLA blends with and without diisocyanates.

	T_m (°C)	X_c (%)	T_c (°C)	$T_{5\%}$ (°C)	T_{d1} (PHBV) (°C)	T_{d2} (PLA) (°C)
Neat PHBV	171.8±0.2	66.6±0.6	122.4±0.1	274±1	289±1	-
PHBV/PLA	172.05±0.1	63.3±2.3	120.9±0.1	275±1	288±2	350±1
1HMDI	171.7±0.0	68.7±0.4	120.5±0.1	275±2	289±1	350±1
10HMDI	170.2±0.3	63.6±0.4	111.7±0.1	274±1	288±1	338±2
20HMDI	170.2±0.2	63.1±4.9	111.2±0.2	274±2	289±1	346±1
1polyHMDI	170.6±0.2	63.0±6.2	115.9±0.1	275±1	288±2	350±1
10polyHMDI	170.7±0.0	63.2±2.7	113.0±0.1	272±1	287±1	338±1
20polyHMDI	170.0±0.2	62.3±2.5	111.5±0.2	274±2	286±2	326±2
1PDI	170.7±0.3	63.3±0.7	112.2±0.2	276±1	288±1	350±1
10PDI	170.5±0.0	62.9±1.6	113.4±0.0	276±1	290±2	349±1
20PDI	170.5±0.0	64.7±1.0	112.2±0.1	276±2	290±2	322±2

The PHBV/PLA blends exhibit a two-stage mass loss step, with an onset degradation temperature ($T_{5\%}$) at about 275 °C. The first step is characterised by a maximum mass loss rate (T_{d1}) at about 288 °C and another (T_{d2}) at around 350 °C. The first one is related to the thermal degradation of PHBV, which consists of a single weight loss step between 240 and 320 °C, corresponding to a random chain scission reaction [37]. The second step is a consequence of the thermal degradation of PLA that takes place by the cleavage of bonds on the backbone to form cyclic oligomers, lactide and carbon monoxide as products [38].

The thermal decomposition process of the blends containing the diisocyanates did not show significant variations with respect to the uncompatibilized blend in $T_{5\%}$, with the exception of 10polyHMDI which showed a decrease in $T_{5\%}$ of about 3 °C. Regarding the maximum degradation rate temperatures, T_{d1} corresponding to the PHBV remained unchanged, whereas T_{d2} shifted to lower temperatures with increasing addition of diisocyanates. It is worthwhile highlighting the values of 326 and 322 °C for 1:20 molar ratios of polyHMDI and PDI, respectively. This behavior, which is also seen in other PLA/diisocyanates systems, can be attributed to the reaction of the remaining diisocyanates with the PLA chains and/or their degradation products [39].

Even though the maximum degradation rate temperature corresponding to the PLA fraction of the blends is reduced, the effect of diisocyanates on the overall thermal stability of the compounds, from a practical point of view, led by the PHBV matrix, is negligible.

In order to establish if the addition of diisocyanates alters the crystallization behavior of PHBV/PLA blends, DSC measurements were performed for samples with and without compatibilizers. Representative DSC curves of cooling and heating scans, after removal of the thermal history, are displayed in Fig. 5.3. Table 5.2 summarises the main parameters, crystallization and melting temperatures, crystallization enthalpies and degrees of crystallinity for all the samples studied in this work.

As shown in Fig. 5.3, the PHBV/PLA blends exhibit a mixed behavior corresponding to their blend ratio. In the blends, two peaks (a melting peak around 172 °C and a crystallization peak around 122 °C) can be related with the typical PHBV thermal behavior (neat PHBV in Table 2). Also, the PLA melting signal can be appreciated as small shoulders in the blend thermograms, although the endothermic cold crystallization peak of PLA (present in the neat PLA at 112.6 °C) cannot be easily determined.

After analysing the resulting DSC thermograms for the compatibilized blends, it can be noted that the T_c of PHBV was significantly shifted to lower temperatures (Fig. 5.3b) when the diisocyanates were incorporated in the PHBV/PLA blends. This shift in T_c is more pronounced as the diisocyanate content is increased. Since the PHBV used in this study contains boron nitride, as nucleating agent, the resulting decrease in T_c can be attributed to the reaction products of the diisocyanates with PHBV and PLA, which would be able to hinder the crystallization of PHBV, and some side reactions

of the isocyanates with the boron nitride particles, which would decrease the nucleating effect on PHBV. SEM micrographs of uncompatibilized blends and compatibilized ones show that boron nitride particles are detached in the first ones, but show some polymer stuck to them in the presence of compatibilizers (Fig. 5.4).

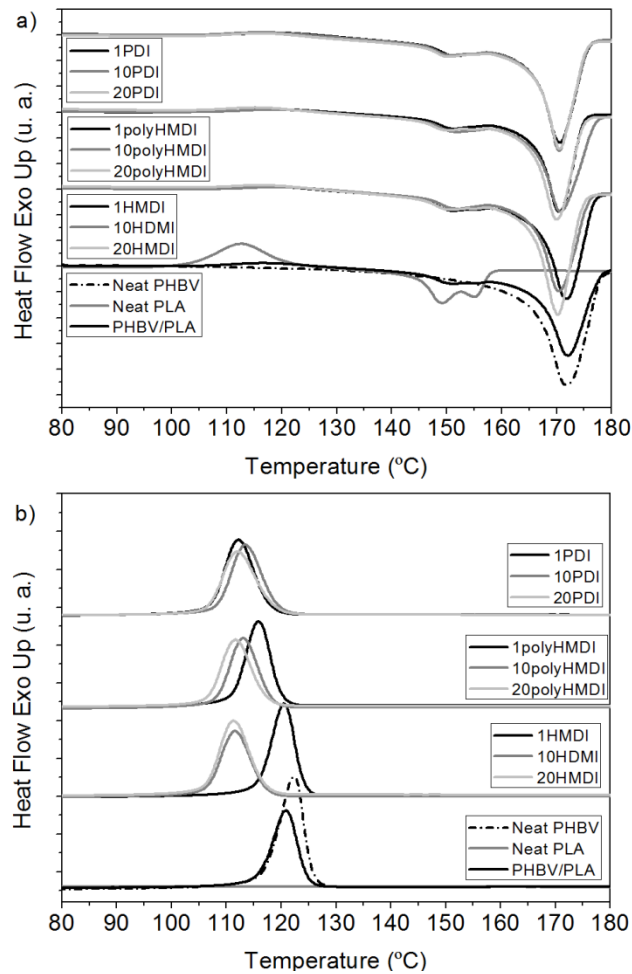


Fig. 5.3: DSC curves of neat PHBV, PHBV/PLA and PHBV/PLA blends with a 1:20 molar ratio of diisocyanates.

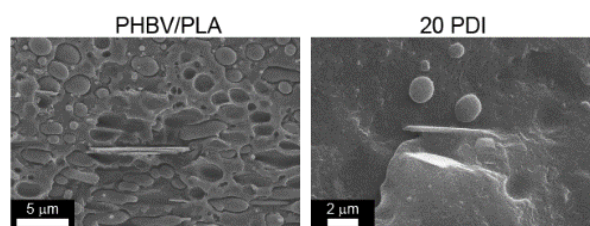


Fig. 5.4: SEM micrographs of boron nitride particles in PHBV/PLA blend and PHBV/PLA blend with a 1:20 molar ratio of PDI.

The degree of crystallinity (X_c) for the compatibilized blends, as shown in Table 5.2, remained similar to those observed for the uncompatibilized PHBV/PLA blend. Nevertheless, this value is about 3-4% lower than the neat PHBV, indicating that the addition of PLA in the PHBV matrix is responsible for such a slight decrease in its crystallinity. Regarding the melting peak temperature of PHBV (T_m) in blends with diisocyanates, it could be observed a drop around 2 °C with respect to neat PHBV or PHBV/PLA.

As mentioned before, isocyanates can combine with terminal alcohol and carboxylic acids. Since terminal groups of PHBV and PLA are alcohol and carboxylic acids, we expect that random reaction will make block copolymers of PLA and PHBV, thus providing a way of compatibilizing both polymers. Indeed, the secondary amines resulting in urethane groups can react with other isocyanates, providing a cross-linking point. In all cases, these species are excluded from crystal lattices, so they would tend to decrease a priori the crystallinity ratio of PHBV. In the case of PolyHMDI, since it is a trifunctional isocyanate, cross-linking is highly expected providing an explanation on why 1:1 ratio of HMDI does not alter the PHBV ability to crystallize, whereas 1:1 polyHMDI does. PDI, on the other hand, is a very reactive diisocyanate, so it may have had an influence on the particle size by starting the compatibilization of the blend sooner in the extrusion barrel, increasing the melt viscosity and making a more effective mixture during the reactive blending.

It is interesting to note that the composition 1:1 HMDI behaves differently from the rest of compatibilized blends, showing a slight increase in crystallinity index and not presenting a variation in T_c with respect to neat PHBV nor the uncompatibilized blend. This may be a consequence of the relative low amount of diisocyanate added, not making crosslinking points as in the case of polyHMDI. Also, there is another case that calls the attention, which is the melting behaviour of

5. Capítulo 3

10polyHMDI, which shows a broader melting signal at higher temperatures, suggesting that it has a larger population of thicker lamellae compared to the rest of the compatibilized blends (Fig. 5.3.a). These findings correlate well with their mechanical properties, analysed subsequently.

5.3.3. Mechanical properties

For the purpose of studying the effect of compatibilizer content and type on the mechanical properties of PHBV/PLA blends, tensile tests to rupture were conducted on specimens obtained from hot-pressed films. The Young's modulus, tensile strength and elongation at break for all the samples were assessed and the values obtained are summarised as a function of compatibilizer content in Fig. 5.5.

In Fig. 5.5.a it can be seen that the addition of 25 wt.% of PLA to PHBV does not significantly affect the average values of the Young's modulus nor the strength at break of neat PHBV. Only a slight decrease in the elongation at break is observed in Fig. 5.5.b.

The role of the compatibilizer in the PHBV/PLA blends is more complex. It can be clearly observed in Fig. 5.5.b that the compatibilizer produces a significant increase in the elongation at break with respect to the uncompatibilized PHBV/PLA blend. However, increasing the compatibilizing content does not produce clear trends for the tensile properties.

It is interesting to highlight the tensile behavior of the 10polyHMDI composition, which shows an increase in tensile strength of 35%, as well as an increase of 53% in the elongation at break with respect to the uncompatibilized blend. Another interesting result can be found in the 1HMDI blend, where a very small amount of compatibilizer produced the highest increase in the elongation at break. This special mechanical behavior observed for 10polyHMDI and 1HMDI can be related to the peculiarities described in the DSC results.

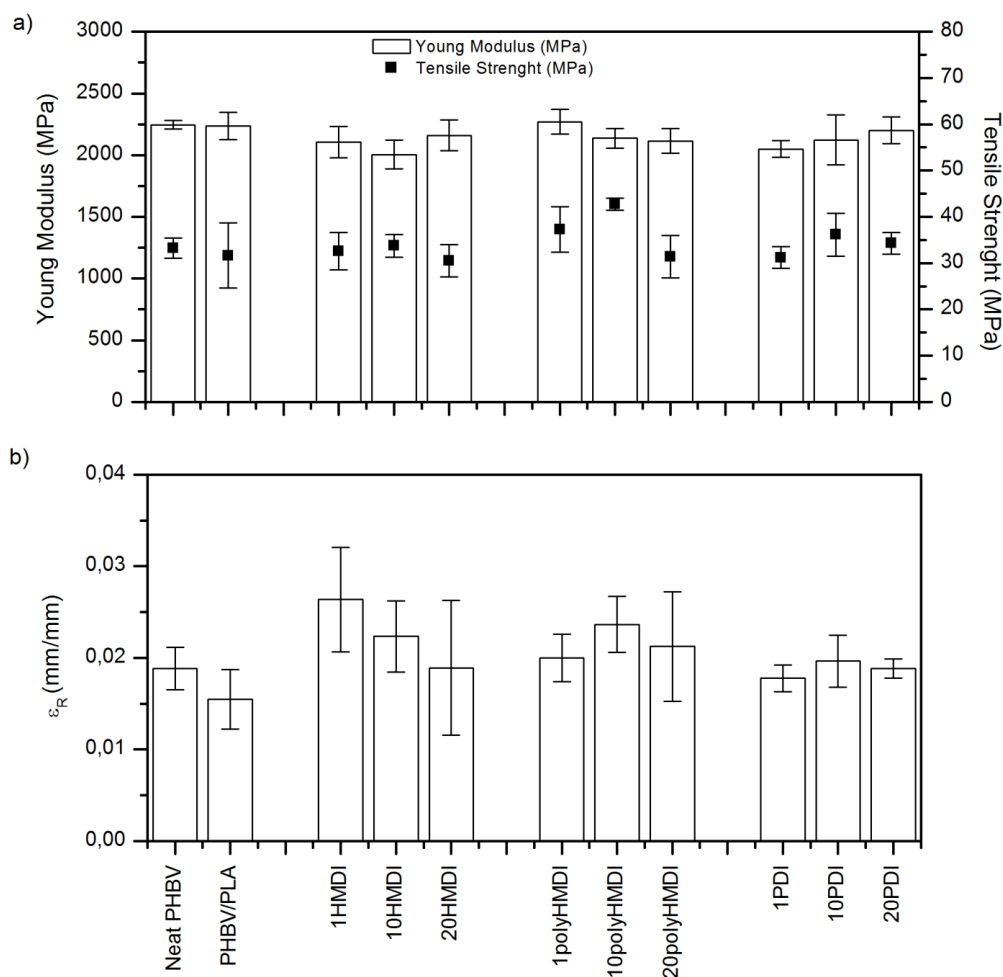


Fig. 5.5: Young's modulus (E), tensile strength (σ_y) and elongation at break (ϵ_R) of neat PHBV and PHBV/PLA blends with diisocyanates versus compatibilizer content.

The viscoelastic behavior and compatibilization degree of the PHBV/PLA blends were studied by DMTA, analysing their storage modulus (G') and $\tan(\delta)$ curves in a temperature range from -10 to 130 °C. The most representative curves (neat PHBV, PHBV/PLA, 1:20 molar ratio of HMDI, polyHMDI and PDI) are shown in Fig. 5.6.

The glass transition temperature of a polymer blend is one of the most important criteria to assess polymer miscibility, and can be directly related with the main peak value of $\tan(\delta)$. Neat PHBV and neat PLA exhibit single peaks of $\tan(\delta)$ at around 17 and 64 °C, respectively, (PLA curve not shown

in Fig. 5.6) and the PHBV/PLA blend exhibits both peaks without a change in the position with respect to the pure polymers. In the presence of diisocyanates, the $\tan(\delta)$ peaks (and subsequently, the T_g values) corresponding to the PHBV-rich and PLA-rich phases are shifted toward each other, indicating a compatibilization effect.

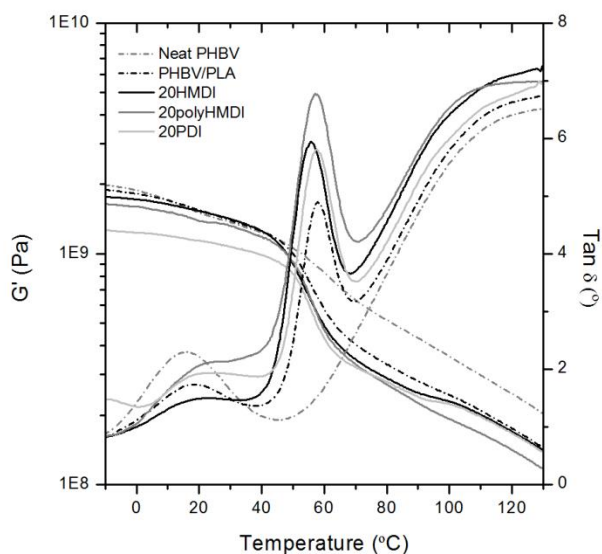


Fig. 5.6: a) Dynamic storage modulus (E') and b) delta tangent of PHBV, PHBV/PLA and PHBV/PLA blends with a 1:20 molar ratio of diisocyanates.

Specifically, it can be seen that the T_g of PHBV is less distinguishable as the compatibilizer content increases. The peak corresponding to the T_g of PHBV is more accentuated in the polyHMDI and PDI compatibilized blends, as can be seen in Fig. 5.6. This suggests a greater increase in the miscibility between PLA and PHBV in presence of these two compatibilizers, implying that there is more interfacial interaction, which is in total agreement with the SEM observations. This behavior was also reported by Zembouai *et al.* for PHBV/PLA nanocomposites by grafting maleic anhydride onto PHBV as a compatibilizing agent in combination with the addition of Cloisite 30B [19].

The storage modulus (G') decreases with increasing temperature and it shows a drastic drop in modulus around the glass transition temperature range. In the case of the blends, the evolution of the G' shows intermediate behavior between the neat PHBV and PLA blends. The moduli of the PHBV/PLA blends do not change below the T_g of PLA with respect to neat PHBV. When the

temperature is raised over the PLA T_g , the storage modulus of the blends decreases due to the lower intrinsic modulus of PLA at that temperature, in comparison to neat PHBV.

As the temperature rises, the reduction in the storage modulus of the blends with respect to neat PHBV is more evident, as seen in Fig. 5.6. In the case of the blend compatibilized with polyHMDI, the decrease in storage modulus is the highest. From this observation, it can be deduced that blending with PLA could provide a way to improve the thermoforming of PHBV. In fact, one of the limitations of thermoforming PHBV is due to its high crystallinity, which makes it very stiff until its melting point and very fluid afterwards, resulting in a very narrow temperature processing window. By blending with PLA, this range can be broadened towards lower temperatures, thus improving its thermoformability.

5.3.4. Rheological behavior

To evaluate the effect of the compatibilizer (type and amount) on the rheological properties of PHBV/PLA blends, dynamic oscillatory shear measurements were carried out as a function of frequency at 180 °C. All rheological measurements were driven from high to low frequencies. Fig. 5.7 shows the variation of the storage modulus (G'), loss modulus (G'') and complex viscosity (η^*) versus frequency for neat PHBV and PHBV/PLA blends, with and without compatibilizers at their different contents.

The storage modulus (G') and the loss modulus (G'') typically increase with frequency, and the difference between G' and G'' values for all the specimens decreases at high frequencies (Figs. 5.7.a, 5.7.c and 5.7.e). This is directly related to the viscoelastic properties of polymers with two overlapped responses: on the one hand, an immediate and non-time dependent elastic response and on the other hand, a time-dependent viscous response. At high frequencies, both PHBV and PLA offer a more elastic response and the viscous contribution is lower. Alternatively, at lower frequencies, viscous phenomena (time dependent) are allowed to a greater extent.

5. Capítulo 3

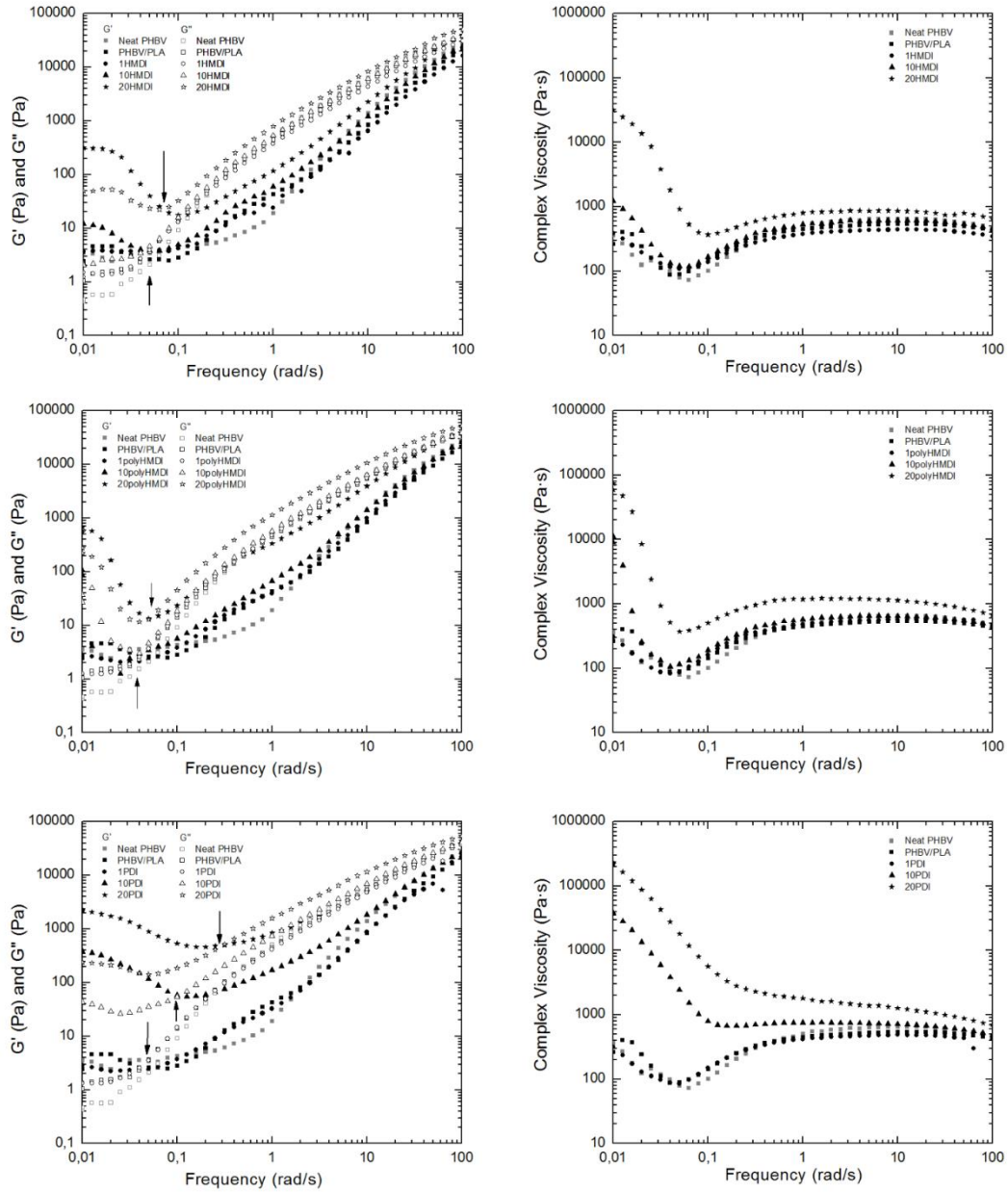


Fig. 5.7: Evolution of a) storage modulus (G'), b) loss modulus (G'') and c) complex viscosity of neat PHBV, PHBV/PLA and PHBV/PLA blends with diisocyanates at 180 °C under 1% dynamical shear strain.

The incorporation of PLA leads to small changes in the rheological behavior. However, with the incorporation of the compatibilizer, an increase in the storage modulus (G') and loss modulus (G'') at low frequencies with respect to those of both neat PHBV and PHBV/PLA can be clearly seen. The different viscoelastic responses of these materials become even more substantial when the compatibilizer content increases, being most pronounced in the case of the addition of PDI as the compatibilizing agent.

Such an increase in the storage and loss modulus (G' and G'') at lower frequencies has been reported by several authors for PHBV/PLA systems. Zhao et al. [40] explained this behavior with the formation of entangled structures in the PHBV/PLA melts. These entanglements lead to highly reversible elastic deformation of melts, partially preventing the relaxation of the melt structures. Furthermore, they raise the possibility that the immiscible nature of PLA/PHBV blends might play a role in the evolution of G' curves at low frequencies. Zembouai et al. [21] also found the same behavior for similar PHBV/PLA blends, also noting the immiscibility of both components [5] and the droplet/matrix morphology [41] as the origin of the phenomenon.

A shoulder in G' , G'' and complex viscosity is observed in all the studied compositions, even neat PHBV. This shift in viscosity at low frequencies has been attributed to the presence of minerals in the PHBV (boron nitride), used as nucleating agents, which can act also as fillers [5].

It can be appreciated that this shoulder shifts to higher frequencies when the diisocyanate content is increased, being most pronounced for the 1:20 molar ratio of compatibilizer (even at 1:10 in the case of PDI). Such a shift, which comes with an increase in complex viscosity at lower frequencies, is observed for 1:10 and 1:20 molar ratios of HMDI, polyHMDI and PDI. This behavior is most enhanced with the addition of PDI with respect to the other two diisocyanates at an equal molar ratio. In agreement with the previous reasoning, an increase in the droplet/matrix surface would lead to such an increase in viscosity at low frequencies, such as that observed in Fig. 5.7, in good agreement with the previous SEM analysis.

This reasoning, however, is called into question by the same authors, arguing that rheological tests performed at 175 °C did not yield the same results as the ones performed at 185 °C [21]. They opened up the possibility that some unmelted PHBV particles could be responsible for the high values of viscosity at low frequencies. To discard this possibility in our experiments, samples were

5. Capítulo 3

placed in DSC pans at the same temperature of their and our rheological measurements, that is at 175, 180 and 185 °C, for 5 min, which is the typical time lapse for the rheological tests. After that, controlled cooling showed that there were no self-seeding phenomenon at 185 or 180 °C, thus proving that complete melting took place and that the thermal history was erased at the rheometer. Samples kept at 175 °C showed some nucleating effect, with a shift of the crystallization peak to higher temperatures.

The possibility of reaching higher values of complex viscosity at low frequencies with high molar ratios of diisocyanate as the compatibilizer is also quite interesting from the processing point of view of PHBV. This result again opens the possibility of improving the thermoforming ability of PHBV, broadening the processing window towards higher temperatures, complementing the effects observed in DMTA analysis towards lower temperatures.

5.4. CONCLUSIONS

PHBV/PLA blends with three different compatibilizers (hexamethylene diisocyanate, (HMDI), poly(hexamethylene) diisocyanate (polyHMDI) and 1,4-phenylene diisocyanate (PDI)) were successfully obtained by melt blending.

Favourable morphologies were achieved during processing for the three compatibilizers, enhancing the miscibility between both polymers, as derived from SEM. The addition of diisocyanates within the range studied slightly decreases the overall crystallinity, and there was a slightly variation in the melting temperature and a marked decrease in crystallization temperature. Nevertheless, no effect on the thermal stability of the compatibilized blends was observed with the addition of the diisocyanates.

The mechanical properties of such blends were characterised by an increase in elongation at break of PHBV/PLA blends through incorporation of HMDI, polyHMDI and PDI as compatibilizing agents.

The processability of PHBV can be facilitated with its blend with PLA and compatibilization with the studied diisocyanates, due to widening the processing window of PHBV, which should contribute to enhancing the thermoforming of PHBV, as concluded by DMTA and rheological results.

Therefore, the use of diisocyanate-type compatibilizers to improve the industrial processability of biopolymer blends may be a promising approach for extending their applications with a view to replacing commodity polymers. Further studies to assess the remaining isocyanate groups and thermoforming properties are requested to find practical applications for these formulations.

ACKNOWLEDGEMENTS

Financial support for this research from Ministerio de Economía y Competitividad (project AGL2015-63855-C2-2-R). Generalitat Valenciana (GV/2014/123) and Pla de Promoció de la Investigació de la Universitat Jaume I (PREDOC/2012/32 and E-2015-22) is gratefully acknowledged. The authors are also grateful to Raquel Oliver and José Ortega for experimental support.

REFERENCES

- [1] A.A. Shah, S. Kato, N. Shintani, N.R. Kamini, T. Nakajima-Kambe, Microbial degradation of aliphatic and aliphatic-aromatic co-polyesters., *Appl. Microbiol. Biotechnol.* 98 (2014) 3437–47. doi:10.1007/s00253-014-5558-1.
- [2] V. Mittal, *Nanocomposites with Biodegradable Polymers*, Oxford University Press, 2011. doi:10.1093/acprof:oso/9780199581924.001.0001.
- [3] R. Auras, L.T. Lim, S.E.M. Selke, H. Tsuji, *Poly(Lactic Acid)*, John Wiley & Sons, Inc., Hoboken, NJ, USA, 2010. doi:10.1002/9780470649848.
- [4] J. Gámez-Pérez, J.C. Velázquez-Infante, E. Franco-Urquiza, P. Pages, F. Carrasco, O.O. Santana, M.L. MasPOCH, Fracture behavior of quenched poly(lactic acid), *Express Polym. Lett.* 5 (2011) 82–91. doi:10.3144/expresspolymlett.2011.9.
- [5] T. Gerard, T. Budtova, Morphology and molten-state rheology of polylactide and polyhydroxyalkanoate blends, *Eur. Polym. J.* 48 (2012) 1110–1117. doi:10.1016/j.eurpolymj.2012.03.015.
- [6] D.Z. Bucci, L.B.B. Tavares, I. Sell, PHB packaging for the storage of food products, *Polym. Test.* 24 (2005) 564–571. doi:10.1016/j.polymertesting.2005.02.008.
- [7] D. Cava, E. Gimenez, R. Gavara, J.M. Lagaron, Comparative Performance and Barrier Properties of Biodegradable Thermoplastics and Nanobiocomposites versus PET for Food Packaging Applications, *J. Plast. Film Sheeting.* 22 (2006) 265–274. <http://www.scopus.com/inward/record.url?eid=2-s2.0-33845203640&partnerID=tZOTx3y1> (accessed January 14, 2015).
- [8] J.M. Lagaron, A. Lopez-Rubio, Nanotechnology for bioplastics: opportunities, challenges and strategies, *Trends Food Sci. Technol.* 22 (2011) 611–617. doi:10.1016/j.tifs.2011.01.007.
- [9] J.W. Rhim, H.M. Park, C.S. Ha, Bio-nanocomposites for food packaging applications, *Prog. Polym. Sci.* 38 (2013) 1629–1652. doi:10.1016/j.progpolymsci.2013.05.008.
- [10] A. Javadi, S. Pilla, S. Gong, L.S. Turng, *Handbook of Bioplastics and Biocomposites Engineering Applications*, John Wiley & Sons, Inc., Hoboken, NJ, USA, 2011. doi:10.1002/9781118203699.

- [11] V. Sridhar, Graphene reinforced biodegradable poly(3-hydroxybutyrate-co-4-hydroxybutyrate) nano-composites, *Express Polym. Lett.* 7 (2013) 320–328. doi:10.3144/expresspolymlett.2013.29.
- [12] J.M. Ferri, O. Fenollar, A. Jorda-Vilaplana, D. García-Sanoguera, R. Balart, Effect of miscibility on mechanical and thermal properties of poly(lactic acid)/ polycaprolactone blends, *Polym. Int.* 65 (2016) 453–463. doi:10.1002/pi.5079.
- [13] A. Martínez-Abad, J. González-Ausejo, J.M. Lagarón, L. Cabedo, Biodegradable poly(3-hydroxybutyrate-co-3-hydroxyvalerate)/thermoplastic polyurethane blends with improved mechanical and barrier performance, *Polym. Degrad. Stab.* 132 (2016) 52–61. doi:10.1016/j.polymdegradstab.2016.03.039.
- [14] L. Cabedo, J. Luis Feijoo, M. Pilar Villanueva, J.M. Lagarón, E. Giménez, Optimization of Biodegradable Nanocomposites Based on aPLA/PCL Blends for Food Packaging Applications, *Macromol. Symp.* 233 (2006) 191–197. doi:10.1002/masy.200690017.
- [15] M.P. Arrieta, J. López, D. López, J.M. Kenny, L. Peponi, Development of flexible materials based on plasticized electrospun PLA–PHB blends: Structural, thermal, mechanical and disintegration properties, *Eur. Polym. J.* 73 (2015) 433–446. doi:10.1016/j.eurpolymj.2015.10.036.
- [16] Y. Deng, N.L. Thomas, Blending poly(butylene succinate) with poly(lactic acid): Ductility and phase inversion effects, *Eur. Polym. J.* 71 (2015) 534–546. doi:10.1016/j.eurpolymj.2015.08.029.
- [17] S. Modi, K. Koelling, Y. Vodovotz, Assessing the mechanical, phase inversion, and rheological properties of poly-[(R)-3-hydroxybutyrate-co-(R)-3-hydroxyvalerate] (PHBV) blended with poly-(l-lactic acid) (PLA), *Eur. Polym. J.* 49 (2013) 3681–3690. doi:10.1016/j.eurpolymj.2013.07.036.
- [18] S. Modi, K. Koelling, Y. Vodovotz, Miscibility of poly(3-hydroxybutyrate-co-3-hydroxyvalerate) with high molecular weight poly(lactic acid) blends determined by thermal analysis, *J. Appl. Polym. Sci.* 124 (2012) 3074–3081. doi:10.1002/app.35343.
- [19] I. Zembouai, S. Bruzaud, M. Kaci, A. Benhamida, Y. Corre, Y. Grohens, J.-M. Lopez-Cuesta, Synergistic Effect of Compatibilizer and Cloisite 30B on the Functional Properties of Poly (3-hydroxybutyrate- co -3-hydroxyvalerate)/ Polylactide Blends, *Polym. Eng. Sci.* 54 (2014) 2239–2251. doi:10.1002/pen.
- [20] I. Zembouai, M. Kaci, S. Bruzaud, A. Benhamida, Y.-M. Corre, Y. Grohens, A study of morphological, thermal, rheological and barrier properties of Poly(3-hydroxybutyrate-Co-3-Hydroxyvalerate)/polylactide blends prepared by melt mixing, *Polym. Test.* 32 (2013) 842–851. doi:10.1016/j.polymertesting.2013.04.004.
- [21] I. Zembouai, S. Bruzaud, M. Kaci, A. Benhamida, Y.-M. Corre, Y. Grohens, A. Taguet, J.-M. Lopez-Cuesta, Poly(3-Hydroxybutyrate-co-3-Hydroxyvalerate)/Polylactide Blends: Thermal Stability, Flammability and Thermo-Mechanical Behavior, *J. Polym. Environ.* 22 (2013) 131–139. doi:10.1007/s10924-013-0626-7.
- [22] V. Jost, Blending of Polyhydroxybutyrate-co-valerate with Polylactic Acid for Packaging Applications – Reflections on Miscibility and Effects on the Mechanical and Barrier Properties, *Chem. Biochem. Eng. Q.* 29 (2015) 221–246. doi:10.15255/CABEQ.2014.2257.
- [23] Q. Liu, C. Wu, H. Zhang, B. Deng, Blends of polylactide and poly(3-hydroxybutyrate- co -3-hydroxyvalerate) with low content of hydroxyvalerate unit: Morphology, structure, and property, *J. Appl. Polym. Sci.* 132 (2015) n/a-n/a. doi:10.1002/app.42689.
- [24] L. Li, W. Huang, B. Wang, W. Wei, Q. Gu, P. Chen, Properties and structure of polylactide/poly (3-hydroxybutyrate-co-3-hydroxyvalerate) (PLA/PHBV) blend fibers, *Polymer (Guildf).* 68 (2015) 183–194. doi:10.1016/j.polymer.2015.05.024.

- [25] J. Li, M.F. Lai, J.J. Liu, Effect of poly(propylene carbonate) on the crystallization and melting behavior of poly(α -hydroxybutyrate-co- β -hydroxyvalerate), *J. Appl. Polym. Sci.* 92 (2004) 2514–2521. doi:10.1002/app.20211.
- [26] E. Bugnicourt, Polyhydroxyalkanoate (PHA): Review of synthesis, characteristics, processing and potential applications in packaging, *Express Polym. Lett.* 8 (2014) 791–808. doi:10.3144/expresspolymlett.2014.82.
- [27] J. Cailloux, O.O. Santana, E. Franco-Urquiza, J.J. Bou, F. Carrasco, J. Gámez-Pérez, M.L. MasPOCH, Sheets of branched poly(lactic acid) obtained by one step reactive extrusion calendaring process: Melt rheology analysis, *Express Polym. Lett.* 7 (2012) 304–318. doi:10.3144/expresspolymlett.2013.27.
- [28] S. Pivsa-Art, N. Srisawat, N. O-Charoen, S. Pavasupree, W. Pivsa-Art, H. Yamane, H. Ohara, Preparation and biodegradability study of polymer blends of poly(lactic acid) and poly[(R)-3-hydroxybutyrate-co-(R)-3-hydroxyvalerate], in: *Annu. Tech. Conf. - ANTEC, Conf. Proc., Society of Plastics Engineers*, 2013: pp. 1777–1779. <http://www.scopus.com/inward/record.url?eid=2-s2.0-84903526709&partnerID=tZOtx3y1>.
- [29] T. Gerard, Polylactide/poly(hydroxybutyrate-co-hydroxyvalerate) blends: Morphology and mechanical properties, *Express Polym. Lett.* 8 (2014) 609–617. doi:10.3144/expresspolymlett.2014.64.
- [30] P. Raffa, M.-B. Coltelli, S. Savi, S. Bianchi, V. Castelvetro, Chain extension and branching of poly(ethylene terephthalate) (PET) with di- and multifunctional epoxy or isocyanate additives: An experimental and modelling study, *React. Funct. Polym.* 72 (2012) 50–60. doi:10.1016/j.reactfunctpolym.2011.10.007.
- [31] N. Torres, J.J. Robin, B. Boutevin, Chemical modification of virgin and recycled poly(ethylene terephthalate) by adding of chain extenders during processing, *J. Appl. Polym. Sci.* 79 (2001) 1816–1824. doi:10.1002/1097-4628(20010307)79:10<1816::AID-APP100>3.0.CO;2-R.
- [32] S.K. Dogan, E.A. Reyes, S. Rastogi, G. Ozkoc, Reactive compatibilization of PLA/TPU blends with a diisocyanate, *J. Appl. Polym. Sci.* 131 (2014) n/a-n/a. doi:10.1002/app.40251.
- [33] J.-B. Zeng, K.-A. Li, A.-K. Du, Compatibilization strategies in poly(lactic acid)-based blends, *RSC Adv.* (2015). doi:10.1039/C5RA01655J.
- [34] M.R. Nanda, M. Misra, A.K. Mohanty, The Effects of Process Engineering on the Performance of PLA and PHBV Blends, *Macromol. Mater. Eng.* 296 (2011) 719–728. doi:10.1002/mame.201000417.
- [35] H. Alata, T. Aoyama, Y. Inoue, Effect of Aging on the Mechanical Properties of Poly(3-hydroxybutyrate-co-3-hydroxyhexanoate), *Macromolecules.* 40 (2007) 4546–4551. doi:10.1021/ma070418i.
- [36] M.D. Sanchez-Garcia, J.M. Lagaron, Novel clay-based nanobiocomposites of biopolyesters with synergistic barrier to UV light, gas, and vapour, *J. Appl. Polym. Sci.* 118 (2010) 188–199. doi:10.1002/app.31986.
- [37] N. Grassie, E.J. Murray, P.A. Holmes, The thermal degradation of poly(α -hydroxybutyric acid): Part 3-The reaction mechanism, *Polym. Degrad. Stab.* 6 (1984) 127–134. <http://www.scopus.com/inward/record.url?eid=2-s2.0-0021208453&partnerID=tZOtx3y1>.
- [38] F.D. Kopinke, K. Mackenzie, Mechanistic aspects of the thermal degradation of poly(lactic acid) and poly(β -hydroxybutyric acid), *J. Anal. Appl. Pyrolysis.* 40–41 (1997) 43–53. <http://www.scopus.com/inward/record.url?eid=2-s2.0-0031144057&partnerID=tZOtx3y1>.

5. Capítulo 3

- [39] B.-K. Chen, C.-H. Shen, A.F. Chen, Preparation of ductile PLA materials by modification with trimethyl hexamethylene diisocyanate, *Polym. Bull.* 69 (2012) 313–322. doi:10.1007/s00289-012-0730-1.
- [40] H. Zhao, Z. Cui, X. Sun, L.-S. Turng, X. Peng, Morphology and Properties of Injection Molded Solid and Microcellular Polylactic Acid/Polyhydroxybutyrate-Valerate (PLA/PHBV) Blends, *Ind. Eng. Chem. Res.* 52 (2013) 2569–2581. doi:10.1021/ie301573y.
- [41] M. Castro, C. Carrot, F. Prochazka, Experimental and theoretical description of low frequency viscoelastic behaviour in immiscible polymer blends, *Polymer (Guildf)*. 45 (2004) 4095–4104. doi:10.1016/j.polymer.2004.04.019.

6. Capítulo 4

Assessing the thermoformability of poly(3-hydroxybutyrate-co-3-hydroxyvalerate) / poly(acid lactic) blends compatibilized with Diisocyanates

6. Capítulo 4

Assessing the thermoformability of poly(3-hydroxybutyrate-co-3-hydroxyvalerate) / poly(acid lactic) blends compatibilized with Diisocyanates

Jennifer González-Ausejo¹, Estefania Sanchez-Safont¹, Jose Maria Lagaron², Richard T. Olsson³, Jose Gamez-Perez¹, Luis Cabedo¹

¹ Polymer and Advanced Materials Group (PIMA). Universidad Jaume I. 12071. Castellon. Spain.

² Novel Materials and Nanotechnology Group. IATA-CSIC. 46980. Paterna (Valencia). Spain

³ Department of Fibre and Polymer Technology, KTH-Royal Institute of Technology, Stockholm, Sweden

ABSTRACT

Poly(3-hydroxybutyrate-co-3-hydroxyvalerate) (PHBV) is a renewable alternative to conventional barrier packaging polymers due to its thermoplastic properties, biodegradability and gas barrier performance but its potential industrial applications are limited by its high price and difficult processability. A thorough study concerning the thermoforming ability of PHBV, and blends with poly(lactic acid) (PLA) incorporating three different diisocyanates as compatibilizers (hexamethylene diisocyanate, poly(hexamethylene) diisocyanate and 1,4-phenylene diisocyanate) is herein presented after component melt blending. A straightforward universal qualitative method is proposed to assess the thermoformability, based on a visual inspection of a thermoformed specimen and the ability to reproduce the mold shape, and the thermoforming window of the material. The results reveal a significant improvement in the thermoforming capacity and a widening of the thermoforming windows as the correct amounts of diisocyanates are incorporated. The barrier properties and the biodisintegrability of the blends was also studied, confirming a predictable slight decrease of the barrier performance when PLA is added, but without negatively affecting the disintegrability under composting conditions with respect to pristine PHBV.

GRAFICAL ABSTRACT

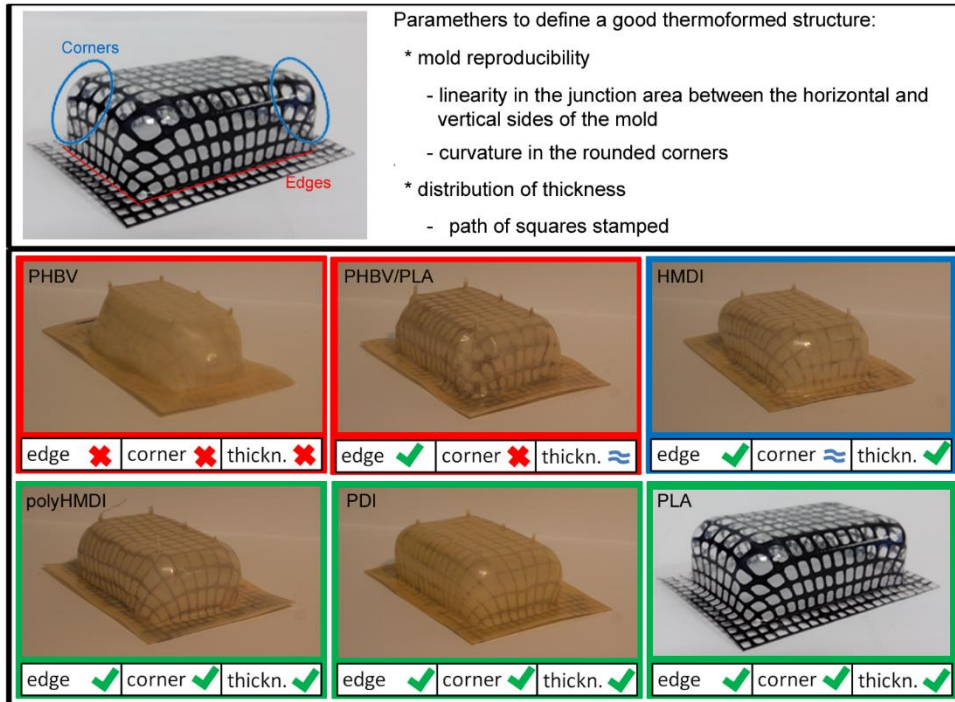


Fig. 6.1: Graphical abstract of the work named Assessing the thermoformability of poly(3-hydroxybutyrate-co-3-hydroxyvalerate) / poly(acid lactic) blends compatibilized with Diisocyanates

6.1. INTRODUCTION

Many of the most widely used rigid packaging products (such as trays, containers, cases or blister packages) are obtained by thermoforming thin thermoplastic sheets. The process is also widely used for preparation of multilayer polymer materials, which are commonly used as high barrier materials in the food packaging industry. Polystyrene (PS), polypropylene (PP), polyvinyl chloride (PVC) and polyethylene terephthalate (PET) are the most widely used polymers for such applications. However, these materials are derived from non-biodegradable fossil fuel resources, which entails environmental problems derived from the large amounts of discarded plastic and their waste management. Biopolymers here arise as a good alternative to replace those commodities, with a special interest in those that come from renewable resources. Poly(lactic acid) (PLA) and some polyhydroxyalkanoates (PHAs), specifically poly(hydroxybutyrate-co-valerate) (PHBV), provide a good alternative to PVC, PP or PET, with the advantage of being 100% biodegradable, and compostable [1–3]. These biopolymers are already being commercialized for packaging applications, such as cosmetic containers, shampoo bottles, covers, milk cartons, among others (reviewed by Keshavarz et al. [4] and Aditi et al. [5]). Nevertheless, these biopolymers still present a number of drawbacks that limit their use in the packaging sector.

PHBV has interesting properties compared to other biopolymers, such as being thermoplastic, presenting high tensile strength, high service temperature (similar to that of PP) [6] and barrier properties to oxygen (close to those of PET and much higher than PLA) [7] [8]. However, its high crystallinity, which is responsible of the excellent barrier performance, restricts its processability by thermoforming. In fact, PHBV can be thermoformed only within a very narrow range of temperatures close to the melting point of the polymer, which leads to sagging phenomenon of the sheet prior to the drawing process, which stems from the sudden loss of mechanical stability. This characteristic limits the geometries and its suitability for thermoformed products in comparison with other conventional polymers, and despite of the importance of the thermoforming process in the packaging sector, few works address this issue in the scientific literature. Among them, Gimenez et al. [9,10] improved the thermoformability of ethylene-vinyl alcohol copolymer (EVOH) by means of blending it with an amorphous polyamide and a compatibilized-ionomer. The ternary blend resulted in an improved forming capacity with a much

6. Capítulo 4

wider forming window than neat EVOH due to a blend composition showing improved dimensional stability during the thermoforming and reduced sensitivity towards sagging. In the same vein of that reported by Gimenez et al., in the present work, blending PHBV with an amorphous biopolymer (PLA) is presented as an approach for fostering the thermoformability of PHBV. PLA shows an excellent thermoformability because of its amorphous state at normal processing conditions [11]. However, the PHBV/PLA blends have some disadvantages: the two biopolyesters exhibit an immiscible behavior when melt blended [12–14] thus yielding to a drop-in-matrix morphology with a poor interface adhesion, and the gas barrier properties decrease by incorporating PLA into PHBV, especially when the PLA content exceeds 25% [14]. These detrimental drawbacks limit the PLA blends for application in high barrier thermoformed packages, which currently are manufactured from PET [15].

In a previous work [16], blends of PHBV with PLA were compatibilized by reactive extrusion blending using three diisocyanates as compatibilizer agents (hexamethylene diisocyanate (HMDI), poly(hexamethylene) diisocyanate (PolyHMDI) and 1,4-phenylene diisocyanate (PDI)). PolyHMDI and PDI resulted in a higher compatibilizing effect, when compared with HMDI. Besides, the rheological behavior of the compatibilized blends suggested that the thermoformability of such systems could improve that of PHBV. In light of those results, the aim of this work is to assess the effect of blending PHBV with 25 wt.% PLA while using the different diisocyanates as compatibilizers, on the thermoforming processability, service properties (barrier to oxygen and water vapor) and biodegradability, as compared to neat PHBV.

6.2. EXPERIMENTAL

6.2.1. Materials

PHBV with 3 mol.% hydroxyvalerate content was purchased from the Tianan Biologic Material Co. (Ningbo, P.R. China) in pellet form (ENMAT Y1000P). PLA Ingeo™ Biopolymer commercial grade 2003D was supplied by the NatureWorks® Co. LLC, USA. The three compatibilizers used, hexamethylene diisocyanate (HMDI), poly(hexamethylene) diisocyanate (PolyHMDI) and 1,4-phenylene diisocyanate (DPI) were supplied by Sigma Aldrich.

6.2.2. Blend preparation

The PHBV and PLA used in this study were dried at 80 °C for 2 h before using by a Piovan DPA 10 (Santa Maria di Sala VE, Italy), while the compatibilizers were used as received. Considering the limited gas barrier properties of PLA with respect to PHBV and in agreement with our previous works [10,11], a fixed PHBV/PLA ratio of 75/25 in weight was kept in all the samples. The PHBV blends were obtained by mixing different amounts of pellets of both polymers and the compatibilizer in an internal mixer (Rheomix 3000P ThermoHaake, Karlsruhe, Germany). To avoid thermal degradation of the biopolyesters during blending, the mixing time was done in less than 4 min, the temperature was set at 180 °C and the rotor speed at 100 rpm. According to the melt temperature sensor during mixing, the polymers were always at temperatures below 195 °C.

The batches were subsequently processed into thin sheets (thickness of 200 and 300 µm) by compression molding, using a hot-plate hydraulic press (Carver 4122, USA) at 180°C, 3 MPa and 4 min. The 300 µm sheets were prepared the same day as they were used in the thermoforming study. In contrast, the 200 µm films were stored in a vacuum desiccator at ambient temperature for 2 weeks to allow full crystallization to take [17] and subsequently used for full characterization.

Samples of both neat PHBV and PLA were processed under identical conditions as the blends, for the sake of comparison. The nomenclature used for the blends is as follows: PHBV/PLA for the blend system without compatibilizer, and HMDI, polyHMDI and PDI for the compatibilized blends. The compatibilizer content was adjusted to 1:20 molar ratio between the functional polymer reactive sites (end groups) and the compatibilizer ones (isocyanates) [16], according to the available Mn and molecular weight data of polymers and isocyanates.

6.2.3. Characterization

Scanning Electron Microscopy (SEM) of all the samples was conducted using a high-resolution field-emission JEOL 7001F microscope. The samples were fractured in liquid nitrogen and then were coated by sputtering with a thin layer of Pt prior to SEM observation. The size of the dispersed phase (i.e. diameter of the spheres) was measured in the SEM microphotographs by using Fiji® software (the number of spheres measured for each sample was never below 400).

6. Capítulo 4

The oxygen permeability (OP) of the films was measured in duplicate by using Oxtran 100 equipment (Modern Control, Minneapolis, MN) at 80% relative humidity (RH) and 24 °C. RH was generated by a built-in gas bubbler and was checked with a hygrometer placed at the exit of the detector. Prior to the measurements, the samples were purged with nitrogen for a minimum 20h in the previously relative humidity equilibrated samples. The oxygen flow during the experiments was fixed at 10 ml/min. the measurements were performed through a 5 cm² samples area by using an in-house development mask. To obtain the oxygen permeability, film thickness was considered in each case.

The water vapor permeability (WVP) of the PHBV/PLA blends was measured according to the ASTM E96 (2011) gravimetric method, using Payne permeability cups (Elcometer SPRI, Hermelle/s Argenteau, Belgium). Measurements were taken in duplicates. The samples were placed between the aluminium top (open O-ring) and bottom part (deposit for the permeant) with a Viton rubber ring between the film and the top part of the cups to ensure their complete sealing. The cups were placed inside a desiccator at 0% RH and the water weight loss through a film area of 0,001 m² was monitored and plotted as a function of time. Water vapor permeability rate was estimated from the slope of the linear part of this plot, thus ensuring the steady-state conditions. Cups with aluminum films were used as control samples to estimate water vapor losses thought the sealing. Water weight loss was calculated as the total cell loss minus the loss through the sealing. Water vapor permeability was obtained multiplying the water vapor permeability by the average film thickness.

Disintegrability of films of neat PHBV, neat PLA and PHBV/PLA compatibilized blends and non-compatibilized blend was assessed by means of a disintegration test under lab scale composting conditions according to the ISO 20200 standard, "Determination of the degree of disintegration of plastic materials under simulated composting conditions in a laboratory-scale test" [18]. For the preparation of solid synthetic waste, 10% of activated mature compost (VIGORHUMUS H-00, purchased from Buras Professional, S.A., Girona, Spain) was mixed with 30% rabbit food, 10% starch, 5% sugar, 1% urea, 4% corn oil and 40% sawdust. The water content of the substrate was around 55 wt.% and the aerobic conditions were guaranteed by gently mixing the compost and periodically adding water according to the standard. The samples were cut from hot pressed plates (10x10x0.2 mm³) and buried inside plastic mesh bags to simplify their extraction and allow the

contact of the compost with the specimens, and were incubated at 58 °C for 31 days. At different composting times samples were recovered for analysis, washed with distilled water, dried at 40 °C under vacuum for 24 h, and weighed. The degree of disintegration was calculated by normalizing the sample weight, at different days of incubation, to the initial weight with Equation (6.1), where m_i is the initial dry mass of the test material and m_f is the dry mass of the test material recovered at different incubation stages.

$$D = \frac{m_i - m_f}{m_i} \times 100 \quad (6.1)$$

The disintegration study was completed by photographs for visual evaluation of the samples and their morphologies were further inspected by SEM analysis.

6.2.4. Thermoforming setup

The thermoforming pilot plant facility (SB 53c, Illig, Helmut Roegele, Germany) presented in Figure 6.2 was used for the vacuum assisted thermoformability study. The heating device is a platform equipped with 15 long waves infrared emitters which slides forward upon the thermoforming chamber during the heating step prior to the forming (see Figure 6.2.b). For all the experiments the emitters were set to 600°C, while the heating time was changed in order to control the temperature of the polymer sheet. The sheet surface temperature was measured at different locations (both in the upper and the lower surface) as function of heating time, thus obtaining relation between the heating time and the sheet temperature (Figure 6.2.d). As shown in Figure 6.2.d, the temperature of the sheet follows a logarithmic trend with respect to the heating time, therefore the dependence of the sheet temperature with the heating time is much higher for lower times, being almost constant for times beyond 50 min, reaching a maximum temperature of ca. 130°C with the current setup.

Sheets having 300 μm thickness were used for the thermoforming study. Before the thermoforming of the sample specimen, a square grid pattern (1x1 cm) was stamped on each sheet in order to track the deformation of the sheet occurring during its mold conformation. The mold used was a female rectangular tray having 40 x 60 x 20 mm (width x length x depth) (see Figure 6.2.c). Thus the maximum draw ratio of the mold was determined by the ratio between the final

6. Capítulo 4

and the initial area of the stamped squares, resulting in a maximum value of 5.2. A minimum of three trays were obtained for every heating time in order to obtain representative information from their thermoforming ability.

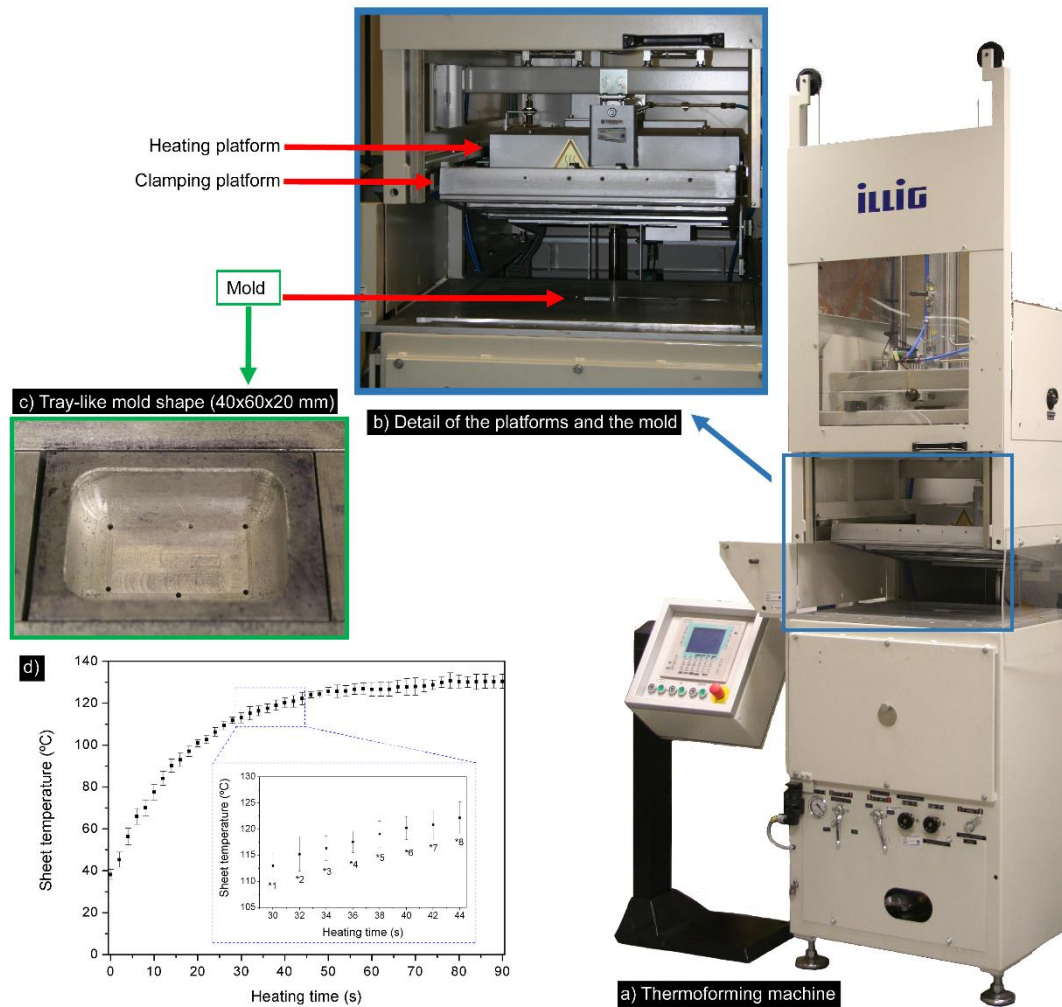


Fig. 6.2: Image of the a) thermoforming facility, b) thermoforming chamber, c) mold and d) Sheet temperature as a function of the heating time.

6.3. RESULTS AND DISCUSSION

6.3.1. Morphology

Figure 6.3 presents SEM micrographs of all the PHBV/PLA blends studied as a function of the diisocyanate type. The micrographs reveal that the blends present a two-phase morphology microstructure can be described as PLA homogeneously dispersed within a PHBV continuous matrix, thus revealing a characteristic discrete-phase structure (DPS, or drop-in matrix). This microstructure proves that the PHBV/PLA blends prepared with high molecular weight commercial polymer grades are immiscible and not fully compatible. The addition of isocyanates to the PHBV/PLA blend was previously studied by our group and we showed that their addition to the blend leads to a decrease in the droplet size of the dispersed phase, as well as decrease on the amount of detached particles [16]. The high compatibilization effect by adding small amounts of diisocyanates, with an improvement in the interfacial adhesion between the two biopolyesters, was herein confirmed.

Image analysis of cryo-fractured specimens was performed to reveal the average droplet size of the PLA droplets in the blends. These results summarized in the histogram plots of Figure 6.3.e. The average droplet diameter for the uncompatibilized PHBV/PLA blend is 1.15 μm with a clear detachment phenomenon between both phases, as can be seen in Figure 6.3.a. However, the incorporation of diisocyanates to the blend (in a 1:20 molar ratio of isocyanates with respect to polymer end-groups) led to a reduction in the PLA domains, with most pronounced results for polyHMDI and PDI. Hence, an average PLA domain size of 0.84, 0.45 and 0.57 μm was determined for the HMDI, polyHMDI and PDI blends, respectively. A similar trend was also found considering the amount of completely detached PLA particles from the matrix, which is in agreement with an increase in the interfacial adhesion and compatibility between PLA and PHBV in the samples containing HMDI, polyHMDI and PDI.

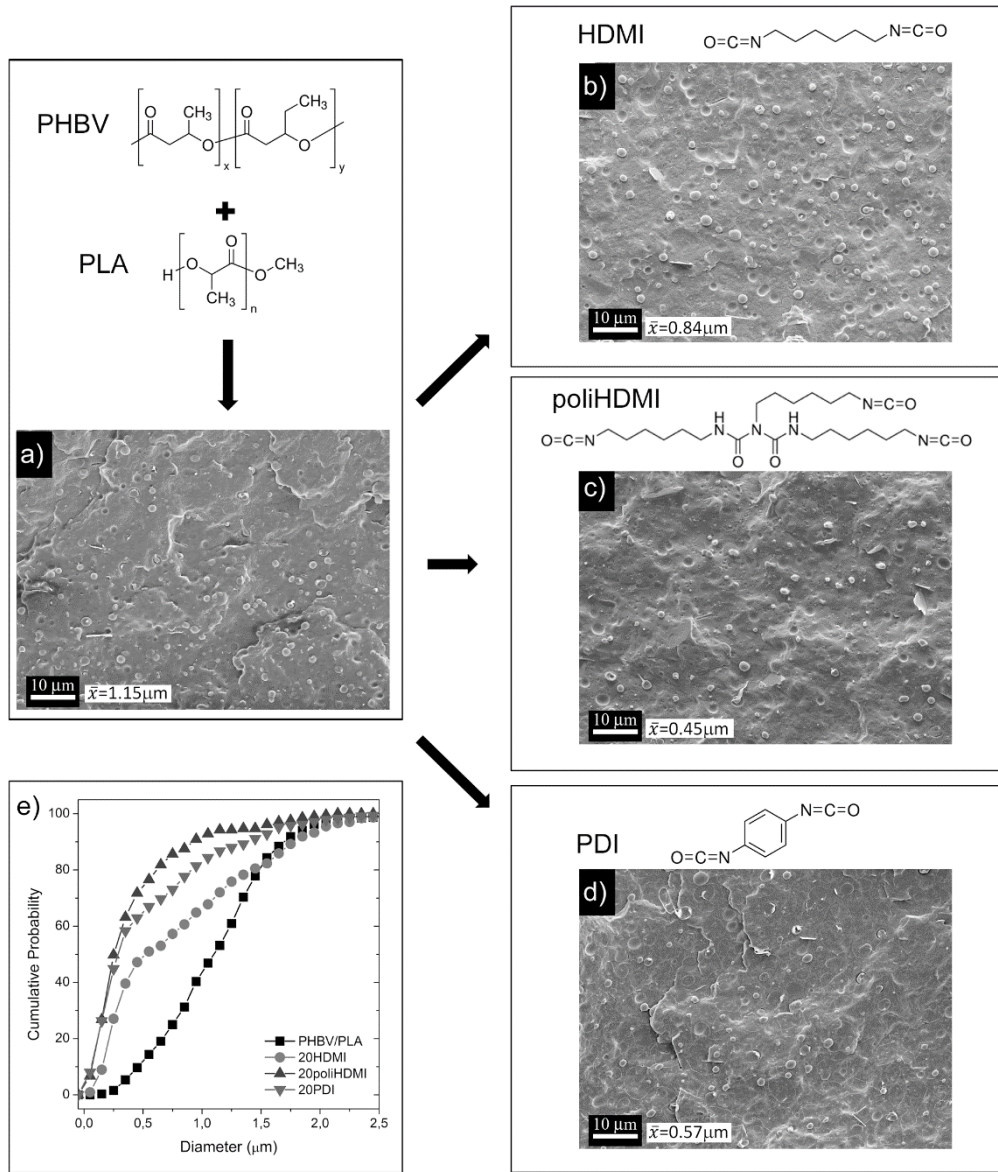


Fig. 6.3: SEM micrographs of a) PHBV/PLA blend, b) HDMI, c) polyHDMI, d) PDI and e) diameter distribution of PLA domains of PHBV/PLA blend and compatibilized blends.

6.3.2. Barrier performance

The assessment of the barrier performance of the polymers and their blends in this work is of utmost interest, since one of the main advantages of the PHBV copolymer is its higher barrier performance, particularly to oxygen, when compared to other biopolyesters such as PLA. The gas barrier properties to water and oxygen of neat PHBV, neat PLA and the PHBV/PLA blends are summarized in Figure 6.4. The best barrier performance corresponds to PHBV, whereas the incorporation of 25 wt.% PLA results in a drop in oxygen and water vapor barrier performance by more than 85 % (86 and 89 % for water and oxygen, respectively). This can be attributed to the lower barrier properties of the PLA, derived from its amorphous state, in agreement with previous studies performed by Zembouai et al. [14], and to some extent the formation of phase interfaces in the two-phase morphology microstructure. The incorporation of the different isocyanates only altered the barrier properties to a small extent in relation to the uncompatibilized blend of PHBV/PLA (see Fig. 6.4). However, the values of the obtained blends, compatibilized and non-compatibilized, were still in the same order of magnitude than those of the neat PHBV.

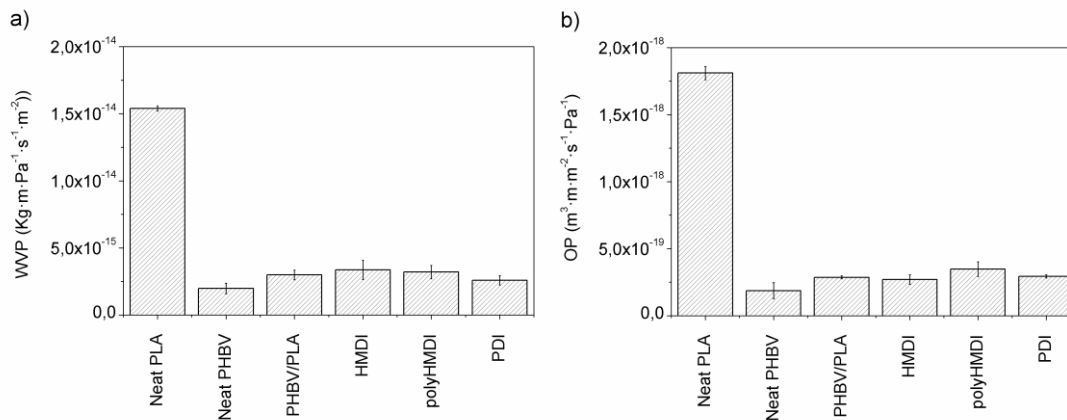


Fig. 6.4: a) Water vapour and b) oxygen permeability of the neat materials and their blends.

6.3.3. Thermoforming study

The present work is framed in a project that aims improving the thermoformability of the PHBV while both the gas barrier performance and the biodisintegrability. For doing so, blends of PHBV with PLA and keeping compatibilization agents were obtained and their barrier performance, thermoformability and disintegrability assessed and compared to that of the pristine PHBV.

To evaluate the thermoforming ability of the compositions prepared, the setup and mold shown in Figure 6.2 was employed. To the best of our knowledge, no standard procedure for assessing thermoformability has been published and/or is being widely used. Generally, the assessment of the thermoformability consist only of a simple visual inspection or, in some cases, in a thickness distribution measurement [19–23]. The absence of a standardized method to compare the thermoformability and process window of the materials has led us to develop a thermoformability evaluation procedure by screening different heating times (i.e. different sheet temperatures), while keeping constant the other processing parameters, which were independently optimized for the specific mold and sheet thickness. Visual inspection of the thermoformed structures was performed and photographs taken for the record.

6.3.3.1. Assessment of the thermoformability and thermoforming window of the PHBV.

We herein define thermoformability as the ability of a material to be successfully thermoformed into a specimen with the shape of the mold and reproducible and controlled thickness distribution. The thermoforming process window is further related to the combination of parameters that allows good thermoformability, being the temperature range the most critical for a particular material. The thermoformability and the determination of the thermoforming temperature range (process window) for PHBV (and all the blends) were accordingly assessed based on screening of the process conditions, visual inspection of the obtained samples, and comparison with the original mold. The method consisted firstly of thermoforming the sheets with the grid drawn on them. After this process, with the aid of the deformed grid, three parameters were related to the reproducibility of the mold's shape, and the thickness distribution of the molded specimen was assessed (both local and overall). These three parameters are summarized in Figure 6.5.a and described as follows:

- a) Edge inspection: it assesses the linearity in the joint section between the flat surface of the original sheet and the onset of the deformation (for the particular case of a tray-shaped mold, this would be the line defined by the intersecting planes of the original flat sheet and the vertical sides of the tray).
- b) Corner inspection: it provides information about the mold reproducibility at the corners of the tray.
- c) Thickness inspection: it evaluates the uniformity in the path and span of the squares in the grid (the shape of the grid elements are related to the local draw ratio and to the thickness distribution; high draw ratios result in high span and low thickness. On the other hand, even square-grid deformation is related to a uniform thickness distribution).

As a comparison, Figure 6.5.b presents two thermoformed trays from PLA and PHBV under the most optimal conditions for each biopolyester. It can be appreciated that PLA reproduces accurately the mold's geometry and keeps a regular thickness distribution. On the other hand, the PHBV specimen exhibits an irregular final shape, which differs from that of the mold. With respect to the thickness distribution, the PHBV presents a non-symmetric and completely irregular path in the grid, in agreement with a random thickness distribution. In order to determine the thermoforming temperature range of PHBV, identical sheets of PHBV were thermoformed varying the heating time. The resulting trays were observed, paying attention to the "edge", "corners" and "thickness" (as stated previously). Each parameter was classified as "bad" (red color, cross sign), "intermediate" (blue color, wave sign) or "good" (green color, tick mark), as depicted in Figures 6.5.b and 6.5.c. The upper and lower limits of the temperature range (that is, the heating time range) were established as those at which all the studied compositions resulted in a poor thermoformability. For the present setup, they were 30 and 44 seconds, respectively, using a step of 2s for the screening (see inset Fig. 6.2.d). When evaluating the thermoformability of the neat PHBV, according to the method proposed in this work, none of the conditions yielded in a good thermoformed tray, as shown in Figure 6.5.c. Thus, it could be concluded that neat PHBV showed poor thermoformability. The overall poor thermoforming behavior of the PHBV, including its narrow thermoforming temperature range, can be ascribed to its high crystallinity, which results in an abrupt loss of mechanical stability when the softening temperature is reached, thus leading

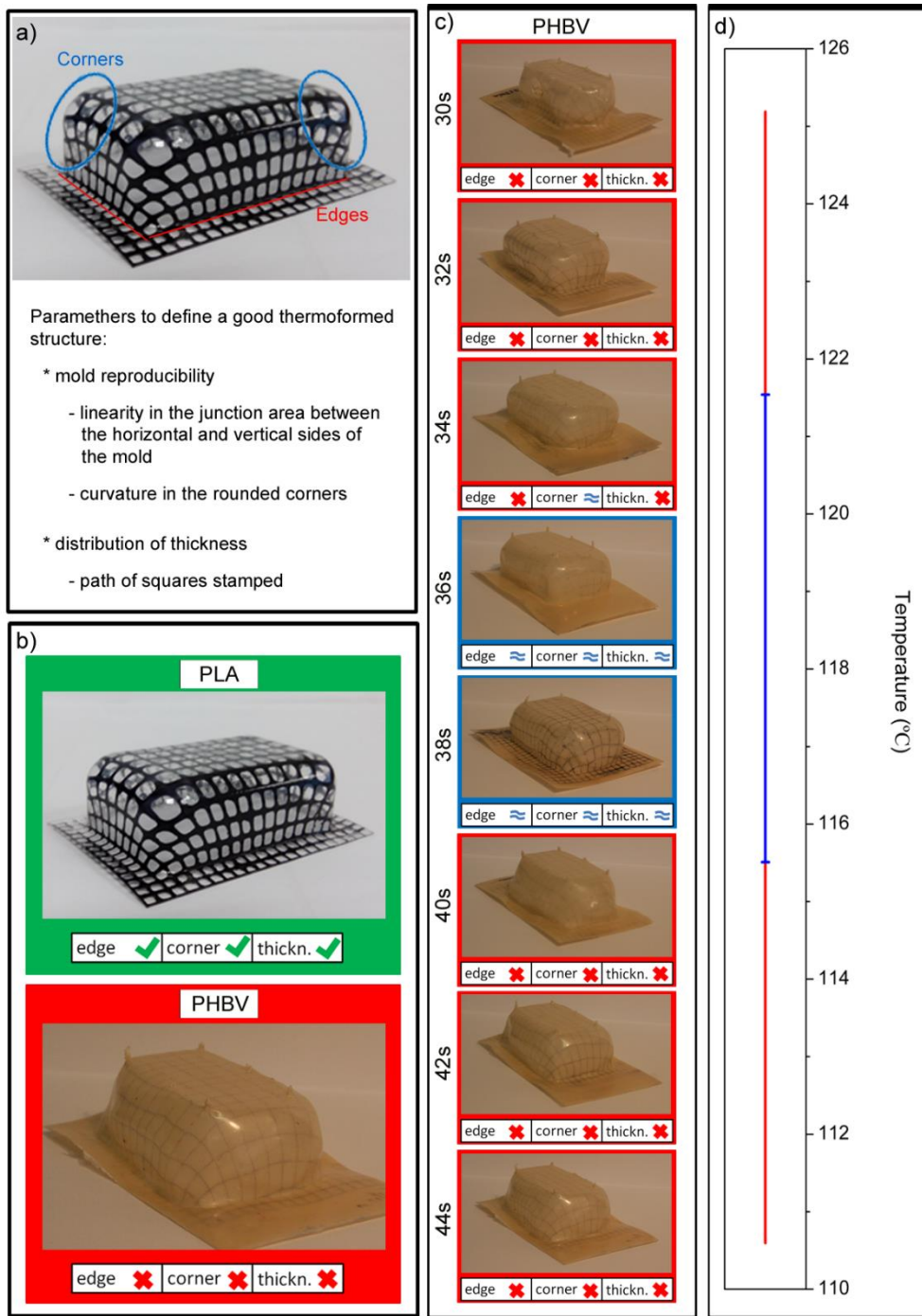


Fig. 6.5: a) parameters defined in the method on a thermoformed PLA tray, b) an example of the thermoformed trays for PLA and PHBV, c) thermoformed PHBV trays at different heating times evaluated according to the method and d) thermoforming temperature range according to the method.

to sagging effect prior to the thermoforming step [9,10]. The sagging effect results in considerable redistribution of material within the molded sheet. Nevertheless, a slight improvement in the shape of the samples was accounted for heating times of 36 and 38s. Under these conditions, the so-obtained thermoformed trays are considered as intermediate (blue color). Figure 6.5.d summarizes the thermoformability of the PHBV trays (represented by the color code) as a function of the thermoforming temperature within the analyzed time range.

6.3.3.2. Thermoformability of the PLA/PHBV blends

Figure 6.6 summarizes the evaluation of the thermoforming ability for all the PHBV/PLA blends studied (with and without the compatibilizers) as a function of the heating time, including representative pictures of the thermoformed trays. From the figure, it can be deduced that the incorporation of the PLA to the PHBV resulted in a slight improvement with respect to the thermoformability of the PHBV. However, neither a more limited thickness variation nor an increase in the thermoforming temperature range could be observed. The limited effect of the addition of the PLA was assigned to the lack of compatibility between the two polymers. The absence of compatibility was reported in a previous work [16] by SEM observations as well as by DSC and DMA, where two independent glass transition temperatures were clearly observed. However, as the compatibilizers were added to the blend, it greatly improved the thermoformability of the PHBV/PLA, with thermoforming enhancements as a function of the used compatibilizer.

The incorporation of HMDI to the PHBV/PLA blend resulted in a wider thermoforming temperature window, although the overall thermoformability of the blend was still classified as intermediate even in the best temperature range (30 to 40s heating). All the HMDI thermoformed trays showed poor reproducibility in the round corners of the mold. A small improvement in the thickness distribution, as determined from a more homogenous and predictable path of the square-grid, was observed. With respect to the samples containing polyHMDI and PDI, both compositions allowed a wider thermoforming temperature window, when compared to the neat PHBV and PHBV/PLA. Moreover, a good thermoformability (green color) was achieved for the first time in the samples obtained in the temperature range from 112

6. Capítulo 4



Fig. 6.6: Photographs of the thermoformed structures depending on the processing temperature and thermoforming temperature range for Neat PHBV, PHBV/PLA blend and the PHBV/PLA compatibilized blends.

to 122 and from 112 to 124 °C for the polyHMDI and PDI, respectively. The samples processed at the limits of the studied temperature range showed however intermediate thermoforming compliance, according to the methodology used. Interestingly, the thickness distribution of the obtained samples was repetitive for all the samples and compositions, thus being predictable and controllable, and the samples resulted in trays that perfectly reproduced the geometry of the mold.

The positive outcome in terms of thermoformability when PLA with the compatibilizers were incorporated to the PHBV, and the expanded thermoforming temperature range can be ascribed to two phenomena: 1. an enhancement in the sheet stability during heating prior to thermoforming and, 2. an increase in the elasticity of the molten blend during the thermoforming. The former phenomenon is attributed to an improved interaction between the dispersed amorphous phase and the continuous crystalline phase. Such interactions are important at temperatures close to the softening point of the crystalline phase, and leads to an increase in the overall viscosity of the system [16]. This higher viscosity results in a reduction of the sagging effect and therefore, a better control of the thickness distribution during the distribution of the thermoplastic in the mold. Increasing thermoformability of highly crystalline polymers by blending them with amorphous polymers was previously reported by Gimenez et al. [9,10]. The increase in the stability of the polymer system during the heating stage, prior to the deformation, and an increase in the elasticity of PHBV blends when compared to the pure PHBV was also reported for processing of PHVB blends in injection molding [24,25].

Overall, both the enhanced stability and the improved elasticity are positive for the thermoforming outcome. Thus, the improvement in the thermoformability and in the thermoforming process windows in this work was a combined effect of enhanced sheet stability, counteracting a sudden drop in viscosity during thermoforming, and an improved phase interaction due to the use of diisocyanates.

6.3.4. Degradation in composting conditions

PHBV and PLA are well known for undergoing biodegradation in composting conditions within a short time, being this one of the main advantages of these materials for short time applications, such as packaging. Therefore, the melt blending of both polymers should, in principle, result in a completely biodegradable material. However, as in this work the blends of the two biopolyesters have been compatibilized with diisocyanates, the possibility of the isocyanates to interfere with the biodegradation was explored. Disintegration tests under composting conditions of all the compositions were therefore performed, monitoring the weight loss of the samples over time according to the ISO 20200 standard [18]. Results are summarized in Figure 6.7.

Figure 6.7.a shows the evolution of disintegration (% of weight loss vs. time) for neat PHBV, neat PLA, PHBV/PLA and the compatibilized blends (HMDI, polyHMDI and PDI). All tests were performed in lab-scale composting conditions. When compared the Neat PLA and Neat PHBV curves, some differences arise. Neat PLA shows a very short induction time in combination with fast disintegration, being fully disintegrated within the first two weeks. Neat PHBV, on the other hand, did not undergo significant weight variations during the first 8 days, in agreement with other reported works performed with the same grade of PHBV [26,27]. Additionally, although both disintegration vs. time curves present an exponential trend, the maximum slope of the Neat PLA is higher than the Neat PHBV one. To visually assess the impact over time of the composting process on the tested samples, images of the studied blends were taken at different time points (Figure 6.7.b). The first sample of Neat PLA taken out from the compost reactor at the 8th day was already broken into pieces showing loss of transparency. According to Arrieta et al. and Fortunati et al. [28,29], this effect is the result of changes in the refraction index, water sorption and/or the presence of hydrolytic products during bacterial biodegradation. With respect to the PHBV-based materials, a noticeable surface roughness can be observed for composting times over 15 days. This surface roughness indicates the onset of the disintegration, since the biodegradation of PHAs takes place by means of a surface erosion by the microorganisms [30,31].

The differences in biodegradation onset time and rate of disintegration for PLA and PHBV can be ascribed to the accessibility of the microorganism involved in the biodegradation to the available amorphous polymer chains, which act as nourishment. Accordingly, the biodegradation takes place

in the amorphous fraction of the biopolyesters rather than on the crystals. Therefore, the biodegradation of the amorphous PLA is favored over the highly crystalline PHBV as reported by Arrieta et al. [32]. This reasoning is consistent with the behavior observed for the PHBV/PLA blends, where the degradation takes place in two steps. The first one, with a weight loss up to 25%, is the fastest one and can be ascribed mostly to the PLA content of the blend, whilst the second one would correspond mainly to the PHBV fraction. On the other hand, during the step attributed to the PHBV fraction, an increase of the disintegration rate is detected when compared with the neat PHBV, which can be related with an increase in the specific surface derived from the voids resulting from the disintegration of the PLA droplets. The differences observed among the biodesintegration curves of the blends can be explained by the accessibility of the microorganisms to the PLA fraction, which results in a delay in the degradation onset with respect to neat PLA and also in variations in the initial disintegration rate, which in turn is faster as is larger the average size of the dispersed phase (c.f Fig. 6.3).

In order to corroborate all the above reasoning, a morphological study of the samples after 20 days in composting conditions has been carried out. Figure 6.7.c presents SEM micrographs of the surface of PHBV and PHBV/PLA blends. The neat PHBV sample shows a uniform rough surface, but the blends show some voids in the surface. The size of these voids is bigger for the uncompatibilized PHBV/PLA blend, following the same order for the rest of the blends as their average particle size decrease. According to our previous assumptions based on weight loss, after 20 days most of the PLA phase should have been already biodegraded, leaving those voids in the samples. In Figure 6.7.d and 6.7.e it is presented a higher magnification detail of the surface of the neat PHBV and the PDI samples, respectively, where the voids in the PDI sample are clearly visible. Indeed, the bacterial growth and the surface erosion of the samples are noticeable in these images. All of the above leads us to the conclusion that the incorporation of diisocyanates as compatibilizers in PHBV/PLA blends in the present dosage does not negatively affect the biodesintegrability, with only small variations related with the size of the dispersed PLA domains within the PHBV matrix.

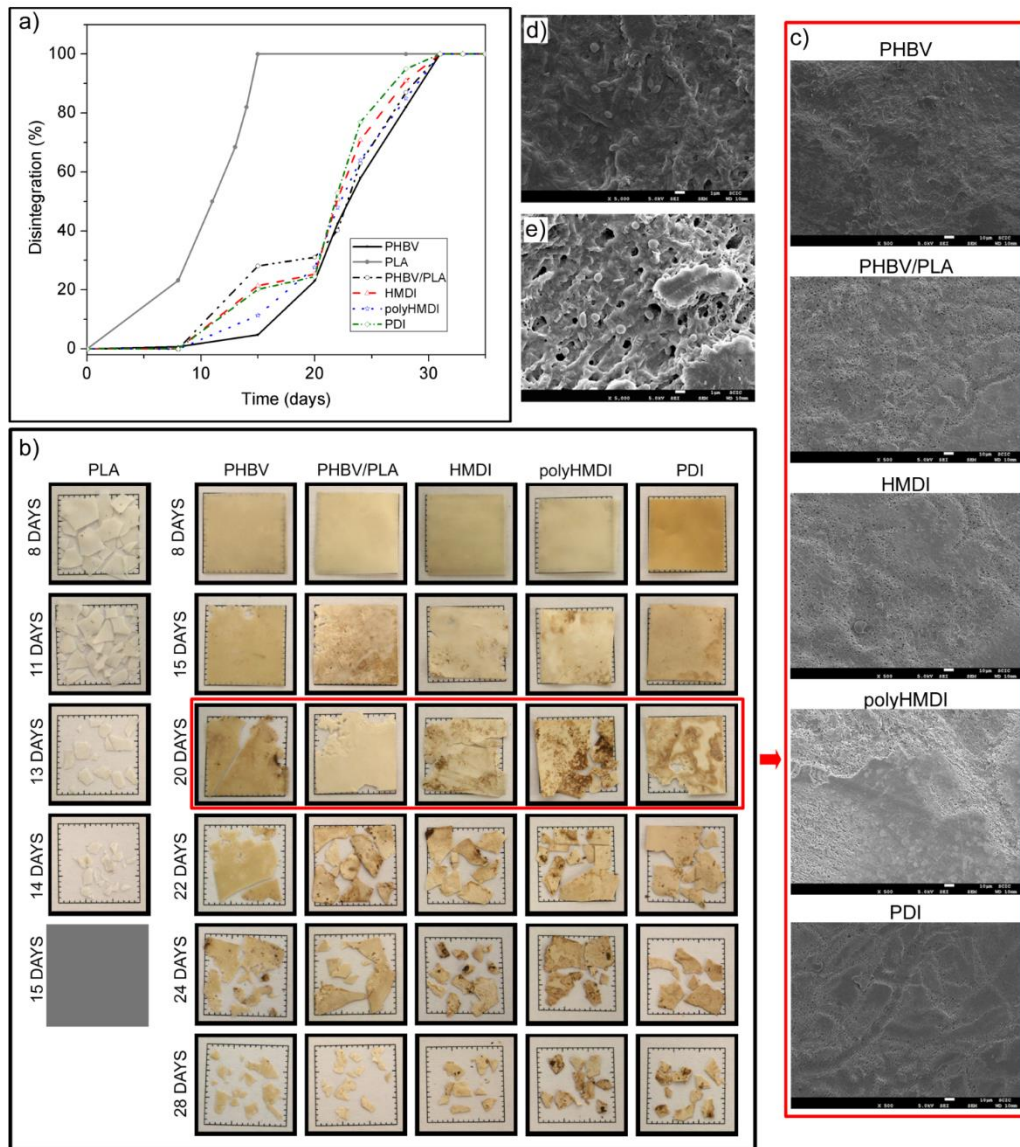


Fig. 6.7: a) Disintegration curve, b) photographs of the disintegrated samples at different times, c) SEM micrographs of eroded surfaces after 20 days under composting conditions, d) and e) SEM micrographs of bacteria colonies after 20 days of composting of PHBV/PLA blend and PDI, respectively.

6.4. CONCLUSIONS

PHBV is a potential good candidate to replace petroleum-based polymers in the packaging sector due to its excellent barrier properties and biodegradability. However, PHBV copolymers present some shortcomings for its direct implementation in this sector. One of the main shortcomings arises from its poor thermoformability (defined as the ability to be successfully reproduced the shape of a mold with a controlled thickness distribution) and its narrow thermoforming window (defined as the temperature range at which good thermoformability is achieved). In this work, blends of PHBV with PLA and three different compatibilizers (hexamethylene diisocyanate, (HMDI), poly(hexamethylene) diisocyanate (polyHMDI) and 1,4-phenylene diisocyanate (PDI)) diisocyanates have been obtained by melt blending. The thermoformability, barrier properties and biodegradability of the so-obtained were investigated. In order to assess the thermoformability of the materials, a simple method for assessing qualitatively the thermoforming capacity of any polymeric film is proposed. Slight enhancement in the thermoforming capacity of PHBV is observed when HMDI is incorporated to the PHBV/PLA blend. On the other hand, good mold reproducibility is accomplished for a wide range of temperatures for both the polyHMDI and PDI blends, being the best ones obtained with PDI. Besides, the addition of diisocyanates did not substantially change the barrier properties of the PHBV/PLA blends, nor does it negatively affect the biodegradation with respect to PHBV. Overall, the use of diisocyanate-type compatibilizers has proven to be a convenient approach to improve thermoformability of PHBV/PLA blends, thus extending the usability of PHBV in thermoformed packaging applications.

ACKNOWLEDGEMENTS

The authors would like to thank the financial support for this research from Ministerio de Economía y Competitividad (AGL2015-63855-C2-2-R and Pla de Promoció de la Investigació de la Universitat Jaume I (PREDOC/2012/32 and UJI-B2016-35). We are also grateful to Raquel Oliver and José Ortega for experimental support.

REFERENCES

- [1] S. Khanna, A.K. Srivastava, Recent advances in microbial polyhydroxyalkanoates, *Process Biochem.* 40 (2005) 607–619. doi:10.1016/j.procbio.2004.01.053.
- [2] L.S. Serafim, P.C. Lemos, R. Oliveira, M.A.M. Reis, Optimization of polyhydroxybutyrate production by mixed cultures submitted to aerobic dynamic feeding conditions., *Biotechnol. Bioeng.* 87 (2004) 145–60. doi:10.1002/bit.20085.
- [3] M.A.M. Reis, L.S. Serafim, P.C. Lemos, A.M. Ramos, F.R. Aguiar, M.C.M. Van Loosdrecht, Production of polyhydroxyalkanoates by mixed microbial cultures., *Bioprocess Biosyst. Eng.* 25 (2003) 377–85. doi:10.1007/s00449-003-0322-4.
- [4] T. Keshavarz, I. Roy, Polyhydroxyalkanoates: bioplastics with a green agenda., *Curr. Opin. Microbiol.* 13 (2010) 321–6. doi:10.1016/j.mib.2010.02.006.
- [5] S. Aditi, D.S. Shalet, N. Manish, R. Pranesh, T. Katyayini, Microbial production of polyhydroxyalkanoates (PHA) from novel sources : A Review, *Int. J. Res. Biosci.* 4 (2015) 16–28.
- [6] D.Z. Bucci, L.B.B. Tavares, I. Sell, PHB packaging for the storage of food products, *Polym. Test.* 24 (2005) 564–571. doi:10.1016/j.polymertesting.2005.02.008.
- [7] D. Cava, E. Gimenez, R. Gavara, J.M. Lagaron, Comparative Performance and Barrier Properties of Biodegradable Thermoplastics and Nanobiocomposites versus PET for Food Packaging Applications, *J. Plast. Film Sheeting.* 22 (2006) 265–274. <http://www.scopus.com/inward/record.url?eid=2-s2.0-33845203640&partnerID=tZ0tx3y1> (accessed January 14, 2015).
- [8] Y.-M. Corre, S. Bruzaud, J.-L. Audic, Y. Grohens, Morphology and functional properties of commercial polyhydroxyalkanoates: A comprehensive and comparative study, *Polym. Test.* 31 (2012) 226–235. doi:10.1016/j.polymertesting.2011.11.002.
- [9] E. Giménez, J.M. Lagarón, M.L. MasPOCH, L. Cabedo, J.J. Saura, Uniaxial tensile behavior and thermoforming characteristics of high barrier EVOH-based blends of interest in food packaging, *Polym. Eng. Sci.* 44 (2004) 598–608. doi:10.1002/pen.20054.
- [10] E. Giménez, J. Lagaron, R. Gavara, L. Cabedo, J.J. Saura, Study of the thermoformability of ethylene - vinyl alcohol copolymer based barrier blends of interest in food packaging applications, *J. Appl. Polym. Sci.* 96 (2004) 3851 – 3855. <http://onlinelibrary.wiley.com/doi/10.1002/app.13584/full> (accessed December 9, 2014).
- [11] R.M. Rasal, A. V. Janorkar, D.E. Hirt, Poly(lactic acid) modifications, *Prog. Polym. Sci.* 35 (2010) 338–356. doi:10.1016/j.progpolymsci.2009.12.003.
- [12] S. Modi, K. Koelling, Y. Vodovotz, Miscibility of poly(3-hydroxybutyrate-co-3-hydroxyvalerate) with high molecular weight poly(lactic acid) blends determined by thermal analysis, *J. Appl. Polym. Sci.* 124 (2012) 3074–3081. doi:10.1002/app.35343.
- [13] I. Zembouai, S. Bruzaud, M. Kaci, A. Benhamida, Y. Corre, Y. Grohens, J.-M. Lopez-Cuesta, Synergistic Effect of Compatibilizer and Cloisite 30B on the Functional Properties of Poly (3-hydroxybutyrate- co -3-hydroxyvalerate)/ Polylactide Blends, *Polym. Eng. Sci.* 54 (2014) 2239–2251. doi:10.1002/pen.
- [14] I. Zembouai, M. Kaci, S. Bruzaud, A. Benhamida, Y.-M. Corre, Y. Grohens, A study of morphological, thermal, rheological and barrier properties of Poly(3-hydroxybutyrate-Co-3-Hydroxyvalerate)/polylactide blends prepared by melt mixing, *Polym. Test.* 32 (2013) 842–851. doi:10.1016/j.polymertesting.2013.04.004.

- [15] R.A. Auras, B. Harte, S. Selke, R. Hernandez, Mechanical, Physical, and Barrier Properties of Poly(Lactide) Films, *J. Plast. Film Sheeting*. 19 (2003) 123–135. doi:10.1177/8756087903039702.
- [16] J. Gonzalez-Ausejo, E.L. Sanchez-Safont, J.M. Lagarón, R. Balart, L. Cabedo, J. Gamez-Perez, Compatibilization of PHBV/PLA blends with diisocyanates, *J. Appl. Polym. Sci.* (n.d.) Accepted.
- [17] H. Alata, T. Aoyama, Y. Inoue, Effect of Aging on the Mechanical Properties of Poly(3-hydroxybutyrate-co-3-hydroxyhexanoate), *Macromolecules*. 40 (2007) 4546–4551. doi:10.1021/ma070418i.
- [18] UNE-EN ISO 20200 Determinación del grado de desintegración de materiales plásticos bajo condiciones de compostaje simuladas en un laboratorio, (2006).
- [19] A. Guinault, A.S. Nguyen, G. Miquelard-Garnier, D. Jouannet, A. Grandmontagne, C. Sollogoub, The Effect of Thermoforming of PLA-PHBV Films on the Morphology and Gas Barrier Properties, *Key Eng. Mater.* 504–506 (2012) 1135–1138. doi:10.4028/www.scientific.net/KEM.504-506.1135.
- [20] R. McCool, P.J. Martin, The role of process parameters in determining wall thickness distribution in plug-assisted thermoforming, *Polym. Eng. Sci.* 50 (2010). doi:10.1002/pen.21718.
- [21] D. Marathe, D. Rokade, L. Busher Azad, K. Jadhav, S. Mahajan, Z. Ahmad, S. Gupta, S. Kulkarni, V. Juvekar, A. Lele, Effect of plug temperature on the strain and thickness distribution of components made by plug assist thermoforming, *Int. Polym. Process.* 31 (2016). doi:10.3139/217.3060.
- [22] M. Buntinx, G. Willems, G. Knockaert, D. Adons, J. Yperman, R. Carleer, R. Peeters, Evaluation of the Thickness and Oxygen Transmission Rate before and after Thermoforming Mono- and Multi-layer Sheets into Trays with Variable Depth, *Polymers (Basel)*. 6 (2014) 3019–3043. doi:10.3390/polym6123019.
- [23] R.E. Lee, Y. Guo, H. Tamber, M. Planeta, S.N.S. Leung, Thermoforming of Polylactic Acid Foam Sheets: Crystallization Behaviors and Thermal Stability, 55 (2016) 560–567. doi:10.1021/acs.iecr.5b03473.
- [24] H. Zhao, Z. Cui, X. Sun, L.-S. Turng, X. Peng, Morphology and Properties of Injection Molded Solid and Microcellular Polylactic Acid/Polyhydroxybutyrate-Valerate (PLA/PHBV) Blends, *Ind. Eng. Chem. Res.* 52 (2013) 2569–2581. doi:10.1021/ie301573y.
- [25] I. Zembouai, S. Bruzaud, M. Kaci, A. Benhamida, Y.-M. Corre, Y. Grohens, A. Taguet, J.-M. Lopez-Cuesta, Poly(3-Hydroxybutyrate-co-3-Hydroxyvalerate)/Polylactide Blends: Thermal Stability, Flammability and Thermo-Mechanical Behavior, *J. Polym. Environ.* 22 (2013) 131–139. doi:10.1007/s10924-013-0626-7.
- [26] A. Martínez-Abad, J. González-Ausejo, J.M. Lagarón, L. Cabedo, Biodegradable poly(3-hydroxybutyrate-co-3-hydroxyvalerate)/thermoplastic polyurethane blends with improved mechanical and barrier performance, *Polym. Degrad. Stab.* 132 (2016) 52–61. doi:10.1016/j.polymdegradstab.2016.03.039.
- [27] E.L. Sánchez-Safont, J. González-Ausejo, J. Gámez-Pérez, J.M. Lagarón, L. Cabedo, Poly(3-Hydroxybutyrate-co-3-Hydroxyvalerate)/Purified Cellulose Fiber Composites by Melt Blending: Characterization and Degradation in Composting Conditions, *J. Renew. Mater.* 4 (2016) 123–132. doi:10.7569/JRM.2015.634127.
- [28] M.P. Arrieta, J. López, E. Rayón, a. Jiménez, Disintegrability under composting conditions of plasticized PLA-PHB blends, *Polym. Degrad. Stab.* (2014) 1–12. doi:10.1016/j.polymdegradstab.2014.01.034.
- [29] E. Fortunati, D. Puglia, C. Santulli, F. Sarasini, J.M. Kenny, Biodegradation of Phormium tenax/poly(lactic acid) composites, *J. Appl. Polym. Sci.* 125 (2012) E562–E572. doi:10.1002/app.36839.

6. Capítulo 4

- [30] D. Puglia, E. Fortunati, D. a. D'Amico, L.B. Manfredi, V.P. Cyras, J.M. Kenny, Influence of organically modified clays on the properties and disintegrability in compost of solution cast poly(3-hydroxybutyrate) films, *Polym. Degrad. Stab.* 99 (2014) 127–135. doi:10.1016/j.polymdegradstab.2013.11.013.
- [31] K. Iggui, N. Le Moigne, M. Kaci, S. Cambe, J.-R. Degorce-Dumas, A. Bergeret, A biodegradation study of poly(3-hydroxybutyrate-co-3-hydroxyvalerate)/organoclay nanocomposites in various environmental conditions, *Polym. Degrad. Stab.* 119 (2015) 77–86. doi:10.1016/j.polymdegradstab.2015.05.002.
- [32] M.P. Arrieta, J. López, A. Hernández, E. Rayón, Ternary PLA–PHB–Limonene blends intended for biodegradable food packaging applications, *Eur. Polym. J.* 50 (2014) 255–270. doi:10.1016/j.eurpolymj.2013.11.009.

7. Capítulo 5

**Effect of the addition of sepiolite on the morphology
and properties of melt compounded PHBV/PLA blends**

7. Capítulo 5

Effect of the addition of sepiolite on the morphology and properties of melt compounded PHBV/PLA blends

Jennifer Gonzalez-Ausejo¹, Jose Gamez-Perez¹, Rafael Balart², José Maria Lagarón³, Luis Cabedo¹

¹ Polymer and Advanced Materials Group (PIMA), Universidad Jaume I. 12071, Castellon, Spain.

² Instituto de tecnología de Materiales (ITM), Universidad Politécnica de Valencia, Campus de Alcoi. 03801, Alcoy, (Alicante) Spain

³ Novel Materials and Nanotechnology Group, IATA-CSIC, 46980, Paterna (Valencia), Spain

ABSTRACT

A study concerning the incorporation of sepiolite in blends of biopolyesters (PHBV/PLA) to obtain clay / polymer nanocomposites (CPN) was performed in order to improve the gas barrier performance of the final materials and achieve a well dispersed morphology by means of an increase in the melt viscosity during melt blending. The latter is relevant to increase the stability of the PHBV sheets during thermoforming. The samples were analyzed using scanning electron microscopy (SEM), wide angle X-ray diffraction (WAXS), thermogravimetric analysis (TGA), differential scanning calorimetry (DSC), tensile tests at room and high temperatures, dynamo-mechanical thermal analysis in torsion mode (DMTA), oscillatory rheometry with a parallel plate setup, Vicat softening temperature system and oxygen barrier properties. The resulting Sepiolite/PHBV/PLA nanocomposites not only improved the compatibility between the biopolymers and reduced the oxygen permeability, but also improved the mechanical properties at room temperature, showing an increase in the elongation at break, as well as increasing the rigidity and stability of the CPN at higher temperatures, which could make them very attractive for uses in thermoforming applications for food packaging.

GRAFICAL ABSTRACT

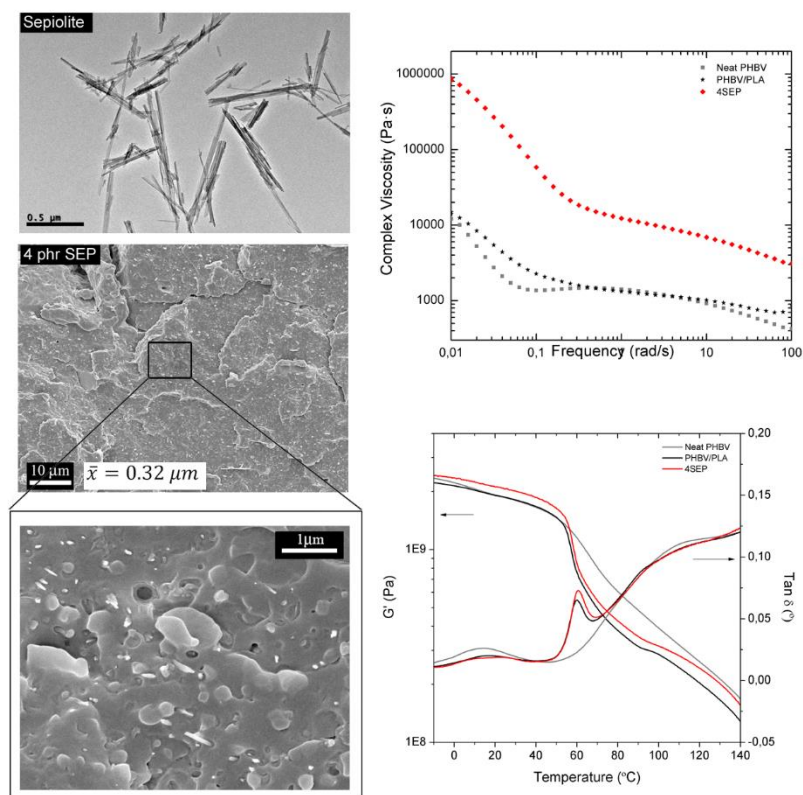


Fig. 7.1: Graphical abstract of the work named Effect of the addition of sepiolite on the morphology and properties of melt compounded PHBV/PLA blend

7.1. INTRODUCTION

The incorporation of clay minerals as nanoadditives in polymer and polymer blends, thus obtaining the so-called clay mineral-polymer nanocomposites (CPN), has raised the interest of both the academia and the industry in the recent years due to the interesting combination of properties of the resulting hybrid materials. In this sense, nanotechnology brings significant opportunities for the biodegradable polymers to improve their applicability to the food packaging field by increasing the performance in the aspects in which the oil-based polymers are still superior [1–3].

The massive use of petroleum-based polymers has resulted in environmental concerns derived not only from their non-renewable origin, but also from the waste management issues resultant from their low degradation rates. Hence, there is a growing interest in the development of renewable and biodegradable materials to partially replace the oil-based ones and minimize the problematics related to waste generation at the end of the life cycle. Two of the most promising biopolyesters are the poly (3-hydroxybutyrate-co-3-hydroxyvalerate) (PHBV) and the poly(lactic acid) (PLA). These biopolymers provide a good alternative to fossil-fuel based plastics as they possess thermoplastic properties similar to conventional polyolefins, with the advantage of being 100% biodegradable, compostable and produced from renewable resources [4–6].

Poly (3-hydroxybutyrate-co-3-hydroxyvalerate) (PHBV) is a polyhydroxyalkanoate (PHA), a family of naturally occurring storage biopolyesters synthesized by more than 300 species of Gram-positive and Gram-negative bacteria [7]. When compared to other biopolyesters, PHBV presents on one hand excellent barrier properties (similar to those of polyethylene terephthalate (PET)) [8], and much better than other biopolyesters such as poly(lactic acid) [9] and, on the other hand, a balanced mechanical performance in terms of stiffness and strength similar to that of polypropylene (PP) [10]. The main reason behind this good barrier properties is the high crystallinity of the PHBV copolymers, being as high as 60% in some cases [11]. However, molten state thermoforming of highly crystalline polymers has a very narrow processing window due to the sagging phenomenon derived from the loss of mechanical stability of the sheet prior to the drawing process [12,13]. Hence, the high crystallinity of PHBV results in a narrower processing window when compared to commodities and other biopolyesters [10], which avoid the application of this biopolymer to some packaging applications, e.g. thermoformed trays and blisters. It has

7. Capítulo 5

been reported that in order to increase the processing window and the sheet stability of highly crystalline polymers for thermoforming applications, blending with amorphous polymers can be a successful approach [13,12]. In the present work blends of PHBV with poly (lactic acid) (PLA) have been obtained in order to increase the stability of the PHBV sheets at thermoforming temperatures, while retaining biodegradability.

When dealing with melt processing, PLA shows better processability compared to other biopolymers, being more easily thermoformed because of its broad processing window, derived from its amorphous state at normal processing conditions [14] and use of chain extenders to produce branching [15]. However, gas barrier properties of PLA are not as good as PHBV and would lead to a drop in the barrier performance of the final material.

Furthermore, PHBV/PLA blends have been widely studied in the literature [16–20] and it is known that the performance of these blends can be compromised by the low interfacial adhesion between the components due to the immiscible nature of PHBV and PLA, leading to a characteristic droplet-matrix morphology or discrete-phase structure. Melt compounding is a most convenient approach for obtaining a homogeneous morphology of immiscible blends, when the blending is conducted in high shear conditions. To do so, the viscosity of the blend has to be high enough to enable shear forces to take place. In the case of PHBV/PLA blends, the molten viscosity is found to be insufficient to achieve good dispersion of the PLA phase, due to the competition between shear forces (break-up mechanism) and the interfacial tension forces (coalescence mechanism) [21,22]. In a previous work [23], PHBV/PLA blends with different diisocyanates as compatibilizers have been assessed, showing a reduction in the PLA dispersed domains in the PHBV matrix. In that work, the increase in compatibility was achieved by reducing the interfacial tension between the blend components.

A novel approach is proposed in the current work, which is the introduction of a natural clay mineral as a nanofiller in the melt blending process, thus obtaining a nanobiocomposite. By doing so, it is intended to improve the two main concerns of blending PHBV with PLA: the decrease in the gas barrier performance of the final blend by incorporating the clay [24] and getting a well dispersed morphology during melt blending, by means of an increase in the melt viscosity. It has been widely reported that the addition of low amounts of nanoparticles, such as, carbon nanotubes, bentonites, halloysite nanotubes and sepiolite needles, among others, provides

improved mechanical, thermal and barrier properties against gases, aromas, and water vapor of biopolymers [25–29].

Sepiolite is a natural clay mineral that has attracted interest as nanoparticles for biopolymers because it is cheap and abundantly available and has rich functionality and good biocompatibility [30–34]. It is a phyllosilicate that exhibits fibrillar needle-shaped porous structure because alternating continuous two-dimensional tetrahedral sheets with non-continuous octahedral sheets, resulting in the formation of channels running parallel to the fiber length [35]. It also has a high hydrophilicity due to high concentration of surface silanol along the length of the needles. This promotes an improved dispersion of sepiolite by melt blending in some polymeric matrices as well as the coupling reaction with the polar areas of the polymer chains, without chemical modification, especially when compared with other clay mineral-based such as montmorillonite [36–38]. Sepiolite has been found to increase the gas barrier properties of PLA [39] and cause higher melt viscosity and stronger shear thinning due to the larger aspect ratio and surface area of sepiolite compared to other natural clay minerals [40].

Although sepiolite has been widely used as nanofiller in many matrices, such as PLA [30,39,41,42] and PLA-based blends [43,44], to the best of our knowledge, the effect of addition of sepiolite in PHBV or PHBV-based blends has never been studied.

In this work, the effect of the addition of a natural sepiolite in the morphology and final properties of blends of biopolyesters (PHBV/PLA) is assessed for the first time.

7.2. EXPERIMENTAL

7.2.1. Materials

Poly(3-hydroxybutyrate-co-3-hydroxyvalerate) (PHBV) with 3 mol% 3-hydroxyvalerate content was purchased from Tianan Biologic Material Co. (Ningbo. P.R. China) in pellet form (ENMAT Y1000P). Commercial poly(lactic acid) PLA 2003D was supplied by NatureWorks® Co. LLC. USA.

An additive based on sepiolite in powder form was kindly supplied by Tolsa (Tolsa Group. Madrid. Spain). It was a polyfunctional additive Pansil manufactured from high purity sepiolite especially recommended to improve the distribution of organic and inorganic fillers and fibers.

7. Capítulo 5

7.2.2. Sample preparation

The PHBV/PLA proportion was set at 75/25 wt./wt.% and CPN of Sepiolite//PHBV/PLA were obtained with Sepiolite contents of 1, 2, 3 and 4 phr (weight parts of sepiolite per hundred weight parts of the PHBV/PLA blend). All materials were dried prior to their processing at 80 °C for 2 h.

The blends were prepared in a twin-screw co-rotating extruder with L/D ratio of 24 and a diameter of 2.5 cm, with a temperature profile of 165/170/175/180 °C (from the hopper to the extruder die) at a speed of 40 rpm to achieve good mixing. The extruded material was pelletized and dried at 80 °C for 2 h.

Standardized tensile specimens (ISO-527 Type 1B for tensile and flexural tests and ISO 179 type 1 for impact tests) were injection molded in a Meteor 270/75 injection molding machine (Mateu & Sole, Barcelona, Spain) with an injection temperature of 180 °C at the nozzle.

Films (0.2 mm thick) for WAXS and barrier properties measurements were compression molded from the blend pellets in a hot-plate press (180 °C, 2 min for melting followed by 2 min at 3 bar). Discs of 25 mm in diameter and 2 mm thick for rheological measurements were also obtained by compression molding from the blend pellets in a hot-plate press at 180 °C and applying 300 bar for 2.5 min. All the samples were stored in a vacuum desiccator at ambient temperature during two weeks to allow full crystallization to take place [45].

Samples of both neat PHBV and PLA (referred to as neat PHBV and neat PLA, respectively) were processed under identical conditions for the intention of comparison. The nomenclature used for the blends is as follows: PHBV/PLA for the blend with 75:25 wt./wt. of PHBV and PLA without sepiolite and XSEP for the CPN where X is the sepiolite content in phr.

7.2.3. Characterization

The morphology of the cryofractured surface of sepiolite/PHBV/PLA nanocomposites and PHBV/PLA blend was evaluated by Scanning Electron Microscopy (SEM) using a JEOL 7001F. The samples were fractured in liquid nitrogen and subsequently coated by sputtering with a thin layer of Pt.

The size of the dispersed phase observed in SEM micrograph was evaluated measuring the length of the spheres in microphotographs with ImageJ software (the number of spheres measured for each sample was never below 400).

Transmission electron microscopy (TEM) of the sepiolite was performed using a Jeol 2100 operated at 200 kV. In order to observe the morphology and size of sepiolite nanofibers preventing large agglomeration of particles, a small droplet of a highly diluted dispersion of sepiolite in deionized water was dropped directly upon a copper grid holder and allowed to dry gently. The length distribution and the average diameter of the sepiolite needles were also measured with ImageJ software.

Wide angle X-ray diffraction (WAXS) measurements were performed using a Bruker AXS D4 ENDEAVOR diffractometer. The samples were scanned at room temperature in reflection mode using incident Cu K-alpha radiation ($\lambda = 1.54 \text{ \AA}$), while the generator was set up at 40 kV and 40 mA. The data was collected over a range of scattering angles (2θ) comprised in the of 2–40° range.

The thermal stability of the blends and CPN was investigated by means of thermogravimetric analysis (TGA) using a TGA/SDTA 851 (Mettler-Toledo Inc., Schwerzenbach, Switzerland). The samples were heated from 50 to 600 °C at a heating rate of 10 °C/min under nitrogen flow. The characteristic temperatures $T_{5\%}$ and T_d corresponded, respectively, to the initial decomposition temperature (5% of weight loss) and to the maximum degradation rate temperature measured at the derivative thermogravimetric (DTG) maximum peak.

Differential scanning calorimetry (DSC) experiments were conducted using a DSC2 (Mettler Toledo) with an intracooler (Julabo modelo FT900). The weight of the DSC samples was typically 7 mg. Samples were first heated from -20 to 200 °C at 10 °C/min, kept for 1 min at 200 °C, cooled down

7. Capítulo 5

to -20 °C at 10 °C/min. and then finally heated to 200 °C at 10 °C/min. The crystallization temperature (T_c), melting temperature (T_m), and melting enthalpy (ΔH_m) were determined from the cooling and second heating curve. T_m and ΔH_m were taken as the peak temperature and the area of the melting endotherm, respectively. The crystallinity (X_c) of the PHBV phase was calculated by the following Equation (7.1).

$$X_c (\%) = \frac{\Delta H_m}{w \cdot \Delta H_m^0} \cdot 100 \quad (7.1)$$

where ΔH_m (J/g) is the melting enthalpy of the polymer matrix. (ΔH_m^0) is the theoretical melting enthalpy of 100% crystalline PHBV (perfect crystal) (146 J/g), and w is the weight fraction of PHBV in the blend and CPN [46]. The DSC instrument was calibrated with an indium standard before use.

PHBV/PLA blends and CPN were characterized by standardized mechanical tests: tensile up-to-failure and flexural. Tensile and flexural tests were carried out at room temperature in a universal test machine Ibertest ELIB 30 (S.A.E. Ibertest, Madrid, Spain) following the guidelines of the ISO 527:2012 and ISO 178:2010 respectively. A 5 kN load cell was used and the crosshead speed was set to 5 mm/min. At least five samples were tested and average values of different parameters were calculated.

Dynamic-mechanic analysis (DMTA) experiments were conducted in an oscillatory rheometer AR G2 (TA Instruments, New Castle, EEUU) equipped with a clamp system for solid samples (torsion mode). Samples sizing 40x10x4 mm³ were subjected to a heating program from -10 °C to 140 °C with a heating rate of 2 °C/min at a constant frequency of 1 Hz. The maximum deformation (γ) was set to 0.1%.

To determine the Vicat softening temperature (VST) a standard VST/HDT cell (model Deflex 687, Metrotec S.A, San Sebastian, Spain) was used following the UNE EN ISO 306:2015. The selected method for evaluate the VST was B50 using a load of 50 N and a heating rate of 50 °C/h.

Rheological analysis were conducted by means of oscillatory shear measurement, being performed using an oscillatory rheometer AR G2 (TA Instruments, New Castle, EEUU) equipped with parallel disks of 25 mm diameter using a gap of 1.5 mm. Sample disks were vacuum dried at 60 °C for 24 h before testing. Strain sweep viscoelastic tests were first performed at a fixed angular frequency of

1 Hz in order to determine the extent of the linear regime. Afterwards, frequency sweep experiments were carried out at a fixed strain in the linear regime, in order to determine the linear viscoelastic moduli, G' (storage modulus) and G'' (loss modulus), as well as the complex viscosity (η^*). The angular frequencies were swept from 100 to 0.01 Hz with five points per decade at 180 °C.

Tensile tests at high temperature and high speed were carried out in a universal testing machine (Shimadzu AGS-X 500N) equipped with a thermostatic chamber (Shimadzu TCE-N300) at a crosshead rate of 500 mm/min and 140 °C. All samples were allowed to reach the equilibrium under 140 °C inside the thermostatic chamber for 5 minutes before the tensile load was applied. Tests were performed according to ASTM D638 with dumb-bell samples die-cut from approximately 200 μm thick films prepared by hot press. Five specimens of each sample were tested and the average results with standard deviation were reported.

The oxygen permeability (OP) of the films was measured in duplicate by using Oxtran 100 equipment (Modern Control, Minneapolis, MN) at 80% relative humidity (RH) and 24 °C, % RH was generated by a built-in gas bubbler and was checked with a hygrometer placed at the exit of the detector. Prior to the measurements, the samples were purged with nitrogen for a minimum of 20 h in the previously relative humidity equilibrated samples. The oxygen flow during the experiments was fixed at 10 ml/min. The measurements were performed through a 5 cm^2 sample area by using an in-house development mask. To obtain the oxygen permeability, film thickness was considered in each case.

Water vapour permeability (WVP) was measured according to the ASTM E96 (2011) gravimetric method. using Payne permeability cups (Elcometer SPRI, Hermelle/s Argenteau, Belgium). Measurements were taken in duplicate. The samples were placed between the aluminium top (open O-ring) and bottom part (deposit for the permeant) with a Viton rubber ring between the film and the top part of the cups to enhance sealability. The cups were placed inside a desiccator at 0% RH and the water weight loss through a film area of 0.001 m^2 was monitored and plotted as a function of time. Water vapor permeability rate was estimated from the slope of the linear part of this plot. thus ensuring the steady-state conditions. Cups with aluminum films were used as control samples to estimate water vapor losses thought the sealing. Water weight loss was

7. Capítulo 5

calculated as the total cell loss minus the loss through the sealing. Water vapor permeability was obtained multiplying the water vapor permeability by the average film thickness.

Water uptake (WU) was assessed from samples dried at 105 °C until a constant weight and then immersed in a distill water bath until a constant weight. WU was calculated according to Equation (7.2):

$$\text{WU (\%)} = \frac{w_f - w_i}{w_i} \cdot 100 \quad (7.2)$$

where w_i and w_f are the initial and final (equilibrium) weight of the samples, respectively. Three replicates for each sample were measured, and the average value is reported.

7.3. RESULTS AND DISCUSSION

7.3.1. Melt compounding and rheology of the blends

This work aims at obtaining a PHBV-based material with enhanced processability, with respect to neat PHBV, while keeping the excellent gas barrier properties of this biopolymer by melt blending the PHBV with PLA and sepiolite. Hence, this paper presents a thorough study of the effect of the sepiolite on the behavior and properties of the biopolyester blends.

In a former step, the morphology of sepiolite was assessed by means of SEM, TEM and WAXS. Figures 7.2.a and 7.2.b present the TEM and SEM micrographs of sepiolite nanofiller, respectively, SEM observation reveals fiber-like morphology of the clay mineral particles, with a high aspect ratio (ratio between length and width or thickness). Size distribution results are presented in Figure 7.2.c. as a result of over 400 nanofibers measurements through image analysis of several SEM and TEM micrographs. No distinction between width and thickness of the fiber has been done; therefore, for the sake of simplicity, a tubular-like shape was assumed, thus having a single parameter in the nanometer range (diameter). Size distribution of the length and diameter (inset) of the nanofibers are plotted in Figure 7.2.c. An average wide length distribution with d_{10} , d_{50} and d_{90} of 0.17 μm , 0.47 μm and 1.4 μm was found out, whilst an average diameter of 14 ± 4 nm was calculated. Therefore, the average aspect ratio (length / diameter) of the sepiolite needles was found to be over 30.

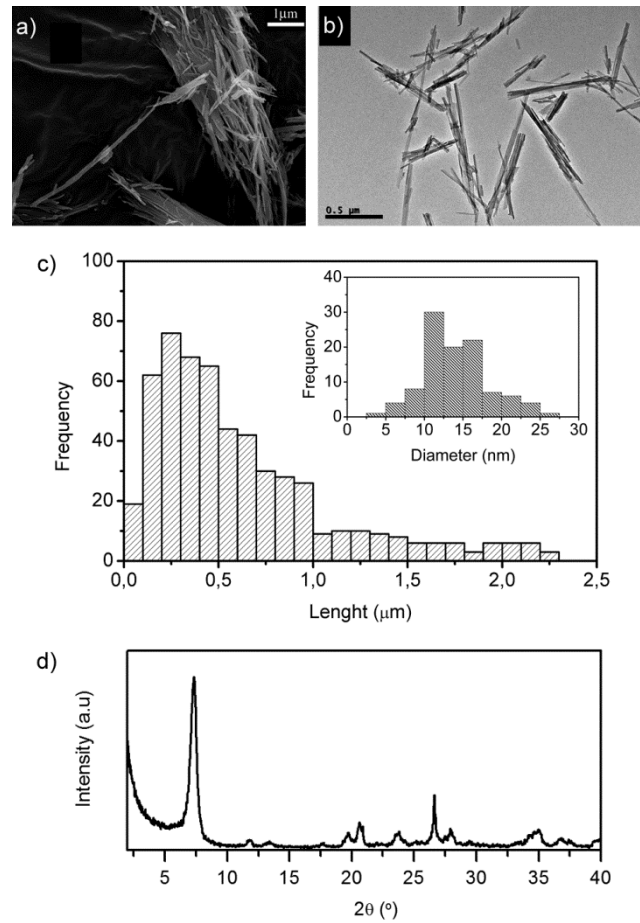


Fig. 7.2: Morphology of sepiolite: a) SEM, b) TEM micrographs, c) length and diameter distribution of sepiolite needles and d) WAXS diffractogram of sepiolite

The WAXS diffractogram of the sepiolite powder is presented in Figure 7.2.d. The diffraction peak at $(2\theta) = 7.34^\circ$ corresponds to the (110) plane, corresponding to a d-spacing of 1.2 nm and revealing that sepiolite is in its natural hydrated form [47]. The hydrated form of the sepiolite is a priori the most convenient for the purpose of blending with a biopolyester, due to the fact that its external surface would be completely covered by hydroxyl groups (from the silanol) that can interact with the ester groups of the biopolyesters, thus forming hydrogen bonds and increasing interaction and effectiveness of the nanofiller.

7. Capítulo 5

Rheological characterization of the blends, with and without sepiolite, was carried out by means of dynamic oscillatory shear measurements as a function of frequency at 180 °C. All rheological measurements were driven from high to low frequencies. Figure 7.3 shows the variation of the complex viscosity (η^*), storage modulus (G') and loss modulus (G'') versus frequency for neat PHBV, PHBV/PLA blends and Sepiolite/PHBV/PLA nanocomposites for different sepiolite contents.

A slight increase in viscosity throughout the whole range of frequencies is registered when the PLA is added to the PHBV; however, no great effect in the rheology of the PHBV is found considering the amount of PLA incorporated (25 wt.%). In contrast, a small quantity of sepiolite can lead to a dramatic change in the rheology of the polymer blend. In this sense, at low frequencies (below 0.1 rad/s), neat PHBV presents a low viscosity value which increases scarcely with the addition of PLA. When the sepiolite is incorporated, a considerable increase in the melt viscosity of the system is observed, particularly at loadings above 2 phr. Thus, the viscosity of the CPN containing 4 phr of sepiolite at these frequencies presented a value 50 times bigger than that of the neat PHBV. This behavior can be explained by the fact that the clay mineral nanofibers imposed a restriction on the polymer chain movements during the melt flowing. The effective degree of interaction can be attributed to the formation of hydrogen bonds between the hydroxyl groups present in the outer surface of the clay mineral and the carbonyl groups of the polyesters [19,48–50]. It is commonly assumed that the rheological behavior of molten polymers at low frequencies can be representative for their behavior during melt blending processes. Hence, an increase in the viscosity under these circumstances would lead to an increase in the shear forces taking place during mixing. Considering that the effectiveness of dispersive mixing is directly related to the shear forces occurring, and that these shear forces are linearly dependent on the viscosity of the melt, it can be inferred that the increase in viscosity when the sepiolite is incorporated to the molten PHBV/PLA blend may result in a more effective blending and, therefore, a better distribution of the PLA phase within the PHBV matrix. Additionally, higher viscosities would decrease the droplet-droplet coalescence phenomenon (which would result in smaller droplet size). This point will be further discussed in the morphology section.

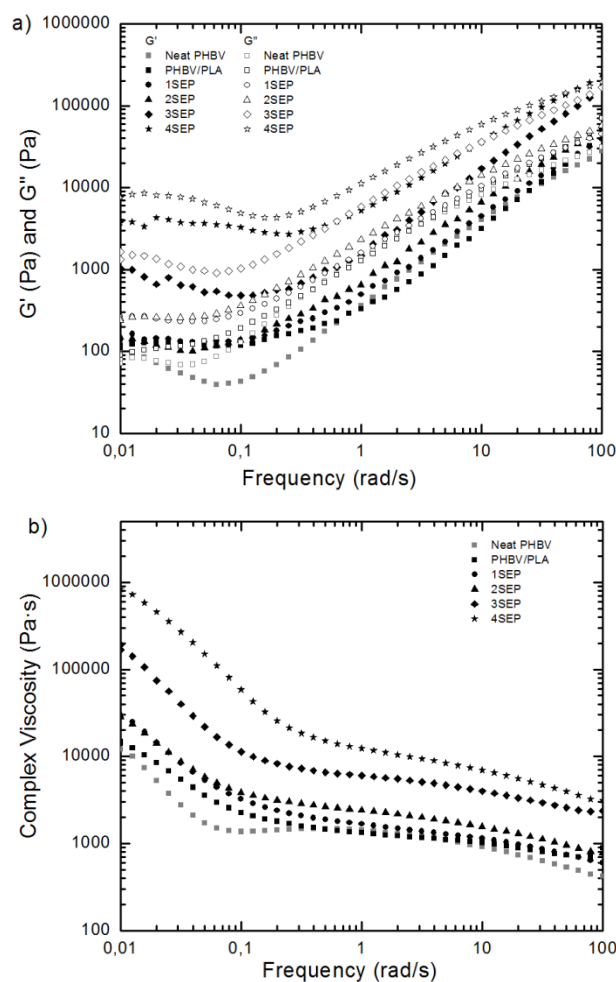


Fig. 7.3: Evolution of a) storage modulus (G'). b) loss modulus (G'') and c) complex viscosity of neat PHBV, PHBV/PLA and sepiolite/PHBV/PLA nanocomposites at 180 °C under 1% dynamical shear strain.

As a common trend, the storage modulus (G') and the loss modulus (G'') typically increase with frequency and the difference between G' and G'' values for all the specimens decreases at high frequencies (Fig. 7.3.a). This is directly related to the viscoelastic properties of polymers, with two overlapped responses: on one hand, an immediate and non-time dependent elastic response; on the other hand, a time-dependent viscous response. Therefore, G' is a measure of the elastic response of the polymer melt. In agreement to what was described in the viscosity behavior of the blends, a slight increase in both G' and G'' throughout the whole range of frequencies is registered

7. Capítulo 5

when the PLA is incorporated to the PHBV. However, the big change is observed with the addition of the sepiolite nanofibers (being more noticeable for loadings over 2 phr). The values of G' at low frequencies register a significant rise with sepiolite contents of 3 and 4 phr. when compared to those of PHBV and the PHBV/PLA blend. Therefore, the elastic response of the melt of compositions with sepiolite is expected to be higher than in the case of pure PHBV and PHBV/PLA blends. The melt elasticity at low speed of deformation is a parameter that can be related to the behavior of the blend when small speed forces are applied (e.g. creep phenomenon). Thus, an increase in the G' at low frequencies could be related to lower creep during heating prior to thermoforming step, i.e. an improved stability of the polymer sheet due to a lower sagging effect taking place.

These results point an enhancement of the blends, which may enable a broadening of the thermoforming window of the material towards higher temperatures. This is in agreement with what is presented and further discussed in section “Mechanical properties at high temperatures”.

7.3.2. Morphology

The morphology of the PHBV/PLA blend and Sepiolite/PHBV/PLA nanocomposites was evaluated by means of SEM and WAXS. Figure 7.4.a present the cryofractured surface of the PHBV/PLA blend, where an immiscible behavior can be clearly detected, as derived from the characteristic discrete-phase structure (DPS, or drop-in matrix). Thus, spheres of PLA are evenly distributed throughout a continuous PHBV matrix. The neat separation between the phases and the presence of detachment phenomenon indicate that the two phases are immiscible and not fully compatible (see Figure 7.4.a). This is in agreement with what has been reported in the literature [23].

SEM micrographs of Sepiolite/PHBV/PLA nanocomposites are presented in Fig. 7.4.a-7.4.e. The sepiolite nanofibers are selective located in the PHBV matrix. as can be observed in the higher magnification detail of Fig. 7.4.f. A uniform and good dispersion of the sepiolite needles within the PHBV matrix is observed for all the compositions, i.e. no aggregates are found even for the SEP CPN. Hence it can be assumed that an effective mixing has been achieved. Moreover, a good degree of adhesion between the filler and the polymer matrix is inferred from the high degree of adhesion at the interface between the nanofibers and the PHBV matrix (Fig. 7.4.f). All this can be

explained by the good interaction between the hydroxyl superficial groups and the ester groups of the PHBV, and is in concordance with the rheology results.

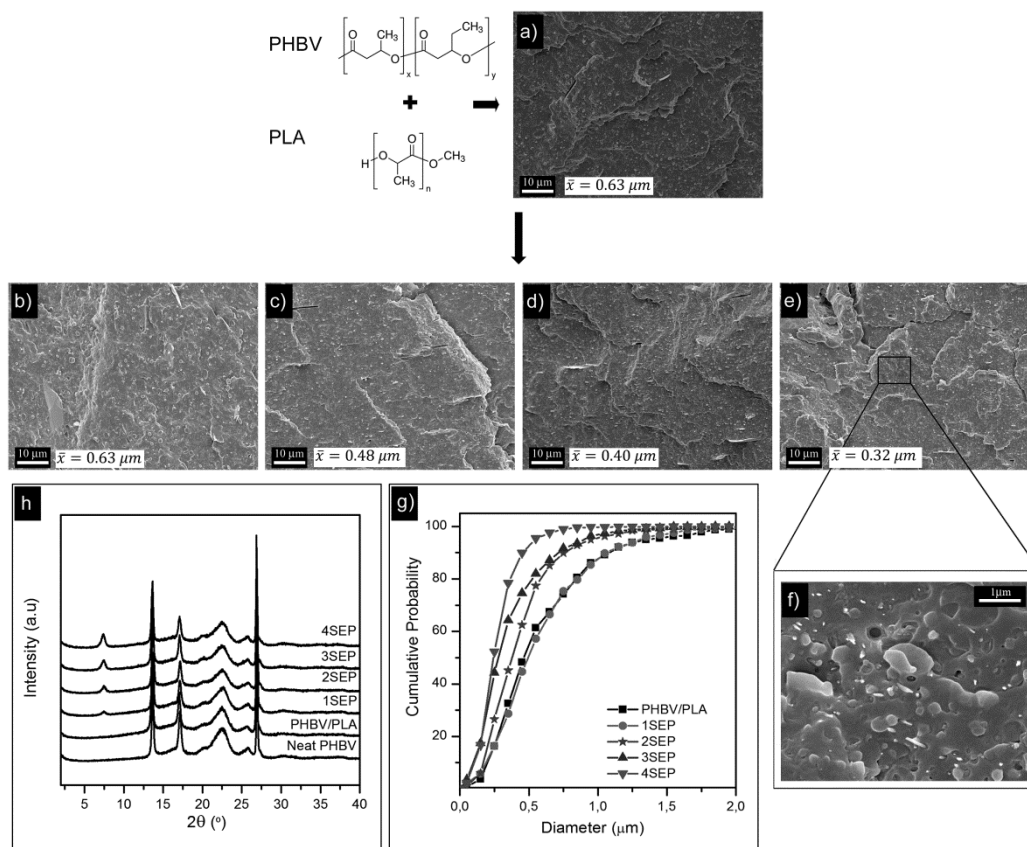


Fig. 7.4: SEM micrographs of a) PHBV/PLA blend, b) 1SEP, c) 2SEP, d) 3SEP, e) 4SEP; h) WAXS diffractograms of PHBV/PLA blend and sepiolite/PHBV/PLA nanocomposites and d) diameter distribution of PLA domains of PHBV/PLA blend and sepiolite/PHBV/PLA nanocomposites

Figure 7.4.b-7.4.e present SEM micrographs of the Sepiolite/PHBV/PLA nanocomposites as a function of the sepiolite content. The morphology of the CPN is similar for all the formulations evaluated, i.e. drop-in matrix morphology with an evenly distributed sepiolite needles in the PHBV matrix. However, when analyzing the size of the PLA droplets, a considerable decrease in the average size is observed: from $0.63 \mu\text{m}$ for the PHBV/PLA without sepiolite to $0.32 \mu\text{m}$ for the sample containing 4 phr of nanofibers. The reduction in the droplet size is representative for the effectiveness of the blending step, thus the addition of the sepiolite has led to a more favorable

7. Capítulo 5

morphology of the polymer blend. The explanation behind the decrease in the average disperse phase domain could be an increase of the viscosity, resulting in higher shear forces while melt mixing. Additionally, to the decrease in the average droplet size, in Figure 7.4.g. a clear decrease in the presence of large size droplets is detected (from a D90 value of 1.05 μm for the PHBV/PLA to 0.45 μm for the SEP). One feasible explanation for this observation could be a decrease in the droplet-droplet coalescence phenomenon; which is known to be responsible of the large size droplets in immiscible polymer blends [51]. This decrease can be related to an increase in the viscosity at low frequencies with the incorporation of the sepiolite, in agreement to the section above.

The WAXS diffractograms of the PHBV, PHBV/PLA blend and CPN are shown in Fig. 7.4.h. The PHBV diffractogram presents three main peaks at 2θ values of 13, 17, and 26° . The first two peaks can be associated with the (020) and (110) reflections of the orthorhombic lattice of the PHBV respectively. The most intense peak at $2\theta = 26^\circ$ corresponds to the (002) reflection of the boron nitride, which is present as a nucleating agent in the commercial grade used in this work. PLA is known to be amorphous, therefore no new peaks are detected in the diffractogram for the PHBV/PLA blend; and only a slight reduction in the relative intensity with respect to the amorphous halo is detected as a consequence of the dilution effect. No effect is also detected in the PHBV crystalline morphology with the addition of PLA accordingly to their immiscible nature.

Regarding the samples containing sepiolite, the most intense reflection of sepiolite (110) at $2\theta = 7.29^\circ$ (Fig. 7.4.h) is clearly visible. No changes were observed in the shape or position of this peak in the Sepiolite/PHBV/PLA nanocomposites, and only an increase in intensity with the increase in sepiolite content is revealed. No noticeable difference in the peak positions and relative intensities of PHBV/PLA blend peaks can be observed when the nanofibers are introduced; therefore, it can be concluded that the crystalline form of the PHBV is not affected by the addition of sepiolite.

For all the above stated it can be concluded that the sepiolite has proven to be an efficient nanofiller for enhancing the melt blending of PHBV and PLA.

7.3.3. Thermal characterization

TGA experiments were carried out to investigate the effect of the presence of the sepiolite nanofibers on the thermal stability of PHBV/PLA blends. Fig. 7.5 plots the mass loss and the derivative thermogravimetry (DTG) curves versus temperature for the neat PHBV and PHBV/PLA blends with and without sepiolite, while Table 1 summarizes the onset degradation temperature ($T_{5\%}$) and maximum degradation rate temperature (T_d) for all the samples studied.

The PHBV/PLA blends exhibits a two-step mass loss, with an onset degradation temperature ($T_{5\%}$) about 276 °C. The first step is characterized by a maximum mass loss rate (T_{d1}) at about at 289 °C and another one (T_{d2}) around 348 °C. The first one is related to the thermal degradation of PHBV, which consists of a single weight loss step between 240 and 320 °C corresponding to a random chain scission reaction [52]. The second step is a consequence of the thermal degradation of PLA that takes place by cleavage of bonds on the backbone to form cyclic oligomers, lactide and carbon monoxide as products [53]. The fact that the blends presented stages of degradation separately confirms once again their immiscibility.

The thermal decomposition process of the Sepiolite/PHBV/PLA nanocomposites shows a slight variation with respect to PHBV/PLA. Maximum degradation rate temperatures, T_{d1} corresponding to the PHBV remained almost unchanged (slight shifted of 1-2 °C with respect to PHBV), whereas T_{d2} shifted to higher temperatures with increasing sepiolite content. This increase varies from 6 to 13 degrees with the sepiolite content. These results are in agreement with the work reported by Mofokeng et al. [18], in which the authors attributed the increase to the shielding or barrier effect of the nanoparticles to heat and/or a retardation effect of the nanoparticles on the movement of free radicals and volatile degradation products.

In order to assess the effect of the addition of sepiolite in the crystallization behavior of PHBV in the PHBV/PLA blends, DSC measurements were performed to samples with and without sepiolite. Table 7.1 summarizes the main parameters obtained from the DSC experiments.

As shown in Table 7.1 the PHBV/PLA blend exhibits a mixed behavior corresponding to their blend ratio. In the blend, two peaks (a melting peak at 169.6 °C and a crystallization peak at 116.3 °C) can be related with the typical PHBV crystallization behavior (neat PHBV in Table 7.1).

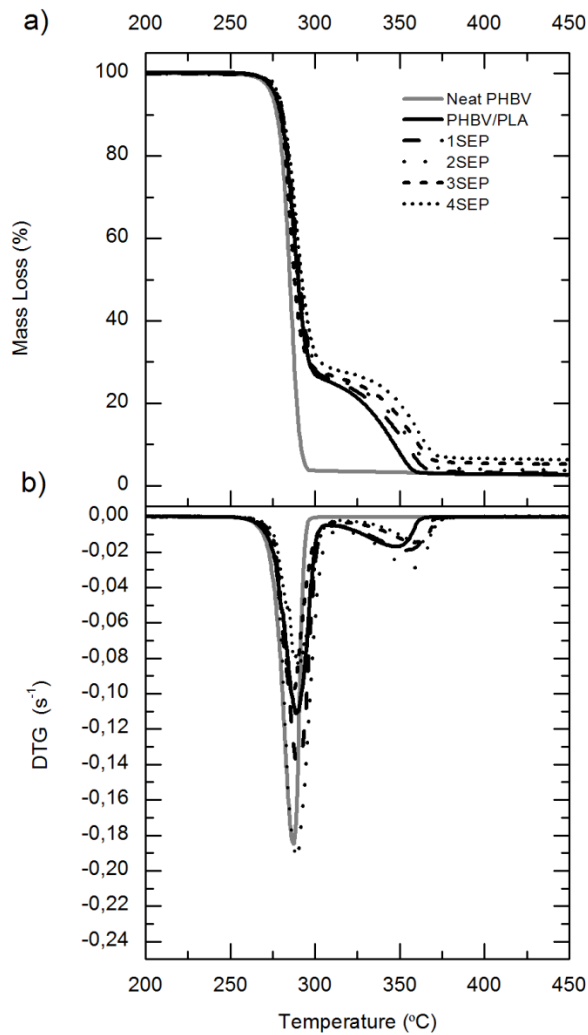


Fig. 7.5: a) Weight loss versus temperature as analysed by TGA and b) DTG curves of PHBV/PLA blend and sepiolite/PHBV/PLA nanocomposites

DSC results for the CPN show a slight shift towards higher temperatures of both the crystallization and the melting temperatures of PHBV for all the cases with the addition of sepiolite, with respect to that of PHBV/PLA blend. This increase, although irrelevant from the overall point of view, may be ascribed to a nucleating effect of sepiolite (in addition to the nucleating effect of the boron nitride incorporated in the commercial grade of PHBV). No relevant change has been detected in the total crystallinity of the PHBV phase.

Table 7.1: Thermal properties of sepiolite/PHBV/PLA nanocomposites: TGA, DSC and VST parameters

Sample	T _{5%} (°C)	T _{d1} (°C)	T _{d2} (°C)	ΔH _{m.PHBV} (J/g)	X _{c.PHBV} (%)	T _{m.PHBV} (°C)	T _{c.PHBV} (°C)	VST (°C)
Neat PHBV	274	288	-	-95	65	169.6	116.3	132.4
PHBV/PLA	276	289	348	-98	67	168.9	119.6	111.8
1SEP	277	288	354	-96	66	171.5	120.7	110.6
2SEP	278	290	358	-98	67	171.3	121.3	118.0
3SEP	278	290	359	-97	66	171.7	122.9	117.6
4SEP	278	290	361	-98	67	171.0	122.9	119.2

7.3.4. Mechanical properties

For the purpose of studying the effect of the addition of the sepiolite on the mechanical properties of PHBV/PLA blends, tensile tests to up-to-rupture were conducted on injected specimens for all the samples studied. Figures 7.6.a-7.6.c plot the evolution of tensile and flexural properties of the PHBV and PHBV/PLA blend with and without sepiolite as a function of the sepiolite content.

Significant increase in Young's modulus, tensile strength, flexural modulus and flexural strength were observed in PHBV/PLA blend, with respect to neat PHBV. This is the result of the difference in the mechanical performance of the PHBV with respect to the PLA. On the contrary, no change was observed in elongation at break with the addition of PLA. Therefore, the mechanical properties of PHBV/PLA blend are significantly affected with respect to those of PHBV in terms of stiffness and resistance. but not in elongation at break.

Regarding the Sepiolite/PHBV/PLA nanocomposites, no clear trend is observed in neither the elastic modulus nor maximum strength (in both tensile and flexural mode) when the nanofibers are incorporated to the PHBV/PLA blend. However, an interesting and unexpected increase in the elongation at break was found (Fig 7.6.b). This increase doesn't seem to depend on the sepiolite content; nevertheless, taking into consideration the low elongation at break of the pristine polymers, it is quite relevant (being close to a raise of 50% in the 3SEP with respect to PHBV/PLA). A possible theory for this behavior would lay upon the reduction of the average interparticle matrix ligament thickness as a result of the reduction in the droplet size, which is reported to have a critical role on the toughness of brittle semi-crystalline polymers [54].

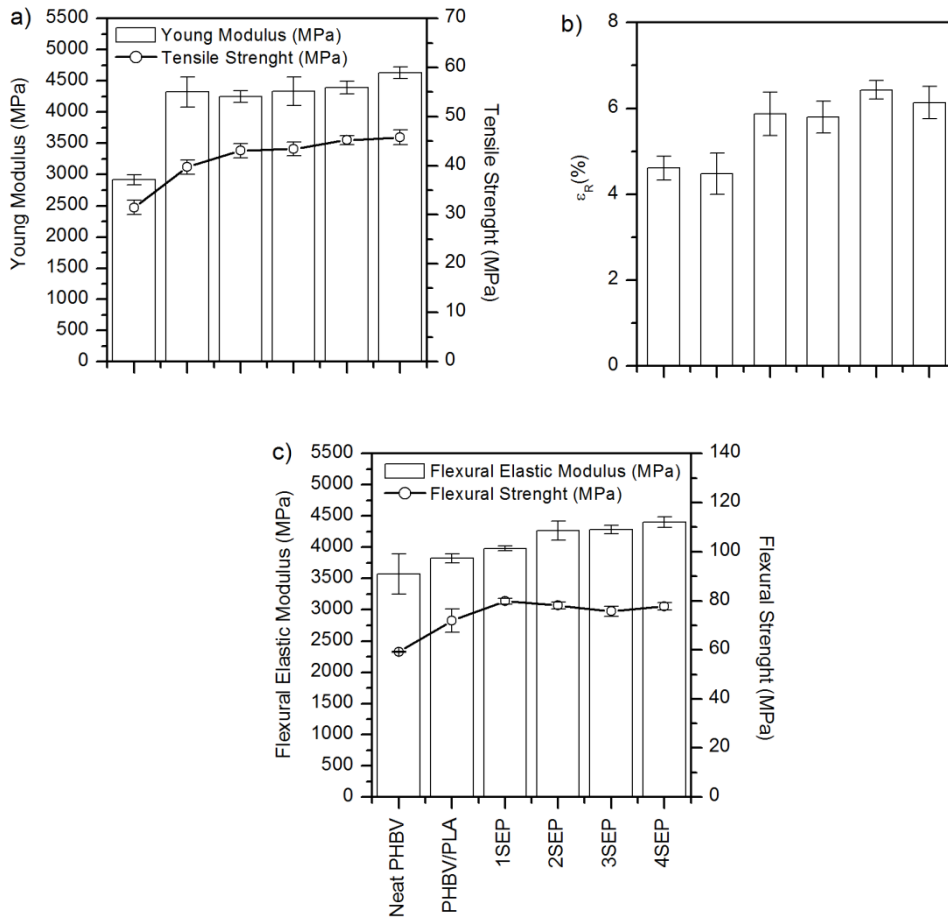


Fig. 7.6: a) Young modulus and tensile strength, b) elongation at break (ϵ_R) and c) flexural elastic modulus and flexural strength of neat PHBV, PHBV/PLA blend and sepiolite/PHBV/PLA nanocomposites

Changes with varying temperature in viscoelastic behavior, mechanical performance and miscibility of PHBV, PHBV/PLA and Sepiolite/PHBV/PLA nanocomposites have been assessed by means of DMTA. Representative curves of storage modulus (G') and tan delta (δ) versus temperature in the range of -10 to 140 °C are plotted in Fig. 7.7.

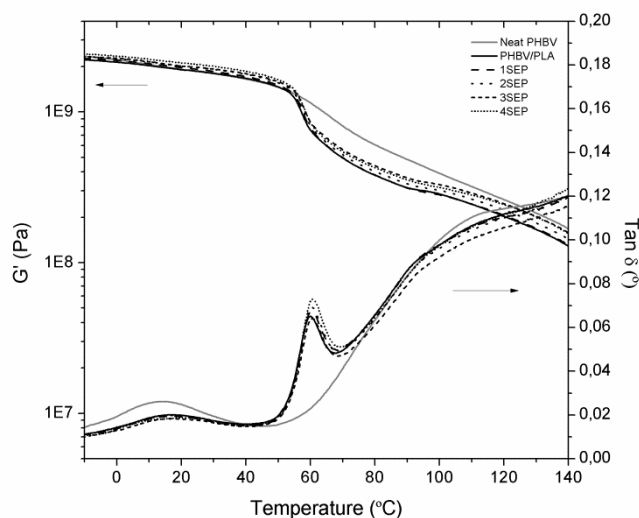


Fig. 7.7: a) Dynamic storage modulus (E') and b) delta tangent of PHBV, PHBV/PLA and sepiolite/PHBV/PLA/nanocomposites.

Tan delta (δ) curve of the neat PHBV present a single peak at temperature close to 16 °C. ascribed to the α -relaxation of the PHBV. The α -relaxation is a second order transition associated to the glass transition (T_g) in PHBV copolymers. The neat PLA, on the other hand, exhibits two events in the tan delta (δ) curve: a sharp peak at 56 °C and a change in the slope at 90.5 °C. The former event is related to the glass transition of the PLA, while the latter can be attributed to its cold crystallization. In the PHBV/PLA blend, an increase in the position of the glass transition of the PHBV is detected, while the PLA T_g and cold crystallization remains unaffected. The increase in the PHBV T_g can be explained by the hindrance imposed to the movement of the chains in the amorphous fraction of the PHBV by the presence of the solid PLA spheres. However, the fact that the T_g of the PLA does not undergo any change when blending with PLA is a prove of the immiscible behavior of the two biopolyesters.

When the sepiolite is incorporated to the polymer blends, no effect is observed in the PHBV peak; however, increase of 2.5 °C in the position of the α -relaxation peak and 5 °C the position of slope change ascribed to the cold crystallization of the PLA are detected. This modest increase can be attributed to the decrease in the PLA domain size. which confines the movement of the polymer chains.

7. Capítulo 5

The storage modulus curve of neat PHBV undergoes a gradual decrease when increasing the temperature only presenting a negligible change in the slope of the curve at the temperatures at which the α -relaxation takes place. Thus, the elastic response of the neat PHBV is governed by the crystalline phase. On the other hand, the pure PLA curve exhibits a severe drop in the elastic response when the glass transition takes place, as a result of its amorphous structure. However, a recovery of the storage modulus is observed with the cold crystallization event. The PHBV/PLA blend, present an elastic response where the contribution of the PHBV is more noticeable, however the effect of the glass transition and subsequent cold crystallization of the PLA phase is detected.

The incorporation of the sepiolite nanofibers resulted in an overall increase in the elastic response, as a consequence of a reinforcing effect of the fibers in the polymeric system. This effect, however, is more noticeable at temperatures above the T_g of the PLA, where the blend undergoes a decrease in the elastic behavior. This reinforcing effect could be attributed to a good polymer-clay mineral interaction which restricts the molecular motion of polymer chains, and is therefore dependent on the amount of nanofibers incorporated. Above the cold crystallization of the PLA, the decrease rate in storage modulus with the increasing temperature is lower for the CPN than for the pure PHBV or the PLA/PHBV sample. Thus, the addition of the sepiolite has led to an increase in the elastic behavior of the material at temperatures close to the processing window of the PHBV. This can potentially enhance the stability of the polymer sheet during heating prior to the thermoforming, decreasing the sagging as previously discussed.

7.3.5. Mechanical properties at high temperatures

The thermal resistance of the neat PHBV and PHBV/PLA blends with and without sepiolite was evaluated by means of the Vicat softening temperature (VST); data is shown in Table 7.1. VST represents an estimation of the material hardness under aggressive thermal conditions.

The VST decreases when PLA is added to the PHBV. due to the amorphous character of this biopolymer, which shows lower VST than PHBV. Nevertheless, the addition of the sepiolite resulted in a significant increase in VST values. Specifically, sepiolite contents over 1 phr raises VST values of the CPN with respect to that of PHBV/PLA by over 8 °C. This is in agreement to what was observed in DMTA experiments. and would confirm a decrease in creep behavior of the system.

For the purpose of studying the performance of the blends under processing conditions, for processes in which high speed forces are applied and high temperatures, such as thermoforming processes, hot tensile test were evaluated. Tensile tests up-to-rupture at 140 °C and crosshead rate of 500 mm/min were conducted on samples die-cut from approximately 200 µm thick films for all the samples studied. Figure 7.8 plots the evolution of tensile properties of the PHBV and PHBV/PLA blend with and without sepiolite as a function of the sepiolite content.

As expected by the DMTA results, the addition of the PLA to the PHBV resulted in a decrease in the rigidity and resistance of the blend at 140 °C, but an increase in the elongation at break is also achieved.

Regarding the Sepiolite/PHBV/PLA nanocomposites, a slightly increase in tensile modulus and tensile strength are observed when the nanofibers content is increased. This is in agreement with the increase in the elastic response of the system as detected by DMTA. On the other hand, the increase in the elongation at break achieved in the PHBV with the incorporation of the PLA, does not seem to be affected by the addition of the nanofibers, on the contrary a slightly increase is observed for the samples containing 1 and 4 phr of sepiolite.

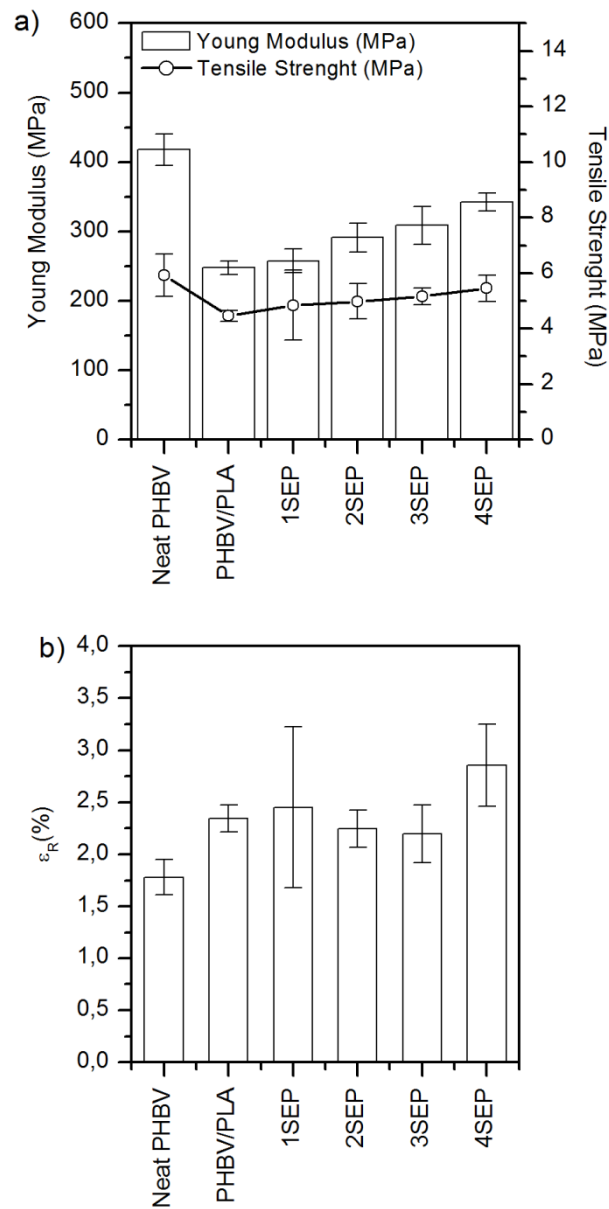


Fig. 7.8: a) Young modulus and tensile strength and b) elongation at break (ϵ_R) of neat PHBV, PHBV/PLA blend and sepiolite/PHBV/PLA nanocomposites at a crosshead rate of 500 mm/min and 140°C.

7.3.6. Barrier properties

One of the main advantages of the PHBV copolymer when compared to other biopolyesters such as PLA is their higher barrier performance particularly to oxygen. Therefore, the assessment of the barrier performance of the obtained systems in this work is of utmost interest. Table 7.2 gathers the oxygen and water permeability of all the samples studied in the present work.

Table 7.2: Barrier properties of sepiolite/PHBV/PLA nanocomposites

Sample	OP·10 ⁻¹⁹ (m ³ ·m·m ⁻² ·s ⁻¹ ·Pa ⁻¹)	WVP·10 ⁻¹⁵ (Kg·m·Pa ⁻¹ ·s ⁻¹ ·m ⁻²)	Water sorption (%)	OP decrease respect to PHBV/PLA (%)	WVP decrease respect to PHBV/PLA (%)
Neat PHBV	1.70±0.00	1.98±0.20	1.52±0.26	53	22
PHBV/PLA	3.64±0.12	2.55±0.60	1.56±0.18	-	-
1SEP	3.28±0.28	2.90±0.31	2.28±0.24	10	-14
2SEP	3.11±0.02	2.70±0.14	2.23±0.22	15	-6
3SEP	3.31±0.06	2.63±0.27	1.91±0.10	9	-3
4SEP	3.22±0.07	2.28±0.26	1.62±0.19	12	11

Blending PHBV with PLA resulted in a sharp increment in the oxygen permeability (O₂P) of the blend, as a result of both the intrinsic lower barrier to oxygen of the PLA and the blending process that can lead to preferential diffusion pathways. Nevertheless, the values of the so-obtained blends are still in the same order of magnitude as those of the neat PHBV. When sepiolite was incorporated to the system, a clear increase in the barrier performance to oxygen was seen. The permeability drop can be as high as 15% for the 4SEP when compared to the PHBV/PLA blend. There can be two reasons behind this positive effect of the addition of the nanofiller: the first one is an increase of the tortuosity in the diffusion pathway of the oxygen through the PHBV matrix (where the clay mineral is located). However, the diffusion of the oxygen across the polymer film is expected to take place mainly through the PLA phase, since the gas barrier O₂P of PLA is 2.2-2.8·10⁻¹⁸ m³·m·m⁻²·s⁻¹·Pa⁻¹, according to the literature [55,56], to be 13-16 times lower than that of the PHBV (Table 7.2). Hence, the key factor in the reduction of the oxygen permeation rate throughout the CPN when compared to that without sepiolite could be the reduction of the PLA droplet size, which

7. Capítulo 5

would impose an increase on the tortuosity of preferential the diffusion path through the PLA phase.

Water vapor permeability (WVP) by weight loss or gain measurements (ASTM E96) are common methods to determine the water barrier properties of materials. WVP of the blend show similar trend to what is observed in the O₂P, but in this case, the drop is less considerable. The addition of the sepiolite, however, resulted in a different behavior to that observed for the oxygen: at low sepiolite contents an increase in the WVP is registered when compared to PHBV/PLA sample, which reduces as the amount of clay mineral is incremented. WVP is very dependent on the water solubility in the polymer. This is undoubtedly the reason behind the decrease in the water barrier properties undergone by the blend when the clay mineral is incorporated. Sepiolite is known to be highly hygroscopic (traditionally used as absorbent [57]), thus boosting the water uptake of the system by 46% beyond the one without nanofibers with just 1 phr of clay mineral (Table 7.2). Russo *et al.* also reported the increase in water vapor permeability when investigated the effect of sepiolite in PLA CPN and also ascribed this behavior to the hydrophilicity of the filler [58]. Nevertheless, the increase in the diffusion coefficient of the CPN (due to the above-mentioned increase in the tortuosity of the diffusion pathways imposed by the sepiolite fibers and the decrease in the size of disperse phase entities) counteracts the increase in the water uptake as the sepiolite content is augmented. Thus, for the 4SEP sample. the overall WVP is lower than that of the blend without nanofiller.

For all the stated above, small quantities of well dispersed sepiolite could yield to an increase in the barrier performance of the PHBV/PLA blends. partially counteracting the decrease in the barrier performance undergone by the PHBV when blended in order to enhance the processability.

7.4. CONCLUSIONS

PHBV polymers are currently a most promising alternative to fossil fuel derived polymers; however, some drawbacks have yet to be overcome without compromising their good properties (particularly the oxygen barrier). Among them, the processability of the PHBV by thermoforming is a relevant issue that takes it apart from its use in some fields of application. In this work, for the first time, the use of sepiolite is investigated as an additive in melt blends of PHBV and PLA. The

incorporation of the nanofibers resulted in a better and more efficient blending of the two immiscible polymers, as derived from a more homogeneous morphology. Sepiolite did not alter the overall crystallinity or the thermal degradation kinetics of the blends. The mechanical tests at room temperature showed an unexpected increase in the elongation at break at room temperature of the CPN. Regarding the mechanical performance at high temperature, the reinforcing effect of the clay mineral, together with the better morphology achieved during blending resulted in higher elastic behavior of the CPN (as derived from both DMTA and tensile tests experiments). This trend may result in a better thermoformability of the final material, thus improving the processability of the biopolyester blend by decreasing the sagging of the polymer sheet and allowing a wider thermoforming window. Finally, the use of a well distributed low amount of sepiolite may counteract the oxygen and water vapor barrier drop undergone by the PHBV when blended with PLA. Overall, the sepiolite has proven to be a convenient additive to PHBV/PLA blends in order to enhance the applicability of these materials in the food packaging sector.

ACKNOWLEDGEMENTS

Financial support for this research from Ministerio de Economía y Competitividad (project AGL2015-63855-C2-2-R (MINECO/FEDER)) and Pla de Promoció de la Investigació de la Universitat Jaume I (PREDOC/2012/32 and E-2015-22) is gratefully acknowledged. The authors are also grateful to laboratory technicians of the Universitat Jaume I (Estefania Sánchez, Raquel Oliver and José Ortega) and all members of the Instituto de Tecnología de Materiales, ITM at Universitat Politècnica de València for their help in experimental support.

REFERENCES

- [1] J. Matusik, E. Stodolak, K. Bahranowski, Synthesis of polylactide/clay composites using structurally different kaolinites and kaolinite nanotubes, 51 (2011) 102–109. doi:10.1016/j.clay.2010.11.010.
- [2] N.F. Magalhães, K. Dahmouche, G.K. Lopes, C.T. Andrade, Using an organically-modified montmorillonite to compatibilize a biodegradable blend, Appl. Clay Sci. 72 (2013) 1–8. doi:10.1016/j.clay.2012.12.008.
- [3] A. Botana, M. Mollo, P. Eisenberg, R.M. Torres Sanchez, Effect of modified montmorillonite on biodegradable PHB nanocomposites, 47 (2010) 263–270. doi:10.1016/j.clay.2009.11.001.

- [4] S. Khanna, A.K. Srivastava, Recent advances in microbial polyhydroxyalkanoates, *Process Biochem.* 40 (2005) 607–619. doi:10.1016/j.procbio.2004.01.053.
- [5] L.S. Serafim, P.C. Lemos, R. Oliveira, M.A.M. Reis, Optimization of polyhydroxybutyrate production by mixed cultures submitted to aerobic dynamic feeding conditions., *Biotechnol. Bioeng.* 87 (2004) 145–60. doi:10.1002/bit.20085.
- [6] M.A.M. Reis, L.S. Serafim, P.C. Lemos, A.M. Ramos, F.R. Aguiar, M.C.M. Van Loosdrecht, Production of polyhydroxyalkanoates by mixed microbial cultures., *Bioprocess Biosyst. Eng.* 25 (2003) 377–85. doi:10.1007/s00449-003-0322-4.
- [7] B.H.A. Rehm, Polyester synthases: natural catalysts for plastics., *Biochem. J.* 376 (2003) 15–33. doi:10.1042/BJ20031254.
- [8] D. Cava, E. Gimenez, R. Gavara, J.M. Lagaron, Comparative Performance and Barrier Properties of Biodegradable Thermoplastics and Nanobiocomposites versus PET for Food Packaging Applications, *J. Plast. Film Sheeting.* 22 (2006) 265–274. <http://www.scopus.com/inward/record.url?eid=2-s2.0-33845203640&partnerID=tZotx3y1> (accessed January 14, 2015).
- [9] Y.-M. Corre, S. Bruzaud, J.-L. Audic, Y. Grohens, Morphology and functional properties of commercial polyhydroxyalkanoates: A comprehensive and comparative study, *Polym. Test.* 31 (2012) 226–235. doi:10.1016/j.polymertesting.2011.11.002.
- [10] E. Bugnicourt, Polyhydroxyalkanoate (PHA): Review of synthesis, characteristics, processing and potential applications in packaging, *Express Polym. Lett.* 8 (2014) 791–808. doi:10.3144/expresspolymlett.2014.82.
- [11] M. Kunioka, A. Tamaki, Y. Doi, Crystalline and thermal properties of bacterial copolyesters: poly(3-hydroxybutyrate-co-3-hydroxyvalerate) and poly(3-hydroxybutyrate-co-4-hydroxybutyrate), *Macromolecules.* 22 (1989) 694–697. doi:10.1021/ma00192a031.
- [12] E. Giménez, J. Lagaron, R. Gavara, L. Cabedo, J.J. Saura, Study of the thermoformability of ethylene - vinyl alcohol copolymer based barrier blends of interest in food packaging applications, *J. Appl. Polym. Sci.* 96 (2004) 3851 – 3855. <http://onlinelibrary.wiley.com/doi/10.1002/app.13584/full> (accessed December 9, 2014).
- [13] E. Giménez, J.M. Lagarón, M.L. MasPOCH, L. Cabedo, J.J. Saura, Uniaxial tensile behavior and thermoforming characteristics of high barrier EVOH-based blends of interest in food packaging, *Polym. Eng. Sci.* 44 (2004) 598–608. doi:10.1002/pen.20054.
- [14] R.M. Rasal, A. V. Janorkar, D.E. Hirt, Poly(lactic acid) modifications, *Prog. Polym. Sci.* 35 (2010) 338–356. doi:10.1016/j.progpolymsci.2009.12.003.
- [15] J. Cailloux, O.O. Santana, E. Franco-Urquiza, J.J. Bou, F. Carrasco, J. Gámez-Pérez, M.L. MasPOCH, Sheets of branched poly(lactic acid) obtained by one step reactive extrusion calendaring process: Melt rheology analysis, *Express Polym. Lett.* 7 (2012) 304–318. doi:10.3144/expresspolymlett.2013.27.
- [16] I. Zembouai, S. Bruzaud, M. Kaci, A. Benhamida, Y. Corre, Y. Grohens, J.-M. Lopez-Cuesta, Synergistic Effect of Compatibilizer and Cloisite 30B on the Functional Properties of Poly (3-hydroxybutyrate- co -3-hydroxyvalerate)/ Polylactide Blends, *Polym. Eng. Sci.* 54 (2014) 2239–2251. doi:10.1002/pen.
- [17] J.P. Mofokeng, a. S. Luyt, Dynamic mechanical properties of PLA/PHBV, PLA/PCL, PHBV/PCL blends and their nanocomposites with TiO₂ as nanofiller, *Thermochim. Acta.* 613 (2015) 41–53. doi:10.1016/j.tca.2015.05.019.

- [18] J.P. Mofokeng, A.S. Luyt, Morphology and thermal degradation studies of melt-mixed PLA/PHBV biodegradable polymer blend nanocomposites with TiO₂ as filler, *J. Appl. Polym. Sci.* 132 (2015) n/a-n/a. doi:10.1002/app.42138.
- [19] H. Zhao, Z. Cui, X. Wang, L.-S. Turng, X. Peng, Processing and characterization of solid and microcellular poly(lactic acid)/polyhydroxybutyrate-valerate (PLA/PHBV) blends and PLA/PHBV/Clay nanocomposites, *Compos. Part B Eng.* 51 (2013) 79–91. <http://www.scopus.com/inward/record.url?eid=2-s2.0-84877837110&partnerID=tZ0tx3y1> (accessed February 15, 2014).
- [20] M.J. John, Biopolymer blends based on polylactic acid and polyhydroxy butyrate-co-valerate: Effect of clay on mechanical and thermal properties, *Polym. Compos.* (2014). doi:10.1002/pc.23114.
- [21] A. Monfared, A. Jalali-Arani, Morphology and rheology of (styrene-butadiene rubber/acrylonitrile-butadiene rubber) blends filled with organoclay: The effect of nanoparticle localization, *Appl. Clay Sci.* 108 (2015) 1–11. doi:10.1016/j.clay.2015.02.012.
- [22] J. Huitric, J. Ville, P. Médéric, M. Moan, T. Aubry, Rheological, morphological and structural properties of PE/PA/nanoclay ternary blends: Effect of clay weight fraction, *J. Rheol. (N. Y. N. Y.)* 53 (2009) 1101. doi:10.1122/1.3153551.
- [23] J. Gonzalez-Ausejo, E.L. Sanchez-Safont, J.M. Lagarón, R. Balart, L. Cabedo, J. Gamez-Perez, Compatibilization of PHBV/PLA blends with diisocyanates, *J. Appl. Polym. Sci.* (n.d.) Accepted.
- [24] K.K. Yang, X.L. Wang, Y.Z. Wang, Progress in nanocomposite of biodegradable polymer, *J. Ind. Eng. Chem.* 13 (2007) 485–500. <http://www.scopus.com/inward/record.url?eid=2-s2.0-34547635623&partnerID=40&md5=5e8f39b5cc9bd0cc58014645a6c02a49>.
- [25] N. Bitinis, E. Fortunati, R. Verdejo, I. Armentano, L. Torre, J.M. Kenny, M.Á. López-Manchado, Thermal and bio-disintegration properties of poly(lactic acid)/natural rubber/organoclay nanocomposites, *Appl. Clay Sci.* 93–94 (2014) 78–84. doi:10.1016/j.clay.2014.02.024.
- [26] B.S. Bouakaz, I. Pillin, A. Habi, Y. Grohens, Synergy between fillers in organomontmorillonite/graphene–PLA nanocomposites, *Appl. Clay Sci.* 116–117 (2015) 69–77. doi:10.1016/j.clay.2015.08.017.
- [27] J. González-Ausejo, E. Sánchez-Safont, J. Gámez-Pérez, L. Cabedo, On the use of tris(nonylphenyl) phosphite as a chain extender in melt-blended poly(hydroxybutyrate-co-hydroxyvalerate)/clay nanocomposites: Morphology, thermal stability, and mechanical properties, *J. Appl. Polym. Sci.* 133 (2016). doi:10.1002/app.42390.
- [28] J.M. Lagarón, L. Cabedo, Polylactide (PLA)/clay nano-biocomposites, *RSC Polym. Chem. Ser.* 2015–Janua (2015) 215–224. <http://www.scopus.com/inward/record.url?eid=2-s2.0-84937438672&partnerID=tZ0tx3y1>.
- [29] R. Neppalli, V. Causin, C. Marega, M. Modesti, R. Adhikari, S. Scholtyssek, S.S. Ray, A. Marigo, The effect of different clays on the structure, morphology and degradation behavior of poly(lactic acid), *Appl. Clay Sci.* 87 (2014) 278–284. doi:10.1016/j.clay.2013.11.029.
- [30] J. Wu, X. Zou, B. Jing, W. Dai, Effect of sepiolite on the crystallization behavior of biodegradable poly(lactic acid) as an efficient nucleating agent, *Polym. Eng. Sci.* 55 (2015) 1104–1112. doi:10.1002/pen.23981.
- [31] A. Nuzzo, E. Bilotti, T. Peijs, D. Acierno, G. Filippone, Nanoparticle-induced co-continuity in immiscible polymer blends – A comparative study on bio-based PLA-PA11 blends filled with organoclay, sepiolite, and carbon nanotubes, *Polymer (Guildf.)* 55 (2014) 4908–4919. doi:10.1016/j.polymer.2014.07.036.

- [32] M.D. Samper-Madrigal, O. Fenollar, F. Dominici, R. Balart, J.M. Kenny, The effect of sepiolite on the compatibilization of polyethylene–thermoplastic starch blends for environmentally friendly films, 50 (2014) 863–872. doi:10.1007/s10853-014-8647-8.
- [33] J.B. Olivato, J. Marini, E. Pollet, F. Yamashita, M.V.E. Grossmann, L. Avérous, Elaboration, morphology and properties of starch/polyester nano-biocomposites based on sepiolite clay, 118 (2015) 250–256. doi:10.1016/j.carbpol.2014.11.014.
- [34] H.E. Miltner, N. Watzeels, N.A. Gotzen, A.L. Goffin, E. Duquesne, S. Benali, B. Ruelle, S. Peeterbroeck, P. Dubois, B. Goderis, G. Van Assche, H. Rahier, B. Van Mele, The effect of nano-sized filler particles on the crystalline-amorphous interphase and thermal properties in polyester nanocomposites, 53 (2012) 1494–1506. doi:10.1016/j.polymer.2012.01.047.
- [35] M.F. Brigatti, E. Galan, B.K.G. Theng, Chapter 2 Structures and Mineralogy of Clay Minerals, in: *Dev. Clay Sci.*, 2006: pp. 19–86. doi:10.1016/S1572-4352(05)01002-0.
- [36] T.S. Daitx, L.N. Carli, J.S. Crespo, R.S. Mauler, Effects of the organic modification of different clay minerals and their application in biodegradable polymer nanocomposites of PHBV, *Appl. Clay Sci.* 115 (2015) 157–164. doi:10.1016/j.clay.2015.07.038.
- [37] K. Fukushima, Properties of poly(lactic acid) nanocomposites based on montmorillonite, sepiolite and zirconium phosphonate, *Express Polym. Lett.* 6 (2012) 914–926. doi:10.3144/expresspolymlett.2012.97.
- [38] K. Fukushima, D. Tabuani, G. Camino, Poly(lactic acid)/clay nanocomposites: effect of nature and content of clay on morphology, thermal and thermo-mechanical properties, *Mater. Sci. Eng. C.* 32 (2012) 1790–1795. doi:10.1016/j.msec.2012.04.047.
- [39] N. Moazeni, Z. Mohamad, N. Dehbari, Study of silane treatment on poly-lactic acid(PLA)/sepiolite nanocomposite thin films, *J. Appl. Polym. Sci.* 132 (2015) n/a-n/a. doi:10.1002/app.41428.
- [40] M. Sabzi, L. Jiang, M. Atai, I. Ghasemi, PLA/sepiolite and PLA/calcium carbonate nanocomposites: A comparison study, *J. Appl. Polym. Sci.* 129 (2013) 1734–1744. doi:10.1002/app.38866.
- [41] K. Fukushima, D. Tabuani, C. Abbate, M. Arena, L. Ferreri, Effect of sepiolite on the biodegradation of poly(lactic acid) and polycaprolactone, *Polym. Degrad. Stab.* 95 (2010) 2049–2056. doi:10.1016/j.polymdegradstab.2010.07.004.
- [42] M. Liu, M. Pu, H. Ma, Preparation, structure and thermal properties of polylactide/sepiolite nanocomposites with and without organic modifiers, *Compos. Sci. Technol.* 72 (2012) 1508–1514. doi:10.1016/j.compscitech.2012.05.017.
- [43] K. Nuñez, C. Rosales, R. Perera, N. Villarreal, J.M. Pastor, Nanocomposites of PLA/PP blends based on sepiolite, *Polym. Bull.* 67 (2011) 1991–2016. doi:10.1007/s00289-011-0616-7.
- [44] K. Nuñez, C. Rosales, R. Perera, N. Villarreal, J.M. Pastor, Poly(lactic acid)/low-density polyethylene blends and its nanocomposites based on sepiolite, *Polym. Eng. Sci.* 52 (2012) 988–1004. doi:10.1002/pen.22168.
- [45] H. Alata, T. Aoyama, Y. Inoue, Effect of Aging on the Mechanical Properties of Poly(3-hydroxybutyrate- co -3-hydroxyhexanoate), *Macromolecules.* 40 (2007) 4546–4551. doi:10.1021/ma070418i.
- [46] M.D. Sanchez-Garcia, J.M. Lagaron, Novel clay-based nanobiocomposites of biopolyesters with synergistic barrier to UV light, gas, and vapour, *J. Appl. Polym. Sci.* 118 (2010) 188–199. doi:10.1002/app.31986.
- [47] M. Darder, M. López-Blanco, P. Aranda, A.J. Aznar, J. Bravo, E. Ruiz-Hitzky, Microfibrillar Chitosan–Sepiolite Nanocomposites, *Chem. Mater.* 18 (2006) 1602–1610. doi:10.1021/cm052364z.

- [48] T. Gerard, T. Budtova, Morphology and molten-state rheology of polylactide and polyhydroxyalkanoate blends, *Eur. Polym. J.* 48 (2012) 1110–1117. doi:10.1016/j.eurpolymj.2012.03.015.
- [49] K. Li, J. Peng, L.-S. Turng, H.-X. Huang, Dynamic rheological behavior and morphology of polylactide/poly(butylene adipate-co-terephthalate) blends with various composition ratios, *Adv. Polym. Technol.* 30 (2011) 150–157. doi:10.1002/adv.20212.
- [50] B. Wang, T. Wan, W. Zeng, Dynamic rheology and morphology of polylactide/organic montmorillonite nanocomposites, *J. Appl. Polym. Sci.* 121 (2011) 1032–1039. doi:10.1002/app.33717.
- [51] A. Martínez-Abad, J. González-Ausejo, J.M. Lagarón, L. Cabedo, Biodegradable poly(3-hydroxybutyrate-co-3-hydroxyvalerate)/thermoplastic polyurethane blends with improved mechanical and barrier performance, *Polym. Degrad. Stab.* 132 (2016) 52–61. doi:10.1016/j.polymdegradstab.2016.03.039.
- [52] N. Grassie, E.J. Murray, P.A. Holmes, The thermal degradation of poly(-D)-β-hydroxybutyric acid: Part 3-The reaction mechanism, *Polym. Degrad. Stab.* 6 (1984) 127–134. <http://www.scopus.com/inward/record.url?eid=2-s2.0-0021208453&partnerID=tZOtx3y1>.
- [53] F.D. Kopinke, K. Mackenzie, Mechanistic aspects of the thermal degradation of poly(lactic acid) and poly(β-hydroxybutyric acid), *J. Anal. Appl. Pyrolysis.* 40–41 (1997) 43–53. <http://www.scopus.com/inward/record.url?eid=2-s2.0-0031144057&partnerID=tZOtx3y1>.
- [54] J.A. van Dommelen, W.A. Brekelmans, F.P. Baaijens, Micromechanical modeling of particle-toughening of polymers by locally induced anisotropy, *Mech. Mater.* 35 (2003) 845–863. doi:10.1016/S0167-6636(02)00307-1.
- [55] J.M. Lagaron, Novel Clay-Based Nanobiocomposites of Biopolyesters with Synergistic Barrier to UV Light, Gas, and Vapour, (2010). doi:10.1002/app.
- [56] M.J. Fabra, A. Lopez-Rubio, J.M. Lagaron, Nanostructured interlayers of zein to improve the barrier properties of high barrier polyhydroxyalkanoates and other polyesters, *J. Food Eng.* 127 (2014) 1–9. doi:10.1016/j.jfoodeng.2013.11.022.
- [57] E. Galan, Properties and applications of palygorskite-sepiolite clays, *Clay Miner.* 31 (1996) 443–453. <http://www.scopus.com/inward/record.url?eid=2-s2.0-0030375877&partnerID=tZOtx3y1>.
- [58] P. Russo, S. Cammarano, E. Bilotti, T. Peijs, P. Cerruti, D. Acierno, Physical properties of poly lactic acid/clay nanocomposite films: Effect of filler content and annealing treatment, *J. Appl. Polym. Sci.* 131 (2014) n/a-n/a. doi:10.1002/app.39798.

8. Discusión general

8. Discusión general

Este trabajo busca contrarrestar las principales limitaciones técnicas que plantea el copolímero PHBV para su aplicabilidad en el sector del envasado. Utilizando el PHBV como material base comercial se han desarrollados nuevas formulaciones biodegradables por adición de una segunda fase con el fin de modular su comportamiento. Se ha estudiado la adición de materiales cerámicos (C30B, HNT), un elastómero (TPU) o un polímero rígido (PLA), así como la mezcla ternaria de PHBV con PLA y sepiolita. Todas las composiciones se han obtenido mediante mezclado en fundido en equipos convencionales de procesamiento de polímeros termoplásticos haciendo uso, en ocasiones, de agentes reactivos compatibilizantes.

Al introducir la segunda fase se obtienen distintos resultados en función de la naturaleza de la misma. A continuación, se compara la influencia de la naturaleza de los materiales adicionados sobre la estabilidad térmica, el comportamiento mecánico, el comportamiento a barrera, la biodegradabilidad y la procesabilidad por termoconformado de las composiciones estudiadas basadas en PHBV.

a) Estabilidad térmica

En el procesamiento de envases, los materiales suelen ser sometidos a distintos ciclos térmicos, como son, por ejemplo, el procesamiento de láminas, el estirado, el termoconformado o el sellado en caliente, entre otros. En estas etapas puede producirse cierta degradación térmica local, siendo los productos de tal degradación susceptibles de migrar hacia el contenido del envase.

Las composiciones de estudio en las que se ha adicionado una segunda fase cerámica y un extensor de cadena han demostrado mejorar la estabilidad térmica del PHBV, por lo que estas composiciones son susceptibles de ser utilizadas para este tipo de requerimientos de procesamiento. Concretamente, la adición de HNT, TNPP o la adición conjunta de C30B y TNPP revela una mejora en la resistencia a la degradación térmica. En cuanto a las mezclas en las que ha sido adicionada una fase elastomérica (TPU) o una fase polimérica rígida (PLA), los resultados muestran que el efecto de la adición de la segunda fase sobre la estabilidad térmica del PHBV es despreciable. Esto es debido a la falta de interacción entre ambas fases poliméricas, de modo que la presencia de la segunda fase no altera la cinética de degradación del PHBV. En el caso de las muestras PHBV/PLA

8. Discusión general

compatibilizadas con los diisocianatos, aun indicándose una mejora en la adhesión interfacial entre ambas fases poliméricas, la morfología matriz-gota que poseen estas mezclas resulta en un proceso de degradación térmica de las fases poliméricas de manera independiente. En cuanto a la adición de fase cerámica, a través de la sepiolita, sobre las mezclas PHBV/PLA (fase secundaria polimérica rígida) se observa que la degradación del PLA se ve ralentizada y la del PHBV no se ve afectada por la adición de las arcillas. Esto es debido al efecto barrera de las nanopartículas de sepiolita que dificultan el movimiento de los radicales libres y productos de degradación volátiles del PLA.

b) Comportamiento mecánico

Una de las funciones primordiales de los envases es la protección del producto que contienen frente a contaminaciones externas y el deterioro. En este sentido los envases deben poseer unas propiedades mecánicas y barrera adecuadas en función del uso y del contenido. De acuerdo con la bibliografía consultada y mencionada en el marco teórico de este documento, el PHBV posee un comportamiento mecánico equilibrado en términos de rigidez y resistencia similares a la del PP. Sin embargo, el PHBV posee una alta fragilidad que limita su aplicabilidad en el sector del envasado, especialmente para aquellas aplicaciones en las que se requiere cierta tenacidad o ductilidad del envase.

De entre las composiciones de estudio, la adición de arcillas, resultan en un marcado incremento de la rigidez y la resistencia mecánica a temperatura ambiente, debido al efecto de refuerzo mecánico logrado con la adición de una fase nanométrica. Estos resultados sugieren que la adición de materiales nanométricos podría paliar el problema de falta de estabilidad termomecánica del PHBV a temperaturas superiores al ambiente.

En el caso de la adición de la fase polimérica rígida, se observa distinto comportamiento mecánico a temperatura ambiente en función de la técnica de obtención de la muestra. Es decir, las mezclas PHBV/PLA compatibilizadas y sin compatibilizar desarrolladas mediante mezclador interno y posterior prensado desde el fundido no muestran variación apreciable en las propiedades mecánicas con respecto al PHBV (Capítulo 3). Sin embargo, el estudio realizado con probetas inyectadas a partir de granza obtenida mediante extrusión de doble husillo muestra un aumento considerable de la rigidez y la resistencia del material con respecto al PHBV (Capítulo 5). Estas diferencias observadas en función de la técnica de obtención de la muestra son debidas a las

diferencias morfológicas de las muestras tras el procesado. El tamaño de los dominios de PLA en las muestras obtenidas por extrusión de doble husillo y posterior inyección es de $0.63 \mu\text{m}$, frente a $1.15 \mu\text{m}$, en el caso de uso de mezclador interno y posterior prensado desde el fundido. Al tener el PLA una mayor rigidez y mostrar las entidades de PLA un menor tamaño y una mejor distribución en la matriz de PHBV actúan como refuerzo mecánico de la matriz de PHBV.

En cuanto a la introducción de sepiolita en el sistema PHBV/PLA, los nanocompuestos inyectados muestran un incremento considerable en la elongación a rotura. Este hecho se debe a la reducción de la longitud media del ligamento de la matriz entre dominios de la fase dispersa, como resultado de la reducción en el tamaño de estos dominios esféricos de PLA en presencia de sepiolita.

En este trabajo, se ha explorado el uso de un modificador, una segunda fase elastomérica (TPU). Las muestras con TPU son aquellas que mayor incremento de la ductilidad y la tenacidad han resultado de todas las composiciones estudiadas (Capítulo 2). Se observa un incremento considerable de la elongación a rotura para contenidos de TPU superiores al 30% en peso. Sin embargo, como cabría esperar, este aumento de la ductilidad se consigue a expensas de generar una reducción de rigidez y resistencia del material.

Dados los resultados mecánicos a temperatura ambiente obtenidos en las distintas investigaciones desarrolladas y analizadas, las composiciones con una segunda fase cerámica o polimérica rígida son susceptibles de ser utilizadas para envases que requieran una mayor rigidez y resistencia. En el caso de requerirse envases con mayor ductilidad las composiciones estudiadas con TPU parecen ser prometedoras.

Ciertas aplicaciones de los envases requieren de preservar el contenido a temperaturas superiores a la temperatura ambiente. En tales casos, se deben garantizar las propiedades mecánicas a las condiciones de exposición. En el capítulo 3, estudiando las mezclas PHBV/PLA se muestra cómo la adición de PLA produce la caída del módulo de almacenamiento para temperaturas superiores a la T_g del PLA, lo que se podría traducir en una pérdida de la consistencia mecánica del envase debido al reblandecimiento de la fase dispersa. Este hecho haría que, a pesar de que la adición del PLA mejora la aplicabilidad del material base en aplicaciones donde el envase se produzca mediante termoconformado (como se discutirá más adelante), la presencia del mismo pueda condicionar su empleabilidad cuando este envase vaya a estar sometido a temperaturas superiores a la ambiente.

8. Discusión general

Este comportamiento se ha observado tanto en las mezclas PHBV/PLA puras como en las composiciones compatibilizadas con diisocianatos.

Este hecho motivó la introducción de un tercer componente en el sistema: una fase cerámica. La fase cerámica nanométrica genera un ligero aumento de la rigidez y la ductilidad a elevadas temperaturas (ensayos de tracción a elevadas temperaturas), además de mantener una temperatura de reblandecimiento Vicat en valores cercano a los 120 °C. Por consiguiente, las composiciones en las que se adicionan conjuntamente la fase polimérica rígida y la fase cerámica parecen prometedoras para aplicaciones en las que elevadas temperaturas son requeridas.

c) Comportamiento a barrera

Controlar el transporte de materia a través del envase es vital para el envasado de alimentos, bebidas, cosméticos, productos farmacéuticos, de limpieza, agroquímicos, etc. El PHBV tiene como principal ventaja en este campo su excelente capacidad barrera, muy superior a la de otros biopolíesteres similares. Es precisamente este aspecto el que hace del PHBV un material de alto interés en la actualidad, por consiguiente, mantener su comportamiento barrera se ha buscado en el presente trabajo como una condición prioritaria. Así, la premisa del presente trabajo era generar formulaciones que mejoren la aplicabilidad del PHBV para la industria del envasado sin afectar en exceso su comportamiento barrera ni su biodegradabilidad.

El efecto sobre la permeabilidad con la adición de una segunda fase elastomérica ha sido estudiado en función del contenido en TPU. Se ha observado que la adición de contenidos de hasta el 30% en peso de TPU no afecta significativamente a las propiedades barrera a vapor de agua y limoneno del PHBV.

En el presente estudio, la incorporación de 25% en peso de PLA da como resultado una estructura inmisible con el PLA disperso en la matriz de PHBV y que conlleva una caída en el rendimiento a barrera a oxígeno y vapor de agua en 89 y 86%, respectivamente. Sin embargo, los valores obtenidos para las mezclas compatibilizadas y no compatibilizadas, todavía se encuentran en el mismo orden de magnitud que las del PHBV puro. Un ligero incremento en las propiedades barrera es observado cuando la sepiolita es adicionada a las mezclas PHBV/PLA. En este caso existen dos efectos simultáneos, por un lado, la adición de una fase de tamaño nanométrico incrementa la

tortuosidad de la trayectoria de difusión de gases y vapores a través de la matriz de PHBV. Por otro lado, la adición de sepiolita logra una reducción considerable del tamaño de los dominios dispersos de PLA, lo que a su vez incrementa la tortuosidad en la trayectoria preferencial de difusión a través de la fase de PLA.

d) Biodegradabilidad

Como consecuencia de la vasta cantidad de materiales de envase que se producen, así como del gran impacto medioambiental asociado a sus residuos, la industria del envasado considera un valor añadido adicional la biodegradabilidad de los envases al finalizar la vida útil de estos.

El mantenimiento de la biodegradabilidad intrínseca del PHBV, debido a su síntesis biológica y a sus enlaces éster fácilmente hidrolizables, ha prevalecido a la hora de seleccionar la composición y el contenido de los aditivos utilizados como segunda fase en este estudio, así como los compatibilizantes y el extensor de cadena usados. En este trabajo, la desintegrabilidad en condiciones controladas de compostaje según la norma UNE EN ISO 20200 ha sido seleccionada como el indicador de la biodegradabilidad en compostaje de los materiales. La utilización de esta norma ha sido ampliamente aceptada por la comunidad científica para estudiar el comportamiento de los materiales en condiciones de compostaje a escala de laboratorio, como se puede contrastar por el gran número de publicaciones que hacen uso de ésta en la última década.

Todas las composiciones estudiadas han mostrado la desintegración completa según la norma citada para tiempos comprendidos entre 31 y 36 días, a excepción de la muestra con un contenido del 50% en peso de TPU. El ensayo de compostaje de las mezclas PHBV/TPU fue desarrollado para un máximo de 41 días. En este periodo la muestra con un contenido de TPU del 50% en peso alcanzó una desintegración del 65%. Cabe remarcar que la tendencia que muestra la curva permite estimar un grado de desintegración mayor si se consideran períodos de compostaje más largos y, en todo caso, inferiores a los 6 meses que establece como límite la norma.

8. Discusión general

e) Procesabilidad por termoconformado

Un gran número de envases rígidos se obtienen mediante termoconformado de láminas termoplásticas delgadas, como son, por ejemplo, las bandejas, las carcasas, las cajas o los blísteres. El PHBV presenta una estrecha ventana de procesamiento derivada de su alta cristalinidad, lo que limita la idoneidad del PHBV para ser utilizado como materia prima para el diseño de productos termoconformados.

En este trabajo, el estudio de la procesabilidad del PHBV ha sido abarcado en distintos capítulos. En el caso de las mezclas PHBV/PLA se estudia la procesabilidad por termoconformado del PHBV haciendo uso del análisis reológico y dinamo-mecánico, estimando las variaciones en la ventana de procesamiento de las mezclas obtenidas al ser adicionada la fase secundaria polimérica rígida y su compatibilización con diisocianatos o con la adición de sepiolita a las mezclas. En ambos estudios se concluye que la procesabilidad del PHBV puede ser favorecida mediante el mezclado del PHBV con PLA y la compatibilización de la mezcla mediante diisocianatos o en presencia de sepiolita. En el caso concreto del estudio de compatibilización de la mezcla PHBV con diisocianatos se detecta un incremento de la ventana de procesamiento para termoconformado (aumentando el rango térmico y disminuyendo las temperaturas a las que se logra un buen termoconformado). Sin embargo, en el caso de adición de la fase cerámica y la fase polimérica rígida el incremento de la ventana de procesamiento para el conformado por termoconformado se vería incrementada únicamente hacia mayores temperaturas.

En el caso de las mezclas PHBV/PLA compatibilizadas, se han realizado ensayos de termoconformado variando la temperatura de calentamiento de la lámina con el fin de determinar la ventana de termoconformado del material. Los resultados muestran el incremento de la ventana de termoconformado del PHBV cuando las mezclas PHBV/PLA son compatibilizadas con dos de los diisocianatos, polyHMDI y PDI. Además, los prototipos termoconformados obtenidos con estas composiciones reproducen fielmente el molde y resultan en una distribución de espesores homogénea.

Por consiguiente, las mezclas estudiadas de PHBV con PLA incrementan la aplicabilidad del PHBV como materia prima para el diseño de productos termoconformados.

9. Conclusiones

9. Conclusiones

Del análisis de las investigaciones realizadas en este trabajo se puede extraer la siguiente conclusión general:

Es posible mejorar la aplicabilidad del PHBV al sector del envasado mediante la obtención de composiciones a partir de la introducción de una segunda fase polimérica y/o cerámica. Esta mejora se deriva del aumento de la estabilidad térmica del material base, así como de su ductilidad y su procesabilidad mediante termoconformado, mientras se mantienen sus excelentes propiedades barrera y su rápida biodegradabilidad. Cabe destacar que para la obtención de estas composiciones se han empleado materiales comerciales y se han aplicado técnicas de procesado convencionales de termoplásticos, lo que asegura su viabilidad industrial en el sector del envasado.

Las conclusiones parciales de cada uno de los estudios realizados se describen a continuación:

- La adición de un extensor de cadena adecuado (tris(nonilfenil) fosfito, (TNPP)), se ha revelado como una solución adecuada para mejorar la estabilidad térmica y propiedades mecánicas del PHBV. Similares resultados se han logrado mediante la obtención de nanocompuestos PHBV/haloisita y nanocompuestos PHBV/montmorillonita organomodificada en presencia de TNPP. No obstante, cuando el extensor de cadena se añade al nanocompuesto con haloisita no se produce una mejora de las propiedades con respecto al nanocompuesto sin extensor de cadena. (Capítulo 1)
- Se ha mejorado la ductilidad del PHBV a temperatura ambiente mediante el mezclado en fundido con un poliuretano termoplástico manteniendo las propiedades barrera a vapor de agua y aromas para contenidos máximos del 30 % en peso Además se preserva la biodegradabilidad de la mezcla para contenidos en aditivo de hasta el 40 % en peso. (Capítulo 2)
- El mezclado de PHBV con un 25 % en peso de PLA y distintos contenidos de tres diisocianatos (HMDI, polyHMDI y PDI) mejora la compatibilidad entre las fases poliméricas, el comportamiento mecánico y aumenta la viscosidad compleja a bajas frecuencias con

9. Conclusiones

respecto al PHBV. Los mejores resultados son obtenidos con la adición de polyHMDI o PDI en proporción molar 1:20. (Capítulo 3)

- Se desarrolló una metodología cualitativa de evaluación sencilla y universal de la termoconformabilidad de polímeros. La aplicación de esta metodología en el PHBV y sus mezclas PHBV/PLA compatibilizadas con distintos diisocianatos ha permitido, a su vez, un análisis sistemático del rango de temperaturas empleado en el procesado por termoconformado del PHBV y sus mezclas estudiadas. (Capítulo 4)
- Se ha mejorado la capacidad de moldeo por termoconformado del PHBV y se ha incrementado el rango de temperaturas de procesado por termoconformado mediante mezclado en fundido de PHBV con un 25 % en peso de PLA y la adición de diisocianatos como compatibilizantes de la mezcla de biopolímeros sin repercutir negativamente sobre el comportamiento a barrera (vapor de agua y oxígeno) ni la biodesintegración de las mezclas con respecto al PHBV. (Capítulo 4)
- La adición de sepiolita mejora el mezclado en fundido del PHBV y del PLA, reduciendo el tamaño de la fase dispersa. Esto, junto con el efecto de las nanopartículas, conduce a una reducción en la permeabilidad a oxígeno, mejora las propiedades mecánicas, mediante el incremento de la elongación a rotura, e incrementan la rigidez y estabilidad de los nanocompuestos a altas temperaturas con respecto al PHBV puro. (Capítulo 5)

10. Conclusions

10. Conclusions

The analysis of the research in this work result in the following general conclusion:

It is possible to improve the applicability of PHBV to the packaging industry by making compounds, with the introduction of a second phase, which can be polymeric and / or ceramic. Such improvement comes out from the increase in thermal stability of the base material as well as its ductility and thermoforming processability, while maintaining its excellent barrier properties and fast biodegradability. It should be noted that commercial products have been used to obtain these compositions and conventional thermoplastic processing techniques have been applied, which ensures their industrial viability.

The partial conclusions of each of the studies performed are described below:

- The addition of a suitable chain extender (tris (nonylphenyl) phosphite, (TNPP)) has been revealed as a solution to improve the thermal stability and mechanical properties of PHBV. Similar results have been achieved by obtaining PHBV/Halosisite nanocomposites and nanocomposites PHBV/organomodified montmorillonite in the presence of TNPP. However, when the chain extender is added to the halosisite nanocomposite there is no improvement in properties with respect to the nanocomposite without chain extender. (Capítulo 1)
- The PHBV ductility at room temperature has been improved by melt blending it with a thermoplastic polyurethane while maintaining the water vapor and aromas barrier properties for maximum contents of 30 wt.%. In addition, the biodegradability of the blend for additive content up to 40 wt.% is preserved. (Capítulo 2)
- Blending PHBV with 25 wt.% of PLA and different contents of three diisocyanates (HMDI, polyHMDI and PDI) improves the compatibility between polymer phases, the mechanical behavior, and increases complex viscosity at low frequencies with respect to PHBV. The best results are obtained with the addition of polyHMDI or PDI in 1:20 molar ratio. (Capítulo 3)

10. Conclusions

- A qualitative, simple and universal evaluation methodology for polymer thermoformability was developed. The application of this methodology in the PHBV and its PHBV/PLA compatibilized blends with different diisocyanates has allowed to determine the thermoforming process temperature range of PHBV and its studied blends. (Capítulo 4)
- The thermoforming moldability of the PHBV has been improved and the temperature range has been increased by melt blending PHBV with 25% by weight of PLA and the addition of diisocyanates as compatibilizers of the blend, without negative repercussion on the barrier behavior (water vapor and oxygen) nor the biodesintegration of the blend with respect to PHBV. (Capítulo 4)
- The addition of sepiolite improves the melt mixing of PHBV and PLA, reducing the size of the dispersed phase. This, along with the effect of the nanoparticles, leads to a reduction in oxygen permeability, improves mechanical behavior by increasing the elongation at break, and increases the rigidity and stability of nanocomposites at high temperatures with respect to pure PHBV. (Capítulo 5)

11. Trabajos en curso y futuros

11. Trabajos en curso y futuros

A continuación, se muestran varias líneas de investigación en curso y futuras para aumentar el conocimiento y la aplicabilidad de los polihidroxialcanoatos en el sector del envasado. Algunas de las siguientes líneas están actualmente en desarrollo en el marco de la presente tesis y se plantean como continuación de la misma:

- Una de las líneas futuras para la continuación de este trabajo de investigación es el desarrollo y caracterización de envases multicapa aplicando las composiciones de estudio, así como los conocimientos de los sistemas estudiados.
- Durante el desarrollo de esta tesis se han evaluado las propiedades barrera y la desintegrabilidad de las composiciones de estudio a través de las películas obtenidas por extrusión o prensado en fundido. Los resultados de permeabilidad y desintegrabilidad de los materiales son función del espesor de la lámina de estudio. Con el fin de poder evaluar estas propiedades en los envases termoconformados finales sería deseable el diseño y desarrollo de una metodología de medida de las propiedades barrera y biodegradación de envases termoconformados completos. El método a desarrollar permitiría obtener un valor más real de estas propiedades ya que se tendría en cuenta la distribución de espesores real de los envases.
- Actualmente existe una gran preocupación por la revalorización de desechos procedentes de la industria alimentaria, agrícola, etc. La adición de estos materiales, como material de relleno, en formulaciones basadas en PHBV podría reducir el coste del producto final. El desarrollo de compuestos basados en las composiciones estudiadas en este trabajo de tesis y la adición de desechos procedentes de la industria alimentaria y agrícola forma parte de las líneas futuras de esta tesis. Los objetivos concretos a desarrollar son la optimización del contenido de relleno y la compatibilización con la matriz polimérica y la segunda fase estudiada en este trabajo para mantener las propiedades y la capacidad de termoconformado estudiadas reduciendo el coste del envase final. El estudio de la viabilidad de la adición de paja de trigo a las mezclas de PHBV/TPU estudiadas está siendo desarrollado actualmente en colaboración con el grupo de Nuevos materiales y nanotecnología para aplicaciones alimentarias del Dr. José María Lagarón en el Instituto de Agroquímica y Tecnología de los Alimentos (IATA-CSIC).

11. Trabajos en curso y futuros

Dado el óptimo rendimiento de las mezclas PHBV/TPU, estudiadas en el Capítulo 3, para contenidos de TPU del 20% en peso, en este estudio, se ha fijado en esta cantidad el contenido en elastómero y se ha adicionado paja de trigo en contenidos desde el 5 al 50% en peso. El comportamiento mecánico, térmico, barrera y desintegración en compostaje de las mezclas ternarias obtenidas no varía sustancialmente con respecto a la mezcla binarias PHBV/TPU para bajos contenidos en paja de trigo. Por consiguiente, es posible reducir los costes del material adicionando desechos agroalimentarios, valorizando éstos, sin repercutir sustancialmente en el comportamiento del PHBV. Actualmente se está trabajando en la redacción de un artículo conjunto con el Dr. Lagarón y su equipo (grupo de Nuevos materiales y nanotecnología para aplicaciones alimentarias del IATA-CSIC).

- El comportamiento mecánico del PHBV sufre un cambio muy marcado en las siguientes horas a ser procesado. Este efecto de envejecimiento puede comprometer su uso en determinadas aplicaciones, como pueden ser aquellas en las que se necesite un procesado secundario por termoconformado. Por ello, actualmente se está llevando a cabo un estudio acerca del efecto del envejecimiento del PHBV y si la adición de la fase elastomérica podía compensar este mecanismo. Concretamente, se estudia la influencia del envejecimiento a temperatura ambiente, debido a la cristalización secundaria y el envejecimiento físico, sobre la capacidad de termoconformado del PHBV. Los resultados muestran que la adición de TPU afecta al proceso de envejecimiento del PHBV. Con el paso del tiempo de almacenamiento las muestras termoconformadas que contienen TPU mantienen la perfecta reproducción del molde. Sin embargo, las muestras termoconformadas de PHBV obtenidas a partir de las 24h tras el procesado presentan una serie de irregularidades. Actualmente se están realizando unos ensayos para poder finalizar el artículo de este trabajo.

- Otro de los objetivos de estudio en curso y futura línea de trabajo es el estudio de la relación que se establece entre procesado-estructura-propiedades de los materiales poliméricos cuando son procesados por impresión 3D. Se pretende aumentar del conocimiento del que se dispone de las propiedades resultantes de ser aplicada esta novedosa tecnología de procesado en biopolímeros biodegradables para aumentar la aplicabilidad de estos materiales en el sector del envasado.

Los primeros trabajos en esta línea han sido iniciados mediante la caracterización de probetas obtenidas por impresión 3D basadas en la utilización de filamentos comerciales de biopolíesteres biodegradables para su aplicación en el sector del envase. Este trabajo ha sido desarrollado durante una estancia de investigación en Zabrze (Polonia) en colaboración con el Centre of Polymer and Carbon Materials Polish Academy of Sciences, Zabrze (Polonia).

Concretamente, en esta primera toma de contacto con la técnica de impresión 3D, se pretende aumentar el conocimiento que se tiene del comportamiento mecánico, térmico y la respuesta a la degradación hidrolítica de probetas de PLA y una mezcla de PLA/PHA obtenidas por impresión 3D variando la dirección de producción.

Los primeros resultados de los que se dispone muestran una gran diferencia en las propiedades mecánicas y la morfología de las muestras resultantes del procesado por impresión 3D en dirección horizontal y vertical. En cuanto al estudio de degradación hidrolítica, no se observan diferencias considerables en el comportamiento y velocidad de degradación hidrolítica en función de la dirección de procesado, ni de la composición del filamento. Las probetas desarrolladas están siendo estudiadas en mayor profundidad actualmente, con el fin de determinar el peso molecular, la distribución de peso molecular, la estructura química y las propiedades térmicas previas al proceso de degradación hidrolítica. Asimismo, un extenso análisis de las probetas sometidas a degradación hidrolítica está siendo desarrollado a fin de describir con mayor precisión el proceso de degradación que ha tenido lugar. Concretamente, se están analizando los oligómeros liberados durante la degradación hidrolítica, determinando la composición y el peso molecular de los mismos.

Actualmente se está trabajando en la redacción de un artículo conjunto con el Professor Marek Kowalczyk colaborando con el Centre of Polymer and Carbon Materials Polish Academy of Sciences (Zabrze, Poland) y la Faculty of Science and Engineering at the University of Wolverhampton (Inglaterra).

- Los envases activos están siendo objeto de gran interés en la industria del envasado de alimentos ya que implica la posibilidad de dotar de una mayor funcionalidad al envase. Una de las posibilidades que ofrece el envasado activo es la de permitir prolongar la vida útil y aumentar la seguridad de los alimentos mediante el control de la actividad microbiana. En este sentido, el interés en envases con comportamiento antimicrobiano se ha incrementado considerablemente,

11. Trabajos en curso y futuros

dado el aumento que suponen desde el punto de vista de la seguridad alimentaria. En esta línea, en colaboración con el grupo de Nuevos materiales y nanotecnología para aplicaciones alimentarias del IATA-CSIC se ha realizado un estudio en el que se han desarrollado compuestos basados en PHBV con actividad antimicrobiana mediante la incorporación de partículas de sulfato de plata. Los resultados de este estudio constatan el comportamiento antimicrobiano de las composiciones estudiadas sin repercutir sobre la biodegradación en condiciones de compostaje de los materiales. Actualmente se está trabajando en la redacción de un artículo conjunto con el Dr. Lagarón y su equipo del IATA-CSIC.

12. Anexos

12. Anexos

12.1. Lista de publicaciones

A continuación, se expone el listado de los trabajos difundidos en revistas internacionales indexadas fruto del trabajo experimental expuesto en este trabajo, así como de otras líneas de investigación en las que se ha colaborado durante el periodo de desarrollo de la tesis doctoral:

- González-Ausejo J., Sánchez-Safont E., Gámez-Pérez J., Cabedo L. On the use of tris(nonylphenyl) phosphite as a chain extender in melt-blended poly(hydroxybutyrate-co-hydroxyvalerate)/clay nanocomposites: Morphology, thermal stability, and mechanical properties. *J Appl Polym Sci* 2016;133.
- Sánchez-Safont E.L., González-Ausejo J., Gámez-Pérez J., Lagarón J.M., Cabedo L. Poly(3-Hydroxybutyrate-co-3-Hydroxyvalerate)/Purified Cellulose Fiber Composites by Melt Blending: Characterization and Degradation in Composting Conditions. *J Renew Mater* 2016;4:123–32.
- Martínez-Abad A., González-Ausejo J., Lagarón J.M., Cabedo L. Biodegradable poly(3-hydroxybutyrate-co-3-hydroxyvalerate)/thermoplastic polyurethane blends with improved mechanical and barrier performance. *Polym Degrad Stab* 2016;132.
- González-Ausejo, J.; Sánchez-Safont, E.; Cabedo, L.; Gamez-Perez, J. Toughness enhancement of commercial Poly(Hydroxybutyrate-co-Valerate) (PHBV) by blending with a Thermoplastic Polyurethane (TPU). *J. Multiscale Model.* 2016;7.
- Gonzalez-Ausejo J., Sanchez-Safont E.L., Lagarón JM., Balart R., Cabedo L., Gamez-Perez J. Compatibilization of PHBV/PLA blends with diisocyanates. *J Appl Polym Sci.*, Accepted. Under production.
- Gonzalez-Ausejo J., Gamez-Perez J., Balart R., Lagarón J.M., Cabedo L. The effect of the addition of sepiolite on the morphology and properties of melt compounded PHBV/PLA blends. *Polymer Composites*, Under revision.
- González-Ausejo J., Sánchez-Safont E., Lagarón JM., Gámez-Pérez J., Cabedo L. Assessing the thermoformability of poly(3-hydroxybutyrate-co-3-hydroxyvalerate)/ poly(acid lactic) blends compatibilized with Diisocyanates. *Polymer engineering science*, Under revision.
- González-Ausejo J., Sánchez-Safont E., Lagarón JM., Gámez-Pérez J., Cabedo L., Gámez-Pérez J. Incorporation of thermoplastic polyurethane in Poly(3-hydroxybutyrate-co-3-hydroxyvalerate): changes in mechanical properties and thermoforming ability. In preparation.

12. Anexos

- González-Ausejo J., Musioł, M., Sikorska, W., Adamus, G., Janeczek, H., Kowalczuk, M., Rydz, J. Characterization of 3D printed samples of biopolymer in two different processing conditions. Hydrolytic degradation study. In preparation.
- Martínez-Abad A., González-Ausejo J., Gamez-Perez J., Lagarón J.M., Cabedo L. Characterization and disintegrability under composting conditions of PHBV-based composite films with silver sulfate particles. In preparation.
- Martínez-Abad A., González-Ausejo J., Lagarón J.M., Cabedo L. Poly(hydroxybutirate-co-hydroxyvalerate)/Thermoplastic polyurethane/Wheat straw ternary blend with improved performance. In preparation.

12.2. Imagen de la primera página de los artículos publicados expuestos en la sección de resultados y discusión

CAPÍTULO 1

JOURNAL OF
Applied Polymer
SCIENCE

On the use of tris(nonylphenyl) phosphite as a chain extender in melt-blended poly(hydroxybutyrate-co-hydroxyvalerate)/clay nanocomposites: Morphology, thermal stability, and mechanical properties

Jennifer González-Ausejo, Estefanía Sánchez-Safont, José Gámez-Pérez, Luis Cabedo

Polymer and Advanced Materials Group (PIMA), Universidad Jaume I, 12071 Castellon, Spain

Correspondence to: L. Cabedo (E-mail: lcabedo@uji.es)

ABSTRACT: The influence of the incorporation of tris(nonylphenyl) phosphite (TNPP) as a chain extender on the morphology and thermal stability of poly(hydroxybutyrate-co-hydroxyvalerate) (PHBV)/clay nanocomposites obtained by melt mixing has been studied. Two different clays have been used: a laminar organomodified montmorillonite (Cloisite® 30B) and a tubular unmodified halloysite (HNT). The morphology of the so-obtained nanocomposites has been assessed by transmission electron microscopy, scanning electron microscopy, and wide angle X-ray diffraction, showing a partially exfoliated structure for PHBV/Cloisite® 30B nanocomposites, as well as a good dispersion of the HNT in the PHBV matrix. The crystallinity of the resulting nanocomposites, determined by DSC, does not change when clays or TNPP are added. An increase in the onset temperature of thermal degradation of PHBV has been obtained with the addition of TNPP, as determined by TGA. With regard to the effect of the nanoclays on the thermal stability of PHBV, the onset temperature of the PHBV/HNT nanocomposites is higher than that of the pure PHBV, while this trend is not observed for the nanocomposites containing Cloisite® 30B. The addition of TNPP to the PHBV/Cloisite® 30B nanocomposites resulted in an improved thermal stability; however, for the HNT nanocomposites, the TNPP does not seem to have a significant effect. For all studied systems, it was shown that the variation of mechanical properties of the nanocomposites is due to the reinforcing effect of the nanoclays on the PHBV matrix. In the case of TNPP, it is due to the increased molecular weight and formation of a long-chain branching structure. © 2015 Wiley Periodicals, Inc. *J. Appl. Polym. Sci.* **2016**, *133*, 42390.

© 2015 Wiley Periodicals, Inc.

Materials
Views

WWW.MATERIALSVIEWS.COM

42390 (1 of 8)

J. APPL. POLYM. SCI. **2016**, DOI: 10.1002/APP.42390



Contents lists available at ScienceDirect

Polymer Degradation and Stability

journal homepage: www.elsevier.com/locate/polydegstab

Biodegradable poly(3-hydroxybutyrate-co-3-hydroxyvalerate)/thermoplastic polyurethane blends with improved mechanical and barrier performance



Antonio Martínez-Abad ^a, Jennifer González-Ausejo ^b, José María Lagarón ^a, Luis Cabedo ^{b,*}

^a Novel Materials and Nanotechnology Group, IATA, CSIC, Avda. Agustín Escardino 7, 46980, Burjassot, Spain

^b Polymers and Advanced Materials Group (PIMA), Universitat Jaume I, 12071, Castellón, Spain

ARTICLE INFO

Article history:

Received 17 December 2015
Received in revised form
22 March 2016
Accepted 31 March 2016
Available online 5 April 2016

Keywords:

PHBV
TPU
Biodisintegration
Melt blending
Biodegradable polymers

ABSTRACT

Poly(3-hydroxybutyrate-co-3-hydroxyvalerate) (PHBV) polymers pose a green alternative to fossil-fuel derived polymers, as they exhibit good biocompatibility, biodegradability and outstanding barrier performance compared to other biopolyesters. However, their excessive brittleness has not yet been overcome without compromising barrier performance. In this work, a native ester-based thermoplastic polyurethane (TPU) not stabilised against hydrolysis, has been thoroughly assessed for the first time as an additive in melt blends with PHBV. Phase segregation in scanning electron microscopy (SEM) confirmed the immiscibility of the two polymers, however a degree of interaction has been found. Wide-angle X-ray scattering and differential scanning calorimetry revealed no major effect of the TPU on the crystallinity of the PHBV phase. The onset and kinetics of thermal degradation was not altered by the presence of the TPU up to 50 wt% content. Blends with increasing TPU contents showed a gradual decrease in the modulus of elasticity and tensile strength, while a substantial increase in elongation at break has been found for contents of TPU above 20 wt%, which resulted an improvement in the overall toughness of the blends. The excellent barrier performance of the PHBV against water vapour and aroma compounds was shown to be unaffected by TPU loads of ≤ 30 wt%. Full decomposition of neat PHBV and PHBV/TPU blends below 50 wt% TPU content was achieved after 40 days according to biodisintegration standards (ISO 20200). The study puts forward the potential use of TPU to improve the mechanical performance of these natural biopolyesters without compromising the barrier properties or the biodegradability of the melt blends.

© 2016 Elsevier Ltd. All rights reserved.

CAPÍTULO 3

Journal of Applied Polymer Science - Decision on Manuscript # APP-2016-10-1585.R1

Journal of Applied Polymer Science <onbehalfof+sergionaz@gmail.com@manuscriptcentral.com>
Respon: sergionaz@gmail.com
Per a: ausejo@uji.es

9 de desembre de 2016, 20:41

09-Dec-2016

Dear Miss Gonzalez-Ausejo,

I am delighted to inform you that your manuscript # APP-2016-10-1585.R1 entitled "Compatibilization of PHBV/PLA blends with diisocyanates" has been found to be worthy of publication in the Journal of Applied Polymer Science.

Please note, however, that final acceptance of your manuscript is contingent on submission of a clean, production-ready manuscript, along with tables in the proper format and figures with the correct resolution for publication.

Your most recently uploaded manuscript files are currently being examined; if adjustments are required we will contact you shortly with more details and guidance on how to upload your files.

Once you receive our format instructions, please upload your production-ready files WITHIN 3 BUSINESS DAYS.

Delays in uploading production-ready files will unnecessarily delay final acceptance and publication, and might lead to eventual withdrawal of your manuscript.

COVER: We believe your images might be appropriate for use on the cover of the journal, and the paper worthy of being highlighted in this way. If you would like images from your paper, or an alternative image related to the work, to be considered for the cover, please email your layout suggestions with a short description to appmc@wiley.com. Please see our Cover FAQ at [http://onlinelibrary.wiley.com/journal/10.1002/\(ISSN\)1097-4628/homepage/Cover_FAQ.html](http://onlinelibrary.wiley.com/journal/10.1002/(ISSN)1097-4628/homepage/Cover_FAQ.html) for details on cover image preparation.

OPEN ACCESS option: if you would like to make your article freely accessible to everyone even if they do not have a subscription to the journal, which might increase usage of your research, you can order it at: https://authorservices.wiley.com/bauthor/onlineopen_order.asp paying the OnlineOpen fee of \$3000. You can find more information on Wiley OnlineOpen initiative at <http://olabout.wiley.com/WileyCDA/Section/id-406241.html>.

Your article cannot be published until the publisher has received the appropriate signed license agreement. Within the next few days the corresponding author will receive an email from Wiley's Author Services system which will ask them to log in and will present them with the appropriate license for completion.

COLOR FIGURES: color figures ONLINE are FREE; therefore If you are happy for your figures to appear in color online and in black & white in the print version of the journal, you do not need to do anything.
If you would like your figures to be in color in the PRINT VERSION of the journal, you will have to pay \$850 for one figure, \$1495 for two figures, or \$1995 for three or more figures. Please email appmc@wiley.com to arrange payment in the case you would like color figures in the PRINT VERSION of the article.

Thank you for your contribution to the Journal of Applied Polymer Science: we look forward to your continued contributions to the Journal.

Best wishes,

Prof. Sergei Nazarenko,
Journal of Applied Polymer Science
sergionaz@gmail.com, sergei.nazarenko@usm.edu

12. Anexos

12.3. Presentaciones en congresos nacionales e internacionales

A continuación, se expone el listado de los trabajos difundidos en congresos nacionales e internacionales durante el periodo de desarrollo de la tesis doctoral:

2016

González-Ausejo, J.; Gámez-Pérez, J.; Balart, R.; Lagarón, J.M.; Cabedo, L.; PHBV/PLA/Sepiolite nanocomposites for food packaging applications. International Conference on Nanotechnology Applications (Nanotec 2016), 26-27 Septiembre 2016, Valencia, España (Comunicación oral)

González-Ausejo, J.; Sánchez-Safont, E.; Cabedo, L.; Gámez-Pérez, J.; Toughness enhancement of commercial poly(hydroxyl butyrate-co-valerate) (PHBV) by blending with a thermoplastic polyurethane (TPU). 15th International Conference on Fracture and Damage Mechanics, 14-16 Septiembre 2016, Alicante, España (Póster)

Cabedo, L.; González-Ausejo, J.; Sánchez-Safont, E.; Martínez-Abad, A.; Fabra, M. J.; Lagarón, J.M.; Gámez-Pérez, J.; Estrategias para mejorar la aplicabilidad del Poli(3-hidroxivalerato-co-3-hidroxibutirato) (PHBV) al sector del envasado. XIV Reunión del grupo especializado de polímeros (GEP) de la RSEQ y RSEF (GEP 2016), 5-8 Septiembre 2016, Burgos, España (Comunicación oral)

González-Ausejo, J.; Sánchez-Safont, E.; Lagarón, J.M.; Balart, R.; Cabedo, L.; Gámez-Pérez, J.; Extending the usability of PHBV in thermoforming stages. 9th International Conference on Modification, Degradation and Stabilization of Polymers (MoDeSt 2016), 4-8 Septiembre 2016, Cracovia, Polonia (Comunicación Oral)

González-Ausejo, J.; Lagarón, J.M.; Balart, R.; Gámez-Pérez, J.; Cabedo, L.; Effect of addition of sepiolite in biodegradable biopolyesters. POLYMAT 2016 - SILESIAN MEETINGS ON POLYMER MATERIALS, 27-28 Junio 2016, Zabrze, Polonia (Póster)

González-Ausejo, J.; Lagarón, J.M.; Balart, R.; Gámez-Pérez, J.; Cabedo, L.; Efecto de la adición de sepiolita en biopoliésteres biodegradables. XIV Congreso Nacional de Materiales, 8- 10 Junio 2016, Gijón, España (Póster)

2015

González-Ausejo, J.; Martínez-Abad, A.; Gámez-Pérez, J.; Lagarón, J.M.; Cabedo, L.; Biodegradable and High Performance PHBV/TPU Blends. 5th International Conference on BIODEgradable and BIObased POLymers (BIOPOL 2015), 6-9 Octubre 2015, San Sebastian, País Vasco, España (Póster)

González-Ausejo, J.; Sanchez-Safont, E.; Izquierdo-Escrig, R.; Balart, R.; Cabedo, L.; Gámez-Pérez, J.; Use of poly(hexamethylene) diisocyanate as compatibilizer in PHBV/PLA blends. 5th International Conference on BIODEgradable and BIObased POLymers (BIOPOL 2015), 6-9 Octubre 2015, San Sebastian, País Vasco, España (Póster)

González-Ausejo, J.; Sánchez-Safont, E.; Lagarón, J.M.; Gámez Pérez, J.; Cabedo Mas, L.; Enhancement of the thermoformability of PHBV by blending with a TPU. 1st French-Spanish Joint Congress for Young Researchers in Polymers (JIP-JEPO2015), 14-18 Septiembre 2015, San Sebastian, País Vasco, España (Comunicación oral)

González-Ausejo, J.; Sánchez-Safont, E.; Gámez-Pérez, J.; Cabedo, L.; Mejora de la termoconformabilidad del PHBV mediante mezclas biodegradables con poliuretano. III CONGRESO I+D+i CAMPUS DE ALCOI, CREANDO SINERGIAS, 14 Julio 2015, Alcoi, Comunidad Valenciana, España (Póster)

González-Ausejo, J.; Gámez-Pérez, J.; Cabedo, L.; Boronat, T.; Garcia-Garcia, D.; Mejora de las propiedades mecánicas y compatibilidad de mezclas de PHBV/PLA con plastificantes comerciales de origen bio. III CONGRESO I+D+i CAMPUS DE ALCOI, CREANDO SINERGIAS, 14 Julio 2015, Alcoi, Comunidad Valenciana, España (Póster)

Sánchez-Safont, E.; González-Ausejo, J.; Gámez-Pérez, J.; Lagarón, J.M.; Cabedo, L.; Cellulose fiber reinforced PHBV composite with improved performance at high temperature. COST Action FP1205 Joint Meeting Working Groups & Management Committee meetings: "Advances in cellulose processing and applications-research goes to Industry, 10 Marzo 2015, Iasi, Rumania (Comunicación oral)

12. Anexos

2014

Sánchez-Safont E.; Guevara F.; González-Ausejo, J.; Gámez-Pérez, J.; Lagarón, J.M.; Cabedo, L.; Caracterización y biodegradación en condiciones de compostaje de compuesto de PHBV/Microcelulosa. XIII Reunión del grupo especializado de polímeros (GEP) de la RSEQ y RSEF (GEP 2014), 7-9 Septiembre 2014, Girona, España, (Póster)

González-Ausejo, J.; Sánchez-Safont, E.; Gámez-Pérez, J.; Cabedo, L.; Efecto de la adición de extensores de cadena sobre la estabilidad térmica durante el procesado de PHBV. XIII Reunión del grupo especializado de polímeros (GEP) de la RSEQ y RSEF (GEP 2014), 7-9 Septiembre 2014, Girona, España (Comunicación oral)

2013

Gámez-Pérez, J.; González-Ausejo, J.; Sánchez-Safont, E.; Cabedo, L.; Kinetics of thermal decomposition of poly (3-hidroxybutyrate-CO-3-hidroxyvalerate)(PHBV): Effect of processing and chain extenders. POLYMAR 2013, 1st International Conference in Polymers with special Focus in Early Stage Researchers, 3-7 Noviembre 2013, Barcelona, España (Comunicación oral)

Guevara, F.; González-Ausejo, J.; Sánchez-Safont E.L.; Gámez-Pérez, J.; Lagarón J.M.; Cabedo, L.; PHBV/Microcelulose composites: Characterization and biodegradation in composting conditions. POLYMAR 2013, 1st International Conference in Polymers with special Focus in Early Stage Researchers, 3-7 Noviembre 2013, Barcelona, España (Comunicación oral)

Sánchez-Safont E.; González-Ausejo, J.; Gámez-Pérez, J.; Cabedo, L.; Thermally Stabilized PHBV nanocomposites: obtention and characterization. POLYMAR 2013, 1st International Conference in Polymers with special Focus in Early Stage Researchers, 3-7 Noviembre 2013, Barcelona, España (Comunicación oral)

González-Ausejo, J.; Sánchez-Safont, E.; Gámez-Pérez, J.; Cabedo, L.; Development and characterization of PHBV-CLAY nanocomposites by melt blending with improved thermal stability. BIOPOL- 2013, 1-3 Octubre 2013, Roma, Italia (Póster)

12.4. Lista de abreviaturas y siglas

- PE Polietileno
- PET Polietilentereftalato
- PVC Policloruro de vinilo
- PP Polipropileno
- PS Poliestireno
- PA Poliamida
- PHAs Polihidroxicanoatos
- PHB Polihidroxitirato
- HV Hydroxyvalerate
- PHBV Polihidroxitirato-co-hidroxicvalerato
- PLA Poli (ácido láctico)
- PGA Poli (ácido glicólico)
- PCL Poli (ϵ -caprolactona)
- PBS Poli (sucinato de butileno)
- PVA Poli (alcohol vinílico)
- PHB Poli (β -hidroxitirato)
- ABS Acrilonitrilo butadieno estireno
- SBS Estireno-butadieno-estireno
- HIPS Poliestireno de alto impacto

12. Anexos

- PEG Polietilenglicol
- PBAT Adipato-tereftalato de polibutileno
- TNPP Tris(nonilfenil)fosfito
- C30B Arcilla montmorillonítica modificada con sales de amonio cuaternarias, Cloysite®
30B
- HNT Nanotubos de halloysita
- TPU Poliuretano termoplástico
- HMDI Diisocianato de hexametileno
- PolyHMDI Polihexametilendiisocianato
- PDI 1,4-fenilén diisocianato
- CPN Nanocompuesto arcilla mineral-polímero
- SEM Microscopia electrónica de barrido
- TEM Microscopia electrónica de transmisión
- WAXS Difracción de rayos x a altos ángulos
- DSC Calorimetría diferencial de barrido
- TGA Análisis termogravimétrico
- PPMM Propiedades mecánicas
- PPBB Propiedades barrera a gases y vapores (oxígeno, vapor de agua y limoneno)
- DMTA Análisis dinamo-mecánico a torsión
- VST Temperatura de reblandecimiento Vicat

- T_g Temperatura de transición vítrea
- T_c Crystallization temperature
- T_m Melt temperature
- X_c Degree of crystallinity (%)
- $T_{5\%}$ or T_{max} Initial decomposition temperature (5% of degradation) determined by TGA
- T_d Maximum degradation rate temperature measured at the DTG peak maximum.
- DPS Discrete-phase structure or drop-in matrix morphology
- CLTE Coefficient of linear thermal expansion
- Res Residual charge
- KUT Kerner–Uemura–Takayanagi model
- NN Nicolais–Narkis model
- BP Béla Pukánszky model
- O_2P Permeabilidad a oxígeno
- WVP Permeabilidad a vapor de agua

12. Anexos

12.5. Lista de figuras

Introducción

Fig.1.1: Demanda de plásticos en Europa por segmentos, datos de 2016. Fuente: Plastics Europe, Association of Plastics Manufacturers [2].

Fig.1.2: El tratamiento para los residuos plásticos post-consumo, datos de 2016. Fuente: Plastics Europe, Association of Plastics Manufacturers [2].

Fig. 1.3: Esquema de las líneas de investigación desarrolladas en el presente trabajo

Marco teórico

Fig.2.1: Investigaciones científicas publicadas cada año desde 1980 hasta 2016 acerca de a) PLA y b) PHBV. Fuente de datos Scopus.

Fig. 2.2: PHB acumulado en el interior de las células como gránulos intracelulares. Imagen reportada por Lee en la revista *Biotechnology and bioengineering* en 1996 [56].

Fig. 2.3: Estructura química del PHBV

Fig. 2.4: El mecanismo general de degradación del PHBV [31].

Fig 2.5: Rango de temperaturas en el que diferentes técnicas de procesamiento pueden ser aplicadas en función de la cristalinidad del polímero. Adaptación de [115]

Fig. 2.6: Reacciones potenciales en el sistema PLA-TNPP. (I) Reacción entre grupos hidroxilo terminales del PLA con el TNPP y (II) transesterificación entre un grupo terminal PLA fosfatado y un grupo terminal ácido carboxílico del PLA. [117]

Fig. 2.7: Esquema de un sistema de termoformado asistido a vacío. Reproducción del sistema de termoconformado utilizado en esta investigación.

CAPÍTULO 1

Fig. 3.1: Graphical abstract of the work named On the use of TNPP as a chain extender in melt blended PHBV/clay nanocomposites: morphology, thermal stability, and mechanical properties.

Fig. 3.2: TEM micrograph of (a) PHBV-C30B and (b) PHBV-HNT

Fig. 3.3: SEM images of the fracture surface of a) PHBV-C30B, b) PHBV-C30B-TNPP, c) PHBV-HNT, and d) PHBV-HNT-TNPP

Fig. 3.4: WAXS pattern of neat PHBV, PHBV-C30B, and PHBV-HNT nanocomposites

Fig. 3.5: TGA and DTG curves of PHBV and PHBV/clay nanocomposites with and without chain extender

Fig. 3.6: Stress-strain curves of PHBV and PHBV/clay nanocomposites with and without chain extender

Fig. 3.7: Young's modulus (E), tensile strength (σ_y), and elongation at break (ϵ_R) of PHBV/clay nanocomposites with and without chain extender

CAPÍTULO 2

Fig. 4.1: Graphical abstract of the work named Biodegradable poly(3-hydroxybutyrate-co-3-hydroxyvalerate)/ thermoplastic polyurethane blends with improved mechanical and barrier performance.

Fig. 4.2. Morphology of PHBV/TPU blends. Figure 1a-1f: Scanning electron images of 95/5 (a), 90/10 (b), 80/20 (c), 70/30 (d), 60/40 (e) and 50/50 (f). Particle size distribution for the PHBV/TPU blends (g). D10, D50 and D90 values of the PHBV/TPU blends (h). Accumulated frequency of particle sizes in the ester-blends (i). Detail of PHBV/TPU blend interfaces (j).

Fig. 4.3. WAXS patterns of neat PHBV, TPU and PHBV/TPU blends.

Fig. 4.4. DSC thermograms of neat PHBV, TPU and PHBV/TPU blends: a) Second heating run, b) Cooling run.

12. Anexos

Fig. 4.5. Weight loss versus temperature of the tested materials as analysed by TGA. Inset displays the DTG curves for the same samples.

Fig. 4.6. Tensile stress curves of the PHBV/TPU blends. Inset displays the tendency in elongation at break of blends with increasing TPU content (a). Variation of the tensile modulus of elasticity (b) and tensile strength (c) with the incorporation of TPU and fitting to the respective predictive models.

Fig. 4.7. Vapour permeability of the neat materials and their tested blends to water and limonene.

Fig. 4.8. Disintegration of the PHBV/TPU blends over time under composting conditions.

Fig. 4.9. Visual appearance of the tested blend films (PHBV/TPU) after selected time points during the composting process.

CAPÍTULO 3

Fig. 5.1: Graphical abstract of the work named Compatibilization of PHBV/PLA blends with diisocyanates.

Fig. 5.2: SEM images of the fracture surfaces of PHBV/PLA blends with diisocyanates.

Fig. 5.3: DSC curves of neat PHBV, PHBV/PLA and PHBV/PLA blends with a 1:20 molar ratio of diisocyanates.

Fig. 5.4: SEM micrographs of boron nitride particles in PHBV/PLA blend and PHBV/PLA blend with a 1:20 molar ratio of PDI.

Fig. 5.5: Young's modulus (E), tensile strength (σ_y) and elongation at break (ϵ_R) of neat PHBV and PHBV/PLA blends with diisocyanates versus compatibilizer content.

Fig. 5.6: a) Dynamic storage modulus (E') and b) delta tangent of PHBV, PHBV/PLA and PHBV/PLA blends with a 1:20 molar ratio of diisocyanates.

Fig. 5.7: Evolution of a) storage modulus (G'), b) loss modulus (G'') and c) complex viscosity of neat PHBV, PHBV/PLA and PHBV/PLA blends with diisocyanates at 180 °C under 1% dynamical shear strain.

CAPÍTULO 4

Fig. 6.1: Graphical abstract of the work named Assessing the thermoformability of poly(3-hydroxybutyrate-co-3-hydroxyvalerate)/poly(acid lactic) blends compatibilized with Diisocyanates

Fig. 6.2: SEM micrographs of a) PHBV/PLA blend, b) HDMI, c) polyHMDI, d) PDI and e) diameter distribution of PLA domains of PHBV/PLA blend and compatibilized blends.

Fig. 6.3: a) Water vapor and b) oxygen permeability of the neat materials and their blends.

Fig. 6.4: a) parameters defined in the method on a thermoformed PLA tray, b) an example of the thermoformed trays for PLA and PHBV, c) thermoformed PHBV trays at different heating times evaluated according to the method and d) thermoforming temperature range according to the method.

Fig. 6.5: Photographs of the thermoformed structures depending on the processing temperature and thermoforming temperature range for Neat PHBV, PHBV/PLA blend and the PHBV/PLA compatibilized blends.

Fig. 6.6: a) Disintegration curve, b) photographs of the disintegrated samples at different times, c) SEM micrographs of eroded surfaces after 20 days under composting conditions, d) and e) SEM micrographs of bacteria colonies after 20 days of composting of PHBV/PLA blend and PDI, respectively.

CAPÍTULO 5

Fig. 7.1: Graphical abstract of the work named Effect of the addition of sepiolite on the morphology and properties of melt compounded PHBV/PLA blends.

Fig. 7.2: Morphology of sepiolite: a) SEM, b) TEM micrographs, c) length and diameter distribution of sepiolite needles and d) WAXS diffractogram of sepiolite

12. Anexos

Fig. 7.3: Evolution of a) storage modulus (G'), b) loss modulus (G'') and c) complex viscosity of neat PHBV, PHBV/PLA and sepiolite/PHBV/PLA nanocomposites at 180 °C under 1% dynamical shear strain.

Fig. 7.4: SEM micrographs of a) PHBV/PLA blend, b) 1SEP, c) 2SEP, d) 3SEP, e) 4SEP; h) WAXS diffractograms of PHBV/PLA blend and sepiolite/PHBV/PLA nanocomposites and d) diameter distribution of PLA domains of PHBV/PLA blend and sepiolite/PHBV/PLA nanocomposites

Fig. 7.5: a) Weight loss versus temperature as analysed by TGA and b) DTG curves of PHBV/PLA blend and sepiolite/PHBV/PLA nanocomposites

Fig. 7.6: a) Young modulus and tensile strength, b) elongation at break (ϵ_R) and c) flexural elastic modulus and flexural strength of neat PHBV, PHBV/PLA blend and sepiolite/PHBV/PLA nanocomposites

Fig. 7.7: a) Dynamic storage modulus (E') and b) delta tangent of PHBV, PHBV/PLA and sepiolite/PHBV/PLA/ nanocomposites.

Fig. 7.8: a) Young modulus and tensile strength and b) elongation at break (ϵ_R) of neat PHBV, PHBV/PLA blend and sepiolite/PHBV/PLA nanocomposites at a crosshead rate of 500 mm/min and 140°C.

12.6. Lista de tablas

CAPÍTULO 1

Table 3.1: DSC and TGA data of the samples studied.

CAPÍTULO 2

Table 4.1: Thermal properties of the PHBV/TPU blends.

Table 4.2: Mass transfer parameters through PHBV/TPU blends.

CAPÍTULO 3

Table 5.1: Nomenclature of studied PHBV, PLA and PHBV/PLA blends.

Table 5.2: DSC and TGA data of PHBV and PHBV/PLA blends with and without diisocyanates.

CAPÍTULO 5

Table 7.1: Thermal properties of sepiolite/PHBV/PLA nanocomposites: TGA, DSC and VST parameters

Table 7.2: Barrier properties of sepiolite/PHBV/PLA nanocomposites

12. Anexos

12.7. Lista de ecuaciones

$$\lambda = 2 \cdot d \cdot \sin\theta \quad (3.1)$$

$$X_c (\%) = \frac{\Delta H_m}{w \cdot \Delta H_m^0} \cdot 100 \quad (3.2), (4.1), (5.1), (7.1)$$

$$P = DS \quad (4.2)$$

$$D = \frac{m_i - m_f}{m_i} \times 100 \quad (4.3), (6.1)$$

$$E_b = E_m \left(\frac{(7-5v_m)x E_m + (8-10v_m)x E_d - (7-5v_m)x (E_m - E_d)x \phi_d}{(7-5v_m)x E_m + (8-10v_m)x E_d + (8-10v_m)x (E_m - E_d)x \phi_d} \right) \quad (4.4)$$

$$E_b = E_m \left(\frac{(7-5v_m)x E_m - (7-5v_m)x E_m x \phi_d}{(7-5v_m)x E_m + (8-10v_m)x E_m x \phi_d} \right) \quad (4.5)$$

$$E_b = E_m (1 - \phi_d^{2/3}) \quad (4.6)$$

$$\sigma_b = \sigma_m (1 - K \phi_d^{2/3}) \quad (4.7)$$

$$\sigma_b = \sigma_m \left(\frac{1 - \phi_d}{1 + 2.5 \phi_d} \right) e^{B \phi_d} \quad (4.8)$$

$$WU (\%) = \frac{w_f - w_i}{w_i} \cdot 100 \quad (7.2)$$